OMEE-2017

Ministry of Education and Science of Ukraine
Lviv Polytechnic National University

Book of Abstracts

International Conference on Oxide Materials for Electronic Engineering – fabrication, properties and applications

OMEE-2017

May 29 – June 2, 2017
Lviv, Ukraine

Lviv
Lviv Polytechnic Publishing House
2017

Міністерство освіти і науки України
Національний університет “Львівська політехніка”

Збірник
тез

Міжнародної наукової конференції “Оксидні матеріали електронної техніки – отримання, властивості, застосування”

OMEE-2017

29 травня – 2 червня, 2017
Львів, Україна

Львів
Видавництво Львівської політехніки
2017

УДК 521.315.61
О 64

Збірник тез Міжнародної наукової конференції “Оксидні
О 64 матеріали електронної техніки – отримання, властивості, застосування” (ОМЕЕ-2017) / упор. В. Швед. – – Львів: Видавництво Львівської політехніки, 2017. – 1 електрон. опт. диск (CD-ROM).
ISBN 978-966-941-062-7

У збірнику подані тези доповідей Міжнародної наукової конференції “Оксидні матеріали електронної техніки – отримання, властивості, застосування” (ОМЕЕ-2017). Конференція присвячена актуальним проблемам технології отримання та дослідження структурних, оптичних, магнітних та електрофізичних властивостей оксидних матеріалів, а також можливості їх практичного застосування у пристроях електронної техніки та розроблення нових функціональних пристроїв на їх основі.

Для науковців та аспірантів, які працюють в галузі фізики оксидних матеріалів.

УДК 521.315.61

Відповідальна за випуск – В. Швед
Усі матеріали подано в авторській редакції

ISBN 978-966-941-062-7

Preface

Dear colleagues,

Welcome to the International Conference on Oxide Materials for Electronic Engineering – fabrication, properties and applications (OMEE-2017) in Lviv, Ukraine, May 29 - June 2, 2017.

Lviv Polytechnic National University has an honour to host this scientific meeting that continues the good tradition that has been commenced as a local workshop in Lviv, which gathered researchers and engineers of several educational and scientific institutions of our city engaged in technology, studying and practical developments of oxide materials for electronic engineering. Afterwards this tradition was continued as series of international scientific workshops. The first one, in 2007, was devoted to the memory of Prof. Andriy O. Matkovskii (1954-2004) who initiated this meetings. The extended subject matters as well as geography of participants of the second workshop in 2009 allowed thinking about new format of the OMEE meeting. Since 2012 this event was hold as an international conference. Thus, it is already the fifth international scientific forum on Oxide Materials for Electronic Engineering in Lviv Polytechnic National University in 2017.

We are very happy that about 200 participants representing contributions from scientific, educational and R&D institutions from 23 countries (Algeria, Armenia, Belarus, Brazil, China, Czech Republic, Germany, Greece, India, Israel, Italy, Kazakhstan, Latvia, Lithuania, Poland, Portugal, Russia, Saudi Arabia, Slovakia, South Korea, Turkey, Ukraine, United Kingdom, USA) decided to participate in OMEE-2017 and have kept up this tradition. Experienced scientists and young researchers, experimentalists and theoreticians in different fields of chemistry and physics, technology and engineering will have a forum for direct and unimpeded discussion of their results and new trends, exchange of knowledge and ideas, joining their efforts in collaboration and multidisciplinary research. The current Conference Program covers the topics of material science and technology, chemistry and physics of solid state, structure peculiarities on different scales, interconnection of chemical composition, structure and properties of oxides, their modification under external influence, developments of new methods of study and new applications of oxide materials in variety fields of electronic engineering.

This book contains abstracts of contributions submitted to the OMEE-2017 Conference. I would like to thank to members of the Program Committee and other experts having made it possible to issue the OMEE-2017 Conference Book of abstracts.

On behalf of the Local Organizing Committee, I would like to thank to all participants of the OMEE-2017 Conference, co-organizing institutions – the Scientific Research Company "Carat" (Lviv, Ukraine), Institute of Physics of the Polish Academy of Sciences (Warsaw, Poland) and Representative office „Polish Academy of Sciences" in Kyiv (Ukraine), as well as to International Centre for Diffraction Data (ICDD) (USA), who promoted the Conference organization and supported it financially.

We are looking forward for successful meeting as well as a pleasant and memorable stay in the ancient Lviv.

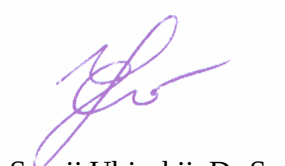

Sergii Ubizskii, Dr.Sc., Prof.
Chairman of Local Organizing Committee
Lviv, May, 2017

Conference Board

Organizers

Lviv Polytechnic National University (Ukraine)
Scientific Research Company "Carat" (Ukraine)
Institute of Physics of the Polish Academy of Sciences (Poland)
Representative office „Polish Academy of Sciences" in Kyiv (Ukraine)

Under support of

Ministry of Education and Science of Ukraine
International Centre for Diffraction Data (ICDD) (USA)

International Advisory Committee

V. Baryakhtar (Ukraine)
D.K. Becker (Germany)
A. Belous (Ukraine)
U. Bismayer (Germany)
Yu. Bobalo (Ukraine)
M. Brodin (Ukraine)
R. Gladyshevskii (Ukraine)
Yu. Gorobets (Ukraine)
Yu. Grin (Germany)
B. Grinyov (Ukraine)
M. Leoni (Italy)
V. Pecharsky (USA)
B. Raveau (France)
H. Sobczuk (Poland)
H. Szymczak (Poland)
A. Suchocki (Poland)
M. Vakiv (Ukraine)
R. Waser (Germany

Program Committee

E. Antipov (Russia)
L. Arizmendi (Spain)
M. Berkowski (Poland)
I. Blonskii (Ukraine)
T. Endo (Japan)
P. Esquinazi (Germany)
H. Gocmez (Turkey)
M. Godlewski (Poland)
R. Golovchak (USA)
V. Grachev (USA)
M. Grinberg (Poland)
E. Hristoforou (Greece)
A. Kamińska (Poland)
A. Kareiva (Lithuania)
M. Kosmyna (Ukraine)
L. Kovacs (Hungary)
M. Kučera (Czech Republic)
A. Luchechko (Ukraine)
V. Lutsyk (Russia)
V. Mykhaylyk (United Kingdom)
S.G. Nedilko (Ukraine)
S.A. Nedilko (Ukraine)
B. Padlyak (Poland)
W. Paszkowicz (Poland)
A. Popov (Latvia)
T. Prikhna (Ukraine)
R. Przenioslo (Poland)
A. Senyshyn (Germany)
V. Sirutkaitis (Lithuania)
S. Sholom (USA)
A. Serga (Germany)
M. Shatruk (USA)
G. Suchanek (Germany)
D. Sugak (Ukraine)
A. Tolmachev (Ukraine)
A. Tovstolytkin (Ukraine)
M. Trubitsyn (Ukraine)
S. Ubizskii (Ukraine)
M. Valerio (Brazil)
L. Vasylechko (Ukraine)
O. Vasylyev (Ukraine)
R. Vlokh (Ukraine)
A. Voloshinovskii (Ukraine)
A. Weidenkaff (Germany)
H. Yükselici (Turkey)
P. Zavalij (USA)
Ya. Zhydachevskyy (Ukraine/Poland)
Yu. Zorenko (Poland)

Local Organizing Committee

S. Ubizskii (Chairman)
N. Martynyuk (Scientific Secretary)

O. Buryy
L. Kovalyk
A. Luchechko
V. Hreb
S. Hurskii
O. Pavlovska
M. Shpotyuk
V. Shved
H. Sobczuk
I. Solskii
D. Sugak
S. Turchak
L. Vasylechko
U. Yakhnevych
Ya. Zhydachevskyy

TABLE OF CONTENTS

Abstracts

SECTION 1

TECHNOLOGY OF ACTIVE MEDIA FOR ELECTRONIC ENGINEERING

Spark-Plasma-Sintering for Preparation of Oxidic and Ceramic Materials

Yuri Grin, Felix Kaiser, Igor Veremchuk

Max. Planck-Institut für Chemische Physik fester Stoffe, Dresden, Germany

Spark Plasma Sintering (SPS) was developed as an efficient technology for compacting of powder materials [1]. A particular feature of SPS is the surface cleaning and activation of the initial powders [2]. This allows the compacting of materials which cannot be efficiently treated by conventional methods. Moreover, the targeted materials can be shaped, e.g. for distinct measurements of physical properties or producing of working parts [3].

In the solid state research, SPS is successfully used for synthesis of new materials, in particular oxides [5,6]. Advantages of this kind of chemical preparations are the use of pulsed electrical dc current as additional – in respect to the usual preparation techniques - possibility of the process influence. This allows chemical reactions at low total temperature of the green good, when locally, in very small volumes, the temperature is high enough for target chemical transformation. The nanoparticle structure of materials can be preserved [7,8]. Employing the dc current within the SPS setup allows performing electrochemical reactions yielding new compounds. Further advantage of SPS for chemical preparations is the acceleration of the diffusion-controlled in combination with the heterophase processes. In selected cases, it leads even to formation of single crystals within the green good [9].

Application of the SPS technique allow to prepare and shape oxidic and ceramic materials for thermoelectric applications [10-12] or for conditioning and sequestration of the active waste [13.14].

[1] M. Tokita, Trends in Advanced System and FGM Technology, in: NEDO Int. Symp. on FGM, 1999.
[2] Z. A. Munir et al., *J. Mat. Sci.* **41** (2006) 763.
[3] R. Orru et. al., *Mat. Sci. Eng. R* **63** (2009) 127.
[5] I. Veremchuk et al., *Inorg. Chem.* **52** (2013) 4458.
[6] G. Kieslich et al., *Phys. Chem. Chem. Phys.* **15** (2013) 15399.
[7] D. Portehault et al., *ASC Nano* **5** (2011) 9052.
[8] S. Conze et al., *J. Solid State Chem.* **229** (2015) 235.
[9] M. Beekman et al., *JACS* **131** (2009) 9642.
[10] B. Feng et al., *Adv. Eng. Mat.* **16** (2014) 1252.
[11] H. Zhang et al., *J. Electron. Mater.* **39** (2010) 1772.
[12] G. Kieslich et al., *Phys. Status Solidi A* **213** (2016) 808.
[13] L. Campayo et al., *J. Nucl. Mat.* **457** (2015) 63.
[14] N. Massoni et al., *J. Eur. Ceram. Soc.* **35** (2015) 297.

Synthesis of Complex Oxide Compounds and Oxide/Polymer Composites with High Temperature Superconducting and Others Especially Valuable Physicochemical Properties

S. Nedilko, A. Dzyazko, T. Voitenko, I. Fesych, M. Zelenko

Taras Shevshenko National University of Kyiv, 12 L'va Tolstogo Str., 01033 *Kyiv, Ukraine*

Properties of complex oxides compounds and oxide/polymer composites, which contain transition metals, are known to depend on synthesis method. A choice of one or the other technique allows us to vary valence state of a transition metal, crystallographic parameters, morphological characteristics (crystallinity degree, porosity, granule size), high temperature superconducting (HTSC), optical and catalytic properties [1]. However, numerous studies showed that there are difficulties at obtaining of the samples with the reproducible properties. In addition, properties of the ceramic materials depend on the temperature conditions of treatment, chemical composition, cation and anion substitutions medium and oxygen content in most cases.

Influence of synthesis method and synthesis conditions on cuprates, nickelates, cobaltate, vanadates, manganites with perovskite and perovskite-like crystalline structures (Ruddlesden-Popper phases, brownmillerite) and oxide/polymer composites with HTSC and others especially valuable physicochemical properties investigated. We studied possibility of synthesis these complex oxides compounds and oxide/polymer composites by solid-state reaction, co-precipitation, sol-gel and secondary induction heating technique [2].

Bi- and Y-containing HTSC cuprates was synthesis by solid-state method. HTSC ceramics of Bi-2212 composition doped with aluminum, zirconium, niobium and tantalum. For the bismuth ceramics samples, the T_c value changes considerably after addition of 5 mass percent Al_2O_3. Besides, a trend for ΔT_c increase observed. The size of particles was 0.5 – 1.5 μm. It was found that the $Y_3Ba_5Cu_8O_{18+\delta}$ (Y358) compound cannot be obtained by means of a method, which involves hydroxooxalate co-precipitation. At $T > T_c$ the $\rho - T$ plot for the Y358 compound, which has been obtained with a solid-state method, looks like that for semiconductors. At the same time, the compound synthesized with a carbonate co-precipitation method behaves like a metal. The results of physicochemical measurements allow us to suggest heterogeneity of the phase composition for the compounds obtained from solutions. Moreover, superconducting properties of the Y358 sample deteriorate (decrease of the T_c value from 92 K to 86 K and the superconducting transition width ΔT_c from 15 K to 9 K, respectively).

Barium cuprate was synthesized using secondary induction heating. It was found that the single-phase product is formed when the equimolar mixture of $Ba(NO_3)_2$ and CuO was kept in the induction furnace for 40 min at 1173 K.

Use of wet chemical methods leads to increase of oxygen indexes and average oxidation degree of transitions metal ions. It was found, that calcination temperature under solid state synthesis is much higher in a comparison with co-precipitation and sol-gel techniques, the period of heating is longer even taking into consideration a previous stage of precursor formation.

[1] S.A. Nedilko, A.G. Dzyazko, M.A. Zelenko, *High temperature superconductivity*, VPC "Kyiv University", Kyiv, 2010, p.191 (in Ukrainian).

[2] S.A. Nedil'ko, I.V. Fesych, O.G. Dzyazko, A.S. Bulachok, S.O. Solopan, T.O. Plutenko, Synthesis of Barium Cuprate by Secondary Induction Heating and its Electrical Properties, *Powder Metallurgy and Metal Ceramics* **55** (2016) 347.

Thin-Film Oxide Scintillators

M. Kucera[1], Z. Lucenicova[1], O. Lalinsky[2], and M. Nikl[3]

[1]*Charles University, Faculty of Mathematics & Physics, 12116 Prague, Czech Republic*
[2]*Institute of Scientific Instruments, CAS, 61264 Brno, Czech Republic*
[3]*Institute of Physics, CAS, 16000 Prague, Czech Republic*

In scintillators, the high energy particles (electrons, protons, neutrons, alpha particles) or photons (X- rays or gamma rays) excite electrons in atoms, which thereafter return to the ground state accompanied by emission of visible or UV photons. These photons are easily detected by existing photodetectors. The de-excitation can be prompt (in nanosecond time scale) or delayed (milliseconds up to hours).

The films with thickness of several micrometres are used in high resolution electron or X-ray screens and in various applications for imaging of microscopic objects with submicron spatial resolution. The single crystalline film scintillators have found applications in many synchrotron X-ray light sources where luminescence image of a scintillation screen is coupled to a CCD digital camera.

The single crystalline films can be grown by the liquid phase epitaxy (LPE) from the flux. The LPE is a versatile method suitable for the growth of films of typical thickness from submicron to tens of microns on single crystal substrates. The method is more flexible as compared to the growth of bulk single crystals by Czochralski or Bridgman methods and is often used in material research for development of new scintillators.

Here we focus on oxide scintillator films, particularly aluminium garnets, perovskites, and oxyorthosilicates doped with rare earth ions, especially Ce^{3+} and Pr^{3+}. Their luminescent and scintillation properties will be reviewed and discussed in comparison with bulk single crystal counterparts. Special attention will be paid to recently discovered high efficient multicomponent garnets $(LuGd)_3(GaAl)_5O_{12}$:Ce (GAGG:Ce) due to their particularly high light yield (up to 58000 photon/MeV) approaching their theoretical limit and good energy resolution reaching 4.2% at 662 keV [1]. The scintillation characteristics of this garnet system are further improved by intentional co-doping by divalent Mg^{2+} or Ca^{2+} ions which results in significant reduction of the afterglow signal and thermoluminescence signal [2-4]. These results demonstrate significant suppression of shallow electron traps which otherwise result in parasite delayed emission or non-radiative recombination channels with negative influence on scintillation properties. The favorable role of Mg^{2+} doping of GAGG:Ce is mostly caused by creation of tetravalent Ce^{4+} ions as effective electron trap center which successfully compete with the intrinsic electron traps [2].

[1] K. Kamada, S. Kurosawa et al., *Opt. Mater.* **36** (2014) 1942.
[2] M. Nikl, K. Kamada et al., *Crystal Growth & Design* **14** (2014) 4827.
[3] P. Prusa, M. Kucera et al., *Crystal Growth & Design* **15** (2015) 3715.
[4] P. Prusa, M. Kucera et al., *Advanced Opt. Mater.* (2017), doi: 10.1002/adom.201600875.

Last Trends in Micromachining of Transparent Materials with Femtosecond Laser Pulses

V. Sirutkaitis[1], S. Butkus[1], D. Paipulas[1], R. Sirutkaitis[2], G. Slekys[3], M. Barkauskas[4,1]

[1]*Laser Research Centre, Vilnius University, Sauletekio Av. 10, 10233 Vilnius, Lithuania*
[2]*Institute of Biochemistry, Vilnius University, Sauletekio Av. 7, 10233 Vilnius, Lithuania*
[3]*Workshop of Photonics, Mokslininku St. 6A, 08412 Vilnius, Lithuania,*
[4]*Light Conversion Ltd., Keramiku St. 2B, 10233 Vilnius, Lithuania*

Due to the forever growing industrial demand for quality and fast fabrication of transparent materials, femtosecond laser systems are rapidly becoming a topic of interest in industry [1]. Femtosecond laser microfabrication differs from long pulse or CW laser fabrication systems due to nonlinear optical effects arising from high intensity (~TW/cm^2) laser radiation. At these intensity limits, transparent materials become opaque due to strong nonlinear absorption, thus enabling fabrication of virtually any type of material regardless of the wavelengths the laser is emitting. Multiphoton absorption and avalanche ionization occur in a confined space of wide bandgap material, and above some intensity could lead to laser-induced refractive index variations, which are used for creation of waveguides and diffractive gratings in bulk transparent glasses, crystals and plastics or in some range of higher fluencies nanogratings are formed in some transparent materials, which show polarization rotation futures or selectivity in chemical etching in HF or other solutions. At some fluency, which exceeds many times the fluencies required for the nanogratings formation dielectric breakdown is induced and it could be used for microfabrication of transparent materials by ablation or void formation.

In this report, brief fundamentals and original results on investigations performed at participating organizations on such topics will be presented:

a) the fundamentals of femtosecond laser pulse interaction with transparent materials and its application for micromachining,

b) microfabrication of transparent materials by nanograting formation and etching in HF and KOH solutions,

c) the review of an alternative front-side ablation technique by immersing in water the machined samples and focusing the femtosecond pulses through a low NA objective [2],

d) developed at Workshop of Photonics a break through transparent material cutting technology, which enables scribing tempered, non-tempered glass and sapphire in straight or curved lines [3],

e) femtosecond ytterbium laser systems for micromachining of transparent materials developed at Light Conversion Ltd. [4].

[1] R. Osellame, G. Cerullo and R. Ramponi, *Femtosecond Laser Micromachining*, Springer-Verlag, Berlin, Heidelber, 2012.
[2] S. Butkus, E. Gaižauskas, D. Paipulas, Ž. Viburys, D. Kaškelytė, M. Barkauskas, A. Alesenkov and V. Sirutkaitis, Rapid microfabrication of transparent materials using filamented femtosecond laser pulses, *Applied Physics A* **114** (2014) 84-90.
[3] http://wophotonics.com/product/laser-technology-for-cutting-glass-and-sapphire/.
[4] http://lightcon.com/Products/femtosecond-lasers.html.

1D Zinc Nanostructures Obtained by Electrodeposition in Porous Titania

M.G.S. Ferreira[1,*], M. Starykevich[1], A. N. Salak[1], D.K. Ivanou[2], M.L. Zheludkevich[1,3]

[1]*Department of Materials and Ceramic Engineering, CICECO-Aveiro Institute of Materials, University of Aveiro, 3810-193 Aveiro, Portugal*
[2]*Faculty of Engineering, University of Porto, 4200-465 Porto, Portugal*
[3]*Institute of Materials Research, Helmholtz-Zentrum Geesthacht, 21502 Geesthacht, Germany*
* *mgferreira@ua.pt*

The use of high-ordered porous templates on valve metals for formation of nanostructures via electrochemical deposition is a cheap and convenient method. Filling of the matrixes by other materials is applied to produce solid state solar cells, photodetectors, magnetic sensors, metal–insulator–metal capacitors[1]. Dire ct investigation of deposition and nucleation processes in porous templates is hindered because the interface is hidden. Besides, the diffusion limitations in the pores can create additional effects. However, deep understanding of the nucleation process and other processes, which occur in the beginning of the deposition, is extremely important because exactly in the beginning of the deposition it is easy to change properties and structure of the deposited materials.

In the current work, zinc electrodeposition from a deep eutectic mixture of $ZnCl_2$ and choline chloride/ethylene glycol on titanium covered by a dense and porous anodic titania film was studied.

It was shown that thin titanium dioxide layers work as high resistive media and the rate of zinc deposition decreases with film thickness. Thicker titania layers (23 nm and higher) have opposite properties and the zinc reduction rate starts gradually increasing with thickness.

The results firstly obtained on planar electrodes have been transferred to the non-detached porous anodic titania templates. Titania nanotubes were formed in ethylene glycol based electrolyte with ammonium fluoride. Matrix modification such as annealing and crystallization of the pore bottom have strong influence on the electrodeposition process and allow preparation of zinc coaxial structures or nanorods.

[1] D. Kannadassan, R. Karthik, M. Shojaeib Baghini, *Materials Science in Semiconductor Processing* **16** (2013) 274-281.

Improved Performance of TFTs through Low Temperature Annealing of a-InGaZnO for Flexible Electronics

J. G. Troughton[1,2], P. Downs[2], R. Price[2], and D. Atkinson[1]

[1]*Department of Physics, University of Durham, England*
[2]*Pragmatic Printing, NETPark, Sedgefield*

Amorphous Indium Gallium Zinc Oxide (a-IGZO) is at the forefront of thin film transistor (TFT) technology, leading a revolution in both display and communication technologies. While a great deal of work has focused on the use of a-IGZO in next generation displays, producing thinner, lighter, and cheaper screens, less has been done on the implementation of this technology in low cost, flexible applications. This is, in a large part, due to the low thermal budget of the polymeric substrates used for such applications, however, it is arguably this use of a-IGZO that represents the biggest potential market, with applications in NFC and RFID, flexible and shock proof low power memory, the Internet of Things, and many more emerging areas [1].

While there is a growing body of work looking at the deposition of a-IGZO for such applications, there is a lack of study looking at post deposition treatments which can significantly enhance performance of these devices.

Thermal annealing has previously been shown to significantly improve device performance when carried out between 250°C and 500°C in devices on glass, but has not been reported at temperatures compatible with flexible substrates. Here we present a study looking at low temperature thermal annealing, post a-IGZO deposition, carried out between 150°C and 300°C. [2] We show a significant variation on a-IGZO density with such annealing for up to 36 hours, and propose a two-part energy barrier description to explain this change. In addition, it will be shown that such annealing, at 200°C, has a significant smoothing effect on the material interfaces. Finally, these changes in material properties are linked to significant improvement in multiple key performance indicators for transistor devices with a top gate, coplanar device structure. This work represents both guidance for device fabrication, and an enhancement in understanding of physical behaviour of such devices that will help push forward this rapidly growing sphere of research and engineering.

[1] D. Gamota, M. Joyce, A. Schaller, & J. Zhang, In iNEMI Roadmap 2015, chap. Large Area Flexible Electronics (2015).
[2] J. G. Troughton et al., *Appl. Phys. Lett.* **110** (2017) 011903.

An Easy Method for Oriented Conductive Nanowires Formation on $SrTiO_3(100)$

D. Wrana[1], C. Rodenbücher[2], B. R. Jany[1], J. Rysz[1], K. Szot[2,3], F. Krok[1]

[1]*Marian Smoluchowski Institute of Physics, Jagiellonian Univeristy, Krakow*
[2]*Forschungszentrum Jülich GmbH, Peter Grünberg Institute (PGI-7), Jülich*
[3]*August Chelkowski Institute of Physics, Silesian Univeristy, Katowice*

One of the most promising classes of oxide materials are perovskites ABO_3, with $SrTiO_3$ as a model material. For such ternary oxides it is crucial to control the actual chemical composition during preparation, especially near the surface. E.g. it was found that high mobility two-dimensional electron gas (2DEG) between grown $LaAlO_3$ and $SrTiO_3$ substrate is formed for TiO_2 termination only [lao_sto]. A driving force for the stoichiometry changes is related to oxygen activity – for oxidizing conditions SrO-rich structures are preferred [szot_afm], whereas for oxygen depleted conditions various TiO_x phases evolve [sqr5]. Reduction of $SrTiO_3$ results in d-electrons emergence, improving electronic properties, towards novel applications such as memristive devices fabrication.

We studied the thermal reduction of $SrTiO_3(100)$ single crystals at ultrahigh vacuum conditions. Our approach was holistic – combining crystallographic information (LEED), topography (STM, C-AFM, NC-AFM, SEM) with local work function (KPFM) and conductivity (conductive-AFM). Chemical composition was analysed by SIMS, EDX and EELS measurements, whereas actual atomic arrangements were obtained by HR-STEM.

Controlled reduction provides an easy method of tuning electronic structure of $SrTiO_3$. From conductivity measurements we found out that there is a transition from semiconducting to metallic behaviour on the surface after annealing to 800-900^{o}C. Up to 1000^{o}C the surface is flat, however reconstruction changes. Above a threshold temperature, phase segregation occurs and crystalline TiO nanowires of micrometer length are formed. The thickness of the nanowires increased with temperature following an Arrhenius behaviour, indicating that the underlying diffusion process is activated with temperature. Nanowires have a few orders of magnitude better conductivity than the rest of the surface and higher work function by as high as 0.8 eV. Unlike the reduced $SrTiO_3$ surface, nanowires are indifferent to ***in situ*** pure oxygen exposure.

SIMS measurements show that the surface is depleted by Sr (nanowire region) but no Sr segregation towards the bulk was observed. A lamella was cut by FIB in the nanowire region and analysed by HR-TEM. It could be seen that the nanowire consists of TiO in a rocksalt structure, however surface betweent them is still $SrTiO_3(100)$. On the nanowire/$SrTiO_3$ interface there is a small region with valence +3 as seen by EELS indicating an additional interfacial phase.

Due to their stability, electronic properties and epitaxial growth, the created nanowires may have technological potential as micro-nanoscale electrodes, substrate for selective thin films growth or for catalytic applications.

[1] A. Ohtomo, and H. Y. Hwang, *Nature* **427**(6973) (2004) 423-426.
[2] K. Szot, and W. Speier, *Physical Review B* **60**(8) (1999) 5909.
[3] David T. Newell et al., *Physical Review B* **75**(20) (2007) 205429.

Growth and Characterization of $Ca_3Y_2(BO_3)_4$:Er,Yb Laser Crystal

L.V. Gudzenko[1], M.B. Kosmyna[1], A.N. Shekhovtsov[1], K.N. Gorbachenya[2], V.E. Kisel[2], A.S. Yasukevich[2], N.V. Kuleshov[2], W. Paszkowicz[3], A. Sulich[3], J.Z. Domagała[3]

[1]Institute for Single Crystals NAS of Ukraine, 60 Nauki Ave., Kharkov, Ukraine
[2]Center for Optical Materials and Technologies, Belarusian National Technical University, 65 Nezavisimosti Ave., Minsk, Belarus
[3]Institute of Physics, PAS, 32/46 Aleja Lotników, Warsaw, Poland

1.5 μm lasers are of great interest for several industrial applications: laser range-finding, environmental sensing, telecommunication due to eye-safety, high transparency in atmosphere, low losses and minimal value of the group velocity dispersion in fused-silica waveguides. Binary borate $REAl_3(BO_3)_4$:Er,Yb (RE=Y, Gd, Lu) crystals are promising materials for the gain media. Efficient continuous-wave and Q-switched lasing operations were demonstrated [1]. But these compounds have incongruent melting and can be grown only by TSSG technique [2]. This peculiarity significantly limits the application of the crystals. Thus the search for the 1.5 μm gain media which could be produced by direct crystallization from melts is actual task. This report is devoted to the crystal growth by the Czochralski technique and characterization of pure and Er,Yb-doped $Ca_3Re_2(BO_3)_4$ single crystals.

Pure and Er,Yb-doped $Ca_3Y_2(BO_3)_4$ single crystals were grown by the Czochralski method using an automated and equipped with a weight control system “Kristall 3M” puller. The growth processes was carried out in argon from Ir crucible. The crystal and defect structure were characterized. Volumetric chemical methods without prior separation of the components were developed and applied for the determination of the dependence of chemical compositions of the crystals on the growth conditions. Powder XRD technique was used for the study of crystal structure and characterization of defects in the crystals.

Polarized spectroscopic properties of the doped crystal were studied at room temperature. Polarized absorption spectra manifested a weak anisotropy of absorption properties. A strong absorption band corresponding to $^2F_{7/2} \rightarrow {}^2F_{5/2}$ transition of Yb^{3+} ions in $Ca_3Y_2(BO_3)_4$:Er,Yb crystal was centered at 976 nm, with the maximal absorption coefficient of 6.8 cm^{-1} for light polarization E//*b*. The luminescence decay time of $^4I_{13/2}$ erbium level was measured to be of 580 μs. The measured lifetime was significantly shorter than that calculated from the Judd–Offelt analysis (2.41 ms [3]). The luminescence quantum yield for the $^4I_{13/2}$ manifold of $Ca_3Y_2(BO_3)_4$:Er,Yb crystal was estimated about 24%. Thus $Ca_3Y_2(BO_3)_4$:Er,Yb crystal are expected to be suitable for application as gain medium for diode pumped 1.5 μm lasers.

[1] K.N. Gorbachenya et al, *Opt. Lett.* **41**(5) (2016) 918.
[2] V.V. Maltsev et al, *J. of Crystal Growth* **401** (2014) 807.
[3] B. Wei et al, *Materials Research Innovations* **11(**3) (2007) 154.

3D Computer Models of the Ag-{In, Sb}-Sn T-x-y Diagrams

V. Lutsyk[1,2], V. Vorob'eva[1]

[1]*Institute of Physical Materials Science, Siberian Branch of Russian Academy of Sciences, Ulan-Ude, Russia*
[2]*Buryat State University, Ulan-Ude, Russia*

The universal description of all phase transformations within the ternary system can be obtained by its T-x-y diagram 3D computer model [1,2]. All available data are analysed before the model construction. Usually this information is limited by binary systems, x-y liquidus projection, table of phases compositions, participated in the invariant reactions, by several isothermal sections and isopleths [3-6]. Further a scheme of the uni- and invariant states is constructed. This modernized Sheil' scheme is the excellent tool for "the conclusion" of the description of the T-x-y diagram geometric structure in the tabular, and then in the 3D form. It occurs, with the aid of this scheme, in the system Ag-In-Sn that, besides mentioned one peritectic, five quasi-peritectic and one eutectic invariant transformations [3,7], one eutectoid and six quasi-peritectoid transformations take a place thanks to tin's allotropy in the sub-solidus. The 3D scheme of uni- and invariant states is the base of the T-x-y diagram, which contains only three-phase regions (ruled surfaces) and isothermal (horizontal) planes, corresponding to invariant transformations. The unruled surfaces of liquidus, solidus, solvus etc finalize the T-x-y construction. Thus, the 3D model of the Ag-In-Sn T-x-y diagram contains from the crystallization beginning to 0^{o}C 251 surfaces and 85 phase regions. Final 3D model after the refinement of the curvature of unruled surfaces is possible to visualize in axonometric and x-y projection, on any iso- and polythermal sections, and to obtain also the results of the calculations of the mass balances for any concentrations at any temperature [1].

In the case of essential divergences in the data of the different authors a 3D model is conveniently used for the results verification and for the resolving of the questionable moments [2]. For example, the binary compound Sb_2Sn_3 both in the Ag-Sb-Sn T-x-y diagram, represented in [5,6], and in [8], exists at temperatures up to 0^{o}C. However this compound is decomposed at 242.4^{o}C in [3,9]. Its existence is limited by the same temperature in the analogous system Ni-Sb-Sn [4] too. Therefore the 3D model is designed in two versions. The first one corresponds [5,6,8], where the polymorphous transfer of allotropies is passed as the eutectoid reaction, and the 3D model consists of 99 surfaces and 62 phase regions. In the different version, constructed according to [3,9], one additional eutectoid reaction precedes the polymorphous transformation, and the 3D model consists of 109 surfaces and 66 phase regions. Consequently, the conditions for the compound Sb_2Sn_3 existence require additional experimental study.

Acknowledgements. This work has been performed under the program of fundamental research SB RAS (project 0336-2016-0006), and was partially supported by the RFBR projects 15-43-04304, 17-08-00875 and the RSF project 17-19-01171.

[1] V.I. Lutsyk, V.P. Vorob'eva, *Russ. J. Inorgan. Chem.* **61** (2016) 188.
[2] V.I. Lutsyk, V.P. Vorob'eva et al., *Russ. J. Inorgan. Chem.* **61** (2016) 858.
[3] *Atlas of Phase Diagrams for Lead-Free Solders* compiled by A. Dinsdale, A. Watson et al., COST 531. ESF, Brno, Czech Rep.: Vydavatelstvi KNIHAR, Vol. 1, 2008.
[4] *COST MP0602-Handbook of High-Temperature Lead-Free Solders: Atlas of Phase Diagrams* compiled by A. Dinsdale, A. Kroupa et al., Vol. 1, 2012.
[5] S.-W. Chen, P.-Y. Chen, H.-J. Wu et al., *Metall. Mater. Trans. A.* **39** (2008) 3191.
[6] W. Gierlotka, Y.-C. Huang, S.-W. Chen, *Metall. Mater. Trans. A.* **39** (2008) 3199.
[7] X.-J. Liu, Y. Inohana, Y. Takaku et al., *J. Electron. Mat.* **31** (2002) 1139.
[8] S.-W. Chen, C.-C. Chen, W. Gierlotka et al., *J. Electron. Mat.* **37** (2008) 992.
[9] A. Kroupa, J. Vizdal, *Defect and Diffusion Forum* **263** (2007) 99.

Hafnium Oxide as Efficient Material for a New Generation Dielectric

A.P. Mukhachov[1], O.A. Kharitonova[2], O.A. Terentieva[2]

[1]*Chemical Technology of AISU, Kamyanske, Ukraine*
[2]*Dniprodzerzhinsk State Technical University, 2 Dniprobudivska Str., 51900 Kamyanske, Ukraine*
* *eah@ukr.net*

In the early 2000-ies, world leaders in the field of computer engineering, such companies as IBM, Intel and Samsung Electronics announced the development of a new technology for the production of boards based on multilayer films "HfO_2-Al_2O_3" on a silicon pad using the method of atomic layer deposition (ALD) [1]. The board has a high dielectric constant value thus making it possible to produce smaller transistors with increased operational speed, to reduce leakage current and electric energy consumption. It has been known that hafnium oxide is used in the production of optical devices, resistors, electronic ceramics, neutron absorption compositions and catalysts. High purity of material is one of key conditions for its application. As source material, hafnium concentrate was used that was enriched to 10% in the form of $K_2(ZrHf)F_6$ salt – the product of fractional crystallization of zirconium and hafnium fluorides in the production of zirconium for nuclear applications. Another source material is a HFO2 commercial-grade hafnium oxide produced at Vilnogorsk Mining and Smelting Works. Key process stages are fusion with alkali at a temperature of 800°C, dissolution in nitric acid and extraction. The impurities content of resultant hafnium re-extract is 10-5% (mass). The prime objective of the process technology is the preservation of hafnium purity in its oxide production, which is attained by the application of materials and equipment items having a high corrosion resistance, such as stainless steel, crucibles made of high-purity silicon, reaction vessels made of zirconium and fluoroplastic. Centrifugal extractors [2] allow the key critical process of hafnium extraction purification to be sufficiently effective, resulting in obtaining the product of a required 99.99% purity. Physical properties of hafnium oxide are presented in sufficient detail in [3]. Hafnium oxide can by produced using various methods to be selected based on the requirements to product quality, process efficiency and cost considerations.

[1] G. Resnik, Technology on the Verge; Metally Mira, *International Review* **12**(48), December 2002.
[2] G.I. Kuznetsov, A.A. Pushkov, A.V. Kosogorov, *Centrek Type Centrifugal Extractors*, M. 2000, 216 p. (in Russian).
[3] I.A. Shcheka, K.F. Karlysheva, *Chemistry of Hafnium*, Naukova Dumka, Kiev, 1973 (in Russian).

Growth and Characterization of Titanium Doped Spinel Crystals

V.T. Gritsyna[1], Yu.G. Kazarinov[2], V.A. Kobykov[1], L.A. Lytvynov[3]

[1]*V.N. Karazin Kharkiv National University, 4 Svoboda Sq., 61022 Kharkiv, Ukraine*
[2]*NRC "Kharkov Institute of Physics and Technology", 1 Akademicheskaya Str., 61108 Kharkiv, Ukraine*
[3]*Institute for Single Crystals of NAS of Ukraine, 60 Nauky Ave., 61001 Kharkiv, Ukraine*

Recently there appear the interest for growth and investigation of properties of titanium doped magnesium aluminates spinel (Ti:MAS) crystals for possible laser application [1-3]. It was turned out that the optical properties of grown crystals are depended on the growth conditions. Grown by Verneuil method Ti:MAS crystals demonstrates absorption bands at 790, 490 nm and strong absorption in UV range. In absorption spectra of crystals grown by micro-pulling-down method Ti:MAS of different titanium concentration also three bands were observed [2]. But crystals grown using the floating zone method under oxidizing atmosphere have no absorption bands except UV-range [3]. The luminescence properties of grown crystals are also different. In this paper we have grown Ti:MAS crystals doped with titanium at concentration 0.1 – 0.5 mass% using Verneuil method which were non-uniformly colored in bluish and investigated optical properties.

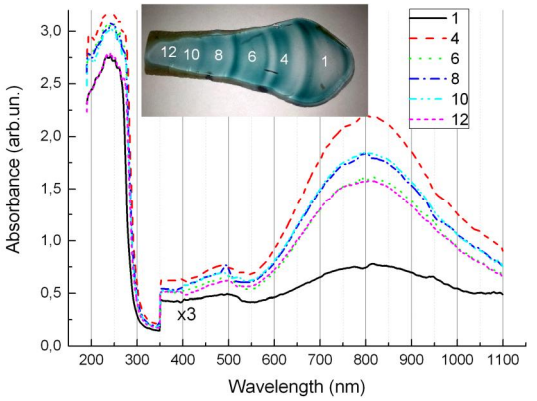

Fig. 1. Cross section view of Ti:MAS crystals doped with titanium 0.2 mass%

The crystals sizes of 30-40 mm in length and about 20 mm in width were obtained at growth rate about 20 mm per hour. The measured lattice parameter a= 0.7996±0.0004 nm which corresponds to crystal lattice of non-stoichiometric spinel $MgO{\cdot}2.5Al_2O_3$. No variation in spinel composition across the boule was registered. Optical absorption spectra and radio luminescence of Ti:MAS crystals have been investigated in order to find out the nature of bluish coloration in obtained crystal. The absorption spectra of spinel crystals doped with titanium contains strong and wide band of maximum at 800 nm, low intensity asymmetrical band at 480 nm. In the UV range a strong absorption edge arising from 300 nm is observed and red shift of this edge increases with growth of titanium concentration. There was registered the correlation of the red shift with intensity of optical absorption band at 800 nm. No variation of titanium atoms concentration measured by X-ray fluorescent analysis along the crystal growth direction was observed, Also, the variation of optical absorption band at 800 nm is correlated to content of iron atoms. The measurement of absorption spectra of Ti:MAS crystals intentionally irradiated with X-rays and/or UV light allow us to distinguish several absorption bands in UV-range related to presence of titanium ions.

[1] L.E. Bausa, I. Vergara, J. GarsiaSole, W. Strek, P.J. Deren, *J. Appl. Phys.* **68** (1990) 736-740.
[2] A. Jouini, H. Sato, A. Yoshikawa, T. Fukuda, *J. Mat. Res.* **21** (2006) 2337-2343.
[3] T. Sato, M. Shirai, K. Tanaka. Y. Kawabe, E. Hanamura, **114** (2005) 155-161.

Growth and Investigation of Colorless Lithium Tantalate Single Crystals for Optoelectronics

I. Solskii[1], D. Sugak[1,2], I. Groshovyj[1], Ye. Kapeliuh[1], V. Hajduchok[1,2], B. Kopko[1,2], M. Vakiv[1,2], V. Gaba[2], S. Ubizskii[2]

[1]*Scientific Research Company "Carat", Lviv, Ukraine*
[2] *Lviv Polytechnic National University, Ukraine*

Lithium tantalate ($LiTaO_3$, LT) ferroelectric single crystal is isostructural to lithium niobate ($LiNbO_3$, LN) crystal and has properties similar to it. Despite a number of advantages compared with LN (higher temperature stability of properties, higher electro-optical coefficients values, etc.) usage of LT is not so extensive as LN. This occurs particularly due to the higher melting temperature (T_m = 1650 ^oC) and significantly lower Curie temperature (T_C ~ 660 ^oC).

Because of the relatively high T_m the growth of LT crystals is carried out usually in the Pt-Rh crucible. But Rh, entering into the crystal causes formation of color centers which result in LT becomes dark brown. For use in acoustoelectronic color of LT does not a matter but for use in acoustooptics or electrooptics elements made of crystal must have high transparency in the visible range of the spectrum. This problem can be solved if the LT growth process occurs in the Ir crucible. The paper presents results of experiments on growing $LiTaO_3$ from iridium crucibles and further study of obtained crystals.

High purity powder raw materials were used for the $LiTaO_3$ growing. Powder was pressed in tablets before loading into the crucible. Growth was carried out by the Czochralski method on Physiterm (France) fasilities. Special thermal unit was designed to provide the necessary temperature distribution field and as well as its gradient. The growth was carried out on oriented seed in X, Y and Z crystal directions. Optimal crystal pulling and rotation rates during crystal growth were determined.

As a result, single crystals with diameter of 60 mm and 60 mm length were obtained. Grown crystals were annealed in air at 1200 °C for 24 hours. The procedure monodomainization of the single crystal was performed in an external electrical field at temperature about 700 °C using platinum electrodes. Single domain state checking was carried out by optical methods.

Active element for acousto-optical, electro-optical and acoustoelectronic devices were made from single domain crystal. Crystal machining modes and characteristics of the treated surfaces are established. Their optical homogeneity was investigated. Optical absorption spectra of crystals were registrated including OH groups region. Antireflection coating structures on certain wavelengths for LT optical elements were calculated. It was concluded that $LiTaO_3$ grown crystals are quite suitable for manufacturing optoelectronic components.

This work performed in the frames of State Order of Ukraine and partially supported by DB/EMSh project of Ukrainian Ministry of Education and Science.

The Effect of Growing Conditions and Thermal Treatment on Luminescent Properties of $CaWO_4$ Crystals

Ya.M. Zakharko[1], I.M. Solskii[2], A.P. Luchechko[1], D.Yu. Sugak[2,3]

[1]*Ivan Franko National University of Lviv, Ukraine*
[2]*Scientific Research Company "Carat", Lviv, Ukraine*
[3]*Lviv Polytechnic National University, Ukraine*

Calcium tungstate crystals are one of the most widely used phosphors due to their excellent luminescent properties, in particular, strong visible luminescence, high light yield as well as high resistance to external environmental influences. Moreover, $CaWO_4$ is perspective material for lasers, acousto-optic components or scintillators [1, 2]. However, spectroscopic and physical characteristics of $CaWO_4$ can vary significantly depending on a difference in the quality of samples. It should be noted also, the presence of a strong afterglow emission component quite often undermines $CaWO_4$ use.

Single crystals were grown by the Czochralski technique from raw materials having purities of 99.99%. The excitation and luminescence spectra of different kind of $CaWO_4$ single crystals were investigated at room temperature.

The $CaWO_4$ single crystals exhibit a strong luminescence emission in the wavelength range of 350-650 nm with X-ray and UV excitations. The position of this band maximum varies from 450 to 520 nm for crystals of different origin. Accordingly, the luminescence intensity and band position of phosphors depend strongly on the starting materials of which are single crystals grown.

The maxima of elementary emission bands, as well as half-widths, were determined. It was established also, that the type of crystals, as well as the excitation wavelength, affect the relative intensity of elementary emission bands.

Measured emission spectra at high energy excitations, in particular, more than 4.9 eV, are mainly attributed to the charge-transfer transitions within the $[WO_4]^{2-}$ anion complex and is interpreted as an emission of self-trapped excitons. The relative intensity of the long-wavelength luminescence band, attributed to the emission of structural defect of the lattice, for example, oxygen-deficient WO_3 complex, in $CaWO_4$ crystals, increases at low energy excitations (4.2-4.4 eV). The nature of the additional luminescence band located between two the above-mentioned is under discussion.

The mechanism of afterglow emission in $CaWO_4$ crystals also is investigated by means of X-ray luminescence and thermally stimulated luminescence (TSL). It was established, that decreasing of the afterglow intensity is accompanied by a lowering of the deep traps concentration.

The influence of annealing in an oxygen atmosphere on luminescent properties of $CaWO_4$, including the relative intensity of elementary emission bands as well as afterglow emission, was also investigated.

[1] D. Spassky, V. Mikhailin, M. Nazarov, M.N. Ahmad-Fauzi, A. Zhbanov, *Journal of Luminescence* **132** (2012) 2753–2762.
[2] V. Yakovyna, Ya. Zhydachevskii, V.B. Mikhailik, I. Solskii, D. Sugak, M. Vakiv, *Optical Materials* **30** (2008) 1630–1634.

Growth and Optical Properties of Ce^{3+} Doped $Y_{3-x}Ca_xAl_{5-x}Si_xO_{12}$ Single Crystalline Films

A. Iskaliyeva[1], V. Gorbenko[1], T. Zorenko[1], K. Paprocki[1], K. Fabisiak[1], S. Dolasiński[1], A. Fedorov[2], F. Schröppel[3], E. Levchuk[3], A. Osvet[3], M. Batentschuk[3], Yu. Zorenko[1]

[1]*Institute of Physics, Kazimierz Wielki University in Bydgoszcz, 85090 Bydgoszcz, Poland*
[2]*SSI Institute for Single Crystals, National Academy of Sciences of Ukraine, 60 Nauki Ave., 61178 Kharkiv, Ukraine*
[3]*Institute of Materials for Electronics and Energy Technology (i-MEET), Department of Materials Science and Engineering VI, University of Erlangen-Nürnberg, 91058 Erlangen, Germany*

In this work, we present for the first time results on crystallization and investigation of the structural and optical properties of luminescent materials based on the single crystalline films (SCFs) of Ce^{3+} doped solid solution of $Y_{3-x}Ca_xAl_{5-x}Si_xO_{12}$ garnet where x=0-0.55. The SCFs were grown by the liquid phase epitaxy (LPE) method onto $Y_3Al_5O_{12}$ (YAG) substrates from the super-cooling melt–solution based on the $PbO-B_2O_3$ flux. The absorption, luminescence and scintillation properties of $Y_{3-x}Ca_xAl_{5-x}Si_xO_{12}$:Ce SCFs at x=0-0.55 were compared with the properties of the reference YAG:Ce SCF sample. The influence of the thermal annealing at 1000 ^oC and 1300 ^oC in 95% N_2 - 5% H_2 reducing atmosphere on the optical properties of $Y_{3-x}Ca_x\ Al_{5-x}Si_xO_{12}$:Ce SCFs was investigated as well. The results of this research can be useful for the development of luminescent materials for white LED converters, scintillators and cathodoluminescent screens based on the epitaxial structures of Ca^{2+}-Si^{4+} containing garnets, grown by LPE method onto undoped or doped substrates of garnet compounds.

Acknowledgements. The work was performed in the NANOLUX2014 No 286 and framework of NCN 2016/21/B/ST8/03200 projects.

Comparison of the Luminescent Properties $Y_3Al_5O_{12}$:Pr Crystal and Single Crystalline Film under Synchrotron Radiation Excitation

Yu. Zorenko[1,2], T. Zorenko[1,2], V. Gorbenko[1,2], S. Nizankovskiy[3]

[1]*Institute of Physics, Kazimierz Wielki University in Bydgoszcz, 85-090 Bydgoszcz, Poland*
[2]*Department of Electronics, Ivan Franko National University of Lviv, 79017 Lviv, Ukraine*
[3]*Institute for Single Crystals, National Academy of Sciences of Ukraine, 61001 Kharkiv, Ukraine*

Pr-doped $Y_3Al_5O_{12}$ (YAG:Pr) garnet, apart from their applications in single crystal (SC) form, attract also an attention as the single crystalline film (SCF) cathodoluminescent screen in the UV emitting electron beam tubes in optical scanning microscopes [1]. Properties of these materials are strongly influenced by the differences in the methods and conditions of their preparation. The aim of our report is to compare the luminescent properties of YAG:Pr SC and SCF using synchrotron radiation (SR) excitation. The YAG:Pr SC were grown by the horizontal direct crystallization method at 1930^{o}C. The YAG:Pr SCF were prepared by the liquid phase epitaxy (LPE) method from melt-solutions based on the $PbO-B_2O_2$ flux in air atmosphere onto YAG substrates at temperatures 960-1000^{0}C.

Luminescent and scintillation properties of the YAG:Pr SCF were recently compared with those of reference SC using the traditional spectral methods (absorption, cathode- and photoluminescence and light yield (LY) measurements under excitation by α–particles) [2]. We found that the emission spectra and decay kinetic of YAG:Pr SCF due to the $5d_1$-4f transition of Pr^{3+} ions are different in comparison with SC counterparts due to (i) the presence of Y_{Al} antisite defects as emission centers in UV range and trapping centers in the case of SC, growth from the melt at high temperatures; (ii) the strong influence of Pb^{2+} flux related dopants in the case of YAG:Pr SCF, grown from PbO based flux at significantly lower temperatures.

Using the time-resolved luminescent spectroscopy of YAG:Pr SC and SCF under excitation by SR at Superlumi station at HASYLAB at DESY at 10 K, we exactly determined the positions of the Pr^{3+} 5d energy levels in YAG host and estimated the differences in the energies of creation of excitons bound with the isolated Pr^{3+} ions in YAG:Pr SCFs and dipole Pr-Y_{Al} AD center in SC counterpart. We also found the notable differences in the excitation spectra and luminescence decay kinetics of YAG:Pr SC and SCF caused by the involving of the antisite defects and oxygen vacancies in SC and Pb^{2+} flux related dopant in SCF in the excitation processes of Pr^{3+} luminescence in YAG hosts.

Acknowledgements. The work was performed in the frameworks of Polish NCN 2016/21/B/ST8/ 03200 project and Ministry of Education and Science of Ukraine in frame of SF-20F project.

[1] Yu. Zorenko, L. Limarenko, I. Nazar, M. Pashkovskii, *Journal Applied Spectroscopy* **55** (1991) 1100.
[2] V. Gorbenko, Yu. Zorenko, V. Savchyn, T. Zorenko et al., *Radiation Measurements* **45** (2010) 461.

$Na_{0.5}Bi_{0.5}TiO_3$ Thin Films on Substrates with Different Structure

T. Kruzina, S. Popov, Yu. Potapovich, M. Trubitsyn, A. Rutskiy, M. Koptev

Oles' Honchar Dnipropetrovsk National University, 72 prosp. Gagarina, 49010 Dnipropetrovsk , Ukraine

Polycrystalline thin films of $Na_{0.5}Bi_{0.5}TiO_3$ (NBT) [1] demonstrate good parameters (P_r=12 μC/cm^2, d_{33}=60-90 Pm/V) that shows prospects for the further development of technology. Researches performed earlier show strong influence of the substrate properties on the structure and electro physical properties of NBT thin films.

In the abstract we report influence of substrate on the structure of NBT thin films deposited by RF magnetron sputtering and synthesized by ex-situ method. NBT films were deposited in Ar/O_2 mixture (1:1) atmosphere (chamber pressure 10 mTorr) on fused quartz and Si(100) substrates which were initially annealed at T=700^{0}C in air for 1 hour. During the deposition process the substrate temperature was kept at T=250^{0}C. Deposited thin films were synthesized by annealing in air for 1 hour at temperature T=700^{0}C. The XRD patterns show presence of NBT structure for both (amorphous quartz and crystalline Si(100)) substrates. Pattern of NBT deposited on quartz shows NBT peaks in their correct positions [2]. Besides there are reflexes from $Bi_4Ti_3O_{12}$ (BiT) structure showing two-phase composition of the films deposited. Taking into account amorphous state of the quartz substrate, the probabilities of generation of these two phases are nearly equal.

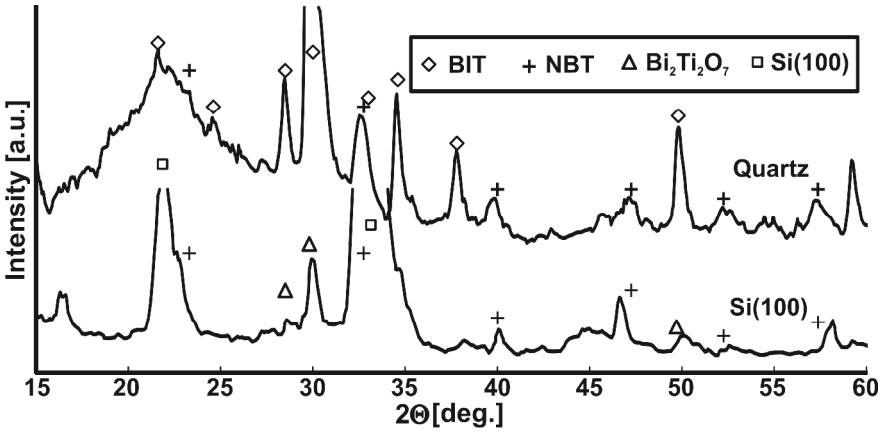

Pattern of NBT deposited on the Si(100) substrate also shows that the films have two-phase composition, but in this case additional phase is pyrochlore, presumably $Bi_2Ti_2O_7$. For this substrate portion of NBT phase is visibly increased. According to Frank–van der Merwe theory [3] pseudo-morphological states should not appear as far as the lattice parameters of substrate and NBT differ each other for more than 15% and NBT films should be formed according to the misfit dislocation model. However, the XRD pattern shows that the NBT peaks are shifted from their correct positions and thus pseudo-morphological states are present. Details of the mechanisms of films structure formation are discussed.

[1] S. Quignon, C. Soyer, and D. Remien, *Am. Ceram. Soc.* **95** (2012) 3180-3184.
[2] S. Popov et al., *Visnyk Dnipropetrovsk University. Seria Fizika, radioelektronika* **23**(24), 100.
[3] J.H. van der Merwe, *Single-crystal films*, Mir, 1996, pp. 172-201 (in Russian).

Electrical Properties of the MIS Structures Based on MBE HgCdTe with SiO_2/Si_3N_4 and Al_2O_3 Insulating Layers

I. Izhnin[1], A. Voitsekhovskii[2], S. Nesmelov[2], S. Dzyadukh[2], G. Sidorov[3], V. Varavin[3], V. Vasil`ev[3], S. Dvoretsky[3], N. Mikhailov[3], M. Yakushev[3]

[1]*Scientific Research Company "Carat", Lviv, Ukraine*
[2]*National Research Tomsk State University, Tomsk, Russia*
[3]*Rzhanov Institute of Semiconductor Physics SB RAS, Novosibirsk, Russia*

$Hg_{1-x}Cd_xTe$ (MCT) solid solutions have remained the basic material for the fabrication of highly effective photodetectors operating in the infrared part of the spectrum (2.5–20 μm) due to dependence of band-gap on the composition *x* (the CdTe content) [1]. Developing large–area HgCdTe/Si(GaAs) structures is one of the key issues in modern HgCdTe molecular-beam epitaxy (MBE) growth technology. The method provides the possibility of growth MCT films with a given thickness distribution of composition. Creation of near-surface graded-gap layers with high content of CdTe allow to improve the working performances of detectors based on MCT by reducing the effect of surface recombination on the lifetime of charge carriers in the semiconductor bulk [2].

An important practical problem in the development of highly sensitive infrared detectors based on MCT is the choice of an optimal passivation coating [3]. Properties of MIS structures based on graded-gap MBE *n*-$Hg_{1-x}Cd_xTe$ with double-layer low-temperature plasma-chemical insulator SiO_2/Si_3N_4 have been studied in detail by authors [4]. However, passivation on high-aspect-ratio HgCdTe mesa array detectors produce a new challenge for the traditional thin-film deposition technologies such as physical vapor deposition and chemical vapor deposition. Low-temperature plasma-enhanced atomic layer deposition (PE ALD) of aluminium oxide (Al_2O_3) is the unique technique to overcome these challenges because of its precise control of the film thickness, excellent uniformity, and conformance to a high-aspect-ratio pattern [5, 6].

The aim of this work was an experimental investigation of the properties of MIS structures based on graded-gap MBE *n*(*p*)-$Hg_{1-x}Cd_xTe$ (x=0.22-0.40) with Al_2O_3 and SiO_2/Si_3N_4 insulator and comparative analysis of their characteristics. The report presents the results of studies of the admittance of these MIS structures in the test signal frequency range 1 kHz - 2 MHz at temperatures ranging from 8 to 300 K. It was revealed that MIS structures with Al_2O_3 have a large enough insulator capacitance (compared to SiO_2/Si_3N_4), a significant modulation of capacitance on the CV characteristics, high dielectric strength and low values of the flat-band voltage. The effective charge density found from the value of the flat-band voltage and slow interface trap density for structures with Al_2O_3 comparable with the corresponding densities for structures with SiO_2/Si_3N_4.

Acknowledgements. The work was financially supported by RFBR and the Administration of Tomsk region as a part of the research project p_a No. 16-42-700759.

[1] A. Rogalski, *Infrared detectors*: *2nd. ed.*, CRC Press, Taylor & Francis Group, New York, 2011, p. 876.
[2] S. Dvoretsky, N. Mikhailov, Y. Sidorov et al., *J. Electron. Mater.* **39** (2010) 918.
[3] R. Singh, A.K. Gupta, K.C. Chhabra, *Defence Science J.* **41** (2013) 205.
[4] Y. Nemirovsky, I. Bloom, *J. Vac. Sci. Technol. A* **6** (1988) 2710.
[5] A.V. Voitsekhovskii, S.N. Nesmelov, and S.M. Dzyadukh, *Thin Sold Films* **522** (2012) 261.
[6] R. Fu, J. Pattison, *Optical Engineering* **51** (2012) 104003.
[7] P. Zhang, Z. Ye, C. Sun et al., *J. Electron. Mater.* **45** (2016) 4716.

Improving the Efficiency of Heat Transfer through Thermal Interfaces with Aluminum Nitride Films

E.M. Rudenko[1], I.V. Korotash[1], A.A. Krakovny[1], D.Yu. Polotskiy[1], A.V. Suvorov[1], M.A. Belogolovskii[1], V.V. Chmil[2]

[1]G.V. Kurdyumov Institute for Metal Physics, 03028 Kyiv, Ukraine
[2]PJSC NPP "Saturn", 03148 Kyiv, Ukraine

The trend towards miniaturization of electronic devices and simultaneous increase of microelectronics packaging density results in a large amount of heat generated during their operation. To reduce the thermal contact resistance between a silicon chip, the heat source and a substrate of integrated circuits, the heat sink is one of the main tasks at the moment. The same problems are actual also for different electrical appliances like, for example, light emitting diodes (LEDs). In this work, we propose aluminum nitride as an efficient thermal interface material and prove it with experiments performed on high power LEDs where the overheating has significant impact on their lifetime and performance.

Replacement of some traditional dielectric layers with high thermal conductive AlN thin films has already improved thermal management in some electrical devices. Moreover, good thermal conductivity is not a sole advantage of this material. AlN is a wide-band-gap semiconductor with such unique properties as high value of surface acoustic velocity, high hardness, and very good electrical insolation. These characteristics can be useful for different applications as well.

To obtain AlN films on various substrates, an original combined ion-plasma facility based on helicon and magnetic-filtered arc plasma sources was used. 3W LEDs were mounted on 1.4-1.6 mm thick aluminum plates of the 200-260 mm^2 area. The plate thickness was about 1.4-1.6 mm. LEDs were installed in two ways, on a conventional metal substrate with a thermal grease and on that coated with aluminum nitride (mounted with a hot adhesive at high pressures). A family of current-voltage curves was recorded in the oven at various temperatures from 30^0 C to 120^0 C with a half-second duration of the sweep current. After that a 20 sec. load current of 300 and 550 mA was warming the LEDs. Then immediately the current-voltage curves were measured with a current pulse of the 0.5 sec. duration. Two representative figures for different LED installations are shown, the upper one corresponds to a standard installation way while the lower one was obtained with the AlN interlayer. If we compare current-voltage characteristics of currently loaded LEDs with heated ones, we can see that the LED mounted directly on a metal substrate (with a thermal grease) is strongly heated and the temperature is increasing to 60-70^0 C for a load current of 550 mA. At the same time, such a load current almost no heats the LED mounted on an AlN coated substrate.

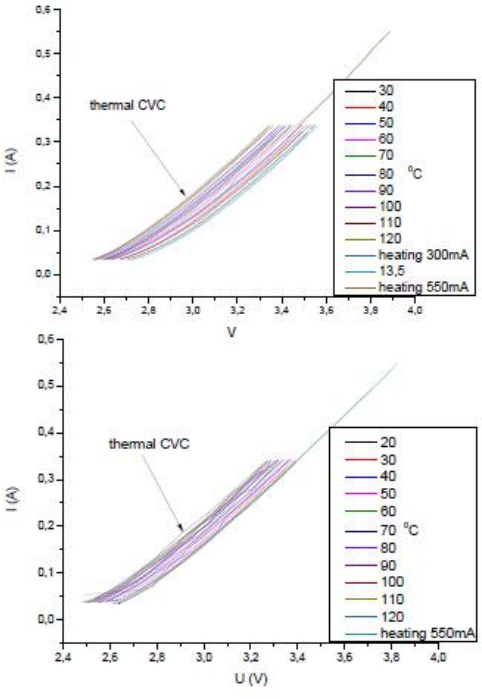

The overall observations indicate that AlN is a very perspective thermal-interface material for electronics applications.

The Increase in Thermal Stability of Anodic Alumina Films on Aluminum

V. Shulgov

Belarusian State University of Informatics and Radioelectronics (BSUIR)

Thermal stability of the "aluminum – anodic alumina film (AAF)" system for the oxide films formed in the surfactant-containing electrolytes is discussed.

Anodized aluminum is widely used in microelectronics to produce switching plates, multiterminal VLSI packages, multichip modules, various sensors, etc. [1]. One of the factors limiting the wide use of aluminum substrates coated with the Al_2O_3 films is low thermal stability of the "Al – AAF" system due to differences in the linear thermal expansion coefficients of aluminum ($\alpha_{Al} = 23 \cdot 10^{-6}$ K^{-1}) and alumina ($\alpha_{ox} = 5 \cdot 10^{-6}$ K^{-1}).

A number of technical solutions allowing improving thermal stability of the "Al – AAF" system such as a thermal annealing to 477 K, anodizing in different electrolytes followed by pore filling with pyrolytic Al_2O_3, etc. is known. However, these methods lead to an increase in the process duration and are not always effective.

A high voltage anodizing of aluminum porous was found on the basis of the theoretical analysis and electron-microscopic studies to be one of the possible ways for reducing the level of thermal stresses in the aluminum – anodic alumina system. The two-stage anodization was used. First, a low-voltage anodization of aluminum substrate was carried out, then the anodizing electrolyte was changed and the aluminum substrate was anodized at high anodizing voltages. The choice of the electrolyte for the second anodizing stage is very important at that.

The 1.5 mm thick aluminum substrates made of commercially available alloy AMg-2 were used. The anodization was performed in three types of electrolytes, namely: 2% oxalic acid, 1% citric acid, and 4% phosphoric acid with the addition of triethanolamine. The study of the thermal stability of the "Al – AAF" system was made by measuring the bending deflection under heating.

The stress calculation was carried out according to the formula [2]:

$$s = \frac{(a_{Al} - a_{ox}) \cdot \Delta T}{h_0 (1-n)\left(\frac{1}{E_0 h_0} + \frac{1}{E_2 h_2}\right)}$$

where a_{ox} and a_{Al} are the linear thermal expansion coefficients of aluminum and alumina; n is the Poisson's ratio of the substrate; DT is the increment of temperature; E_0 is the Young's modulus of the alumina; E_2 is the Young's modulus of aluminum; h_0 and h_2 are the thicknesses of the film and substrate correspondingly.

As was revealed, the sequential anodizing of aluminum first in the oxalic acid electrolyte and further in the electrolyte of phosphoric acid with the addition of triethanolamine at 200 V allows the stress at the "Al – AAF" interface resulting from the high temperature treatments to be reduced significantly. This can be explained by the presence of a plastic deformation zone at the Al – AAF interface, where the stress relaxation takes place.

[1] V. Sokol, V. Shulgov, Electrochemical Aluminium Oxide Technology for Production of Electronics, *Proceedings of International Conference on Oxide materials for electronic engineering – fabrication, properties and application*, OMEE-2012, Lviv, Ukraine, 2012, pp. 55-56.

[2] D.H. Bradhurst, J.S.L. Leach, The mechanical properties of thin anodic films on aluminum, *J. Electrochem. Soc.* **113** (1966) 1245-1249.

The Effect of Deposition Temperature, Flux of N_2 and Sputtering Power on Si/SiO/NbN Superconducting Thin Films

A. Altinkok[1,2], Y. Takamura[2,3,4], Rafael S. Goncalves[5], Renan P. Loreto[5], Juan P. Cascales[2], H. Zenk[1], Jagadeesh S. Moodera[2]

[1]*Department of Electrical and Electronics, Giresun University, Giresun, Turkey*
[2] *Francis Bitter Magnet Laboratory, Massachusetts Institute of Technology (MIT), Cambridge Massachusetts, United States*
[3] *JSPS, Japan*
[4] *Tokyo Institute of Technology, Japan*
[5] *Federal Univ. of Viçosa, Brazil*

NbN thin films are the good candidate for superconducting integrated devices. The sputter deposition of NbN on Si or SiO is desirable due to its low cost and availability of high volume equipment. In this study, The NbN thin films films have been deposited over Si and buffer layers including oxidized Si by reactive magnetron sputtering. Sputtering of a Nb target in different compositions of Ar/N2 gas was also used for the preparation of NbN superconducting thin films. Influence of various sputtering power, substrate temperatures and Ar/N2 gas ratio was also investigated on the superconducting transition temperature (*Tc*). The results showed that increase in the sputtering power and substrate temperature caused increased on the T_C. Thus optimum values are observed via *R-T* curves and calculation of Residual-resistance ratio RRR values. It is shown that the deposition temperature and the flux of N_2 have a strong effect on the preferred orientation, while the critical temperature of the films is influenced by the quality of the original vacuum. Finally, we found that the conditions for T_C depend primarily on the N and Ar sputter deposition pressures on sputter deposited NbN films.

Acknowledgment. This work was supported by the Scientific and Technological Research Council of Turkey TUBITAK BIDEB-2219 International Postdoctoral Research Scholarship Programme, National Science Foundation (NSF) grant no. DMR-1207469 and Office of Naval Research (ONR) Grant No. N00014-13-1- 0301.

Synthesis and Investigation of Glass-ceramic $Na_4M_{3-x}M'_x(PO_4)_2P_2O_7$ (M, M' - Co, Ni, Mn) for Na^+-Ion Batteries

Ie.V. Odynets, I.V. Zatovsky, and N.I. Klyui

College of Physics, Jilin University, 2699 Qianjin Str., 130012 Changchun, P.R. China

Currently, research and development efforts on sodium-ion batteries (SIBs) those is considered as an alternative to lithium-ion batteries (LIBs) due to their lower cost, environmental friendliness and abundance of sodium in comparison with lithium [1]. As a result, in the last few years the publications of results devoted to various types of Na^+-ion electrodes and conducting electrolytes dramatically increases. In particular, compounds with general formula $Na_4M_3(PO_4)_2P_2O_7$ (M - Co, Ni, Mn) have considerable prospects of practical use as a positive electrode in SIBs, due to significant cyclic stability, providing extended lifetime. The successful technological implementation of such materials is possible if the cost of their fabrication will be lowered. Glass-ceramic technology fully satisfies this requirement to manufacture successfully electrode materials [2]. In this work, we obtained and investigate glass-ceramics based on solid solutions $Na_4M_{3-x}M'_x(PO_4)_2P_2O_7$ (M, M' - Co, Ni, Mn) to optimize technology of SIB production.

Glasses based on $Na_4M_{3-x}M'_x(PO_4)_2P_2O_7$ (M, M' - Co, Ni, Mn) were synthesised by a conventional melt-quenching method. Starting reagents $NaPO_3$, Co_3O_4, NiO and MnO_2 in appropriate stoichiometric ratios were melted in a platinum crucible at 1000-1200 °C for 30-120 min. The melts were quickly poured onto a copper plate. Obtained glasses were subsequently annealed at 300-600 °C, this procedure led to formation of crystalline phases in bulk material. The glass transition and crystallization temperatures were determined by differential thermal analysis (DTA). Further, samples were ground by mechanical milling in a planetary ball mill. In order to confirm glass formation and to characterize crystallized phase, all samples were investigated experimentally by FTIR spectroscopy, X-ray powder diffraction, SEM and TEM analysis. Electrical conductivities of glasses and glass-ceramics were measured by impedance spectroscopy method. Few composites for positive electrode were produced from mixture of glass-ceramic powder with conductive carbon black and conducted electrochemical tests for capacity retention and cyclability.

It was shown that the glass-ceramic technique exhibits good applicability in fabrication of solid solutions of $Na_4M_{3-x}M'_x(PO_4)_2P_2O_7$ (M, M' - Co, Ni, Mn) for subsequent use as cathode active materials for SIBs.

Acknowledgements. Funding: This work was supported by the national long-term project [no. WQ20142200205] of “Thousand Talents Plan of Bureau of Foreign Experts Affairs” of People’s Republic of China.

[1] N. Yabuuchi, K. Kubota, M. Dahbi, S. Komaba, Research Development on Sodium-Ion Batteries, *Chem. Rev.* **114** (2014) 11636-11682.

[2] S. Nakata, T. Togashi, T. Honma, T. Komatsu, Cathode properties of sodium iron phosphate glass for sodium ion batteries, *J. Non-Crystall. Solids* **450** (2016) 109-115.

Glass-Ceramic Formation Tendency for System $LiCoPO_4$-$NaCoPO_4$

I. Zatovsky[1], N. Klyui[1], J. Li[1], N. Strutynska[2], W. Han[1], N. Slobodyanik[2], O. Marchenko[2]

[1]*College of Physics, Jilin University, 2699 Qianjin Str., 130012 Changchun, P.R. China*
[2]*Taras Shevchenko National University, 64/13 Volodymyrska Str., 01601 Kyiv, Ukraine*

Complex phosphates of $LiCoPO_4$ and $NaCoPO_4$ are well known as cobalt redox-active electrode materials in rechargeable lithium or sodium batteries [1]. In addition, this compounds is efficient water oxidation catalyst [2]. The possibilities of formation of solid solutions of general compositions $Li_{1-x}Na_xCoPO_4$ have not been reported so far. Herein, we report glass-ceramic formation tendency and electrical conductivity of lithium-sodium cobalt phosphates are examined for Li/Na-ion batteries.

Starting the melt compositions in this study is $(1-x)Li_2O$-xNa_2O-$2CoO$-P_2O_5 (x = 0, 0.25, 0.5, 0.75 and 1.0). Reagents Li_2CO_3, Na_2CO_3, Co_3O_4 and $(NH_4)_2HPO_4$ in appropriate stoichiometric ratios were melted in a platinum crucible at 1000 °C. The melts were exposed during 1 h at the temperature, and then were poured onto a copper sheet to freeze processes. The glass transition and crystallization temperatures were determined by differential thermal analysis (DTA). Obtained samples were subsequently annealed at 600 °C (1 h). Obtained glass-ceramics were characterized by XRD, FTIR, SEM, TEM and impedance spectroscopy method.

Crystalline phases have been obtained in all cases. In particular, XRD pattern revealed low- and high-temperature forms for $NaCoPO_4$, the estimated ratio α-$NaCoPO_4$ (space group *Pnma*) : β-$NaCoPO_4$ (space group $P6_5$) was approximately 1:1. For this sample the phase transition β-$NaCoPO_4$ → α-$NaCoPO_4$ was observed when heated to 600 °C. For the system $(1-x)Li_2O$-xNa_2O-$2CoO$-P_2O_5 (x = 0-1.0) the formation of solid solutions $Li_{1-x}Na_xCoPO_4$ was not happening. Two types of general compositions have been obtained, namely: $LiCoPO_4$ + $NaCoPO_4$ (α- and β- polymorphs) at fast cooling or $LiCoPO_4$ + β-$NaCoPO_4$ (samples were annealed at 600 °C). Thus, although crystal structures of $LiCoPO_4$ (space group *Pnmb*, a = 5.922, b = 10.206, c = 4.701 Å) and β-$NaCoPO_4$ (space group *Pnma*, a = 8.896, b = 6.8007, c = 5.0341 Å) are very similar, but these compounds do not form solid solutions. The report discussed the conductive properties of the obtained composites also.

Acknowledgements. Funding: This work was supported by the national long-term project [no. WQ20142200205] of "Thousand Talents Plan of Bureau of Foreign Experts Affairs" of People's Republic of China.

[1] D. Kundu, E. Talaie, V. Duffort, L. Nazar, The Emerging Chemistry of Sodium Ion Batteries for Electrochemical Energy Storage, *Angew. Chem. Int. Ed.* **54** (2015) 3431.
[2] H. Kim, Jimin Park, I. Park, K. Jin, S.E. Jerng, S.H. Kim, K.T. Nam, K. Kang, Coordination tuning of cobalt phosphates towards efficient water oxidation catalyst, *Nat. Commun.* **6** (2015) 8253.

Mesoporous Titania: Synthesis, Structure, Electrochemistry

V. Kotsyubynsky[1], I. Myronyuk[1], A. Hrubiak[2], M. Kuzyshyn[1], P. Kolkovsky[1]

[1]*Vasyl Stefanyk Precarpathian National University, 57 Shevchenko Str., 76018 Ivano-Frankivsk, Ukraine*
[2]*Institute of Metal Physics, National Academy of Science, 36 Acad. Vernadsky Boulevard, 03680 Kyiv, Ukraine*

Nanostructured titania (TiO_2) is one of the most wide used oxide nanomaterial due to its various applications in industry and medicine as a microbiocide, active material for gas sensors and photocatalytic systems, electrode material of dye-sensitized solar cells and electrochemical power sources. Functional characteristics of titania depend on its phase composition, structural and electronic properties. For example, anatase and brookite phases have higher photoactivity in comparison to rutile. Particle size and morphology are also important factors that determine the electric and catalytic parameters of nanodispersed titania. At the same time synthesis of high defect non-homogeneous porous materials with increased reactivity and conductivity is a very topical issue. The properties of TiO_2 and possibility of its successful technological application crucially depend on the synthesis method. The sol-gel synthesis of titania involves the chemical conversion of titanium alkoxides, titanyl compounds or titanium tetrachloride into a colloidal product in the liquid phase reaction medium. The nucleation of specific titanium dioxide polymorph is caused mostly by the spatial arrangement of the primary monomers $[Ti(OH)_h(OH_2)_{6-h}]^{(4-h)+}$ formed at the hydrolysis and determined by the pH of reaction medium [1].

Titanium butoxide $Ti(OC_4H_9)_4$ was used as a precursor to obtain titania, sulfate acid water solution was used as a hydrolysis agent and cetyltrimethylammonium chloride (CTMA-Cl) was a template. Five titania samples were obtained at the different pH (1.0, 1.2, 1.4, 1.6 and 1.8 respectively). The possibilities of rutile and anatase phases formation are close at these conditions. At the same time the presence of SO_4^{2-} leads to chelating bidentate complex formation and the anatase phase nucleation is initiated. All materials obtained by initial xerogels drying at 80°C were amorphous (XRD data) and crystallize to nanostructured anatase after annealing at 500°C. It was determined (by low angle X-ray scattering data) that the obtained titania samples have mesoporous morphology with the mesopore sizes in a range 1.7 - 4.3 nm. Specific surface areas (low temperature nitrogen adsorption data) non-linear vary depending on the pH during the particles nucleation in a range of 88-348 m^2/g with the maximum for sample obtained at pH=1.4. Specific volume of mesopores changes in a range of 0.56 - 1.68 cm^3 / g.

The obtained materials were used as a base of the cathode for the lithium power sources. Cathode composition consists of titania (90 wt %) acetylene black (8 wt %) and PVF (2 wt %). Counter and reference electrodes were made from lithium foil, 1M $LiBF_4$ in γ-butyrolactone was used as electrolyte. The discharges were carried out in galvanostatic conditions at current density of C/10. The obtained values of specific power density were within range of 870-1750 W/kg. The direct correlation between specific power density and specific volume of mesopores was found. At the same time the specific surface area is not so important characteristic. The kinetic of the discharge process was investigated by impedance spectroscopy. The analysis of changes in the values of the equivalent schemes parameters for different intercalation degrees was carried out. The presence of the only one kinetic process during discharge was determined. Calculated diffusion coefficients decline exponentially with the intercalation degree increasing in a range of $1 \cdot 10^{-8}$-$2 \cdot 10^{-11}$ cm^2/s.

[1] V. O. Kotsyubynsky, I. F. Myronyuk, V. L. Chelyadyn, M. H. Mizilevska, O. Kh. Tadeush, The effect of pH on the nucleation of titania by hydrolysis of $TiCl_4$, *Materials Science and Engineering Technology* **47** (2-3) (2016) 288–294.

Image Formation by Ink-Jet Printing in Micro- and Nanoporous Anodic Alumina Film with Capsulating

B. Kazarkin, Y. Mukha, A. Stsiapanau and A. Smirnov

Belarusian State University of Informatics and Radioelectronics, Minsk, Belarus

The method of functional layers topology formation was tested by ink-jet printing in a film of nanostructural anodic aluminum oxide. The layers were obtained with a resolution of about 50 microns, depth of 150 microns, as directly on the aluminum foil, as on the foil welded to glass substrate by anode welding. A partial and through anodization of aluminum foil were realized, as well as anodic oxide pores capsulation. Thermal and chemical stability of the obtained functional layers capsulated in a matrix of anodic oxide were shown. This low-temperature inexpensive technology is promising for the «roll-to-roll» organic electronic and display devices.

Circular samples of 12 mm diameter and 400 microns thickness contained at least 99,55% Al (fig.1a). Anodizing process was performed in the DC mode with 15% sulfuric acid solution. Profiles of anodizing processes are presented in Table. 1.

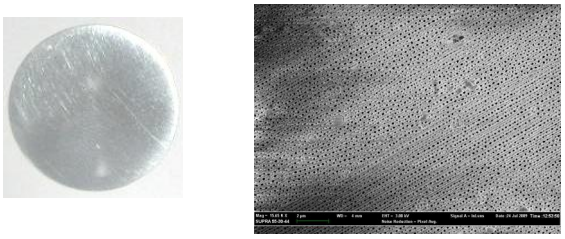

a b

Figure 1. a – image of sample, b – SEM photo of PAO structure

Table 1 - Profiles of anodizing processes

№	1	2	3	4
Sample				
Anodizing time, s	6000	3000	15000	3000
Current density, mA/cm^2	15	30	7.5	15
Total current density, A·s/ cm^2	90	90	112.5	45

At research of the samples was revealed exceptional resistance to mechanical, thermal and chemical stresses. The obtained results show the fundamental possibility of the formation of functional layers for organic electronics and display applications by ink-jet printing in a matrix of anodic alumina. Encapsulation of matrix pores allows obtaining functional films, resistant to mechanical, physical and chemical effects.

[1] V. Zhylinski, A. Chernik, N. Bagamazava, O. Volynets, I. Zharski, V. Bezborodov, A. Smirnov, A. Stsiapanau, *Proc. Int. Conf. on Physics, Chemistry and Applications of Nanostructures*, NANOMEETING-2015, Minsk, Belarus, 2015, pp. 560-563.

[2] S. Theohari, I. Iakovidis, A. Karampotsos, I. Sianoudis, *Open Journal of Applied Sciences* **6**(11) (2016) 783-795.

SECTION 2

ACTIVE MEDIA FUNDAMENTALS: CRYSTAL STRUCTURE AND DEFECTS

How Computer Modelling Can Aid Materials Processing and Defect Driven Effects

M. E. G. Valerio[1], R. A. Jackson[2]

[1]*Physics Department, Federal University of Sergipe, São Cristóvão, 49100-000, SE, Brazil*
[2]*School of Chemical and Physical Sciences, Keele University, Keele, Staffordshire, ST55BG, UK*

Modelling techniques have become common for the investigation of material properties on many scales. The number of methods available now ranges from very detailed quantum mechanical codes, suitable for understanding electronic properties of fairly simple materials, up to finite element approaches where an entire macroscopic object the size of a car can be treated and general, average bulk properties can be targeted. In the present communication the use of empirical potential and energy minimisation based methods are reported in an investigation of simple and complex materials at a scale where the defects can be related to energetics of materials synthesis, the transport properties, and other defect related or driven processes affecting the materials processing.

The focus is on case studies where a complete picture was developed from the empirical potential fitting, calculation of intrinsic and extrinsic defect energies, to the energetics of transport mechanisms. The following systems are considered: $LiNbO_3$, MAl_2O_4 (M=Ca, Sr or Ba) and $CaYAl_3O_7$. Lithium niobate, $LiNbO_3$, is an important technological material, and computer modelling provides a useful means of determining its properties, including defect chemistry, and the effect of doping on the structure. $LiNbO_3$ has been considered in a series of papers [1-4], including empirical potential fitting, intrinsic defect calculation and doping by a range of divalent, trivalent and tetravalent ions. More recently, predictions from defect modelling were used to help interpret EXAFS results on Zn-doped $LiNbO_3$ [5]. Alkaline-earth aluminates, MAl_2O_4 (M=Ca, Sr or Ba) are known as persistent luminescence phosphors when doped with trivalent and divalent rare-earth ions. Defect modelling will be reported, connecting the luminescence properties to the predicted rare-earth site symmetries [6]. The key issue here is the Eu3+ **à** Eu2+ reduction processes, which can be treated via computer modelling [7]. Calcium yttrium aluminate, $CaYAl_3O_7$, which has the melilite structure, is interest because its luminescence properties arise from doping with rare earth ions. This material is challenging because Ca and Y share the same crystallographic site with equal occupancy. A strategy based on the supercell method was developed, and intrinsic and extrinsic defects were modelled.

[1] R.A. Jackson, M.E.G. Valerio, A new interatomic potential for the ferroelectric and paraelectric phases of $LiNbO_3$, *J. Phys. Condensed Matter* **17** (2005) 837–843, doi:10.1088/0953-8984/17/6/005.

[2] R.M. Araujo, K. Lengyel, R.A. Jackson, L. Kovács, M.E.G. Valerio, A computational study of intrinsic and extrinsic defects in $LiNbO_3$, *J. Phys. Condensed Matter* **19** (2007) 046211, doi:10.1088/0953-8984/19/4/046211.

[3] R.M. Araujo, M.E.G. Valerio, R.A. Jackson, Computer modelling of trivalent metal dopants in lithium niobate, *J. Phys. Condensed Matter* **20** (2008) 035201, doi:10.1088/0953-8984/20/03/035201.

[4] R.M. Araujo, M.E.G. Valerio, R.A. Jackson, Computer simulation of metal co-doping in lithium niobate, *Proc. R. Soc. A* **470** (2014) 20140406, http://dx.doi.org/10.1098/rspa.2014.0406.

[5] M.E.G. Valerio, R.A. Jackson, F. Bridges, EXAFS simulations in Zn-doped LiNbO3 based on defect calculations, *IOP Conf. Series: Materials Science and Engineering* **1**(69) (2017) 012003, doi:10.1088/1757-899X/169/1/012003.

[6] R.M. Araujo, M.E.G. Valerio, R.A. Jackson, M.V. dos S. Rezende, Intrinsic Defects in Strontium Aluminates studied via Computer Simulation Technique, *J. Phys: Conf. Series* **249** (2010) 012042, doi:10.1088/1742-6596/249/1/012042.

[7] M.V. dos S. Rezende, M.E.G. Valerio, R.A. Jackson, Computer modelling of the reduction of rare earth dopants in barium aluminate, *J. Solid State Chemistry* **184** (2011) 1903–1908, doi: 10.1016/j.jssc.2011.05.053.

Assembled Phase Diagram as a Novel Tool of Materials Science

V. Lutsyk[1,2]

[1]*Institute of Physical Materials Science, Siberian Branch of Russian Academy of Sciences, Ulan-Ude, Russia*
[2]*Buryat State University, Ulan-Ude, Russia*

Special approach to the construction of the multidimensional phase diagrams in the form of their assembling from the surfaces or the phase regions into the N-dimensional computer models is proposed. To decode the T-x-y diagrams topology, the schemes of uni- and invariant states had been elaborated. This sort of schemes with phase's routes designations makes possible to calculate the number of phase regions, surfaces and to know a type of every surface (plane, ruled or unruled surface). This constructing is fulfilled in several stages: 1) the two-dimensional (2D) table and then the 3D scheme of uni- and invariant states (planes of invariant reactions and ruled surfaces), 2) the prototype (unruled surfaces), 3) transformation of the prototype into the real system model.

Reference book of 3D and 4D models of virtual T-x-y and T-x-y-z diagrams of basic topological types is created. And to construct the real T-x-y diagram of a simple topology it suffices to take from the Reference book the finished model (or the combination of 2-3 simple models). The 3D model is obtained after the input of the coordinates of base points (corresponding to invariant transformations in the binary and ternary system) and correction of the lines and surfaces curvature. Next step is to obtain the prototype of the T-x-y diagram by designing of the liquidus, solidus, solvus, transus surfaces. And last step includes the refinement of the curvature of the directing curves of ruled surfaces, closing the contours of unruled surfaces by curves of binary systems and correcting their isothermal lines. In this stage the 3D model of the real system T-x-y diagram is formed. Finished T-x-y diagram allows to construct any arbitrarily assigned sections and to calculate mass balances of the coexisting phases in all stages of the crystallization for any arbitrarily assigned concentration. Furthermore, the option of the determination of conditions for changing the type of three-phase reaction in any three-phase region is provided.

Acknowledgements. This work was been performed under the program of fundamental research SB RAS (project 0336-2016-0006), it was partially supported by the RFBR (projects 15-43-04304, 17-08-00875) and the RSF (project 17-19-01171).

[1] V. Lutsyk, V. Vorob'eva, From topology to computer model: ternary systems with polymorphism, *Abstracts of the international conference on phase diagram calculations and computational thermochemistry*, CALPHAD XXXVIII, Prague, Czech Republic, 2009, p. 66.

[2] V.I. Lutsyk, V.P. Vorob'eva, Computer models of eutectic-type T-x-y diagrams with allotropy. Two inner liquidus fields of two low-temperature modifications of the same component, *J. Therm. Anal. Calorim.* **101** (2010) 25-31.

[3] V.I. Lutsyk, V.P. Vorob'eva, A.E. Zelenaya, 3D reference book on the oxide systems space diagrams as a tool for data mining, *Solid State Phenomena* **230** (2015) 51-54.

[4] V.I. Lutsyk, V.P. Vorob'eva, S.Ya. Shodorova, Determining the conditions for changes of the three-phase rreaction type in a V-Zr-Cr systems, *Rus. J. Phys. Chem. A* **89** (2015) 2331-2338.

[5] V.I. Lutsyk, V.P. Vorob'eva, Three-dimensional model of phase diagram of Au-Bi-Sb system for clarification of thermodynamic calculations, *Rus. J. Phys. Chem. A* **89** (2015) 1715-1722.

[6] V.I. Lutsyk, V.P. Vorob'eva, 3D model of the T-x-y diagram of the Bi-In-Sn system for designing microstructure of alloys, *Rus. J. Inorg. Chem.* **61** (2016) 188-207.

[7] V.I. Lutsyk, V.P. Vorob'eva, S.Ya. Shodorova, Verification of the T-x-y diagram of the Ag-Au-Bi system using a 3D computer model, *Rus. J. Inorg. Chem.* **61** (2016) 858-866.

[8] V.I. Lutsyk, V.P. Vorob'eva, Verification of Phase Diagrams By Three-Dimensional Computer Models, *Mod. Chem. Appl.* **5** (2017) 215, doi: 10.4172/2329-6798.1000215 (to be published).

Basic Properties of Point Defects in Wide-Band Gap Metal Halides, Oxides and Perovskites

A.I. Popov and E.A. Kotomin

Institute of Solid State Physics, University of Latvia, Latvia

We present a short survey of the optical properties of primary radiation-induced point defects in alkali halides, simple oxides and some ABO_3 perovskites [1].We discuss in details the optical properties of single electron *F* and F^+ centers in rock-salt (f.c.c.) alkali halides and oxides and show that the Mollwo-Ivey law well-known for the *F*-type centers in alkali halides may be extended for other rock-salt structure insulators [2]. We also discuss the major differences in point defect production mechanisms in halides and oxides. We show that the Rabin-Klick diagram may be generalized for a whole family of alkali halides [2]. We discuss also the correlation between the temperatures at which hole polarons start migration in a series of alkali halides (fluorites, chlorides, bromides, iodides) and the lattice displacement around quasi-molecule [3]. Finally,the *F*-type center migration and aggregation into metal colloids in alkali halides and oxides is also discussed [4,5].

[1] E. A. Kotomin, A. I. Popov, Radiation-induced point defects in simple oxides, *Nucl. Instr. Meth. B* **141** (1998) 1.

[2] A. I. Popov, E. A. Kotomin, J. Maier, Basic properties of the F-type centers in halides, oxides and perovskites, *Nucl. Instr. Meth. B* **268** (2010) 3084.

[3] A. I. Popov, E. A. Kotomin, J. Maier, Analysis of self-trapped hole mobility in alkali halides and metal halides, *Solid State Ionic* (2017) (in press), http://dx.doi.org/10.1016/j.ssi.2016.12.004.

[4] E. A. Kotomin, A. I. Popov, The kinetics of radiation-induced point defect aggregation and metallic colloid formation in ionic solids, *Radiation Effects in Solids*, NATO Science Series, vol. 235, Springer, 2007, p. 153.

[5] E. A. Kotomin , V. N. Kuzovkov , A. I. Popov, R. Vila , Kinetics of F center annealing and colloid formation in Al_2O_3, *Nucl. Instr. Meth. B* **374** (2016) 107.

Reflections on Rust: Iron Oxide Photoelectrodes for Solar Energy Conversion and Storage

Avner Rothschild

Department of Materials Science and Engineering, Technion – Israel Institute of Technology, Haifa, Israel

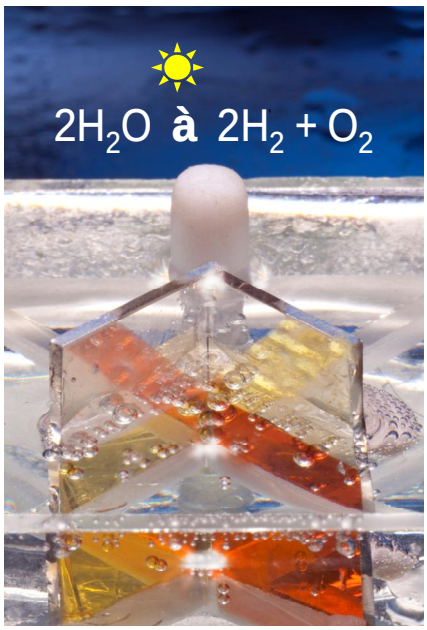

Reliable utilization of solar power on a large scale requires affordable energy storage technology, much cheaper than batteries, in order to synchronize the variable power production with the changing demand. Likewise, there is a need for renewable fuels to replace fossil fuels. These challenges can be achieved, potentially, by splitting water into hydrogen and oxygen, H_2O **à** $H_2 + ½O_2$, using solar power to drive this endergonic reaction uphill. The hydrogen can be stored and converted to electricity and heat on demand. Alternatively, it may serve as feedstock for the production of drop-in liquid fuels for transportation by reaction with CO_2, paving the road towards carbon-neutral synthetic fuels, so-called solar fuels. The first and foremost challenge toward this ambitious goal is the development of chemically stable, efficient and affordable photoelectrodes for water splitting.

Photoelectrodes for solar-powered water splitting must employ a semiconductor material with exceptional stability against corrosion, as well as visible-light absorption. On top of that, it should also be abundant, inexpensive and non-toxic. Iron oxide (□-Fe_2O_3, hematite) is one of few materials meeting these criteria, but its poor transport properties and ultrafast charge carrier recombination present a challenge for efficient charge carrier generation, separation and collection. We explore an innovative solution to this challenge using ultrathin (20-30 nm) quarter-wave films on back reflector substrates. This simple optical cavity design effectively traps the light in otherwise nearly translucent ultrathin films, amplifying the intensity close to the surface wherein photogenerated charge carriers can reach the surface and split water before recombination takes place. This is the enabling key towards the development of high efficiency photoelectrodes that could potentially lead to affordable solar energy storage and solar fuel production.

Brief Biography – Avner Rothschild is an associate professor at the Department of Materials Science and Engineering of the Technion – Israel Institute of Technology in Haifa, Israel. He graduated from the Technion (BSc in Physics and in Materials Engineering, 1997, PhD in 2003) and spent 3 years as a postdoc at MIT. Since 2006 he is a faculty member of the Technion. The Rothschild group has ~20 researchers working on photoelectrochemical water splitting for solar hydrogen production. The group is currently involved in two EU projects: ETASECS - Extremely Thin Absorbers for Solar Energy Conversion and Storage (ERC) and PECDEMO – PhotoElectroChemical DEMOnstration devices. Prof. Rothschild is one of the founding directors of the Israeli Center of Research Excellence on Solar Fuels.

Acceptor and Donor Related Photoluminescence from ZnO Films Doped with Nitrogen

Elzbieta Guziewicz, Ewa Przeździecka, Dmytro Snigurenko, Dawid Jarosz, Bartlomiej S. Witkowski, and Wojciech Paszkowicz

Institute of Physics, Polish Academy of Sciences, 02-668 Warsaw, Poland

The stable *p*-type conductivity of zinc oxide has still encountering problems and is the main obstacle in a wide application of this material in optoelectronics. Regardless a considerable number of papers reporting *p*-type conductivity in ZnO films, in many cases the obtained results remain controversial and the interplay between point and/or extended defects and acceptor states needs to be clarified. It has been reported that doping ZnO with group V elements results in enhancement of luminescence intensity around 3.30-3.32 eV. However, this emission line is commonly observed in a ZnO material irrespective on the chemical nature of dopant or even in a ZnO material without any intentional doping. It has been shown that in epitaxial films the 3.31 eV luminescence is related to structural defects as it is emitted from distinct lines on sample surfaces and cross-sections representing intersections with basal planes of wurzite hexagons [1]. Even in this case the 3.31 eV emission is unambiguously related to a shallow acceptor state located 130 meV above the valence band.

In this paper we report on a photo- and cathodoluminescence study on intentionally undoped and nitrogen doped ZnO layers. The 2 µm thick polycrystalline ZnO films were grown on a highly resistive silicon substrate at low temperature (100^{o}C) under oxygen rich conditions and doped with nitrogen during the Atomic Layer Deposition process [2]. Photoluminescence spectra reveal two dominant emission bands in the excitonic region. Apart from the D^{o}X line at about 3.36 eV also a characteristic emission around 3.30 – 3.32 eV appears. The 3.31 eV emission band appears both in undoped and nitrogen-doped samples, however the RTP annealing in oxygen atmosphere leads to a considerable enhancement of this band only in samples intentionally doped with nitrogen and this enhancement is accompanied by shifting the conductivity towards *p*-type.

The SEM and related spatially resolved low-temperature CL studies show that the area showing donor-related 375 nm emission is complementary to the area showing acceptor-related 370 nm band, which suggests that both *p*-type and *n*-type regions simultaneously coexist in this material. This points out that the 3.31 eV band cannot be clearly associated with structural defects as was suggested before [1].

Acknowledgements. The work was partially supported by the Polish NCN project DEC-2012/07/B/ST3/03567. The Author D.S. acknowledges the partial support from the EU 7th Framework Programme Project No. REGPOT-CT-2013-316014 (EAgLE).

[1] M. Schirra, R. Schneider, A. Rieser, G.M. Prinz, M. Feneberg, J. Biskupek, U. Kaiser, C.E. Krill, K. Thonke and R. Sauer, *Phys. Rev. B* **77** (2008) 125215.

[2] D. Snigurenko, K. Kopalko, T.A. Krajewski, R. Jakiela, E. Guziewicz, *Semicond. Sci. Technol*. **30** (2015) 015001.

The Oxygen Ternary Comlex $V_{Zn}Zn_iO_{Se}$ in the Mixed Crystals $ZnS_xSe_{(1-x)}$

O.G. Trubaeva, S.N. Galkin, A.I. Lalayants

Institute for Scintillation Materials NAS of Ukraine, 60 Nauki Ave., 61001 Kharkiv, Ukraine

Recently, set out new demands, to materials for a wide range of radiation instrumentation. Scintillators based on $ZnS_xSe_{(1-x)}$ mixed crystals are perspective luminescent materials for X-ray and computer tomography. Their advantage over traditional scintillators is a high light output, low level of afterglow and a slight temperature quenching in the operating temperature range.

Mixed crystals were grown by the Bridgman-Stockbarger method from the following compositions: $ZnS_{0,05}Se_{0,95}$; $ZnS_{0,1}Se_{0,9}$; $ZnS_{0,15}Se_{0,85}$; $ZnS_{0,2}Se_{0,8}$; $ZnS_{0,25}Se_{0,75}$; $ZnS_{0,3}Se_{0,7}$. The sulfur distribution along the length of the crystal boule is not constant and it concentration decrease in the tail section.

The RL spectra of $ZnS_xSe_{(1-x)}$ shown a broad band with a max of 590 nm, corresponding to the glow of the ternary complex $V_{Zn}Zn_iO_{Se}$. With the increase in sulfur content, RL intensity increases and reaches a maximum for $ZnS_{0,15}Se_{0,85}$ composition. The intensity of the mixed crystals luminescence increases by 2-3 times after it annealing in zinc vapor. Measurements of light output by two methods showed a higher light yield of mixed crystals $ZnS_xSe_{(1-x)}$ with respect to the commercial crystals of ZnSe(Te) and ZnSe(Al). The high temperature stability of $ZnS_xSe_{(1-x)}$ scintillators, opens up prospects for their use in the medical imaging technique.

Role of Defects in Formation of the Luminescence Properties of Zinc Molybdate Crystals

Y. Hizhnyi[1], S. Nedilko[1], T. Nikolaenko[1], P. Nagornyi[1], R. Boyko[2], V. Boyko[2]

[1]*Taras Shevchenko National University of Kyiv, 64/13 Volodymyrska Str., 01601 Kyiv, Ukraine*
[2]*National University of Life and Environmental Sciences of Ukraine, 5 Geroiv Oborony Str., 03041 Kyiv, Ukraine*

The luminescence properties of zinc molybdate crystals $ZnMoO_4$ are intensively studied at present since these crystals are considered as perspective scintillation materials for various experiments in particle physics. The luminescence spectra of undoped $ZnMoO_4$ crystals usually reveal two components peaking near 530 and 620 nm. According to current opinion, the short-wavelength component originates from radiation annihilation of self-trapped excitons localized on MoO_4 groups of the crystal. However, the origin of the long-wavelength component is still the subject of discussion. According assumption made by several authors, this component should be related to existence the oxygen vacancies in the crystal lattice which form the oxygen-deficient molybdate groups MoO_3. The present work is aimed to examine this assumption in complex experimental and computational studies. Dependences of intensity of the long-wavelength emission component and other luminescence characteristics of zinc molybdate on concentration of the oxygen vacancies are analyzed as result of luminescence spectroscopy studies carried out for the set of samples synthesized at different conditions.

The polycrystalline samples of $ZnMoO_4$ with varying concentration of structural defects were synthesized by solid-state reaction method. The luminescence properties were studied in the VUV region of excitation photon energies on SUPERLUMI station at HASYLAB (Hamburg, Germany). Additional bands in the optical absorption spectra were characterized by diffuse reflectance spectroscopy. The influence of several kinds of defects (V_o, V_o+V_{Zn} and W_{Mo}) on the electronic structure of $ZnMoO_4$ crystal was studied by FP-LAPW method [1].

As the experimental results show, the increase of the oxygen vacancies concentration leads to increase of the relative intensity of the 620 nm emission component of $ZnMoO_4$ and to appearance of additional bands in luminescence excitation spectra in 3.7 – 4.7 eV range of exciting photons energies. The electronic structure results indicate existence of the electronic states of oxygen-deficient MoO_3 groups in the crystal band-gap. Obtained results and their analysis support assumption on the oxygen vacancy-related origin of the long-wavelength emission component of zinc molybdate.

[1] P. Blaha et al, ISBN 3-9501031-1-2, 2001.

Structural and Luminescence Peculiarities for Scheelite-Related Binary Molybdates

K.V. Terebilenko[1], K.L. Bychkov[1], K.E. Klimishina[1],V.N. Baumer[2], M.S. Slobodyanik[1]

[1]*Taras Shevchenko National University of Kyiv, Kyiv, Ukraine*
[2]*STC "Institute for Single Crystals" NAS of Ukraine, Kharkiv, Ukraine*

Pure and doped scheelite-related oxides containing rare-earth metals and molybdate or tungstate anions have been intensively studied during the past decade due to their attractive structures and topologies as well as their potential applications in luminescence and optics [1-2]. Although numerous complex derivatives from the ideal tetragonal structure e (space group $I4_1/a$, Z = 4) have been synthesized, rational theory about the relationship between the structures and the components constructing them has not been developed yet.

Having general chemical formula $(M_{0.5}RE_{0.5})MoO_4$, where M – is alkaline metal and RE – rere-earth one, both metals are located in $(M,RE)O_8$ dodecahedra, which constitute square antiprisms, while molybdenum ions have a tetrahedral oxygen environment MoO_4^{2-} with almost equal cation–oxygen interatomic distances (Fig. 1a). Due to the statistical distribution of alkaline and rere-earth metals within the crystallographic sites of the scheelite structure these crystals provide large bandwidths of the optical absorption and luminescence bands of rare-earth ions. Alternatively the crystal structure can be regarded as a regular intergrowth of these metals in a way of diamond-like framework (fig.1b).

On the basis of structure determination from single crystal data and luminescence properties of a number of binary molybdates the peculiarities of crystal structure – luminescence relationships are explored for isostructural compounds $KCeMo_2O_8$ and $KPrMo_2O_8$. The key trends in scheelite –related structural motifs are compared for known luminescent hosts with common building blocks.

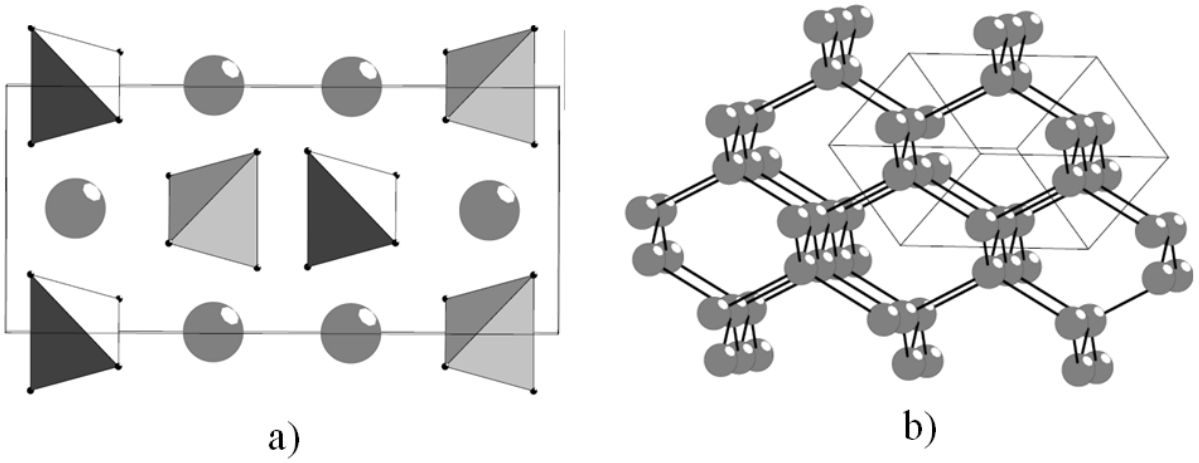

Fig.1. a) The typical representation of the scheelite unit cell and b) formation of diamond-like architecture by rare-earth metals network

[1] G.M. Kuz'micheva, I.A. Kaurova, E.A. Zagorul'ko, N.B. Bolotina, V.B. Rybakov, A.A. Brykovskiy, E.V. Zharikov, D.A. Lis, K.A. Subbotin, *Acta Materialia* **87** (2015) 25-33.

[2] G.M. Kuz'micheva, I.A. Kaurova, V.B. Rybakov, P.A. Eistrikh-Geller, E.V. Zharikov, D.A. Lis, K.A. Subbotin, *Cryst. Eng. Comm.* **18** (2016) 2921-2928.

Recharge Cr^{3+} Ions in Cr,Ca:YAG Ceramics

M. Chaika, O. Vovk, N. Dulina, A. Doroshenko, S. Parkhomenko, A. Tolmachev

Institute for Single Crystals of National Academy of Sciences of Ukraine,
60 Nauky Ave., 61001 Kharkiv, Ukraine

In recent years tetrahedral coordinated Cr^{4+}-doped YAG have attracted a great deal of attention due to its potential use as tunable solid state lasers in the spectral range 1.35-1.55 μm [1] or passive Q-switcher for laser systems based on YAG doped with rare earth ions such as Nd and Yb [2]. As a single dopant Cr incorporated into YAG as a Cr^{3+}, existence of the Cr^{4+} in the crystal requires containing divalent additives such as Ca or Mg to compensate difference in charge. After vacuum sintering ceramic of Cr:YAG contains only Cr^{3+} even the divalent ions presented in the ceramics, and to been recharging up to Cr^{4+} the oxidative annealing is needed.

Therefore, purpose of this work is to investigation of recharge kinetics Cr^{3+} to Cr^{4+} and exchange kinetics of Cr^{4+} ions between octahedral and tetrahedral lattice sites under the air annealing.

Cr,Ca:YAG ceramics with concentration Ca 0.5 at.% and Cr 0.1 at.% were sintered by solid state reaction sintering in vacuum at 1750 °C for 50 hours. After vacuum sintering samples contain Cr^{3+} only. Recharge $Cr^{3+} \rightarrow Cr^{4+}$ was provide in special furnace which allow fast remove sample. Concentration of Cr^{4+} ions was measured by optical absorption spectroscopy. The time dependence of Cr^{4+} ion concentration at four evaluated temperature was carried out to determine activation energy of both the recharge and exchange processes.

According to the literature, during air annealing Cr^{3+} recharge into Cr^{4+} in octahedral position and them replace Al into tetrahedral position. Therefore Cr^{4+} (octahedral) determinate only recharge Cr^{3+} ions but for Cr^{4+} (tetrahedral) formation transfer position also needed.

Time dependence of concentration of Cr^{4+} ions was described with Jander model. Kinetic of recharge Cr^{4+} ion in octahedral and tetrahedral crystallographic position show same behaviour dependence concentration from time. That indicate forming Cr in these position have same limited stage.

The value of activation energy process of recharge Cr^{3+} was calculated as 2,67 ± 0.21 eV, which coincides with literature data for energy of activation oxygen into YAG ceramics [3]. That allows to conclude that recharge of Cr^{3+} to Cr^{4+} in ceramics Cr,Ca:YAG Cr4+ ions controlled by diffusion oxygen through ceramics.

The concentration ratio between tetrahedral and octahedral Cr^{4+} ions no time and temperature depended under air annealing at 1000 to 1300 °C and equal of 0.55. That means the transfer of Cr^{4+} between octahedral and tetrahedral crystallographic position occurs without energy barrier and enthalpy of exchange reaction is close to zero.

[1] N. B. Angert, N. I. Borodin et al., *Soviet Journal of Quantum Electronics* **18**(1) (1988) 73.
[2] Zhu, Siqi et al., *Journal of Laser Applications* **26**(3) (2014) 032009.
[3] Li, Zhen et al., *Journal of the American Ceramic Society* **95**(11) (2012) 3628-3633.

Inelastic Defect Characteristic Internal Friction in SiO_2, GeSi and Anisotropy Automated System "KERN-DP"

A.P. Onanko, G.T. Prodayvoda, Y.A. Onanko, A.V. Shabatura, A.N. Onischenko

Kyiv National University, Kyiv, Ukraine

Influence of direct and variable electrical current is considered at simultaneous act of ultrasonic deformation on internal friction (IF) and elastic module of GeSi single-crystal after cutting and polishing. The diminishing of elastic module E of and the growth of internal friction Q^{-1} is found out at achievement of critical value of electrical current. Kinetics of annealing of structural defects is studied.

The results of examinations of the relaxation processes in a crystalline lattice at thermal and ultrasonic (US) processing on the temperature spectrum of internal friction and elastic module (directional surface of inelastic-elastic body) of SiO_2, GeSi are presented. The growth of IF $Q^{-1}(J^{\sim})$ is observed for an alternating current $J^{\sim}$ at achievement of critical value of electrical current thickness $J^{*}_{cr} \approx 60 \cdot 10^3$ A/m^2 with the simultaneous diminishing of the elastic module value $E(J^{\sim})$ at the consequent increasing of current thickness, as evidently from fig. 1.

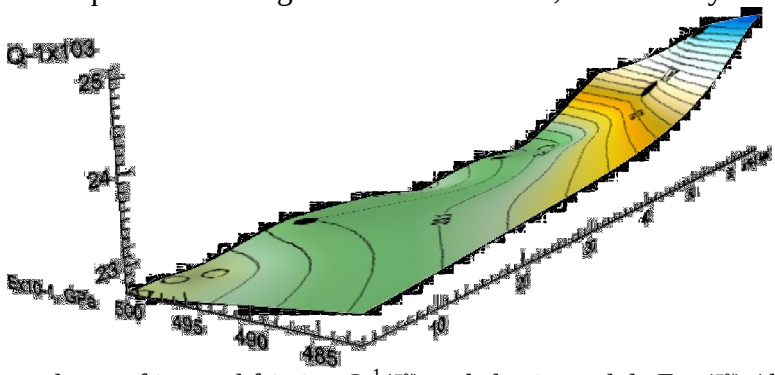

Fig. 1. Current dependence of internal friction $Q^{-1}(J^{\sim})$ and elastic module $E_{111}(J^{\sim})$ (directional surface inelastic-elastic body) of monocrystal GeSi after cutting and polishing from an alternating electrical current thickness with frequency $\omega_J = \omega_{US}$.

The software "KERN-DP" is developed for the automated system of anisotropy parameters analysis. The structure of database is developed on language of mySQL information, physical properties, the special procedures of data management are developed.

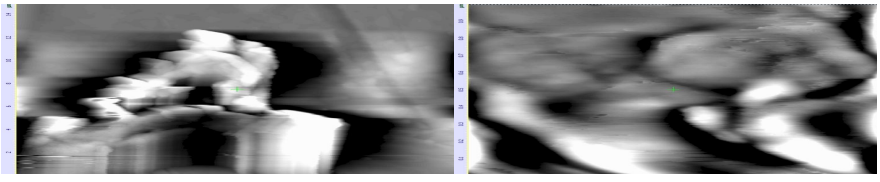

Fig. 2. Atomic force microscopy microstructure of SiO_2 pores on Si (100) ($15x15x10^3$ nm; $1x1x10^3$ nm).

Conclusions

1. The measuring of internal friction background Q^{-1}_0 after different heat, mechanical, radiation treatments gives information about the changing of the thermoelastic strains fields σ_i in SiO_2.

2. The dynamic characteristics of interstitial atoms Si_j, vacancy V and O-complexes can be applied for account of a condition of an annealing with the purpose of deriving specific structural defects in SiO_2.

Deep Levels in β-Ga_2O_3 Single Crystals Doped with Mg^{2+} Ions

A. Luchechko*, V. Vasyltsiv, L. Kostyk, O. Tsvetkova

[1]*Department of Sensor and Semiconductor Electronics, Ivan Franko National University of Lviv, 107 Tarnanavskogo Str., 79017 Lviv, Ukraine*
* luchechko@electronics.lnu.edu.ua

The widespread adoption of energy-saving technologies and development of new low-power devices is needed to provide a stable supply of energy. The transition to efficient power electronics can be achieved by replacing the silicon components (transistors, diodes) to the components made from wide-gap semiconductors that provide lower loss at switching.

The large breakdown field (8 MV/cm) and large band gap (4.8 - 4.9 eV) of gallium oxide (β-Ga_2O_3) have excellent perspective for application in power electronics devices. Recently reported the successful production of Schottky diodes [1] and field effect transistors (MOSFETs) [2] based on β-Ga_2O_3. MOSFETs have good characteristics, including the breakdown voltage (over 400 V), extremely low leakage current, and excellent ratio currents in switched on and switched off states (more than 10 orders of magnitude). Transistors have shown good performance at high temperatures (250 °C) without significant impairment of parameters. These results indicate that β-Ga_2O_3 has more potential than Si and other typical wide-gap semiconductors such as SiC and GaN for applications in power electronics.

However, the successful using of β-Ga_2O_3 as a material for devices of power electronics, optoelectronics in UV range and other applications is hampered by small amount of papers devoted to studying the fundamental properties of β-Ga_2O_3, including the role of impurities and host defects in donor and acceptor levels creating as well as of capture and recombination levels, which play a crucial role in the charge transfer.

This paper presents the investigation results of the optical absorption, photoconductivity, thermally stimulated luminescence (TSL) and thermally stimulated conductivity (TSP) of undoped and Mg^{2+} activated β-Ga_2O_3 single crystals with various heat treatments. Additional bands in the UV region 3.6-4.6 eV and near IR region 0.4-1.2 eV were found in the optical absorption and photoconductivity spectra. Peaks with maxima at about 285 K, 314 K and 354 K and the activation energy of 0.65, 0.72 and 0.84 eV, respectively, were detected on the TSL and TSP curves. The intensities of TSL peaks vary depending on heat treatment and the introduction of Mg^{2+} impurities.

The correlation between bands of the optical absorption and photoconductivity with energy levels of intrinsic defects in β-Ga_2O_3, arising in gallium oxide at a divergence of the oxygen stoichiometry and Mg^{2+} impurities entering have been established. Electronic transitions from shallow donor levels and F-centers are concentrated in the IR region 0.4-1.2 eV and define high conductivity and transparency in long wavelength edge of the material. Absorption and photoconductivity bands in the UV region are associated with transitions of electrons from deep acceptor levels created by host defects and impurities.

[1] K. Sasaki, M. Higashiwaki, A. Kuramata, T. Masui and S. Yamakoshi, *IEEE Electron Device Lett.* **34** (2013) 493-495.
[2] M. Higashiwaki, K. Sasaki, A. Kuramata, T. Masui, S. Yamakoshi, *Appl. Phys. Lett.* **100** (2012) 013504.

The Influence of Europium Impurity on the Recombination Luminescence in Y_2O_3

S.S. Novosad*, I.S. Novosad, O.M. Bordun, I.O. Bordun, O.Ya. Tuzyak

[1]*Ivan Franko National University of Lviv, 1 Universytetska Str., 79000 Lviv, Ukraine*
* novosadss@rambler.ru

Europium as doping impurity for X-ray and cathodoluminophors is mainly interest due to its spectral features of the luminescence, property to change its valence and easily capture electrons and holes. It was revealed in [1–3] works, that F-type centers appear in monocrystals on the base of yttrium oxide after X-ray and ultraviolet light irradiations at the temperature of liquid nitrogen. F-type centers spectra are easily discolored by optic lighting from 1 μm region and thermally.

In this paper we have done the comparative study and have analyzed the spectra of X-ray luminescence (XRL) and the curves of thermostimulated luminescence (TSL) of Y_2O_3 and Y_2O_3:Eu^{3+} ceramics at X-ray excitation in 85–295 K range for the obtaining of additional information about the influence of Eu^{3+} ions on the features of recombination processes in Y_2O_3. At 85 K XRL spectrum of Y_2O_3 ceramic characterizes by wide nonelementary 3.19 eV band. Heating of Y_2O_3 sample from 85 to 210 K leads to insignificant increase of XRL intensity in spectrum maximum and from 210 to 295 K causes the sharply monotonically decrease to ~0.15 numeric value of maximum intensity. XRL spectrum of undoped ceramic at 85 K is fitted into elementary Gaussian shape bands with maxima near 3.40, 3.06, 2.67, 2.33, 2.09 and 1.91 eV considering the features of Y_2O_3 crystallization [4] and possibility of formation of short lifetime and stable hole and electron centers of V- and F-type [1–3] by ionizing radiation. 3.40 and 3.06 eV main bands of XRL are caused by self-trapped excitons of $(YO)^{9-}$ complex when the cation is localized in the field of trigonal (C_{3i}) and monoclinic (C_2) symmetries. Emission at 2.67 eV and weak bands in 1.65–2.61 eV region are considered as radiation of localized excitons on anion vacancies and electron centers of F-type (F^+, F and F^-). Doping of material by europium ions leads to appearance of Eu^{3+} centers luminescence. Eu^{3+} ions form the emission centers with C_2 symmetry in Y_2O_3:Eu^{3+}. Weak bands observed in XRL and TSL spectra are caused by $^5D_0 \rightarrow {}^7F_j$ electronic transitions in Eu^{3+}. 2.03 eV main band is associated with $^5D_0 \rightarrow {}^7F_2$ transition. It is suggested, the energy comes to Eu^{3+} ions through $(Eu^{2+}O^-)$ complexes at both X-ray quanta and optical excitations of Y_2O_3:Eu^{3+} in a charge transfer band.

At 85 K three groups of peaks with different intensity in 85–140, 140–230 and 230–280 K ranges are observed in TSL curve after X-ray excitation of Y_2O_3. TSL in 185 and 203 K main peaks range is connected with thermal destruction of self-trapped states of O^- ions that located in the field of trigonal and monoclinic symmetries. Doping of Y_2O_3 by europium impurity leads to change of TSL peaks intensity ratio in 140–230 K range for 179 K peak and more effective detection of peaks in 230–280 K range. On the base of obtained results of TSL study the main parameters of capture centers of charge carriers in Y_2O_3:Eu^{3+} have been calculated.

[1] V.S. Vayner, A.I. Veynger, Yu.A. Polonskyy, Investigation of F-centers in Y_2O_3 by ESR method, *Physics of the Solid State* **18**(2) (1976) 409–412.

[2] V.S. Vayner, A.I. Veynger, Investigation of formation and transformation of point defects in Y_2O_3 monocrystals, *Physics of the Solid State* **19**(2) (1977) 528–532.

[3] V.S. Vayner, T.M. Bragina, A.I. Veynger, Yu.A. Polonskyy, Direct observation of change of the carge state sign of F-centers in Y_2O_3, *Physics of the Solid State* **21**(9) (1979) 2818–2820.

[4] F. Hanic, M. Hartmanova, S. Bagejasarov et al., Real structure of undoped Y_2O_3 single crystal, *Acta Crystallogr. Sect. B* **40**(2) (1984) 76–82.

Optical Detection of Paramagnetic Centres in Activated Oxyfluoride Glass-Ceramics

U. Rogulis, A. Fedotovs, A. Antuzevics, Dz. Berzins

Institute of Solid State Physics, University of Latvia, 8 Kengaraga Str., Riga, Latvia

Oxifluoride glass-ceramics are transparent composite materials consisting of the oxide glass matrix and fluoride micro- and nanocrystals obtained by a thermal annealing of the initial oxyfluoride glass [1]. Activated oxyfluoride glass ceramics have found an application as infrared convertors [2], and are considered for applications as scintillators [3] and phosphors for white LED's [4].

Activator centres as well as colour centres are often paramagnetic and may affect the properties of the glass-ceramics significantly. Investigations of the paramagnetic centres by the conventional electron paramagnetic resonance (EPR) techniques usually do not allow to directly attribute these centres to particular optical bands of the given sample. For this purpose the most convenient is optically detected EPR via the magnetic circular dichroism (MCD-EPR) [5,6].

MCD-EPR could be observed in the MCD bands which have paramagnetic behaviour. Paramagnetic MCD has been observed in the oxyfluorides activated by Mn^{2+}, Eu^{2+}, Gd^{3+}, Ho^{3+}, Sm^{3+} and Er^{3+}. Oxyfluorides activated by Tb^{3+} and Dy^{3+} showed no paramagnetic components.

The results of the MCD-EPR measurements at the 377 nm and 521 nm MCD bands at the 1.5 K temperature for the oxyfluoride glass-ceramics showed that Er^{3+} ions in the CaF_2 crystallites in these ceramics embed only in the cubic symmetry environment.These results are similar to the previous observations that the Gd^{3+} ions in the glass-ceramics with CaF_2also embed in the cubic environment [7]. For the SrF_2 containing glass ceramics the location of Gd^{3+} in the cubic environment has been observed, too.

As a conclusion, in small CaF_2 crystallites (with the size of few tens of nm) the trivalent rare earth ions prefer to embed in the cubic symmetry environment.

Results of recent measurements on $YAlO_3$:Mn will be reported and compared with the Mn-doped oxyfluorides.

Acknowledgements. The financial support of Latvian-Ukrainian Joint Research Project No. LV-UA/2016/1 is greatly acknowledged.

[1] P.P. Fedorov, A.A. Luginina, A.I. Popov, *J. of Fluorine Chem.* **172** (2015) 22-50.
[2] J.M. Dejneka, *MRS Bull.* **23** (1998) 57-62.
[3] Z. Pan, K. James, Y. Cui, A. Burger, N. Cherepy, S.A. Payne, R. Mu, S.H. Morgan, *Nucl. Instr. and Meth. in Phys. Res. A* **594** (2008) 215-219.
[4] S.H. Lee, S.-R. Bae , Y.G. Choi , W.J. Chung, *Optical Materials* **14** (2015) 71-74.
[5] J.-M. Spaeth, H. Overhof, *Point defects in Semiconductors and Insulators*, Springer-Verlag, Berlin, Heidelberg, 2003.
[6] U. Rogulis, *Low temperature physics* **42** (2016) 689-693.
[7] A. Fedotovs, A. Antuzevics, U. Rogulis, M. Kemere, R. Ignatans, *J. of Non-Crystalline solids* **429** (2015) 118-121.

Theoretical Study of the Effectiveness of Radiation Coloring of the Oxygen-Containing Fluorite Crystals

S. Kachan[1,*], V. Salapak[2], O. Nagurskyy[1], I. Pirko[2]

[1]*Lviv polytechnic National university, 12 Bandera Street, 79013 Lviv, Ukraine*
[2]*Ukrainian National forestry university, 103 gen. Chuprynka Street, 79057 Lviv, Ukraine*
* sikach@gmail.com

Presence of the oxygen as a background impurity worsens the optical transparency of the fluorites in the ultraviolet spectrum and diminishes their radiation resistance [1]. However, by a purposeful doping of the fluorite crystals with oxygen impurities one can achieve a significant coloring during irradiation of such crystals [2].

In the present paper, the parameters of radiation sensitivity of the oxygen-doped fluorite crystals were calculated in a one-dimensional model. The boundary concentrations of the color centers as a function of the concentration of the oxygen impurity in the fluorite crystal were defined. The table shows the calculation data of the parameters of the CaF_2-O^2– crystals' radiation sensitivity.

c	l	w_1	w_2	w_3	c_1/c_0	n_1 , $см^{-3}$	c_2/c_0	n_2,$см^{-3}$	c_2/c_1
0,50	6a	0,100	0,32	0,067	0,240	$6\cdot10^{18}$	0,60	$1,5\cdot10^{19}$	2,5
0,10	10a	0,069	0,32	0,044	0,180	$9\cdot10^{17}$	0,61	$3,1\cdot10^{18}$	3,4
0,01	21a	0,032	0,33	0,014	0,088	$4,4\cdot10^{16}$	0,70	$3,5\cdot10^{17}$	8,0

Note: c –molar concentration of the oxygen ions in the crystal; l – average distance between impurity ions in the crystal framework; a – parameter of the ion chain; $c_0 = 0.5c$ -molar concentration of IVD-pairs (impurity-vacancy dipoles) in the crystal; c_1 – boundary concentration of color centers emerging during the irradiation of the crystal at low temperatures; c_2 – boundary concentration of color centers emerging in the crystal during its irradiation at $T > 150$ K; n_1 – boundary density of color centers emerging at the stage of color saturation of the crystal being irradiated at $T < 150$ K; n_2 – boundary density of color centers emerging at the stage of color saturation of the crystal being irradiated at$T > 150$ K;n_0 – IVD-pairsconcentration in the crystal before the irradiation.

As evidenced by the data presented in the table, at the low-temperature irradiation of the crystal, the possibility w_1 of color centers emergence is lower than the probability w_2 of their destruction during irradiation. Accordingly, the color centers concentration c_1 is considerably lesser than IVD concentration c_0. Conversely, if the crystals are being irradiated at the room temperature, w_1 is greater than w_3. Hence, at the stage of color saturation of the crystal, the concentration of the color centers exceeds the IVD concentration. As the oxygen content reaches 0.5mole, the color centers concentration runs up to 10^{19} cm^{-3}which is by order of magnitude greater than that in *KCl* crystals. Because of the high radiation sensitivity of the doped fluorite crystals, they are a promising material for micro- and nanoelectronics.

[1] P.W.M. Jacobs, S.H. Ong, A.V. Chadwick, V.M. Carr, An experimental and Theoretical Study of crystals Calcium Fluoride Doped with Allkali Metals Cations, *J. Sol. Stat. Chem.* **33**(2) (1980) 159-167.
[2] W. Bollman, Incorporation of O^{2-} and OH^- ions in CaF_2 crystals, *Phys. Stat. Sol. (a)* **60**(2) (1980) 661-667.

High Pressure Luminescence and Raman Investigation of $Ca_9Nd(VO_4)_7$ Whitlockite-Like Crystals

D. Wlodarczyk[1], K. Kosyl[1], K. Izdebska[1], W. Paszkowicz[1], M. Kosmyna[3], A. Shekhovtsov[3], A. Suchocki[1,2]

[1]*Institute of Physics, Polish Academy of Sciences, Aleja Lotnikow 32/46, PL-02668 Warsaw, Poland*
[2]*Institute of Physics, Kazimierz Wielki Univeristy, Weyssenhoffa 11, 85-072 Bydgoszcz, Poland*
[3]*Institute for Single Crystals NAS of Ukraine, Nauki Ave. 60, 61001 Kharkov, Ukraine*

Whitlockite is a phosphate mineral of $Ca_9(MgFe)(PO_4)_6PO_3OH$ formula, known for its presence in granitic pegmatites and phosphate rock deposits, and in living organisms. Recently, various anhydrous synthetic phosphates and vanadates crystallizing in structures related to that of whitlockite have been studied as materials possibly applicable as phosphors in light-emitting diodes and having a potential in laser engineering as a promising host for active laser media, and nonlinear optics. One of studies compound families is described by the formula $Ca_9(Nd^{III})(V^{V}O_4)_7$.

The studied sample of $Ca_9(Nd^{III})(V^{V}O_4)_7$ was a transparent, violet monocrystal grown by the Czochralski method in inert argon atmosphere. Recently done Raman and XRD studies revealled compositional differences that separate this specific type of whitlockite from others in its family. This brittle (Mohs 5), piezoelectric and pyroelectric material has trigonal crystallographic structure and ditrigonal pyramidal crystal class – it belongs to noncentrosymmetric R3c space group. These crystals are also characterized by polymorphic transition from the noncentrosymmetric to the centrosymmetric phase which occurs roughly between 800-1100ºC at ambient pressure however no signs of pressure-induced phase transition were detected in this study.

High pressure luminescence spectra excited by 532 nm radiation show typical lines of Nd^{3+} associated with transitions from $^4F_{3/2}$ to $^4I_{9/2}$, $^4I_{11/2}$, $^4I_{13/}$ levels in this material [1-4], which exhibit pressure coefficients in the range of $4 – 7$ cm^{-1}/Gpa. High-pressure micro-Raman spectra of $Ca_9Nd(VO_4)_7$ single crystal were examined in this work at room temperature on Monovista CRS+ S&I spectrometer with use of diamond-anvil cell (Diacell CryoDAC-LT) and argon as a pressure transmitting medium. The applied pressure reached 15 GPa. The excitation was provided by green (532 nm) and red (785 nm) lasers. At pressure between between 50 and 60 kbar, additional lines appear in the spectra. Signals emerging at 425 and 665 cm^{-1} could be also strictly related to the high-pressure activation of neodymium ions. Origin of these lines is discussed in this work.

[1] M.P. Demesh et al., *Opt. Mater.* **60** (2016) 387-393.
[2] S. Zhai et al., *Phys. Chem. Minerals* **42** (2015) 303–308.
[3] Z. Zhang et. al., *Opt. Mater.* **7** (2017) 484-493.
[4] M.B. Kosmyna et al., *Acta Phys. Pol. A* **124** (2013) 305-313.

Analysis of Electromigration in MWO_4 (M=Ca, Cd, Pb, Zn) Crystals and their Structural Defects

V.N. Shevchuk*, I.V. Kayun

Department of Electronics and Computational Technologies,
Ivan Franko National University of Lviv, 50 Drahomanov Street, 79005 Lviv, Ukraine
* *shevchuk@electronics.lnu.edu.ua*

The complex oxide crystals characterized by mixed electron-ionic conductivity. The electrical properties and migration of charge carriers of some oxide compounds were investigated previous in connection with the structural building and electrical active defects of crystals in our papers [1, 2]. However, the electrical properties of AWO_4 (where A is Ca, Cd, Pb, or Zn) were studied insufficiently. In the book [3] the data on ionic conductivity of crystals of different structural types based on the crystallographic characteristics are given. The effect of migration of tungstate complexes at high temperatures for $CaWO_4$ crystal was observed in [4]. The ionic conductivity of crystals with scheelite type of structure experimentally investigated [5] in $PbWO_4$ and $PbMoO_4$ compounds. But, the mechanism of ionic conductivity and the migration ways of mobile ions in these crystals are not ascertained.

In this work the stereo-atomic crystal structure analysis using the program package TOPOS [6, 7], with the aim to visualization of probable migration pathway of mobile ion in the crystals with general formula AWO_4 (A=Ca, Cd, Pb, or Zn) was applied. The ionic migration maps for the crystals AWO_4 were constructed. Possible migration paths of W ions in the structure of the AWO_4 crystals with scheelite (Ca, Pb, space group $I4_1/a$) and wolframite (Cd, Zn, space group $P2/c$) structure types at different temperatures (room and higher) were analyzed. Consideration of chemical and structural factors and visualization of conduction pathways are promoted the determination of mechanisms and other spatial features of ions migration in crystals. This approach allowed also the forecast of crystal properties and applications. The some basic concepts on micro-level investigation of the mobile ion migrations in crystal lattice and previous results of calculations were considered in our works [8-10].

We show the mobility of W ions in the crystals AWO_4. The obtained results were applied to design of structural defects. The own point defects are considered. In particular the plurality of the WO_4^{2-} oxy-anion as known basic luminescent centers in AWO_4 crystals was motivated.

[1] V.N. Shevchuk, I.V. Kayun, *Acta Phys. Polon. A* **117**(1) (2010) 150-154.
[2] V.N. Shevchuk, I.V. Kayun, *Chem. Met. Alloys* **4** (2011) 72-76.
[3] A.K. Ivanov-Shits, I.V. Murin, *Ionic of solid state. In 2 vol.,* Vol. 1, St. Peterburg University Press, St. Peterburg, 2000, 616 p.; Vol. 2, 2010, 1000 p.
[4] E.Yu. Konysheva, A.Ya. Neiman, E.M. Gorbunova, *Izvestiya RAN. Seriya Fiz* **66**(6) (2002) 830-833.
[5] J.A. Groenink, H. Binsma, *J. Sol. State Chem.* **29**(2) (1979) 227-236.
[6] V.A. Blatov, G.D. Illyushin, O.A. Blatova, N.A. Anurova, A.K. Ivanov-Shits, L.N. Dem'yanets, *Acta Crystallogr. Sect. B* **62** (2006) 1010-1018.
[7] V.A. Blatov, *IUCr CompComm Newsletter* **7** (2006) 4-38.
[8] V.N. Shevchuk, I.V. Kayun, *Proc. Int. Conf. Oxide Materials for Electronic Engineering,* OMEE-2014, Lviv, Ukraine, 2014, pp. 117-118.
[9] V.N. Shevchuk, I.V. Kayun, *Proc. Fifth Int. Conf. Analytic Number Theory and Spatial Tessellations,* Kyiv, Ukraine, 2013, pp. 83-84.
[10] V. Shevchuk, I. Kayun, *Proc. VIIIth Ukrainian-Polish Sci. Pract. Conf. Electronics and Information Technologies,* Lviv-Chynadiyevo, Ukraine, 2016, pp. 167-170.

The Electric Properties of $Na_{0.5}Bi_{0.5}TiO_3$ and $0.87Na_{0.5}Bi_{0.5}TiO_3$ - $0.13BaTiO_3$ Single Crystals

T.V. Kruzina[1], V.M. Sidak[1], M.P. Trubitsyn[1], S.A. Popov[1], A.Yu. Tuluk[1], J. Suchanicz[2]

[1]*Oles Honchar Dnipropetrovsk National University, 72 prosp.Gagarina, 49010 Dnipro, Ukraine*
[2]*Institute of Physics, Pedagogical University, ul. Podchorazych 2, 30-84 Krakow, Poland*

The sodium bismuth titanate $Na_{0.5}Bi_{0.5}TiO_3$ (NBT) and $Na_{0.5}Bi_{0.5}TiO_3$-based solid solutions are considered as promising ecologically friendly materials for piezoelectric devices and electromechanical transducers [1]. In the abstract we study the effect of heat treatment on the electric properties of NBT and $0.87Na_{0.5}Bi_{0.5}TiO_3$- $0.13BaTiO_3$ (0.87NBT-0.13BT) single crystals. The objective of the study is to reveal the contributions of intrinsic defects to the electric properties of the crystals studied.

The permittivity ε and conductivity σ were measured by using an AC bridge P5083 in the frequency range 0,5÷100 kHz and the temperatures diapason 300K÷800 K. The as-grown samples were annealed in air at the temperature 1100K (1 h) and then in vacuum at 1100K (2 h). Temperature- frequency dependencies of ε and σ were measured for as-grown samples and after each heat treatment. The spectra of complex impedance were measured by Tesla BM-507 impedance meter operating in frequency range $5Hz \div 5 \cdot 10^5 Hz$. Temperature of the samples was regulated within the interval from 600K to 900 K.

It was shown that ε and σ for the studied crystals strongly depended on heat treatment atmosphere and temperature. Annealing at T_{ann}=1100 K in air resulted in disappearance of ε relaxation peak near 670 K and significantly decreased conductivity. Subsequent annealing at T_{ann} in vacuum restored low-frequency relaxation maximum of ε but practically did not change σ. The data obtained are discussed in assumption that heat treating in air decreases content of oxygen vacancies V_O, whereas annealing in vacuum generates additional amount of V_O [2].

In order to clarify the mechanisms of charge transport in NBT and 0.87NBT-0.13BT crystals we studied the spectra of complex impedance $Z^*(\omega)=Z' - i \cdot Z''$. Before the measurements the samples were annealed in air at 900K for 1h in order to remove low-frequency dispersion of ε near 670 K. Experimental spectra were plotted as diagrams on the complex (Z'-Z'') plane and discussed on the basis of the equivalent circuits approach. In the studied temperature-frequency range the hodographs of NBT crystals consist of two arcs which are described by impedance of two parallel RC circuits which are connected in series. The hodographs of 0.87NBT-0.13BT crystals consist of a single arc. It is supposed that charge transfer in the bulk of NBT contains the contributions of electronic and ionic conductance. Ionic conductance can be result of oxygen vacancies $V_O^{\bullet\bullet}$ movement. Electrons can hop via traps such as F^+ centers. The low-frequency arc in the experimental hodographs reflects electron conductivity in the near-electrode regions. The effect of $BaTiO_3$ additive on the mechanisms of charge transfer in NBT crystals is discussed.

[1] S. Nahm, S. Priya, *Lead-Free Piezoelectrics*, Springer, New York, 2012.
[2] T.V. Kruzina, V.M. Sidak, M.P. Trubitsyn et al., *Ferroelectrics* **462** (2014) 140.

3D Model of Phase Diagram for System $MgO-SiO_2-Al_2O_3$ and its Application

V. Lutsyk[1,2], A. Zelenaya[1]

[1]*Institute of Physical Materials Science SB RAS, Ulan-Ude, Russia*
[2]*Buryat State University, Ulan-Ude, Russia*

Systems $CaO(MgO)-SiO_2-Al_2O_3$ have a great practical importance, and their phase diagrams (PD) are used not only for the description of properties of advanced and building materials, but for the characterization of geological objects too. Data for invariant processes in the binary and ternary systems (with taking into account the existence and type of binary and ternary compounds) is the base for creation of schema of mono- and invariant equilibria. At the first stage for construction of 3D model, the invariant horizontal complexes at the temperatures of ternary points are reconstructed. Then they are completed by the ruled and unruled surfaces, and the phase regions are formed [1-3].

The system $MgO-SiO_2-Al_2O_3$ has a rather complex geometric structure. It includes four binary compounds and two ternary compounds. It's characterized by 11 invariant transformations: three eutectics, one peritectic, five quasiperitectic equilibria and two four-phase regroupings of phases with polymorphous modifications of silicon oxide (cristobalite and tridymite). Obtained computer model of phase diagram for system $MgO-SiO_2-Al_2O_3$ includes liquid immiscibility surface, 10 liquidus surfaces, 78 ruled surfaces, 11 horizontal complexes at the temperatures of invariant points, 21 two-phase regions and 29 three-phase regions. Projection of PD is divided into 100 two-, 170 one- and 71 zero-dimensional concentration field.

The diagrams of vertical mass balance have been calculated for each concentration field. They permit to obtain the lists of intersected phase regions and the crystallization stages for given mass center over the entire temperature range. In addition, the list of microconstituents for each field is obtained on the base of this investigation. As a result, we can identify the concentration fields with coinciding sets of crystallization scheme and microconstituents and the fields with individual characteristics [4]. However, some concentration fields can differ by the crystallization stages but coincide by the microconstituents with neighboring fields.

There are a large number of concentration fields with coinciding microconstituents in the SiO_2 angle, unlike other parts of PD. The reason is the presence of phase regions with liquids immiscibility and two polymorphous modifications of SiO_2. Processes occurring in the phase regions L_1+L_1, $L_1+L_1+B_1$, $L+B_1$ (B_1 - cristobalite) not influence on the final set of microconstituents, because the products of reactions for these fields are fully expended. Other parts of PD have the similar influence on the microstructure.

Therefore, analysis of concentration fields using the model of phase diagram is a tool to design the microconstituents sets of the heterogeneous material. All possible crystallization schemas of considered system and the content of each microstructural constituents taking into account its origin are analyzed by means of PD model.

Acknowledgements. This work was been performed under the program of fundamental research SB RAS (project 0336-2016-0006), and was partially supported by the RFBR projects 15-43-04304, 16-48-030851, 17-08-00875 and the RSF project 17-19-01171.

[1] V. Lutsyk, A. Zelenaya, Építőanyag - *Journal of Silicate Based and Composite Materials* **65** (2013) 34-38.
[2] V. Lutsyk, A. Zelenaya, *Solid State Phenomena* **200** (2013) 73-78.
[3] V.I. Lutsyk, A.E. Zelenaya, E.R. Nasrulin, E.S. Bimbaev, *Melts* **3** (2016) 206-215.
[4] V.I. Lutsyk, A.E. Zelenaya, E.R. Nasrulin, A.M. Zyrianov, *Melts* **3** (2016) 216-225.

Defects Related Scintillation Properties of Yttrium-Aluminum Garnet Crystals

N. Shiran, A. Gektin, V. Nesterkina, S. Vasyukov, O. Zelenskaya, K. Hubenko

Institute for scintillation materials NAS of Ukraine, 60 Nauki Avenue, 61001 Kharkov, Ukraine

Crystals of yttrium aluminum garnet (YAG) emit a broad luminescence band peaking at 300 nm under x-irradiation associated with the presence of anionic and cationic vacancies, their complexes and antisites. The summary of the supposed origin of defects is presented in [1-3]. Radio-luminescence of pure crystals most probably related to excitons localized around defects, due to violation of the stoichiometric composition. This is supported by the absence of emission and absorption bands in UV range in the nanocrystalline films and optical ceramics produced at lower temperatures.

The investigation is devoted to reveal the defects related effect on scintillator performance of pure yttrium aluminum garnet crystals.

Absorption in UV-VIS-IR, emission and thermostimulated luminescence as well as scintillation properties were determined for different kind of nominally pure crystals. The variable concentration of defects, which correspond to the absorption band in the range of 200 - 400 nm, was estimated. The undoped crystals excited with X-ray demonstrate the complicated emission band in UV wavelength region with peak at around ~290-310 nm. The experimental results point out that the concentration of native structure defects plays an important role in emission efficiency. The intensification of luminescence is only due to suppressing trapping defects. The results obtained shows that the emission' intensity is enhanced in samples which have the highest transparency in UV region.

According to the pulse height spectra recorded under γ ^{137}Cs, the light outputs of pure YAG crystal is nearly twice higher than BGO, and closed to Ce-doped crystal. Decay times constants were estimated to be approximately 7 ns and 460 ns, which agrees the data resulted in [4]. Factors affecting the scintillation efficiency in YAG have been discussed. Scintillation properties show the promising of YAG crystal application as a scintillator.

[1] C.R. Varney, F.A. Selim, *AIMS Mat. Sci.* **2**(4) (2015) 560.
[2] N. Shiran, A. Gektin, K. Gubenko et al., *Funct. Mat.* **23**(2) (2016) 191.
[3] C.R. Varney, M.A. Khamehchi, F.A.Selim, *Rev. Sci. Instr.* **83** (2012) 103112.
[4] Y. Fujimoto, T. Yanagida, H. Yagi et al., *Opt. Materials* **36** (2014) 1926.

Building-Up of X-Ray Luminescence and Conductivity in ZnSe Crystals

M. Alizadeh[1], V.Ya. Degoda[1], N.Yu. Pavlova[2]

[1]*Taras Shevchenko National University of Kyiv, 64 Volodymyrs'ka Str., 01601 Kyiv, Ukraine*
[2]*National Pedagogical Dragomanov University, 9 Pyrogova Str., 01601 Kyiv, Ukraine*

In high-resistivity ZnSe crystals ($\rho \geq 10^{12}$ ohm•cm), at X-ray excitation luminescence (XRL) intensity observed two luminescence bands with maxima at 630 and 970 nm, and easily recorded the X-ray conductivity (XRC). Experimentally investigated the kinetics of luminescence and conductivity when the continuous X-ray irradiation (0,635 mW/cm^2) at temperatures of 8, 85, 295 and 420 K. The kinetics of luminescence and conductivity in crystal greatly depends not only on the concentration of different luminescence centers, but also on the concentrations of different traps.When the luminescence kinetics studies and conductivity can use the fact that at different temperatures have different relationships between the shallow and deep traps. And it should change the nature of the curves the luminescence and conductivity. An important feature of the measurements is the simultaneous recording of both the intensity of the luminescence emission bands and the amount of conduction current.

Experimentally found that the curves of XRL intensity bands 630 and 970 nm between a curve and the current of XRC building-up differ markedly at low temperatures (when the concentration of deep traps more for the concentration of small traps). But the most interesting feature of the kinetics observed for the building-up conductivity at low temperature (8 K) – be 2 seconds late by almost from the moment when the X-ray excitation starting. Also at low temperatures (8 and 85 K) observed a significantly lower the rate of building-up of current in comparison with the rate of the luminescence.

An explanation of the observed features in the XRL and XRC at different temperatures in these crystals of ZnSe. If you remember that the area of generation of free electron-hole pairs at each photo absorption of X-ray quant (Ø ~ 100-300 nm) is much smaller than the dimensions of the sample, and their concentration in this area of excitations are comparable to concentrations of luminescence centers and traps, the bulk recombination occurs in this area, which create a scintillation flash. Naturally, these recombine at the luminescence centers, free electrons and holes do not participate in current conduction. Thus, the more efficient the crystal as a scintillator, the lower portion of the ionizing radiation-generated free carriers participating in conduction current. In addition, to participate in the conduction current of free charge carriers have markedly spatially displaced from the area of generation due to the drift-diffusion motion, i.e. have a sufficiently long lifetime in the zone. At the helium temperatures, when all the traps in the crystal are deep, and the lifetime of free carriers increases as the traps filling rate. And, accordingly, current conduction occurs only after partial traps filling rate and speed with increasing radiation dose reflects the rate of filling the traps. For luminescence kinetics have an instant increase in intensity due to scintillation, and further a relatively small increase in the expense of increasing the concentration of luminescence centers reloaded during the X-ray crystal phosphor excitation.

Trap Settings for the Free Charge Carriers

V.Ya. Degoda[1], M. Alizadeh[1], N.Yu. Pavlova[2]

[1]*Taras Shevchenko National University of Kyiv, 64 Volodymyrs'ka Str., 01601 Kyiv, Ukraine*
[2]*National Pedagogical Dragomanov University, 9 Pyrogova Str., 01601 Kyiv, Ukraine*

The presence of traps for carriers determine the kinetics of luminescence and conductivity in the crystal. Each type of traps, but their concentration in the material (ν_i), is determined by several parameters: depth local level (E_i), frequency factor (w_{0i}), sections localization of electrons and holes (σ_i^-, σ_i^+). Detailed study of the energy spectrum of traps with curved thermally luminescence (TSL) and conductivity (TSC) give the value of thermal delocalization energies and frequency factors. Then there is the issue and how to find sections localization of free carriers in these traps and their concentration. Note that simple experimental methods to determine these parameters traps there.

The analysis to contain free electrons in various traps, ***shallow*** (for which the probability of high thermal delocalization $w_{(i-1)} = 1/\tau_{(i-1)} >> 1\ s^{-1}$, respectively, the Fermi level is below the local level trap in the restricted area); ***phosphorescent*** (for which the probability of carrier delocalization at temperature T is $w_i \sim 1\ s^{-1}$ and the Fermi level almost coincides with the level of local traps); ***deep*** (for which the probability of thermal delocalization very small $w_{(i+1)} = 1/\tau_{(i+1)} << 1\ s^{-1}$ and the average lifetime of charge carriers in localized states far exceeds ten minutes, i.e. the total time of excitement and registration phosphorescence and, accordingly, the Fermi level is above the local level traps in the bandgap). Please be aware that the distribution of traps in shallow, deep and phosphorescent depends on the temperature (T) at which the sample excitation.

The analysis obtained that all types of traps sections defined localization of free electrons simple equation:

$$s_i^- = \frac{w_{0i}}{u^- N_C}.$$

where: u^- – thermal velocity of free electrons in the conduction band $\left(u^- = \sqrt{\frac{2kT}{3m_e^*}}\right)$; $N_C = 2\left(\frac{2p\, m_e kT}{h^2}\right)^{\frac{3}{2}}$ – the effective density of states for electrons in the conduction band; m_e^* – effective electron mass, h - Planck's constant. Accordingly, the crystal, which traps energy spectrum described formula harmonic oscillator sections localization of free charge carriers will be inversely proportional to the depth of the trap. This conclusion is supported by experimental studies of light-sum accumulation in garnet ($Y_3Al_5O_{12}$) crystals and in high-crystals of ZnSe. In these crystals, there is a rapid accumulation of smaller carriers on traps compared to the deeper traps.

Microstructure Evaluation of Doped Al-Ti and Al-Cr Alloys

K. Labisz[1,2], J. Konieczny[1,2], J. Ćwiek[1,2], Ł. Wierzbicki[1,2]

[1]*Department of Railway Transport, Faculty of Transport affiliation, Silesian University of Technology, Krasińskiego 8, 41-019 Katowice, Poland*
[2]*Reserch and Educational Centre for Specialist of Railway Transport, Silesian University of Technology, Krasińskiego 8, 41-019 Katowice, Poland*

In this paper are presented the results of experimental research on the influence of calcium addition on the microstructure and mechanical properties of the aluminium-titanium and chromium alloy. Al-Ti and Al-Cr alloy systems is a of a group of Al-based peritectic systems with potential for development, and application especially in transport industry.

As alloying additive and refiner of the investigated aluminium alloy there is used the basis alloy in form of Al-Ca. After casting of this material the solution heat treatment was applied in order to investigate the applied solution heat treatment parameters time and temperature, which were changed in a defined range. These alloys contain also intermetallic phases, which act as crystallisation basis in the process of coagulation of aluminium. The chosen alloy contains especially the Al_3Ti and Al_4Cr intermetallic phases particles, in relatively huge amount, which act as active media of heterogenic crystallisation and dissolves rapidly in the investigated liquid Al alloy as well as reveals a modifier effect even after a few minutes of introduction into the molten metal [1-6].

The precipitation process was studied after solution heat treatment and ageing. It was shown that the investigated alloys with ternary additions typically have microstructures with dispersed intermetallic phases, distributed uniformly in an Al matrix. The $TiAl_3$ intermetallic phase is intrinsically stable with a melting point of 1623 K, in a higher temperature compared to the aluminium chromium alloy. Due to the low equilibrium solid solubility and diffusivity, the potential exist for generating a refined microstructure with fine dispersion of intermetallic phases by additions or by controlled solidification during the heat treatment process. Furthermore, the presence of Ca can lead to the occurrence of new unknown phases as well as can enhance the thermal stability of ternary Al-Ti-Ca and A-Cr-Ca systems because of its higher melting point then the base alloys. For investigation the X-ray diffraction (XRD) was used to identify the phases present in the as-cast alloy directly after casting, the microstructure of the samples was characterized using transmission electron microscopy (TEM) together with energy dispersive spectroscopy (EDS). Vickers microhardness tester with a load of 0.05 kg was also performed for mechanical properties investigations.

[1] F. Romankiewicz, Modyfikacja aluminium dodatkiem AlTi6, *Archiwum Odlewnictwa* **1**(1) (2001) 159-162.
[2] L.A. Dobrzanski, K. Labisz, M. Piec, J. Lelatko, A. Klimpel, Structure and properties of the 32CrMoV12-28 steel alloyed with WC powder using HPDL laser, *Materials Science Forum* **530**(531) (2006) 334-339.
[3] L.A. Dobrzanski, M. Czaja, Borek, K. Labisz, T. Tanski, Influence of hot-working conditions on a structure of X11MnSiAl17-1-3 steel for automotive industry, *International Journal of Materials & Product Technology* **51**(3) (2015) 264-280, doi: 10.1504/IJMPT.2015.072246.
[4] M. Gwoździk, Z. Nitkiewicz, Wear resistance of steel designed for surgical instruments after heat and surface treatments, *Archives of Metallurgy and Materials* **54**(1) (2009) 241-246.
[5] F. Pagliara, L. Biggiero, A. Patrone, F. Peruggini, An analysis of spatial equity concerning investments in high-speed rail systems: the case study of Italy, *Trnsport Problems* **11**(3) (2016) 55-68, doi: 10.20858/tp.2016.11.3.6.
[6] P. Folęga, P. Czech, T. Figlus, G. Wojnar, Marking influence of cracking gear-tooth on changes meshing stiffeness by used bem, *Scientific Journal of Silesian University of Technology. Series Transport* **65** (2009) 31–38, doi: https://doi.org/10.20858/sjsutst.1983.1.1.

Heating Influence on the Electric Conductivity of the Epoxy-$Bi_{50}Pb_{25}$ $Sn_{12,5}Cd_{12,5}$ Composite

Ł. Wierzbicki, K. Labisz, J. Konieczny, J. Ćwiek

Department of Railway Transport, Faculty of Transport, Silesian University of Technology

The main object of research is to evaluate the volume resistivity of polymer–metal composites. In the research, $Bi_{50}Pb_{25}Sn_{12,5}$Cd12,5 alloy was used and an epoxy resin with hardener. Used in research alloy, commonly known as Wood's alloy, are a material with a low melting point of approximately 65°C.

Composites were made with different weight fraction of the alloy: 0, 20, 40, 60, 80% by weight fraction of the Wood's alloy in to epoxy resin complex.

The idea of presented research is verification of possibility to a variable in a physical state of the material as polymer fillers. The use of that fillers whose functional properties depend on the ambient temperature gives the possibility to obtain a new class of smart materials. The $Bi_{50}Pb_{25}Sn_{12,5}$Cd12,5 undoubtedly can be included as this type of fillers. The molten Wood's alloy definitely has different physical characteristics than the constant. The tests of electrical conductivity of the epoxy-Wood's alloy composite confirm these assumptions.

The performed research has proven that there resistivity dependence of the concentration of the alloy and the temperature. With the increase of the share of the weight alloy Wood's, resistivity decreases. The resistivity of samples decreases as the ambient temperature increases.

[1] R.A. Mrozek, P.J. Cole, L.A. Mondy, R.R. Rao, L.F. Bieg, J.L. Lenhart, Highly conductive, melt processable polymer composites based on nickel and low melting eutectic metal, *Polymer* **51** (2010) 2954–2958.

[2] R. Strümpler, J. Glatz-Reichenbach, Conducting polymer composites, *J. Electroceram.* **3** (1999) 329–346.

[3] A.L. Holbrook, Aluminum flake filled conductive plastics for EMI shielding and thermal conductivity, *Int. J. Powder Metall.* **22** (1986) 41–45.

Anomalous Thermal Expansion of $NdCo_{1-x}Ga_xO_3$

V. Hreb[1], V. Mykhalichko[1], L. Vasylechko[1], O. Zaharko[2], D. Chernyshov[3]

[1]*Lviv Polytechnic National University, Lviv, Ukraine*
[2]*Paul Scherrer Institut, Villigen, Switzerland*
[3]*Swiss-Norwegian Beamlines at the ESRF, CS40220 38043 Grenoble Cedex 9, France*

New mixed cobaltites-gallates with nominal compositions $NdCo_{0.8}Ga_{0.2}O_3$ and $NdCo_{0.3}Ga_{0.7}O_3$ has been obtained from corresponding oxides by solid state reaction in air at 1373 K. X-ray powder diffraction revealed orthorhombic perovskite structure isotypic with $GdFeO_3$. The unit cell dimensions of the samples under investigation are in good agreement with the structural data of the parent $NdCoO_3$ and $NdGaO_3$ compounds, thus proving formation of continuous solid solution in the $NdCoO_3$–$NdGaO_3$ system. According to *in situ* high-temperature X-ray synchrotron powder diffraction examination performed at SNBL BM1A beamline of ESRF, both samples remain orthorhombic in a broad temperature range of 298–1100 K. No symmetry related structural changes were observed. However, comprehensive analysis of the obtained structural parameters of $NdCo_{0.8}Ga_{0.2}O_3$ and $NdCo_{0.3}Ga_{0.7}O_3$ revealed anomalous nonlinear lattice expansion, which is reflected in a sigmoidal dependence of the unit cell dimensions and in abnormally large values of thermal expansion coefficients (TEC) with broad maxima at around ~640 K and ~700 K, respectively. Evidently, similar to the "pure" rare earth cobaltites, these anomalies are caused by an excitation of Co^{3+} ions from low spin to the higher spin states and the coupled magnetic and insulator-metal (I-M) transition. In particular, corresponding transitions occurred in $NdCoO_3$ at 336 K and 635 K, respectively, are reflected in pronounced anomalies in the lattice expansion and clear maxima at the TEC curve at ~ 440 and 620 K [1]. In contrast, neodymium gallate $NdGaO_3$ does not display detectable lattice anomalies in high-temperature region and its unit cell dimension changes in a "normal" way [2].

The lattice anomalies in the mixed cobaltite-gallate series $NdCo_{1-x}Ga_xO_3$ become less pronounces with decreasing cobalt content and the characteristic maxima at the TEC curves are shifted to the higher temperature comparing with the "pure" $NdCoO_3$. Extra structural anomalies, which are evidently associated with the electronic and magnetic phase transitions occurred in $NdCo_{0.8}Ga_{0.2}O_3$ and $NdCo_{0.3}Ga_{0.7}O_3$, are detected in the temperature dependence of the selected bond lengths and octahedra tilt angles. The *M*–O–*M* angles in RMO_3 perovskites characterize the M^{3+}–O^{2-}–M^{3+} overlaps and determine their main magnetic and transport properties [3]. In the $RCoO_3$ series the increase of cooperative rotations of corner-shared CoO_6 octahedra leds to reduction of the bandwidth of Co(3*d*)–O(2*p*) interactions and increase of the spin-state transition temperature. The temperature dependence of the band width in the mixed cobaltites-gallates $NdCo_{0.8}Ga_{0.2}O_3$ and $NdCo_{0.3}Ga_{0.7}O_3$ shows clearly decreasing behaviour thus proving increasing population of the exited spin states of Co^{3+} ions with the temperature. It is evident that the coupling of the electronic and magnetic transitions combined with the lattice results in extremely complicated magnetic and electronic phase diagram of the mixed cobaltite-gallate systems.

Acknowledgements. The work was supported in parts by the Ukrainian Ministry of Education and Sciences under Project "RZE" and ICDD Grant-in-Aid program. The authors thank Yu.Prots and Yu. Dovgalyuk for the kind assistance with synchrotron powder diffraction measurements during beamtime allocated to the ESRF Experiment MA-2320.

[1] K. Knížek et al., *Phys. Rev. B* **79** (2009) 134103.
[2] A. Senyshyn et al., *J. Alloys Compd.* **382** (2004) 84–91.
[3] J.-S. Zhou, J.-Q. Yan, J. B. Goodenough, *Phys. Rev. B* **71** (2005) 220103.

Thermal Behaviour of $PrCo_{1-x}Fe_xO_3$ Probed by X-Ray Synchrotron Powder Diffraction and Impedance Spectroscopy Measurements

O. Pekinchak[1], D.Yu. Sugak[1], S.B. Ubizskii[1], Yu. Suhak[2], H. Fritze[2], L. Vasylechko[1]

[1] *Lviv Polytechnic National University, Lviv, Ukraine*
[2] *Institute of Energy Research and Physical Technologies, Clausthal University of Technology, Goslar, Germany*

Crystal structure and transport properties of the mixed praseodymium cobaltites-ferrites $PrCo_{1-x}Fe_xO_3$ have been studied in the temperature range of 298–1173 K by a combination of *in-situ* X-ray synchrotron powder diffraction and temperature dependent impedance spectroscopy measurements.

Series of micro- and nanocrystalline powders of $PrCo_{1-x}Fe_xO_3$ were obtained by solid-state reactions technique in air at 1473 K and *via* low-temperature sol-gel citrate route at 973 K, respectively. At the ambient conditions both series of the samples adopt orthorhombic perovskite structure isotypic with $GdFeO_3$. Concentration dependence of the unit cell dimensions of $PrCo_{1-x}Fe_xO_3$ proves a formation of continuous solid solution, peculiarity of which is the lattice parameters crossover and appearance of dimensionally cubic structure at $x = 0.4$ [1]. *In-situ* high temperature powder diffraction examination of $PrCo_{1-x}Fe_xO_3$ series revealed considerable anomalies in the lattice expansion which are especially pronounced for the cobalt-reach specimens. These anomalies, which are reflected in a sigmoidal dependence of the unit cell dimensions and in the considerable increasing of the thermal expansion coefficients, are obviously associated with transitions of Co^{3+} ions from low spin to the higher spin states and the coupled metal-insulator transitions, occurred in in rare earth cobaltites at the elevated temperatures. Observed deviations in the lattice expansion in the $PrCo_{1-x}Fe_xO_3$ series become less pronounced with the decreasing cobalt content, but they are clearly detectable even in the iron-richest $PrCo_{0.1}Fe_{0.9}O_3$ specimen. Indeed, the temperature-dependent impedance measurements clearly prove the change of conductivity type from dielectric to the metallic behaviour in the mixed cobaltite-ferrites $PrCo_{1-x}Fe_xO_3$ at the elevated temperatures (Figure). The temperature of insulator-metal transition in $PrCo_{1-x}Fe_xO_3$ series increases from 723 K for $x = 0.4$ to 1100 K for $x = 0.8$ (Figure), which is in a good agreement with the results obtained from the analisys of thermal expansion data. Activation energy of electrical conductivity in the $PrCo_{1-x}Fe_xO_3$ series derived from the Arrhenius plots increases systematically with increasing Fe content from 0.56 eV for $x = 0.4$ to 0.93 eV for $x = 0.8$ samples, being in good agreement with the literature data for the parent $PrCoO_3$ and $PrFeO_3$ compounds (Figure, inset).

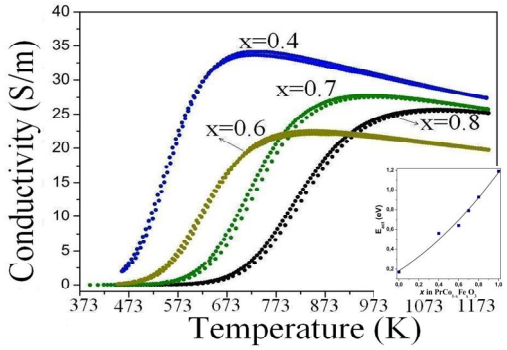

Figure. Temperature dependencies of the electrical conductivity of the $PrCo_{1-x}Fe_xO_3$ samples and concentration dependence of activation energy in the $PrCo_{1-x}Fe_xO_3$ series (inset).

[1] O. Pekinchak et al, *Nanoscale Research Letters* **11**:75 (2016) 1–6.

Acknowledgements. The work was supported in parts by the Ukrainian Ministry of Education and Sciences under Projects “KMON” and “RZE”. Yu. S. acknowledges the support from Energie-Forschungszentrum Niedersachsen.

The Influence of Partial Isomorphic Substitution on Band Structure and Optical Parameters of $ABSO_4$ Group Crystals

P.A. Shchepanskyi[1,2], V.M. Gaba[3], V.Yo. Stadnyk[1], M.Ya. Rudysh[1,2]

[1] *Ivan Franko National University of Lviv, Str. Kyrylo and Mefodiy 8, 79005 Lviv, Ukraine*
[2] *Jan Dlugosz University in Częstochowa, Al. Armii Krajowej 13/15, 42-200 Czestochowa, Poland*
[3] *Lviv Polytechnic National University, Str. S. Bandera 12, 79013 Lviv, Ukraine*

Crystals represented by $ABSO_4$ formulabelong to A_2BX_4 group and are interesting due to their ferroelectric, ferroelastic, superionic, optical and other properties.

In this work partial isomorphic substitution $K \rightarrow NH_4$ study on electronic and optical properties is provided by running first principle calculations ofrepresentative of K_2SO_4 – $(NH_4)_2SO_4$ system, $K_{1.75}[NH_4]_{0.25}SO_4$ crystal.

$K_{1.75}[NH_4]_{0.25}SO_4$ crystal belongs to *Pnma* (№ 62) space group. Its lattice parameters are equal: a = 7.5562(3) Å, b = 5.7917(2) Å, c = 10.1016(4) Å, Cell volume = 442.08(5) Å^3.

Since band structures for K_2SO_4 (PS) [1] and $(NH_4)_2SO_4$ (AS) [2] crystals are known as well as for some other isomorphic crystals of that family, correlation between structure and properties can be revealed.

Calculations of the band structure in this work were carried out self-consistently using the Kohn-Sham formalism within density functional theory (DFT). As input parameters the X-ray analysis data was used. Basis was chosen in a form of plane waves. To describe the exchange-correlation interaction the exchange-correlation functional with the generalized gradient approximation (GGA) was used.

Band energy structure of $K_{1.75}[NH_4]_{0.25}SO_4$ crystal reveals low dispersion of energy levels. Band gap is of a direct type and corresponds to the optical transitions in the Γ point of the Brilluoin zone. Obtained E_g = 4.8eV value is for about 0.4 eV lower then calculated for K_2SO_4 crystal [1].

Two top valence bands (VB) are almost entirely formed by *p*-electrons of oxygen from SO_4^{2-} anion complexes. Contribution of potassium atoms electronic states is major for VB at -28 eV.

The bottom of the conduction band (CB) is formed mainly by hydrogen atoms (*s*-states); higher areas of this band – by mixed set of chemical elements and orbital moments.

Obtained band structure and density of states of the $K_{1.75}[NH_4]_{0.25}SO_4$ crystal are quite similar to calculated for PS [1]. An exception is the fact that bottom of CB in $K_{1.75}[NH_4]_{0.25}SO_4$ is formed by states of hydrogen, while similar role in K_2SO_4 playpotassium states. That leads to decreasing of band gap in the mixed crystal for about 0.4 eV in comparison with PS.

From the calculated dielectric function the refractive indices dispersion for three crystal optics directions is deduced. Order of obtained curves coincides with experimental. The difference is that dispersion of theoretically obtained curves is of the same magnitude for three directions of crystal, while magnitudes for experimental dependences differ, leading to the crossing $n_x = n_y$in the IR spectrum region. Such discrepancy is assumed to occur due to neglect of IR absorption of crystal in the simulations and presence of impurities in real crystal.

[1] B. Andriyevsky, M. Jaskolski, V.Y. Stadnyk, M.O. Romanyuk, Z.O. Kashuba, M.M. Romanyuk, *Computational Materials Science* **79** (2013) 442–447.

[2] B. Andriyevsky, K. Doll, M. Jansen, *Journal of Physics and Chemistry of Solids* **71** (2010) 357–363.

SECTION 3

NANOPARTICLES, NANO-CERAMICS AND NANO-COMPOSITES

Life after Scherrer Formula: Modern Methods of Nanostructure Analysis Using Diffraction

M. Leoni

DICAM University of Trento, 38123 Trento, Italy

Scherrer formula [1] is one of the most common Swiss-knife tools for most scientists working in the nanomaterials field. Albeit being 99 years old, it is in fact still widely employed to extract some "average size" value for a nanocrystalline specimen from a diffraction pattern.

Unfortunately, most of the users ignore that even if the result provided by Scherrer formula has the dimensions of a length, it seldom corresponds to the average size of the nanocrystals composing the specimen under study. To overcome the limitations of Scherrer formula, several approaches have been proposed in the years. The large revolution, however, happened in the last decades with the introduction of full pattern analysis.

In particular, a fast and more physical approach like the Whole Powder Pattern Modelling (WPPM [2]) will be shown, allowing a detailed description of the nanostructure in terms of shape and size distribution of the coherently scattering domains and quantitative information on the defects they might possess. The performance of the WPPM will be shown both on simulated atomistic specimens and on real materials.

The technique is solid when the defects don't alter the overall (global) symmetry of the lattice. When this is no longer the case (e.g. in advanced technologically-relevant materials where stacking defects are present), the modelling of diffraction data is more challenging, but a clear and fast separation of structural and nanostructural features is possible, leading to unexpected results [3-5].

[1] P. Scherrer, Nachr. Ges. Wiss. Goettingen, Math.-Phys. Kl. (1918) 98–100.
[2] P. Scardi, M. Leoni, *Acta Crystallogr. A* **58** (2002) 190-200.
[3] M. Leoni, A. Gualtieri, N. Roveri, *J. Appl. Crystallogr.* **37** (2004) 166-173.
[4] R. Koch, M. Leoni, (2016), (*submitted*).
[5] M. Leoni, (2017), (*in preparation*).

Diversity of Nanocrystal Shape and Morphology: A Brief Review

W. Paszkowicz and K. Fronc

Institute of Physics, Polish Academy of Sciences, Aleja Lotników 32/46, PL-02668 Warsaw, Poland

During recent years the science and technology of nanosized crystals advanced rapidly. This progress became possible by dint of development of electron microscopic techniques enabling the visualisation of an individual nanocrystals. One of fascinating opportunities in this field are the growth techniques permitting for the control of the nanocrystal shape. The nanocrystal shape is an important feature as it influences the physicochemical properties of the material. A large free surface is a shape-dependent factor deciding about the applicability of the nanostructure as catalysts or sensor. A valuable recent development is the synthesis of low-density architectures can be designed for construction of ultralight alloys [1].

The diversity of already reported geometrical nanocrystal forms is quite large. Many techniques of nanocrystal synthesis and growth are known such as hydrothermal route, sputtering, epitaxy. New methods are under development, one of them enables production of metallic and oxide nanoparticles in an original way, namely with a contribution of microbes [2]. They provide nanoparticles of irregular as well as regular shapes. The nanocrystal form and morphology can be controlled through choice of reaction parameters (see e.g. ref. [3,4]), by tuning the fluid composition in the supercritical fluid process [5]; this issue has been a subject of a review [6]. Some techniques lead to the simplest spherical or polyhedral shapes, some others are used to get forms of high geometrical and morphological complexity. The complexity involves both, the geometry of the hierarchical structures (fractals, arrays, superlattices, complexes...) and their building blocks such as nanocapsules, nanoboxes, necklaces, nanoflowers, nanochains, dendrites, multipods, etc. Such unusual forms include, for example, disordered pyramidal pits ('negative pyramids') [7] and hedgehog-like nanocrystals of complex geometrical and chemical nature [8].

Computational approaches are under development aiming for prediction or explanation of the nanocrystal shape and morphology (see, e.g., ref. [9]). Almost twenty simple experimentally found shapes have been distinguished for metallic nanocrystals [10]. The existing shape classification schemes can become a basis for a more detailed shape and morphology classification and analysis.

[1] R. Rettig et al., *Superalloys 2016: Proceedings of the 13th International Symposium on Superalloys*, ed.: M. Hardy, E. Huron, U. Glatzel, B. Griffin, B. Lewis, C. Rae, V. Seetharaman, S. Tin (The Minerals, Metals & Materials Society), 2016.
[2] K.N. Thakkar et al., *Nanomed. Nanotech. Biol. Medicine* **6** (2010) 257-262.
[3] Z.-W. Chou et al., *Chem. Mater.* **21** (2009) 4955–4961.
[4] T.D. Nguyen et al, *Langmuir* **25**(9) (2009) 5322–5332.
[5] Q.D. Truong, *Sci. Rep.* **4** 3975(1-8).
[6] S. Kumar et al., *Small* **2** (2006) 316-329.
[7] E. Guziewicz et al., *Thin Solid Films* **446** (2004) 172-177.
[8] M. Bialoglowski et al., *Cryst. Res. Technol.* **50** (2015) 797-800.
[9] B.B. Kappes et al., *Cryst. Res. Technol.* **50** (2015) 9-10, 801-816.
[10] Y. Xia et al., *Angew. Chem. Intern. Ed.* **48** (2009) 60-103.

Sol-Gel Derived Lanthanide-Substituted Layered Double Hydroxides $Mg_3/Al_{1-x}Ln_x$

A. Kareiva[1], A. Smalenskaite[1], S. Şen[2], A. N. Salak[3], M.G.S. Ferreira[3], A. Beganskiene[1]

[1]*Department of Inorganic Chemistry, Institute of Chemistry, Vilnius University, Naugarduko 24, LT-03225 Vilnius, Lithuania*
[2]*Department of Chemistry, Faculty of Arts and Sciences, Dumlupınar University, 43820 Kütahya, Turkey*
[3]*Department of Materials and Ceramic Engineering/CICECO, University of Aveiro, 3810-193 Aveiro, Portugal*

Recently, considerable attention has been focused on incorporating rare earth ions into LDHs hosts to develop new functional materials, which resemble designed optical properties [1]. LDHs doped with Tb^{3+} ions in the brucite-like layers were prepared by a simple one-step co-precipitation method [2, 3]. Nanosized LDHs doped with Eu^{3+}, Yb^{3+}, Tb^{3+} and Nd^{3+} were prepared through the microemulsion method [4]. The Eu^{3+} and Nd^{3+} were incorporated also into hydrocalumite and mayenite [5]. The Zn/Al/Eu and Zn/Al/Dy LDHs were also reported as perspective and efficient luminescent materials [6-8]. Cerium-doped hydrotalcite-like precursors were also recently synthesized by co-precipitation method [9].

The main aim of this study was to investigate Nd^{3+}, Sm^{3+} and Eu^{3+} substitution effects in the $Mg/Al_{1-x}Ln_x$ systems (the Ln^{3+} concentration in the crystal lattice was changed from 0.05 to 10 mol%) fabricated for the first time to the best our knowledge by sol-gel synthesis route.

The $Mg_3/Al_{1-x}Ln_x$ LDH samples were synthesised by sol-gel method from the solution of metal nitrates, dissolved in 50 ml of distilled water. Secondly, 0.2 M citric acid was added and obtained solution was stirred for 1 h at 80 °C. Next, 2 ml of ethylene glycol have been added to the resulted mixture with continues stirring at 150 °C until the complete evaporation of solvent. The obtained gel was dried at 105 °C for 24 h. The mixed metal oxides were obtained by heating the gels at 650 °C for 4 h. The $Mg_3/Al_{1-x}Ln_x$ LDH specimens were obtained by reconstruction of MMO powders in water at 50 °C for 6 h under stirring. The samples obtained were characterized by X-ray diffraction (XRD) analysis, Fourier Transform Infrared spectroscopy (FT-IR), thermogravimetric (TG) analysis and scanning electron microscopy (SEM). The luminescent properties of $Mg_3/Al_{1-x}Ln_x$ LDH samples were also investigated. The results revealed that lanthanide element enters into a hydrotalcite structure containing Mg^{2+} and Al^{3+} cations in the brucite-like layers.

Acknowledgement. The work has been done in frame of the project TUMOCS. This project has received funding from the European Union's Horizon 2020 research and innovation programme under the Marie Skłodowska-Curie grant agreement No 645660.

[1] P. Gunawan, R. Xu, *J. Phys. Chem C* **113** (2009) 17206-17214.
[2] P. Vicente, M.E. Perez-Bernal, R.J. Ruano-Casero, D. Ananias, P.A.A. Paz, J. Rocha, V. Rives, *Micropor. Mezopor. Mater.* **226** (2016) 209-220.
[3] T. Posati, F. Costantino, L. Latterini, M. Nocchetti, M. Paolantoni, L. Tarpani, *Inorg. Chem.* **51** (2012) 13229-13236.
[4] M. Domiguez, M.E. Perez-Bernal, R. Ruano-Casero, C. Barriga, V. Rives, R.A.S. Ferreira, L.D. Carlos, J. Rocha, *Chem. Mater*. **23** (2011) 1993-2004.
[5] Z. Zhang, G.M. Chen, J.G. Liu, *RSC Adv*. **4** (2014) 7991-7997.
[6] X.R. Gao, L.X. Lei, L.W. Kang, Y.Q. Wang, Y.W. Lian et al., *J. All. Compd*. **585** (2014) 703-707.
[7] D.R.M. Vargas, M.J. Oviedo, F.D. Lisboa, F. Wypych et al., *J. Nanomater*. (2013) 730153.
[8] A.H. Tamboli, A.R. Jadhav, W.J. Chung, H. Kim, *Energy* **93** (2015) 955-962.
[9] A. Smalenskaite, A.N. Salak, M.G.S. Ferreira, A. Katelnikovas, A. Kareiva, *Appl. Clay Sci.* (2017), (*To be published).*

Oxide-Polymer Composites: Toward New Optical Materials

S.G. Nedilko

Taras Shevchenko National University of Kyiv, 64/13 Volodymyrska Str., 01601 Kyiv, Ukraine

There is a well known sentence that the "more new products have been developed in the last twenty years than in the prior history of materials science" [1]. A lot of new materials emerged and not only in traditional and well known technologies like to high-tech aircraft industry, electronics, biomedicine etc., but also in industry of consumer goods, e.g. It is obvious there is now a demand for environmental and human friendly materials. Advanced materials based on polymer matrix and incorporated with some nanosized compounds provide many additional advantages.

This work presents both review and original data about modern state of art concerning structure, physical properties, applications and prospects of some polymer based composites incorporated with micro/nanosized particles of various oxide compounds. Surely, the report emphasises those properties which define such composites as optical materials.

First, the results of synthesis, structure, morphology and spectroscopic study of the luminescent oxides, starting from simple zirconium oxide, ZrO_2, up to complex oxide containing simultaneously 2-3 various metal cations (M^{I} – M^{IV}; Na, Ca, Bi, Zr, e.g.) and 1-2 molecular anions like to $(BO_4)^{n-}$ (B = P, Mo, W, V) are described. These materials can themselves be useful in creation of new optoelectronics devices (WLED, phosphor converting covers of solar elements, e.g.), biomarkers etc.

Second, special attention is paid to description of the study of micro/nanocellulse which was used as polymer matrix. Cellulose based composites have strong promise due to their light weight, high tensile strength and modulus, and comparably low cost. Now, potential market for nanocellulose is very extensive.

That is whytwo sets of micro/nanocellulose samples were prepared using so called "dry' and "wet" procedure and prepared samples were incorporated with some oxides. The last set of the samples provides opportunity to elaborate the method of inorganic pollutions determination in the water. In fact, it is common knowledge that cellulose is a very effective sorbent. Really, synthetic sorbents based on polyethylene, propylene and other polymers show better performance, but they are not eco-friendly enough in comparison to cellulose.

[1] B.E. Brownell, *Transmaterial*. **6** (2006) 237.

Features of Crystal Structure and Luminescent Properties of the $La_{1-(x+y)}Eu_xCa_yVO_4$ Nanosized Compounds

O.V. Chukova, S.A. Nedilko, S.G. Nedilko, A.A. Slepets, T.A. Voitenko, M.A. Zelenko

National Taras Shevchenko University of Kyiv, 63/13 Volodymyrska Str., Kyiv, Ukraine

Among variuos types of optical materials orthovanadates are an important family of compounds those have actual and potential applications in the fields of laser hosts, catalysts, phosphors, sensors and polarizers. These compounds are chemically stable and non-toxic. Currently, some of mentioned applications require vanadate materials with improved efficiency of luminescence emission especially under excitation with light from near UV and violet spectral ranges. Now search for new vanadate compounds for these needs is carried out using variations of two and more cations in their composition including partial iso- and heterovalent substitutions. Intensities of luminescent emission of the RE activators in orthovanadate compounds can be effectively increased with the A^{2+} modifying cations. Properties of compositions with such heterovalent substitutions strongly depend on concentration ratios of the A^{2+} cations. Therefore, we expect that rare earth orthovanadate nanaparticles with heterovalent substitutions could bring an additional raise of luminescence intensity. We used the Ca^{2+} modifying impurities as first step of this elaboration.

In general, the ornhovanadates compounds crystallize in two polymorphs, a tetragonal zircon-type structure (space group: I41/amd, Z = 4) and a monoclinic monazite-type (space group: P21/n, Z = 4). Compounds with small rare-earth cations, $EuVO_4$ e.g., have zircone-type structure. Compounds with a large rare-earth cation, $LaVO_4$ e.g., have monazite-type structure. The aim of this work was to synthesize and study their and structural, morphological and other physical properties of the $La_{1-(x+y)}Eu_xCa_yVO_4$ ($0.05 \le x \le 0.3$, $0.05 \le y \le 0.2$) compounds. The $La_{1-(x+y)}Eu_xCa_yVO_4$ ($0.05 \le x \le 0.3$, $0.05 \le y \le 0.2$) samples were prepared by aqueous nitrate-citrate sol-gel synthesis route taking citric acid (CA) as a complexing agent. Phase compositions and crystal lattice parameters were determined using X-ray diffractometer DRON-3M ($Cu_{K\alpha}$-radiation with a Ni filter). The diffraction patterns were taken at a step of 2^0/min. The microstructure of the compounds was studied with a scanning electron microscope (SEM) Hitachi S – 2400. The pattern of the $La_{0.9}Eu_{0.05}Ca_{0.05}VO_4$, $La_{0.8}Eu_{0.1}Ca_{0.1}VO_4$ compounds fits well with monoclinic monazite-type, and $La_{0.65}Eu_{0.2}Ca_{0.15}VO_4$, $La_{0.5}Eu_{0.3}Ca_{0.2}VO_4$ samples crystallized in tetragonal zircon-type structure.

Luminescence spectra of the samples consist of narrow spectral lines in the 550 – 730 nm spectral range and the lines caused by the $^5D_0 \rightarrow {}^7F_J$ electron transitions in the Eu^{3+} ions. An addition of the Ca^{2+} ions increases intensity and changes spectra of the Eu^{3+} ions luminescence. The structure of the spectra also depends on the excitation light wave length. The carried out analysis has revealed that Eu^{3+} ions form at least two different types of emission centers in the studied materials. The assumption is made that I type centers are formed by the Eu^{3+} ions in their regular positions in the crystal lattice, while the II type centers have complex structure and they consists of Eu^{3+} ions, Ca^{2+} cations and oxygen vacancies. Correlations between luminescence properties and crystal structure of the samples were analyzed. The structure of the both types of emission centers had been analyzed. The samples of the $La_{0.9}Eu_{0.05}Ca_{0.05}VO_4$, $La_{0.8}Eu_{0.1}Ca_{0.1}VO_4$ compounds with monoclinic monazite-type are characterized by better efficiency of luminescence than $La_{0.65}Eu_{0.2}Ca_{0.15}VO_4$, $La_{0.5}Eu_{0.3}Ca_{0.2}VO_4$ samples with tetragonal zircon-type structures if excited from near UV and violet spectral ranges.

Structure, Optical and Dielectric Properties of Opal – Bismuth Silicate Nanocomposites

M. Derhachov[1], V. Moiseienko[1], N. Kutseva[1], B. Abu Sal[2], R. Holze[3], S. Pliaka[1], A. Yevchyk[1]

[1]*Oles Honchar Dnipropetrovsk National University, Dnipro, Ukraine*
[2]*Applied Physics Department, Faculty of Science, Tafila Technical University, Tafila, Jordan*
[3]*Technische Universität Chemnitz, Institute of Chemistry, Chemnitz, Germany*

Synthetic opals filled with oxide materials may be efficiently applied in photonics and energy storage systems [1], and may also serve as an excellent model structure to investigate the charge transfer processes under restricted volume conditions [2]. This work deals with growing bismuth silicate nanocrystals from the Bi_2O_3–SiO_2 melt inside opal pores and characterizing the obtained nanocomposites with employing X-ray diffraction (XRD), scanning electronic microscope (SEM), dielectric and optical spectroscopy technique.

Bulk and film bare opals grown by slow crystallization of silica globules colloidal suspension is impregnated with the melt of $Bi_{12}SiO_{20}$ (corresponding to the 6:1 molar ratio in the Bi_2O_3–SiO_2 system) at temperature slightly higher than 900 ^{0}C, the temperature of the $Bi_{12}SiO_{20}$ congruent melting. After holding for some time period (from 5 to 20 minutes), the samples are cooled down room temperature with the rate no more than 3 ^{0}C per minute.

Melt penetration into opal pores and filler's crystalline state is proved by SEM, XRD, and Bragg light reflection and Raman spectra measurements. The degree of pores filling is no less than 50 vol. %. The $Bi_4Si_3O_{12}$ phase is detected as dominant one in the XRD patterns and Raman spectra of the as-prepared nanocomposites. Its formation is supposed to be caused by changing in the Bi_2O_3–SiO_2 system molar ratio to 2:3 due to the melting of the 5 nm silica particles, involving in the globule structure [3]. The condensation of [SiO_4] tetrahedrons in silica globules should be taken into account, too.

The Raman intensity redistribution revealed by surface scanning may be originated from both the composition inhomogeneity and the structural light focusing together with concentration of the exciting radiation field nearby the surface and bulk defects in the opal matrix.

The obtained active matrix nanocomposites may be involved in process of optical radiation conversion due to their emission properties. Their photoluminescence spectra under 407 nm light-emitting diode and 514 nm laser excitation have a complicated structure, depending on the exciting beam position on the sample surface and the excitation radiation wavelength.

The temperature dependence of direct-current conductivity, presented in the Arrhenius coordinates, demonstrates a step-like conductivity increase in the vicinity of 250 ^{0}C. The dependence at higher temperatures is characterized with activation energy of about 1.1 eV. The frequency dependences of dielectric constant within the 100 Hz – 100 kHz region are measured in the range of temperatures from 100 ^{0}C to 575 ^{0}C.

[1] E. Armstrong and C. O'Dwyer, Artificial opal photonic crystals and inverse opal structures – fundamentals and applications from optics to energy storage, *J. Mater. Chem. C* **3** (2015) 6109, doi: 10.1039/c5tc01083g.
[2] A.E. Lukin et al., Electrical properties of silver iodide nanoparticles system embedded into opal porous matrix, *J. Phys.: Conference Series* **572** (2014) 012047, doi: 10.1088/1742-6596/572/1/012047.
[3] V.M. Masalov et al., Mechanism of formation and nanostructure of Stöber silica particles, *Nanotechnology* **22** (2011) 275718, doi:10.1088/0957-4484/22/27/275718.

Properties of Highly Porous Cr-Doped $SrTiO_3$ as Potential Anode Material for SOFC

Łukasz Łańcucki, Ewa Drożdż

AGH University of Science and Technology, Faculty of Materials Science and Ceramics, al. A. Mickiewicza 30, 30-059 Kraków, Poland

Solid oxide fuel cells (SOFCs) are the power devices that has been attracting great attention due to their fuel flexibility, high efficiency and solid state structure when equaled with other fuel cells. Over the past decade there has been increasing attention in perovskite type based materials that could be used as a substitute for Ni/YSZ cermets that are currently used as anode material in SOFCs. From a wide variety of perovskite type oxides doped strontium titanate (STO) is taken as one most promising materials for SOFCs anode. Such interest is strongly motivated due to its structural stability, excellent catalytic performance, mixed electro-ionic conductivity and high corrosion resistance (especially towards CO_2 and sulfur poisoning). In this work, a series of Cr doped (up to 6%) strontium titanates (STCOs) were prepared. XRD diffractometry revealed that all STCO samples were single phase. Relatively low sintering temperature (1200 ^oC) was chosen in order to maintain high porosity of obtained pellets. The addition of chromium had no effect on porosity of obtained samples as it maintained at about 47 %. In addition to structural research catalytic performance (TPR/TPO) and chemical stability tests of Cr doped STOs was also investigated.

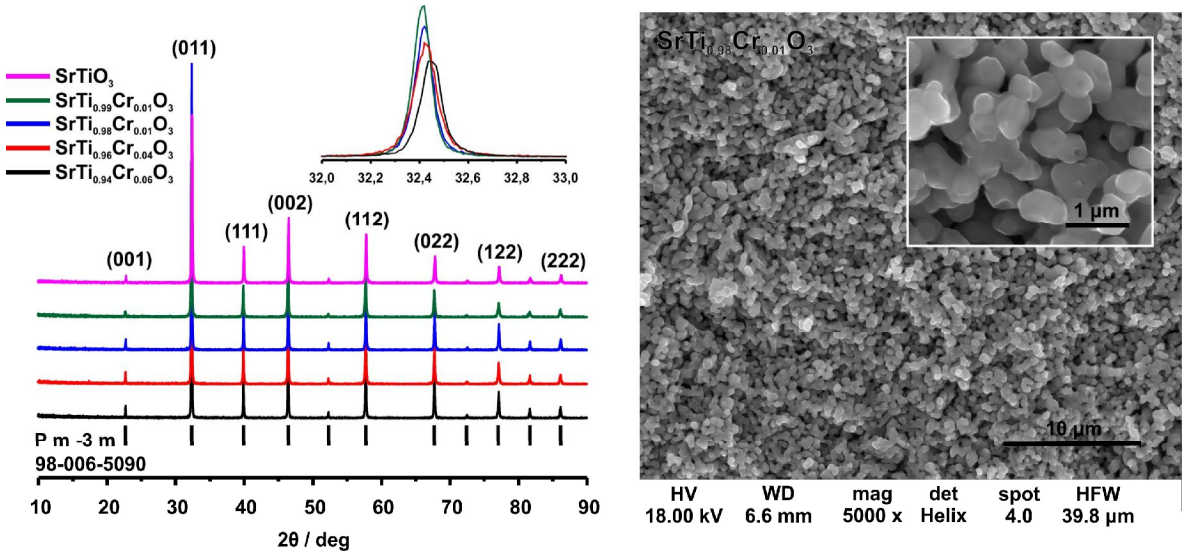

Figure 1. X-ray diffraction pattern of $SrTi_{1-x}Cr_xO_3$ samples after sintering and the SEM microphotographs of $SrTi_{0.98}Cr_{0.02}O_3$

Acknowledgement. This work was financially supported by the National Science Center of the Republic of Poland, Grant No. 2014/14/E/ST5/00763.

Zr-Containing Oxide Compounds: Structure and Optical Properties

V. Chornii[1], S.G. Nedilko[1], K. Terebilenko[1], G. Malashkevich[2], G. Shevchenko[3]

[1]*Taras Shevchenko National University of Kyiv, 64/13 Volodymyrska Str., 01601 Kyiv, Ukraine*
[2]*B.I. Stepanov Institute of Physics, National Academy of Sciences of Belarus, 68 Nezalezhnastsi Ave., 220072 Minsk, Belarus*
[3]*Institute of Physicochemical Problems of Belarusian State University, 14 Leningradskaya Str., 220080 Minsk, Belarus*

Zirconium-containing oxide compounds have been actively studied as perspective materials for various applications: mercury-free lamps, luminescent probes, luminescent materials for solid state lighting, catalyst support, sodium or lithium ion batteries etc. Variety of structures ranging from relatively simple ZrO_2 to complex langbeinite-type $KZr_2(PO_4)_3$ and $K_2BiZr(PO_4)_3$ crystals provides good opportunity to study structure-properties relationships, in particular role of ZrO_x polyhedra in luminescence processes. The most of Zr-containing oxides compounds are insulators with typical band gap values ~ 5 eV [1-3] but these compounds often show an intensive host-related photoluminescence (PL) in the visible spectral region. Obviously, mentioned luminescence is associated with defect-related luminescence centers. The doping with various ions is the most common way to affect the number of defects and therefore to improve optical properties of these oxide compounds.

In this work the structure and luminescence properties of the set of Zr-containing oxide compounds were studied by means of XRD, SEM and luminescence spectroscopy and by electronic band structure calculations. The VUV-excited luminescence properties were measured in 3.5–20 eV region of excitations energies in the 10 - 300 K temperature range. Dependencies of the PL intensities on temperature were obtained for different excitation wavelengths. Luminescence spectra for excitation with N_2-laser (λ_{ex} = 337.1 nm) and three diode-pumped (λ_{ex} = 405, 473 and 532 nm) radiation also were obtained. The electronic structure calculations for ideal and defect-containing crystals were performed by full-potential linear-augmented-plane-wave method implemented in the Wien2K package [4].

The results of experimental the PL studies are discussed together with electronic band structure calculations results, and literature data. The impact of fluorination on the host-related and RE-related luminescence was studied for the case of ZrO_2 compounds. Influence of the rare-earth doping on the ZrO_2, $KZr_2(PO_4)_3$ and $K_2BiZr(PO_4)_3$ compounds are discussed too.

[1] R.H. French, S.J. Glass, F.S. Ohuchi, Y.-N. Xu, W.Y. Ching, *Phys. Rev. B* **49** (1994) 5133-5142.
[2] Yu. Hizhnyi, V. Chornii, S. Nedilko, M. Slobodyanik, I. Zatovsky, K. Terebilenko, V. Boyko, *Radiat. Meas.* **56** (2013) 397-401.
[3] G. Ju, Y. Hu, L. Chen, Y. Jin, Y. Li, *RSC Adv.* **7** (2017) 4190-4195.
[4] P. Blaha, K. Schwarz, G. Madsen, D. Kvasnicka and J. Luitz, WIEN2k, An Augmented Plane Wave + Local Orbitals Program for Calculating Crystal Properties (Karlheinz Schwarz, Techn. Universität Wien, Austria) ISBN 3-9501031-1-2, 2001.

Synthesis and Structure Characterisation of Micro- and Nanocrystalline Powders of $Dy_{1-x}R_xFeO_3$ (R = La, Pr, Nd, Sm, Gd)

O. Pavlovska, I. Lutsyuk, Ya. Vachula, L. Vasylechko

Lviv Polytechnic National University, 12 Bandera Street, 79013 Lviv, Ukraine

The interest in the rare earth ferrites and their solid solutions is stimulated by their unique properties, such as high electrical conductivity, specific magnetic properties including spin reorientation phenomena, as well as significant electrochemical and catalytic activity. These materials have been found diverse technological applications, such as electrode materials for SOFC, HT multiferroics, dielectric, catalysts, sensory materials, etc.

New mixed orthoferrites $Dy_{1-x}R_xFeO_3$ were obtained by two different methods. The samples containing La and Pr were obtained by traditional solid state synthesis in air at the temperatures 1673–1773 K. For a preparation of nanocrystalline powders of $Dy_{0.5}R_{0.5}FeO_3$ (R = Nd, Sm, Gd) a low-temperature sol-gel citrate method was used. Rare earth oxides Dy_2O_3, Sm_2O_3 and Gd_2O_3 as well as $Nd(NO_3)_2{\cdot}6H_2O$ and $Fe(NO_3)_2{\cdot}9H_2O$ were used as an initial reagents. Neodymium and iron nitrates were dissolved in distilled water, whereas nitrate solutions of Dy, Sm and Gd were prepared by dissolving of corresponding oxides in HNO_3. Appropriate amounts of corresponding solutions were mixed on magnetic stirring for 30 min, after that water solution of citric acid (CA) and ethyleneglycol (EG) were sequentially added to the reaction mixture under continuous stirring. The molar ratio of reagents was $n(Dy^{3+}) : n(R^{3+}) : n(Fe^{3+}) : n(CC) : n(EG) = 0.5 : 0.5 : 1 : 2 : 1$ (R = Nd, Sm, Gd). As prepared solutions were gelled at 373–393 K for 4 h after that head treated sequentially at 573 K and 723 K for 1 h. The foamy product obtained was finally calcined at 1273 K for 2 h. In such a way single phase nanocrystalline powders of $Dy_{0.5}R_{0.5}FeO_3$ were obtained with average grain size of 86–300 nm.

Structural parameters of all mixed $Dy_{1-x}R_xFeO_3$ ferrites obtained agree well with the data for the "pure" $RFeO_3$ compounds, thus proving formation of continuous solid solutions with orthorhombic perovskite structure in the $DyFeO_3$–$RFeO_3$ (R = La, Pr, Nd, Sm, Gd) systems. Peculiarity of the $Dy_{1-x}La_xFeO_3$ series is the lattice parameters crossover and formation of dimensionally tetragonal structures at $x \approx 0.97$. The lattice parameters of $Dy_{1-x}R_xFeO_3$ show anisotropic convergent behaviour: the a- and c-parameters increases with increasing R-cation radii, whereas b-parameter decreases (Figure). However, the unit cell volumes in $Dy_{1-x}R_xFeO_3$ series increases almost linearly with according to the Vegard's rule.

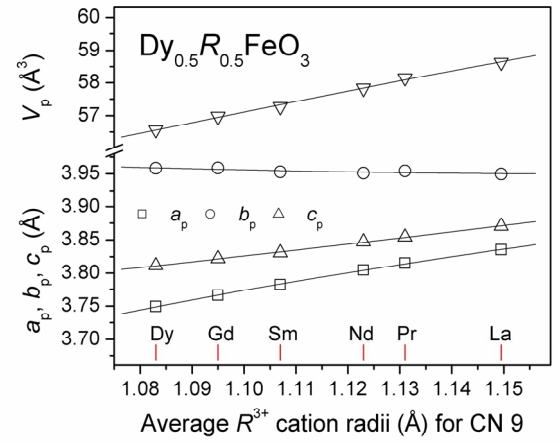

Figure. Unit cell dimensions of $Dy_{0.5}R_{0.5}FeO_3$ series *vs* average R-cation radii. Lattice parameters and unit cell volume of the orthorhombic cell are normalized to the perovskite ones as follows: $a_p = a_o/\sqrt{2}$, $b_p = b_o/\sqrt{2}$, $c_p = c_o/2$, $V_p = V_o/4$.

Acknowledgement. The work was supported by the Ukrainian Ministry of Education and Sciences under Project "RZE".

Peculiarities of XO_4^{2-} (X = Cr, Mo, W) Oxide Molecular Anions Adsorption on the Surface of Carbon Nanostructures

V. Borysiuk[1], S. Nedilko[1], Yu. Hizhnyi [1], A. Shyichuk[2, 3]

[1]*Taras Shevchenko National University of Kyiv, Volodymyrska Street 64/13, 01601 Kyiv, Ukraine*
[2]*Adam Mickiewicz University, Department of Rare Earth, Faculty of Chemistry, Umultowska 89b, 61-614 Poznań, Poland*
[3]*University of Wrocław, Faculty of Chemistry, Joliot-Curie 14, 50-383 Wrocław, Poland*

Chemical functionalization of carbon nanostructures (single-walled carbon nanotubes (SWCNT), graphene sheets, etc.) can modify their physical and chemical properties, leading to the improvement of their performance for specific applications. Carbon nanostructured materials are intensively studied at present as materials for efficient removal and storage of various toxic molecules. Pollution of heavy metals in industrial wastewater has been causing worldwide concern. The main sources of heavy metals are the wastewaters from modern chemical industries. Some studies have already indicated that functionalized CNTs are a promising for the removal of toxic heavy metals traces from water wastes [1]. Theoretical modeling of such molecular adsorption on the CNTs surfaces is a powerful tool what allows to predict some important properties of materials perspective for mentioned use. Adsorption of many kinds of molecules on CNTs of various structures have been considered so far in such computational studies and high predictive power of this theoretical method is now generally accepted.

In this work we studied adsorption characteristics of the XO_4^{2-} (X = Cr, Mo, W) molecular oxyanions on the surfaces of pure and N/B-doped SWCNTs, MWCNTs and graphene sheets. DFT-based geometry-optimized calculations of the electronic structures of carbon nanostructures with adsorbed oxyanions were carried out by Gaussian 09 program package [2].

Binding energies, relaxed geometries, charge states of the adsorbates and the electronic wavefunction profiles were calculated and analyzed. Taken results are supplemented by calculations of the XO_4^{2-}oxyanions adsorption on B/N-doped graphene sheets which are considered as model approximation for large-diameter CNTs. Effects of water solvent on studied adsorption surfaces are considered in a model of polarizable continuum.

Calculation results were discussed in view of potential application of the CNT-based materials as efficient adsorbents of toxic oxides of hexavalent metals. Adsorption mechanism was illustrated by dependence of the binding energy on tube-molecule distance of XO_4^{2-} (X = Cr, Mo, W) molecular oxyanions. Optical characteristics of XO_4^{2-} (X = Cr, Mo, W) anions adsorbed on the surface of carbon nanostructures, such as oscillator strengths of electronic transitions and absorption spectra were calculated. These results were used for verification of computational approach by experimental data.

[1] G. P. Rao, C. Lu, F. Su, *Sep. Purif. Technol.* **58** (2007) 224.
[2] M. J. Frisch, G.W. Trucks, H. B. Schlegel et al., Gaussian 03 (Gaussian, Inc., Wallingford, CT, 2003).

Structure and Properties of Oxides Incorporated Micro/Nanocellulose "Ceramics" - like Materials

M. Nedielko[1], O. Alekseev[2], S. Nedilko[2], V. Chornii[2], S. Revo[2], V. Scherbatskyi[2], V. Boyko[3]

[1]O. *Paton Electric Welding Institute of NASU, 11 Bozhenko Str., 03680 Kyiv, Ukraine*
[2]*Taras Shevchenko National University of Kyiv, 64/13 Volodymyrska Str., 01601 Kyiv, Ukraine*
[3]*National University of Life and Environmental Sciences of Ukraine, 5 Geroiv Oborony Str., 03041 Kyiv, Ukraine*

Cellulose and y its "micro/nanocellulose" forms are ones of advanced materials due to its abundance, multi-functionality, low toxicity of production and biodegradability. They are important for production of the biofuels, biochemicals, etc [1]. The range of new cellulose applications spreads from "paper electronics" to forensic examination and eco-friendly sorbents. Variety of their properties and applications is determined by the porous, micro/nanostructure morphology of the cellulose host and by the unique nature of its interaction with various chemical compounds.

This work is aimed using cool-pressing procedure to fabricate the set of "cellulose-oxide" micro/nanocomposite materials and to study their physical properties.

One set of "ceramics" - like composite materials was prepared as composition of micro/nanocellulose and luminescent oxide particles. The second set contained micro/nanocellulose and carbon nanostructures (fullerens, carbon nanotubes, flakes of the thermoexpanded graphite). The third set was made as composition of micro/nanocellulose matrix, luminescent oxide particles amd additive carbon nanostructures. Prepared composites were studied by means of scanning electron microscopy, XRD and thermogravimetric analysis, and luminescence spectroscopy.

It was found that structure of the composites prepared without oxides is formed by the plaits of near 5 – 50 μm size (crystallinity is about ~ 56%), that allowed us to characterize the samples as "ceramics – like". Structure of the micro/nanocellulose samples which contain oxide particles is similar, but the cellulose plaits are deformed and partially destroyed by oxide particles. The sizes of the last ones are from ~ 10 nm up to tens microns. Strong interaction between cellulose and carbon constituent changes the structure of carbon contained composites compared described above. Physical properties of studied materials (density, crystallinity, spectra and intensity of photoluminescence) depend both on the samples temperature (conditions of the thermal treatment) in the range 25 – 125 C and on the content of oxide or carbon components.

Obtained results showed that these composite materials are promising for creation of advanced mechanical, thermomechanical, electromechanical and optoelectronic devices, WLED, e.g.

[1] K. Nelson et al., *American process: Production of low cost nanocellulose for renewable, advanced materials applications*, Springer, 2016, pp. 267-302.

Preparation and Luminescence Properties of $BiPO_4$-$PrPO_4$ Solid Solutions

V.P. Chornii[1], S.G. Nedilko[1], K.V. Terebilenko[1], M.S. Slobodyanik[1], V. Boyko[2]

[1]Taras Shevchenko National University of Kyiv, 64/13 Volodymyrska Str., 01601 Kyiv, Ukraine
[2]National University of Life and Environmental Sciences of Ukraine, 5 Geroiv Oborony Str., 03041 Kyiv, Ukraine

Currently the new lighting and display devices such as light-emitting diodes (LEDs), plasma display panels (PDPs), and field emission displays (FEDs) have been proposed or developed in industry, which result in great interest in searching novel phosphors for mentioned applications [1–2]. Pr^{3+} doped oxide materials including phosphates, aluminates or borates have been widely used as a red emitting phosphor exhibiting relatively strong absorption in the near ultraviolet range of the light and intense red luminescent emission of good color purity [3].

The $BiPO_4$ represents phosphates of simple monoclinic structure containing bismuth (III) in BiO_8 distorted environment. Therefore, based on the effective ionic radii and charge balance of cations, the activator Pr^{3+} ion is expected to occupy randomly the Bi^{3+} sites in the orthophosphate host [3].

A series of the $Bi_{1-x}Pr_xPO_4$ (x = 0.01 - 0.06) compounds was synthesized by a high temperature solid state reaction method. The initial materials, Bi_2O_3 (99.99%), $(NH_4)_2HPO_4$ (99.999%) and Pr_6O_{11} (99.999%) were weighted in stoicheometry, then thoroughly mixed and milled in agate mortar for more than 30 min till they are uniformly distributed. The obtained mixtures have been heated at 450, 500 and 600°C for 6 h at each temperature with intermediate regrinding in porcelain crucibles along with an atmosphere agent, and then have been naturally cooled to room temperature. In order to measure the characteristics of the phosphor, the samples were grinded into powder.

The phase composition of prepared samples was determined by X-ray diffraction and IR spectroscopy methods. The solid solutions formation in limited range was found for the praseodymium series due to the significant difference in crystal structures of $BiPO_4$ and $PrPO_4$. Therefore, at high praseodymium content (more than 5 %) the mixtures of two phosphates are found on the diffraction patterns.

The luminescence properties of a $Bi_{1-x}Pr_xPO_4$ series were studied. It was found that the samples reveal intensive red luminescence when are excited in the range of the $^3H_4 \rightarrow {}^3P_J$ *f-f* transitions in Pr^{3+} ions. The most intensive peaks in photoluminescence spectra are related with $^3P_0 \rightarrow {}^3H_6$ (602.8 nm) and $^3P_1, {}^1I_6 \rightarrow {}^3F_2$ (610 - 635 nm) radiation transitions in the Pr^{3+} ions.

[1] C.C. Lin, A. Meijerink, R.-S. Liu, *J. Phys. Chem. Lett.* **7** (2016) 495–503.
[2] M. Janulevicius, P. Marmokas, M. Misevicius, J. Grigorjevaite, L. Mikoliunaite, S. Sakirzanovas, A. Katelnikovas, *Sci. Rep.* **6** (2016) 26098.
[3] Y. Zheng, L. Li, M. Zhao, J. Zheng, G. Li, E. Yang, X. Zhang, *Cryst. Eng. Comm.* **16** (2014) 5040-5049.

Intrinsic Luminescence of SrF_2 Nanoparticles

M. Chylii[1], T. Malyi[1], V. Vistovskyy[1], A. Zhyshkovych[1], A. Voloshinovskii[1]

[1]*Ivan Franko National University of Lviv, 8 Kyryla i Mefodiya Str., 79005 Lviv, Ukraine*

The nanophysics development caused intense research in the field of luminescence studies with the aim to create new luminescent materials that can be used as fluorescent labels for biomedical research[1], nanoscintillators for photodynamic radiotherapy[2], loaders for polymer films for X-rays detection[3], etc. However, the research of interaction between radiation and nanoparticles are required for their practical application. One aspect of this study is the dependence of luminescence intensity on the size of nanoparticles and exciting energy. The optimal size of nanoparticles with suitable scintillation parameters will be established during such studies. The luminescence-kinetic properties of SrF_2 nanoparticles were studied in this work.

SrF_2 nanoparticles were synthesized by chemical co-precipitation. Such the synthesis provides the obtaining of nanoparticles with the small enough sizes $\alpha \approx 20$ nm. In order to obtain SrF_2 nanoparticles of different size, the nanoparticles were annealed at temperatures 200, 400, 600 and 800ºC and their sizes were 30, 45, 65 and 85 nm accordingly.

It was revealed that self-trapped exciton luminescence intensity decreases with decreasing size of nanoparticles, but the rate of decrease depends on the mechanism of luminescence excitation. The smallest sensitivity to the size of nanoparticles is characteristic of excitation in the range of optical exciton creation ($h\nu < E_g$). In the case of excitation in the range of low energy band-to-band absorption transitions ($E_g < h\nu < E_{th}^{ex}$), luminescence is the most sensitive to the nanoparticle size. Under excitation in the range of photon multiplication ($h\nu > E_{th}^{ex}$) luminescence intensity dependence on the size of the nanoparticles is intermediate.

The range of sharp decline of X-ray excited luminescence intensity was revealed, which can correspond to the case when the electronic thermalization length exceeds the nanoparticle size. The sizes of nanoparticles associated with the range of rapid decrease in the X-ray intensity are increased in the series of $CaF_2 \rightarrow SrF_2 \rightarrow BaF_2$. The range of self-trapped exciton luminescence intensity sharp variation can be used for rough estimates of the electron thermalization length.

Main mechanisms of quenching of X-ray excited exciton luminescence of SrF_2 nanoparticles are related to (i) recombination of electrons with surface defects, especially if the size of nanoparticles and electron thermalization length is comparable and (ii) non-radiative decay of excitons due to diffusion to the surface of the nanoparticles.

[1] W.C.W. Chan, D.J. Maxwell, X. Gao et al., Luminescent quantum dots for multiplexed biological detection and imaging, *Curr. Opin. Biotechnol.* **1** (2002) 40–46.

[2] N.Y. Morgan, G. Kramer-Marek, P.D. Smith et al., Nanoscintillator conjugates as photodynamic therapy-based radiosensitizers: calculation of required physical parameters, *Radiat. Res.* **2** (2009) 236–44.

[3] S.Z. Shmurak, V.V. Kedrov, N.V. Klassen et al., Pulsed X-ray luminescence of composites consisting of inorganic particles and organic phosphors, *Tech. Phys. Lett.* **8** (2012) 691–694.

Template Synthesis and Luminescent Properties of Lanthanide Impurities Doped YBO_3 Nanoparticles

T. Malyi[1], A. Zhyshkovych[1], M. Chylii[1], V. Vistovskyy[1], A. Zaichenko[1,2], A. Voloshinovskii[1]

[1]*Ivan Franko National University of Lviv, 8 Kyryla i Mefodiya Str., 79005 Lviv, Ukraine*
[2]*Lviv Polytechnic National University, 12 S. Bandera Str., 79013 Lviv, Ukraine*

YBO_3 nanoparticles doped with lanthanide elements attract the attention of researchers because of its possible application for creation of luminescent materials which possess spectrally separated narrow luminescence bands in the visible range of the spectrum [1, 2]. This will provide simultaneous marking of several types of biological objects in mixed biological cultures for visualization of processes at the cellular level. Nanosized borate particles doped with lanthanide luminescent impurities can be synthesized by different methods, such as nucleation, hydrothermal, solvothermal, sol-gel method, solid state reaction, etc.

YBO_3-Ln nanoparticles obtained via nucleation method are characterized by 10 nm size and amorphous state. However, they possess low luminescence intensity. To increase the intensity of luminescence it is necessary to anneal the nanoparticles at high temperatures, which usually leads to unwanted effects of nanoparticles aggregation. The organic surfactants as templates for the nanoparticle growth can be used to prevent the formation of aggregate structures. In order to study the influence of synthesis conditions on the structural and luminescent properties the YBO_3-Ln nanoparticles were prepared using oligoperoxide templates of different types and different concentrations and annealing of samples at temperatures of 400, 600 and 800 °C.

It was revealed that nanoparticles annealed at 800 °C for 30 minutes possess sufficient luminescence intensity. The change of annealing temperature in the range of 200 – 800 °C effects insignificantly on the nanoparticles sizes which are within the 37-50 nm. However, as a result of high-temperature annealing the nanoparticles undergo aggregation. The aggregation is reduced if the nanoparticles are synthesized in the presence of oligomers and additionally covered with the polymer shell after annealing. In this case, most of the nanoparticle aggregates are about of 100 nm size.

The doping of YBO_3 nanoparticles with lanthanide ions provides the triple colour of luminescence under excitation at 366 nm. The obtained YBO_3-Ce nanoparticles possess blue colour of luminescence with λ_{em} = 420 nm. YBO_3-Ce,Tb system possess spectrally narrow green colour luminescence band at λ_{em} = 543 nm due to excitation energy transfer from cerium to terbium ions, as well as narrow red colour luminescence band at λ_{em} = 617 nm in YBO_3-Ce,Tb,Eu nanoparticles due to energy transfer from Ce^{3+} to Tb^{3+} ions and subsequently from Tb^{3+} to Eu^{3+} ions.

[1] R. Ladj, A. Bitar, M. Eissa, Individual inorganic nanoparticles: preparation, functionalization and in vitro biomedical diagnostic applications, *J. Mater. Chem. B* **1** (2013) 1381–1396.

[2] Thanh-Dinh Nguyen, From formation mechanisms to synthetic methods toward shape-controlled oxide nanoparticles, *Nanoscale* **5** (2013) 9455–9482.

Luminescence of Polystyrene Composites with Nanoparticles $LaPO_4$-Pr

T. Demkiv[1], O. Halyatkin[1], A.S. Zaichenko[2] ,V.V. Vistovskyy[1], A.S. Voloshinovskii[1]

[1]*Ivan Franko National University of Lviv, 8a Kyryla i Mefodiya Str., 79005 Lviv, Ukraine*
[2]*Lviv Polytechnic National University, 12 S. Bandera Str., 79013 Lviv, Ukraine*

Plastic scintillators possess high operation speed, large light yield and low cost manufacturing. However, due to the low absorption efficiency for registration of high-energy radiation the scintillators with considerably large size are needed. The efficiency of X-ray and gamma-ray absorption can be increased by embedding the nanoparticles with high atomic number Z. Such polymeric composites filled with inorganic nanoparticles show a substantial increase in light output compared to the polymeric scintillators together with keeping temporal parameters of polymers [1].

In order to enhance the scintillation parameters of polymeric composites with embedded nanoparticles the study of excitation mechanisms in the case of loading with nanoscale particles, in particular the study of energy transfer mechanism from nanoparticles to polymer matrix, is necessary. This will give the possibility to create new organic polymer composites based on polymer scintillators with embedded nanoparticles that combine advantages of polymer and crystal scintillators: high light yield and short decay times of scintillation pulses. Therefore, the polymer composites with $LaPO_4$ nanopaticles doped with Pr^{3+} ions that possess luminescence in the range 220-285 nm spectrally overlapping with absorption region of polymeric matrix are studied [2].

Based on spectral-kinetic studies of $LaPO_4$-Pr polystyrene nanocomposites the significantly larger X-ray luminescence intensity (up to 30 times) of the polymer composites with embedded inorganic nanoparticles was revealed in comparison with such for pure polystyrene scintillator due to fact that absorption capability of ionization radiation for inorganic nanoparticles is significantly larger than that for polystyrene. The dependence of energy transfer mechanism from inorganic nanoparticles to polystyrene matrix on the ratio between the nanoparticle size and free electron path or thermalization length of electron was revealed.

The radiative energy transfer mechanism from Pr^{3+} ions in $LaPO_4$ nanoparticles to polystyrene matrix in composites with embedded micro and nanoparticles with size larger than the free electron path or thermalization length of electron occurs. The nonradiative energy transfer mechanism from nanoparticles to polystyrene matrix in composites embedded with nanoparticles of size smaller than free electron path is dominated. Polystyrene matrix excited by electron that emitted from $LaPO_4$-Pr nanoparticles under X-ray irradiation exhibits luminescent and decay time parameters typical for pure polystyrene scintillator.

[1] T. Demkiv, O. Halyatkin, V. Vistovskyy, A. Voloshinovskii, *Nuclear Instruments and Methods in Physics Research Section A: Accelerators, Spectrometers, Detectors and Associated Equipment* **810** (2016) 1-5.

[2] V. Vistovsky, N. Mitina, A. Shapoval, T. Malyy, A. Gektin, T. Konstantinova, A. Voloshinovskii and A. Zaichenko, *Opt. Mater.* **34** (2012) 2066.

EPR Spectroscopy of the Lithium Tetraborate Glasses Doped with Ag

B.V. Padlyak[1,2], V.Ya. Tataryn[3], A. Drzewiecki[1], T.B. Padlyak[2], V.T. Adamiv[2], I.M. Teslyuk[2]

[1] *University of Zielona Góra, Institute of Physics, Division of Spectroscopy of Functional Materials, 4a Szafrana Str., 65-516 Zielona Góra, Poland*
[2] *Vlokh Institute of Physical Optics, Department of Optical Materials, 23 Dragomanov Str., 79005 Lviv, Ukraine*
[3] *Lviv Polytechnic National University, Institute of Telecommunications, Radioelectronics and Electronic Engineering, Department of Photonics, 1 St. Yura Sq., 79013 Lviv, Ukraine*

The X-band electron paramagnetic resonance (EPR) spectra of the Ag-doped borate glasses with $Li_2B_4O_7$ basic composition have been investigated and analysed. The $Li_2B_4O_7$:Ag glasses were obtained using standard glass synthesis and technological conditions described in [1]. The Ag impurity was introduced into the $Li_2B_4O_7$ composition as $AgNO_3$ compound and as metallic highly dispersed silver in amount 2.0 mol. %. By EPR spectroscopy it was shown that the Ag impurity is incorporated into the network of as-synthesised $Li_2B_4O_7$ glasses as the Ag^{2+} ($4d^9$) paramagnetic ions. The observed broad asymmetric EPR signal with the effective g-factor g_{eff} = 2.05 ± 0.01 at room temperature is typical for highly Ag-doped glasses [2,3] and is associated with Ag^{2+} ions that are coupled by magnetic dipolar interaction. In all investigated $Li_2B_4O_7$:Ag glasses also clearly has been observed the characteristic for glasses EPR signal with $g_{eff} \cong 4.29$ that belongs to the Fe^{3+} non-controlled impurity ions.

Thermal annealing of the $Li_2B_4O_7$:Ag glasses in the air atmosphere at temperature 710 K during 2 hrs leads to complete disappearing of the Ag^{2+} EPR signal, whereas the effective g -factor, integral intensity, and peak-to-peak derivative linewidth of the Fe^{3+} EPR signal practically were not change after this oxidising annealing.

As-synthesised $Li_2B_4O_7$:Ag glasses were annealed at temperature 710 K during 4 hrs in the reducing H_2 atmosphere (gas pressure 700 mm Hg) and in vacuum (10^{-4} Torr with titanium getter) for formation in them of a near-surface layer, containing the Ag nanoparticles [4,5]. The EPR spectroscopy shows complete disappearing of the Ag^{2+} signal in the $Li_2B_4O_7$:Ag glasses, annealed in the H_2 atmosphere and vacuum and practically unchanged parameters of the Fe^{3+} signal after the reducing annealing.

Optical properties of the $Li_2B_4O_7$ glasses and parameters of the metallic silver (Ag) nanoparticles in them, obtained by reducing thermal annealing were described in [4,5]. The obtained results of EPR spectroscopy and published data in [4,5] are discussed in the terms of redox processes, which take place in the $Li_2B_4O_7$:Ag glasses during thermal annealing in the oxidising (air) and reducing (H_2 and vacuum) atmospheres.

[1] B.V. Padlyak, S.I. Mudry, Y.O. Kulyk, A. Drzewiecki, V.T. Adamiv, Y.V. Burak, I.M. Teslyuk, *Mater. Sci. Poland* **30** (2012) 264.
[2] A. Samokhvalov, S. Nair, E.C. Duin, B.J. Tatarchuk, *Appl. Surf. Sci.* **256** (2010) 3647.
[3] R. Stefan, S. Popescu, M. Bindea, A. Popa, O. Raita, *Anim. Sci. Biotech.* **44** (2011) 141.
[4] V.T. Adamiv, I.M. Bolesta, Ya.V. Burak, R.V. Gamernyk, I.D. Karbovnyk, I.I. Kolych, M.G. Kovalchuk, O.O. Kushnir, M.V. Periv, I.M. Teslyuk, *Physica B* **449** (2014) 31.
[5] I.M. Bolesta, O.O. Kushnir, I.I. Kolych, I.I. Syvorotka, V.T. Adamiv, Ya.V. Burak, I.M. Teslyuk, *Adv. Sci. Eng. Med.* **6** (2014) 326.

Luminescent and Structural Studies of $Y_3Al_5O_{12}$ Nanopowders Doped with Different Concentrations of Yb^{3+} Ions

I.I. Syvorotka[1,*], A.P. Luchechko[2], D.Yu. Sugak[1,3], L.O. Vasylechko[3], Ya.A. Zhydachevskii[3,4], S.B. Ubizskii[3], A. Suchocki[4,5]

[1]*Scientific Research Company "Carat", Lviv, Ukraine*
[2]*Ivan Franko National University of Lviv, Ukraine*
[3] *Lviv Polytechnic National University, Ukraine*
[4]*Institute of Physics, Polish Academy of Science, Warsaw, Poland*
[5]*Institute of Physics, Kazimierz Wielki University, Bydgoszcz, Poland*
* syvorotka.jr@yahoo.com

Yttrium aluminum garnet $Y_3Al_5O_{12}$ (YAG) doped with rare-earth ions is an important laser material and phosphor with excellent chemical and thermal stability, as well as good optical-luminescent properties. As a rare-earth ion with the simplest energy-level construction, Yb^{3+} has some important advantages, in particular, a long radiative lifetime of the upper laser level and no excited-state absorption or upconversion loss compared with other rare-earth ions [1]. On the other hand, significant changes in the optical-luminescent properties are observed in nanomaterials and are due to surface-related defects.

The studied YAG nanopowders doped with Yb^{3+} ions have been synthesized by citrate sol-gel method, as described in [2]. In this method following substances were used: yttrium nitrate hexahydrate $Y(NO_3)_3{\cdot}6H_2O$ and aluminum nitrate nonahydrate $Al(NO_3)_3{\cdot}9H_2O$, ytterbium oxide Yb_2O_3, nitric acid HNO_3, citric acid $C_6H_8O_7$ and distilled water H_2O. The temperature of calcinations was 1000 °C. Activator concentration was equal 5, 10, 15, 20 and 30 at.%. The phase formation of YAG: Yb was characterized by X-ray powder diffraction (XRD) techniques. The average size of particles was estimated from the line broadening by using of well-known Scherrer's formula, as well as by Williamson-Hall analysis [3] and was in the range 60...200 nm. Anomalous increase of nanopowder lattice parameter with increasing of Yb concentration was observed, despite that the Yb^{3+} ionic radius is smaller than that of Y^{3+}. This anomalous concentration dependence, apparently, connected with presence of ytterbium ions in aluminum positions of crystal lattice.

The luminescence spectra and decay kinetics of YAG:Yb with various doping levels were measured at room temperature. All emission and excitation spectra are typical of ytterbium ions and correspond to f-f transitions of Yb^{3+}. Two main excitation peaks are centered at 1016 nm and 1039 nm, as well as main emission peak, is at about 1030 nm. The Yb^{3+} luminescence intensity has the maximum for 5% of ytterbium and decreases with increasing concentration to 30 % more than one order. Activator concentration has no effect on the positions of the peaks in the luminescence spectra. Doping levels increasing also leads to shortening of Yb^{3+} lifetimes from 600 to 20 μs at the Yb^{3+} concentration changing from 5 to 30 %, respectively. The decays are related to $^2F_{5/2} \rightarrow {}^2F_{7/2}$ transition in Yb^{3+} ions. The observed decreasing of the luminescence intensities and shortening of the lifetimes are caused most probably by concentration quenching and energy transfer from Yb^{3+} to host or surface-related defects.

The effects of various Yb^{3+} concentrations and thermal treatment on structural distortion and luminescent properties of YAG nanopowders are discussed.

[1] X. Xu, Z. Zhao, P. Song et al., *Journal of the Optical Society of America B* **21**(3) (2004) 543-547.
[2] Ya. Zhydachevskii, I.I. Syvorotka, L. Vasylechko, D. Sugak, I.D. Borshchyshyn, A.P. Luchechko, Ya.I. Vakhula, S.B. Ubizskii, M.M. Vakiv, A. Suchocki, *Optical Materials* **34** (2012) 1984–1989.
[3] G.K. Williamson, W.H. Hall, X-ray line broadening from filed aluminium and wolfram, *Acta Metall*. **1** (1953) 22–31.

Synthesis of Highly Porous $SrTiO_3$ Nanomaterials

Adrian Mizera, Ewa Drożdż, Łukasz Łańcucki

AGH University of Science and Technology, Faculty of Materials Science and Ceramics, al. A. Mickiewicza 30, 30-059 Kraków, Poland

The strontium titanate based perovskites are materials that can be potentially applied as anode material for solid oxide fuel cells (SOFC). One of main requirement for those materials is high porosity (more than 30% vol.). A route of synthesis have a great impact on microstructural properties such as size and shape of pores. It is agreed that microstructure (specially specific surface area) affects the catalytic performance of materials. In case of potential anode materials for SOFCs Three Phase Boundary (TPB) growth is crucial from application point of view.

Therefore, the classical, commonly used, solid-state synthesis can be replaced by one of wet preparation methods. One of the most effective ways of obtaininghighly porous nanomaterials powdersis citrate combustion method. In this research citrate method was modified by application of various surfactants (Triton X-100, Pluronic 123) and/or polymer (PVA) agents. As the precursors for $SrTiO_3$the ethanol/water citrate solutions of strontium nitrate andtitanum (IV) isopropoxidewere used. Moreover, to implement regular porosity, Three Dimensionally Ordered (3DOM) structures of STO were made by using Polystyrene spheres that acted as soft organic template. Deposition of inorganic species on surface of template aggregates results in the formation of particles with certain shape and size.

Microstructures of obtained materials were illustrated using scanning electron microscopy (Fig. 1). All of applied modifications allow to obtain highly porous materials. Final products of soft-templating synthesis present similar shape and size of pores. Powders derived from synthesis with polystyrene spheres present show the presence of larger pores which size is comparable to size of template spheres. The XRD diffractometrymeasurements confirmed $SrTiO_3$ single phase purity.Complementary to SEM data, TPR/TPOxinvestigationswere performed in order to determine the accessibility of $SrTiO_3$ surface.

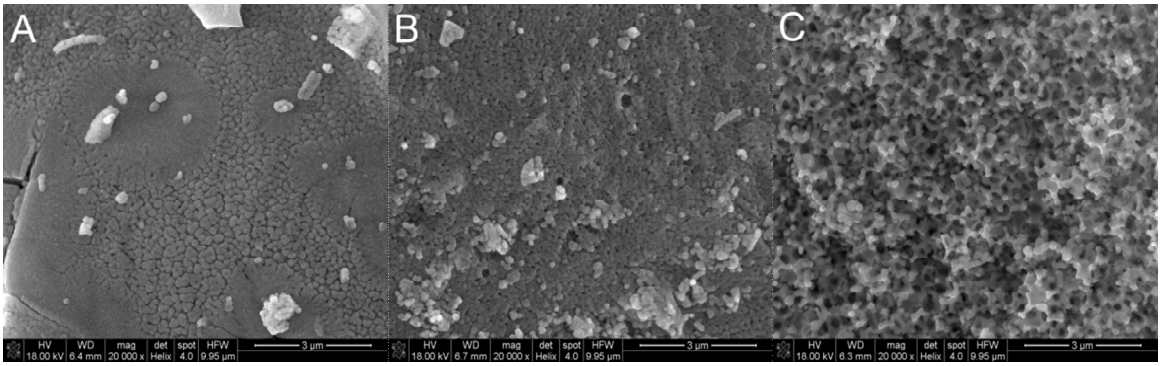

Figure 1. Microphotographs of $SrTiO_3$ powders calcined in 900 °C prepared with usage of A) poly(vinyl alcohol) B) Pluronic P-123 copolymer and C) polystyrene spheres.

Acknowledgement. This work was financially supported by the National Science Center of the Republic of Poland, Grant No. 2014/14/E/ST5/00763.

Exploration of Second Harmonic Generation in KDP-Based Crystalline Nanocomposites

B. Kulyk[1], N. Andrushchak[2], A. Andrushchak[2], B. Sahraoui[3]

[1]*Research and Educational Center "Fractal", Department of Physics, Ivan Franko National University of Lviv, 50 Dragomanova Str., 79005 Lviv, Ukraine*
[2]*Lviv National Polytechnic University, 12 S. Bandery Str., 79013 Lviv, Ukraine*
[3]*University of Angers, MOLTECH-Anjou Laboratory, UMR CNRS 6200, 2 bd Lavoisier, 49045 Angers, France*

In recent years, nanomaterials have been in a primary focus of science and technology with their rigorous research and development. Nanoporous materials as a subset of nanostructured materials possess unique structural-surface properties that underline their importance in various fields of human activity. They offer new opportunities in areas of inclusion chemistry, guest-host synthesis and molecular manipulations and reaction in the nanoscale range.

The exploration of quadratic nonlinear optical response in nanocomposites based on KDP nanocrystalites grown inside nanopores of aluminium oxide Al_2O_3 (Fig.1) has been performed. Growing the KDP nanocrystallites inside these nanopores has been recently confirmed by X-ray analysis [1]. The rotational Maker fringe technique [2] in the transmission scheme has been used for second harmonic generation (Fig.2) measurements employing *s*- and *p*-polarized fundamental 1064 nm laser beam.

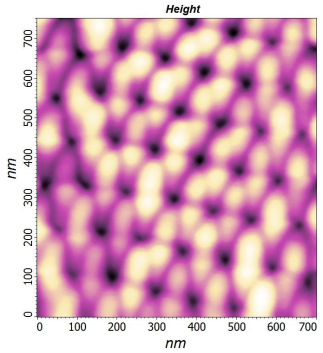

Fig. 1. AFM image of alumina nanoporous matrix

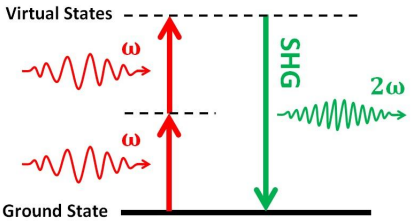

Fig. 2. Schematic energy-level diagram of SHG process

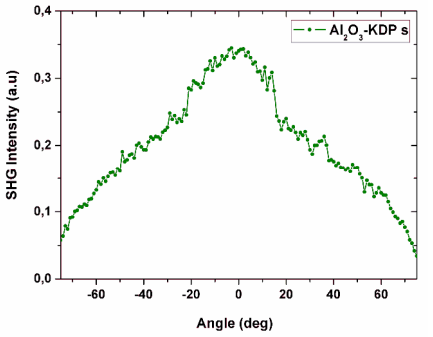

Fig. 3. Angular dependence of SHG in KDP nanocomposite

The second order nonlinear optical response of studied nanocomposites (see Fig.3) again confirms the presence of noncentrosymmetric filler (nanocrystallites of KDP) inside nanopores of Al_2O_3. Furthermore, the polarization dependent intensity of nonlinear response suggests the macroscopic anisotropy of grown KDP nanocrystallites. Thus, second harmonic generation technique may serve as a sensitive tool for diagnostics of crystalline fillers inside nanoporous matrices.

[1] N.A. Andrushchak, O.A. Buryy, V.T. Adamiv, I.M. Teslyuk, A.S. Andrushchak, A.V. Kityk, Development of crystalline nanocomposites with KDP crystals as nanofiller, *Proceedings of the International Conference on Nanomaterials: Applications and Properties*, Lviv, Ukraine, 2016, Vol. 5, No.2, 02NNSA10(3 pp.).

[2] B. Kulyk, A.P. Kerasidou, L. Soumahoro, C. Moussallem, F. Gohier, P. Frère, B. Sahraoui, Optimization and diagnostic of nonlinear optical features of π-conjugated benzodifuran-based derivatives, *RSC Adv.* **6** (2016) 14439-14447.

A Numerical Model of Light Propagation in Porous Composite Structures

Nazariy Jaworski*, Nazariy Andrushchak*

CAD Department, Lviv Polytechnic National University, 12 S. Bandery Str., Lviv, Ukraine
** nazariyjaworski@gmail.com, nandrush@gmail.com*

With development of nanotechnologies, an interest in development and investigation of porous materials as the most promising materials in different areas of science is rapidly growing [1]. The best way to find a set of effective physical characteristics of porous composite material is a numerical simulation of corresponding physical processes in the structural model of that material [2]. Such numerical models give the ability to take into account many microstructural heterogeneities of complex porous composites that cannot be done in analytical models [3].

In order to build a complex porous composite model a microlevel cellular model with a porous generation method based on Bezier curve generation was used [4]. The result of such simulation is shown in Fig. 1. The proposed composite structure is described by representative volume element that is a 3D matrix of scalar intensities, diapasons values of which describe different composite components.

To simulate a light propagation in such model the numerical methods of solving differential equations that are a mathematical model of physical process were used. For example, a beam propagation method that was used for light propagation in complex porous structure of composite is depicted in Fig 2.

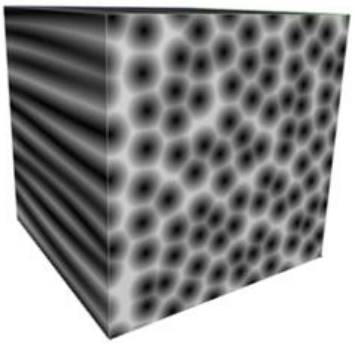

Fig. 1. *Example of porous composite structure*

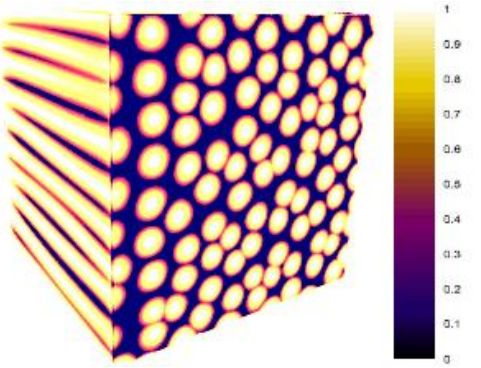

Fig. 2. *Example of light propagation process simulation in porous composite structure*

The results of such simulations can be used for effective refractive index calculation in terms of reverse boundary problem solution. Besides, by using the proposed approach the numerical model of finding the effective optical characteristics in porous matrix composites can be built.

[1] A. Losic, *Nanoporous Alumina. Fabrication, Structure, Properties and Applications*, Springer, 2015, 371 p.

[2] N. Jaworski, I. Farmaga, M. Lobur, P. Spiewak, Research of composite materials optimal design task based on numerical simulation, *Proceedings of the 8th Int. Scientific and Technical Conference on Computer Sciences and Information Technologies*, CSIT'2013, Lviv, Ukraine, 2013, pp. 46-48.

[3] N. Jaworski, I. Farmaga, U. Marikutsa, Building the micro-level composite materials structure models in the problems of their optimal design, *Scientific Bulletin of Ukrainian National Forestry University* **25.8** (2015) 359-366.

[4] N. Jaworski, N. Andrushchak, A method of nanoporous anodic aluminum oxide structure modeling based on Bezier curves generation, *Proceedings of the 14th Int. Conf. on Experience of Designing and Application of CAD Systems in Microelectronics*, CADSM'2017, Polyana-Svalyava, Ukraine, 2017, pp. 63-66.

[5] N.A. Andrushchak, O.A. Buryy, V.T. Adamiv, I.M. Teslyuk, A.S. Andrushchak, A.V. Kityk, Development of crystalline nanocomposites with KDP crystals as nanofiller, *Proceedings of the International Conference on Nanomaterials: Applications and Properties*, Lviv, Ukraine, 2016, Vol. 5, No.2, 02NNSA10(3 pp.).

Computational Study of Electrical Processes in Nanotubes/Dielectric Composite

Andriy Stelmashchuk*, Ivan Karbovnyk

Ivan Franko National University of Lviv, Lviv, Ukraine
* steelandriy@gmail.com

Filling the insulating polymer matrix with nanotubes (e.g. carbon nanotubes, CNTs) improves noticeably the electrical and mechanical properties of the resulting composite [1]. Usually, very low concentration of nanofiller is needed to transform nanocomposite into conductor as the aspect ratio for nanotubes is very high [2]. Electrical conductivity of nanocomposite is to a large extent determined by the configuration of CNTs.

Since the electrical conductivity of nanocomposite is dependent on many factors, significant efforts are required to explore study it experimentally. Therefore, a number of approaches were developed in order to simulate the process using numerical calculations.

In this work, nanocomposite is modelled as 3D volume box also known as representative volume element (RVE) randomly filled with high aspect ratio conductive nanotubes. Electrodes are attached to the opposite sides of nanocomposite in order to test its's electrical properties. CNTs can potentially create connections between each other and, therefore, form long chains of connected tubes between the opposite sides of RVE [2].

In this model, we consider solid CNTs, that means they cannot overlap each other by volume. An electric contact between nanotubes is ensured by tunneling effect.

The simulation process starts with generating a set of CNTs inside the RVE. Start point and the direction in space of each CNTs is randomly chosen. Before adding newly generated CNTs into the system we have to perform additional check to be sure that this CNT doesn't overlap the existing ones. To perform such check, the shortest distance between generated tube and all other CNTs is calculated. Only in case when all these distances are larger than CNT diameter d, the newly generated CNT is going to be added to the system.

If the shortest distance between CNTs is less than tunneling cut-of distance, then we assume that these CNTs are in electrical contact. Several bunches of mutually connected nanotubes form clusters. The cluster is called conductive if it contains CNTs connected to both electrodes. For finding conductive clusters in RVE we utilize the union find algorithm.

Set of connected CNTs can be interpreted as a random network of resistors. After applying the combination of Kirchhoff's current law and Ohm's law the system of linear equations is created. After applying potential boundary conditions and solving the system we obtain the values of potentials V_i at all network nodes then all currents flowing through resistor elements are calculated. Finally, we calculate the total equivalent electrical conductivity of random resistor network using Ohm's law and total current flowing through system and applied potential values.

We have developed software for the simulation of nanotube-dielectric composite conductivity using the method described above. Model nanocomposite sample is characterized by the following parameters. Dimensions of the nanocomposite are 1000 nm, 1000 nm and 100 nm respectively. The CNT diameter is 2 nm and the length is 20 nm, intrinsic conductivity is 10^4 S/m. The tunnel cut-off distance is set to 1.8 nm. Simulation results are in agreement with experimental measurements reported in [2].

[1] R. Khare, S. Bose, Carbon Nanotube Based Composites - A Review, *J. Minerals & Materials Characterization & Engineering* **4**(1) (2005) 31-46.

[2] N. Hu, Z. Masuda, C. Yan, G. Yamamoto, The electrical properties of polymer nanocomposites with carbon nanotube fillers, *Nanotechnology* **19**(21) (2008) 215701.

Influence of Ag Nanofilms on the Optical Properties of $LiNbO_3$

I. Bolesta[1], M. Vakiv[2], V. Haiduchok[2], O. Kushnir[1], A. Demchuk[1], S. Nastyshyn[1], R. Gamernyk[1]

[1]Ivan Franko National University of Lviv, Faculty of Electronics and Computer Technologies, Chair of Radiophysics and Computer Technologies, 107 Gen. Tarnavskogo Str., 79017 Lviv, Ukraine
[2]Scientific Research Company "Carat", 202 Stryjska Str., 79031 Lviv, Ukraine

Lithium niobate (LN) single crystals are very interesting and attractive material, which widely used for designing and production of opto- and acoustoelectronic devices variety. LN has anomalously high pyroelectric, electrooptic and acoustooptic coefficients and thereby can be used for fabrication of optical devices [1]. Technology for formation of photonic crystals using vacuum deposition of microstructures on the LN surface rapidly develops during last years [2]. Experimental investigation of microstructures deposited on the dielectric matrix shows that they greatly influence a linear and none-linear permittivity of the substrate [3, 4]. We expect that formation of metallic microstructures on the LN surface will lead to similar effect and thus application of this material will be expanded. In this paper we will analyze morphology of Ag-nanoparticles on LN surface as well as their influence on the surface properties.

Ag-nanoparticles are prepared by magnetron sputtering in vacuum using COM-TH2-SP2-ION deposition equipment (TORR Corp., USA). LN substrates had dimensions 16×8×0.8 mm. Thickness of nanofilms deposited at rate 0.7 Å/s and temperature 50° C was varied from 1 till 4 nm. The structure of the surface was investigated by Atomic Force Microscope NT-MDT SolverPro 47 in semi-contact mode by the NSG10 tip with the radius of ~10 nm. Optical spectra were measured using the two-beam spectrophotometer Shimadzu UV-3600 in the 300…2000 nm spectral band with the step of 1.0 nm and spectral slit width of 2.0 nm. For study of nonlinear optical effects of the LN with Ag films it has been used a conventional Z-scan technique developed by Sheik-Bahae [5].

It has been observed significant changes in nonlinear properties of LN in particular the nonlinear refraction of the silver nanoparticles, which are present on the substrate. It should be noted that these changes as well as a position of plasmon absorption peak of the silver nanofilms deposited on the LN substrate [6] depend essentially on the sign of electric charge on the crystal surface. This phenomenon can be used to determine easily the charge sign on the LN surface.

[1] R. S. Weis, T. K. Gaylord, Lithium niobate: Summary of physical properties and crystal structure, *Applied Physics A* **37** (1985) 191-203, http://dx.doi.org/0.1007/BF00614817.

[2] M. Manzo, F. Laurell, V. Pasiskevicius, K. Gallo, Electrostatic control of the domain switching dynamics in congruent LiNbO3 via periodic proton-exchange, *Appl. Phys. Lett.* **98** (2011) 122910, http://dx.doi.org/10.1063/1.3571559.

[3] V.T. Adamiv, I.M. Bolesta, Ya.V. Burak, R.V. Gamernyk, I.D. Karbovnyk, I.I. Kolych, M.G. Kovalchuk, O.O. Kushnir, M.V. Periv, I.M. Teslyuk, Nonlinear optical properties of silver nanoparticles prepared in Ag doped borate glasses, *Physica B* **449** (2014) 31–35, http://dx.doi.org/10.1016/j.physb.2014.05.009.

[4] I.M. Bolesta, O.O. Kushnir, I.I. Kolych, I.I. Syvorotka, V.T. Adamiv, Ya.V. Burak, I. M. Teslyuk, AFM Investigations and Plasmon Spectra of Silver Clusters Formed on $Li_2B_4O_7$:Ag Glass Surface in Reducing Atmosphere, *Advanced Science, Engineering and Medicine* **6** (2014) 1–7, http://dx.doi.org/10.1166/asem.2014.1498.

[5] M. Sheik-Bahae, A.A. Said, T.H. Wei, D.J. Hagan, E.W. Van Stryland, Sensitive measurement of optical nonlinearities using a single beam, *JQE* **26** (1990) 760, http://dx.doi.org/10.1109/3.53394.

[6] I.M. Bolesta, M.M. Vakiv, V.G. Haiduchok, A.A. Kushnir, Plasmon absorption by silver nanoparticles on $LiNbO_3$ surface, *Ukr. J. Phys.* **62** (2017) 39-45, http://dx.doi.org/10.15407/ujpe62.01.0039.

Optical and Nonlinear Optical Characterization of Nanosized ZnO

V. Multian[1], A. Uklein[1], O. Boldyrieva[2], V. Lisnyak[2], V. Gayvoronsky[1]

[1]*Institute of Physic of National Academy of Science of Ukraine, 46 Prospect Nauky, 03028 Kyiv, Ukraine*
[2]*Taras Shevchenko National University of Kyiv, Chemical faculty, 62a Volodymyrska Str., 01601 Kyiv, Ukraine*

Wide-gap semiconductor ZnO is characterized with high binding energy of Wannier-Mott excitons (~60 meV) and promising luminescence efficiency. ZnO nanoparticles (NPs) are widely applied in the fields of optoelectronic devices [1]. ZnO NPs have shown a high potential for the biolabeling application [2] that require the NPs size reduction (at least less than 100 nm) within maintaining the same level of the SHG efficiency. Ultra-small size ZnO NPs or QDs should be synthesised for advanced biolabeling under size controlled technique because these particles possess valuable electro-optical properties that differ from their bulk counterparts, and being sensitive to both NP's size and shape.

In the present communication, we report on the nonlinear optical (NLO) properties and SHG efficiency of ultra-small NPs. ZnO NPs with the efficient luminescent and quadratic NLO responses were prepared by a hydrolytic route. The resulted ZnO NPs were characterized with optical and IR spectroscopies. Core stabilization, at the early stages of hydrolysis, limits the further growth. The average size of NPs was estimated to be within 2.0–2.8 nm with absorption measurements. The PL emission and UV-Vis absorption increase with the content of NPs. The efficiency growths from the particles isolated from EtOH to that from MeCN. The PL bands were analysed and the respective band area was addressed to the oxygen vacancies.

The NLO characterization of ZnO NPs was provided by the self-action effect monitoring within the picosecond laser pulses at 1064 nm. It was shown the ZnO NPs isolated from solvents of different nature have a diverse efficiency of the absorptive and refractive NLO responses. The correlation between the $\mathrm{Im}(\chi^{(3)})$ magnitude and the oxygen deficiency in ZnO was shown.

The second harmonic generation (SHG) in the ZnO NPs was studied under the femtosecond-laser excitation at 800 nm. The SHG efficiency is comparable for ZnO NPs of ~2 and ~150 nm. For biolabeling applications, this effect is quite important, if one apply the SHG response techniques with small ZnO NPs.

[1] T. Mei, Y. Hu, Synthesis, self-assembly and optoelectronic properties of monodisperse ZnO quantum dots, Optoelectronic Devices and Properties, Ed. Sergiyenko O, InTech China, Shanghai; pp. 215–240 (2011).

[2] C. Joulaud, Y. Mugnier, G. Djanta, M. Dubled, J.-C. Marty, C. Galez, J.-P. Wolf, L. Bonacina, R. Le Dantec, Characterization of the nonlinear optical properties of nanocrystals by Hyper Rayleigh Scattering, *J. Nanobiotechnology* **11**:S8 (2013), doi:10.1186/1477-3155-11-S1-S8.

Synthesis of Poorly Crystalline Sodium- and Carbonate-Containing Apatite and its Sorption Properties Relatively to Cu^{2+}, Zn^{2+} and Cu^{2+}/ Zn^{2+} Ions

Oksana Livitska, Nataliia Strutynska, Nikolay Slobodyanik

Inorganic Chemistry Department, Taras Shevchenko National University of Kyiv, 64/13 Volodymyrska Str., 01601 Kyiv, Ukraine

Calcium phosphates and their complex substituted analogs are widely used as catalysts of important industrial reactions, hosts for luminescent materials, adsorbents etc. Among them hydroxylapatites possess a high removal capacity for different metals ions which can substitute calcium ions in the structure or stay on the surface due to sorption process.

The similarity of synthetic apatite composition to the inorganic part of bones and teeth in human bodies makes them the most perspective for bone repair in orthopaedics and dentistry. At the same time, the balanced introduction of microelements (copper, zinc) in a matrix of apatite allows to vary its resorption rate in the body.

In this report, sodium- and carbonate-substituted apatite was synthesised by the wet precipitation method in aqueous system $Ca(NO_3)_2/Na_3PO_4/Na_2CO_3$ (molar values Ca/P = 1.67, CO_3^{2-}/PO_4^{3-} = 1). Then obtained poorly crystalline powder (particles of 20-30 nm in diameter) was used as matrix for sorption of cooper, zinc and copper/zinc ions from the aqueous solutions of their nitrates. The influence of heating to 700 °C or a microwave processing on the characteristics of the samples was also investigated. The obtained samples and products of their heating to 700 °C were characterized using X-ray powder diffraction, infrared spectroscopy, elemental and thermal analysis, and scanning electron microscopy.

It was found that microwave radiation (2.45 GHz) during 30 min doesn't effect samples characteristics, such as crystallinity and size of particles (Fig. 1a) but can give the possibility to decrease an amount of adsorbed water.

Annealing at 700 °C resulted in the formation of crystalline products (complex substituted calcium orthophosphate with apatites structure) and the aggregation of particles (Fig. 1b). Elemental analysis indicated that content of Cu^{2+}, Zn^{2+} in the solid samples correlated well with its concentration in the initial solutions. Thermogravimetric analysis for the prepared complex substituted calcium phosphates showed the 15-17 % mass loss up to 1100 °C due to elimination of water and partial losing of carbon dioxide.

Obtained results may give us new insights at creation not only new antibacterial and bioceramic materials but also effective catalysts.

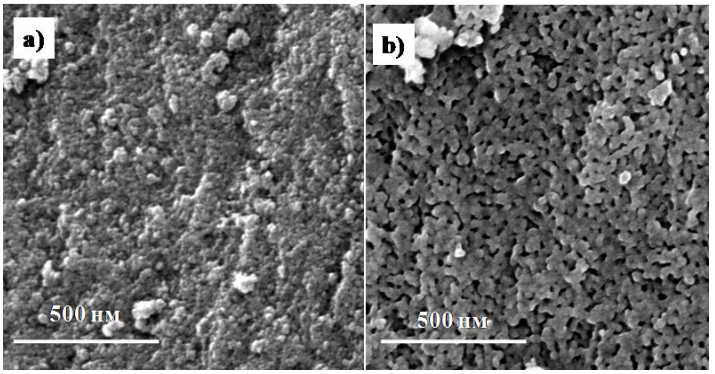

Fig 1. SEM images of Cu^{2+}-containing sample: microwave processed (a) and annealed at 700 °C (b).

Magnetic Behavior of ZnO Nanoparticles Doped with Co and Mn Ions

Myroslava Omelchenko[1], Jacek Wojnarowicz[2], Jaroslaw Rybusinski[1], Andrzej Majhofer[1], Andrzej Twardowski[1] and Jacek Szczytko[1]

[1]*Faculty of Physics, University of Warsaw, Warsaw, Poland*
[2]*Institute of High Pressure Physics, Polish Academy of Sciences, Sokolowska 29/37, 01-142 Warsaw, Poland*

The II-IV valence nanoparticles with semiconducting, luminescent and magnetic properties are under ongoing research in modern spintronic. Magnetic properties of ZnO:Co and ZnO:Mn nanoparticles were investigated in this work. The influence of the concentration of the doping Mn/Co ions on the magnetization of $Zn_{1-x}Mn_xO$ and $Zn_{1-x}CoxO$ nanoparticles was experimentally obtained and analyzed. Superconducting quantum interface device (SQUID) with the applied magnetic field up to 7 T was used for determining the magnetization of ZnO:Co and ZnO:Mn nanapowders and compared with the pure ZnO nanopowder. Zink oxide nanopowders doped with 1%,15% Co and 1%,15% Mn were produced by the microwave solvothermal synthesis. The nanostructures of the particles were investigated by skeleton density, specific surface area (SSA), phase purity (XRD), lattice parameters, average particle size, crystal size distribution, scanning electron microscopy (SEM).

[1] D.P. Joseph, G.S. Kumar, C. Venkateswaran, *Mater. Lett.* **59** (2005) 2720–2724.
[2] P.V. Radovanovic, N.S. Norberg, K.E. McNally, D.R. Gamelin, *J. Am. Chem. Soc.* **124** (2002) 15192–15193.
[3] Jelena Tamuliene, Rimantas Vaisnoras, Goncal Badenes, and Leonas-Mindaugas Balevicius, *J. of Nanomaterials* (2009) 308276(7 p.).
[4] Hengda Li, Xinzhong Liu, Zhigong Zheng, *Journal of Magnetism and Magnetic Materials* **372** (2014) 37–40.
[5] J. Wojnarowicz, S. Kusnieruk, T. Chudoba, J. Mizeracki, W. Łojkowski, *Glass Ceram.* **3** (2015) 8–13.

The Electrode Material for Hybrid Supercapacitor Based on the Nanostructured Iron-Substituted Lithium-Manganese Spinel

R. Lisovsky, B. Ostafiychuk, I. Budzulyak, A. Boychuk, B. Rachiy, V. Kotsyubynsky

Vasyl Stefanyk Precarpathian National University, 57 Shevchenko Str., 76018 Ivano-Frankivsk, Ukraine

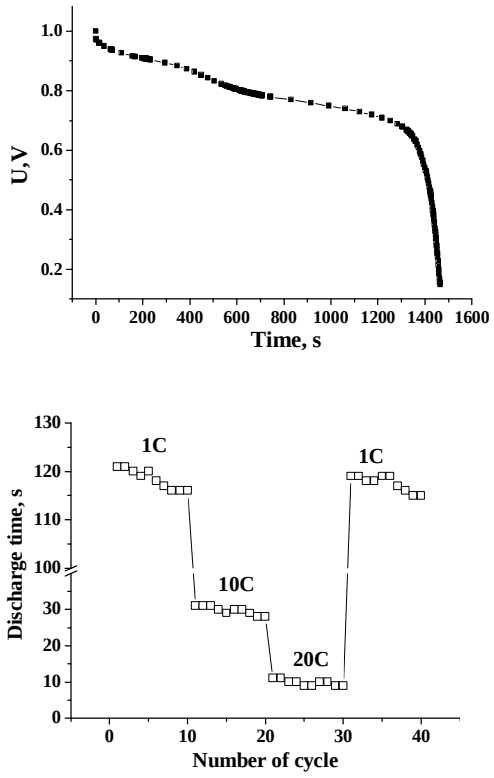

Fig.1. Typical discharge curve cycling characteristics of supercapacitor based on the AC and $LiMn_{1.95}Fe_{0.05}O_4$ spinel

Modern electronic devices and electric transport demand new energy sources with high specific power, capacity and energy. The hybrid supercapacitors (HSC) combine advantages of carbon and Faraday's electrodes and are the most perspective alternative of lithium power sources. We investigated the electrode material of HSC based on the $LiMn_{1.95}Fe_{0.05}O_4$ spinel in $LiNO_3$ and Li_2SO_4 water electrolytes.

The carbonated and activated carbon (specific surface area about 670 m^2/g, average mesopores and micropores sizes are 8 and 1.7 nm, respectively) were used as a polarized electrode. Lithium-manganesespinel was synthesized by sol-gel method without autoburning. As the initial precursors we used $Mn(NO_3)_3 \cdot 6H_2O$, $LiNO_3 \cdot 3H_2O$ and $Fe(NO_3)_3 \cdot 9H_2O$. The electrochemical studies were performed by the galvanostatic cycling and cyclic voltammetry. The diffusion coefficient was calculated by galvanostatic intermittent titration method.

The monophase $LiMn_{1.95}Fe_{0.05}O_4$ spinel with the Fe^{3+}cations substitution in the octahedral sites has been obtained (XRD and Mosssbauer spectroscopy data). The average particle sizes (calculated by Scherrer equation) were about 10-12 nm. The measurement of conductivity's frequency dependencies (impedance spectroscopy data) indicates the presence of the conductivity percolation mechanism in the 10^3 - 10^5 Hz range due to electrons jumps between the iron cations in the the spinel lattice. The obtained values of DC conductivity (about 10^{-3} Sm/m) are significantly higher than typical characteristic of unsubstituted lithium manganese spinel. Discharge curves (current density 1C) are characterized by a lateral region in 0.9-0.8 V range (Fig. 1a). Redox peaks were observed at the CVA curvesin the same voltage range so it's an evidence of lithium intercalation in the spinel structure. Calculated diffusion coefficient vary in 10^{-9}-10^{-10} cm^2/s range. Such comparatively high values are associated to high conductivity of spinel grains. The model capacitor specific capacitance decrease with the current density enlarging to 10 C and 20 C (Fig. 1b), however system are reversible even after high current cycling. The specific power of model capacitors was about 700 W/kg.

[1] B.I. Rachiy, B.K. Ostafiychuk, I.M. Budzulyak, V.M. Vashchynsky, R.P. Lisovsky, V.I. Mandzyuk, The effect of thermochemical treatment of carbon materials on their electrochemical properties, *Journal of Nano- and Electronic Physics* **6**(4) (2014) 040311-040316.

Synthesis and Properties of $Mg(OH)_2$ and MgO Fine Powers

I. Matsukevich, A. Ruchets, N. Krutko, V. Vashook

Institute of General and Inorganic Chemistry of the National Academy of Sciences of Belarus, Belarus

Fine powders of magnesium oxide are technologically important materials as they find very wide range of applications. Magnesium oxide has found application in heterogeneous catalysis, organic synthesis [1, 2], humidity and acid gases sensors, water and gas purification [3, 4], in determination of toxic substances and their subsequent treatment [5], as an antibacterial agent [6] and others. The properties of magnesium oxide are strongly determined by the properties of the precursors used to produce it including $Mg(OH)_2$. The magnesium hydroxide is widely used as a flocculant for wastewater treatment and acids neutralization, and as a catalyst in organic synthesis [7].

Magnesium hydroxide powders were synthesized by precipitation from water solutions. After precipitation the resultant product was repeatedly washed with distilled water and filtered. Samples dried at 105 °C consisted of magnesium hydroxide with a hexagonal crystal structure of brucite (P3m1), with unit cell parameters: a = 0,3143(1) nm, c = 0,4770(2) nm. After annealing at 550°C, the material was identified as a magnesium oxide with the structure of periclase (a = 0,4211(1) nm). The primary particle size decreased from 27 before annealing to 11 nm after annealing, whereas the secondary particle size increased from 79 to 255 nm. This can be explained by evolution of gaseous reaction products during formation of primary particles of MgO and their following agglomeration during sintering.

Isotherms of nitrogen adsorption-desorption for $Mg(OH)_2$ and MgO refer to isotherms of the fourth type, which correspond to mesoporous adsorbents with a pore size of $2 \leq D \leq 50$ nm. In accordance with the shape of the hysteresis loops of capillary condensation the pores in the samples are equivalent to cylindrical and slotted mesopores. The first of these are most likely formed by agglomeration of crystallites, and the second ones by consolidation of lamellar particles to the "packs" and "tapes".

The curves of pore size distribution prove homogeneity of mesoporous samples. The values of dominant pore diameter are 26 and 29 nm for magnesium hydroxide and magnesium oxide respectively. Obtained powders of $Mg(OH)_2$ and MgO showed sufficiently high total pore volume – 0,737 and 1,038 cm^3/g, respectively, which opens up opportunities to use them as nanoreactors for synthesis of isolated nano-sized particles and multidirectional catalysts.

[1] Ch. Jun, T. Shuanghong, L. Jiang, X. Ya, *Applied Catalysis A: General* **506** (2015) 118–125.
[2] S. Demirci, B. Öztürk, S. Yildirim, F. Bakal, M. Erol, O. Sancakoğlu, R. Yigit, E. Celik, T. Batar, *Materials Science in Semiconductor Processing* **34** (2015) 154–161.
[3] J.C. Yu, A. Xu, L. Zhang, R. Song, L. Wu, *Journal of Physical Chemistry B* **108** (2004) 64□70.
[4] W. Rizwan, S.G. Ansari, M.A. Dar, Y.S. Kim and H.S. Shin, *Materials Science Forum* **558□559** (2007) 983□986.
[5] C. Zeyneb, E. Sema (Akyil), and Y. Sabriye (Doyurum), *Environmental Progress & Sustainable Energy* **31**(4) (2012) 536–543.
[6] M.R. Bindhu1, M. Umadevi, M. Kavin Michea, M.V. Arasu, N.A. Al-Dhabi, *Materials Letters* **166** (2016) 19-22.
[7] Kh.M. Saoud, Sh. Saeed, R.M. Al-Soubaihi, M.F. Bertino, *American Journal of Nanomaterials* **2**(2) (2014) 21-25.

Nano-Composites in the System $Ce_{0.8}Sm_{0.2}O_{1.9}$ - MgO

V. Vashook[1,2], I. Matsukevich[1], J. Zosel[2], E. Sperling[3], K. Ahlborn[3], U. Guth[3], M. Mertig[3]

[1]*Institute of General and Inorganic Chemistry NAS of Belarus, 220072 Minsk, Belarus*
[2]*Kurt-Schwabe-Institut für Mess- und Sensortechnik e.V. Meinsberg, 04736 Waldheim, Germany*

Grain boundaries of single-phase solid electrolyte ceramics are often less conductive in comparison with grain volumes [1,2]. Another situation can appear in composite materials consisting of solid electrolytes (SE) and dielectric phases (Ins). The SE/Ins grain boundaries can exhibit higher conductivities compared to the bulk of the solid electrolyte grains in composites where the epitaxial connecting zone between SE and Ins is characterized with certain structures containing irregularities and additional defects [3]. It was found for example, that epitaxial films of yttria stabilized zirconia (YSZ), formed on MgO single crystals, have oxide ion conductivities, which are 3–4 orders of magnitude higher than those of YSZ in the temperature range 600–800 °C [4]. Herewith, the formation of intermediate layers between YSZ and MgO phases with the thickness 1.6 nm was observed.

Elevated oxygen ion conductivities of such composites can be realized with ceramic structures in connection with appropriate conductivity parameters of the composite components. For example, this phenomenon was observed in systems like LiJ/Al_2O_3, $Ce_{1-x}Sm_xO_{2-x/2}$/Na_2CO_3, Na_2CO_3/Na_2SO_4, $Ba(NO_3)_2$–Al_2O_3 and $Ce_{0.8}Gd_{0.2}O_{1.9}$/MgO [5].

Conductivity model of the nano-composite ceramics consisting of solid electrolyte (SE) and the dielectric phases (Ins) proposed in the assumption that the conductivity of the grain boundaries (SE/Ins) is higher than the bulk conductivity of the SE particle and the conductivity of SE/SE grain boundaries. The particle size of composite ceramics (SE+Ins) at which the conductivity may exceed the conductivity of the single phase solid electrolyte ceramics is estimated depending of grain boundary thickness and the bulk and grain boundary conductivities of the composite ceramic components. To test the model, the composite ceramics based on magnesium oxide (MgO) and cerium dioxide doped with samarium oxide (SDC) were prepared.

The total electrical conductivity of the SDC/MgO composite ceramics with 50 % mol. of dielectric magnesium oxide measured in air at temperature 250-550 °C was comparable with the conductivity of the pure SDC single phase ceramics. Such situation can be explained by appearance of new more conductive areas in composite ceramics. We propose that these high conductive areas can be SDC/MgO grain boundaries, which are only the new conductivity areas in composite ceramics in comparison with the single phase SDC ceramics.

Optimization of grain size and uniformity of distribution of components in the composite ceramics can open up the possibility to produce more conductive oxide solid electrolyte materials, but verification of this assumption requires additional investigations with composition and structure of new nano-composites in this system.

[1] T. Kudo and H. Ohayashi, *J. Electrochem. Soc.* **122** (1975) 142-147.
[2] M.C. Martin, M.L. Mecartney, *Solid State Ionics* **161** (2003) 67–79.
[3] H. Mehrer, *Springer Ser. Solid State Sci.* **155** XIX (2007) 654.
[4] I. Kosacki, Ch.M. Rouleau, P.F. Becher, J. Bentley, D.H. Lowndes, *Solid State Ionics* **176** (2005) 1319–1326.
[5] V. Vashook, J. Zosel, E. Sperling, K. Ahlborn, F. Gerlach, W. Fichtner, M. Schelter, U. Guth, M. Mertig, *Solid State Ionics* **288** (2016) 98-102.

Effects of Physical- and Chemical-Adsorbed Water near Grain Boundaries in Modified MgO-Al_2O_3 Nanoceramics Tested with Positron-Positronium Trapping Algorithm

H. Klym[1], A. Ingram[2], O. Shpotyuk[3,4], I. Hadzaman[5], D. Chalyy[6]

[1]*Lviv Polytechnic National University, 12 Bandera Str., 79013 Lviv, Ukraine*
[2]*Opole University of Technology, 75 Ozimska Str., 45370 Opole, Poland*
[3]*Vlokh Institute of Physical Optics, 23 Dragomanov Str., 79005 Lviv, Ukraine*
[4]*Jan Dlugosz University, 13/15 al. Armii Krajowej, 42201 Czestochowa, Poland*
[5]*Drohobych Ivan Franko State Pedagogical University, 24 I. Franko Str., 82100 Drohobych, Ukraine*
[6]*Lviv State University of Life Safety, 35 Kleparivska Str., 79000 Lviv, Ukraine*

The positron annihilation lifetime (PAL) spectroscopy method based on the fact that the unstable positron-electron system (positronium Ps) is repelled from ionic cores of atoms and tends to location in open pores. In the ground state, the Ps exists as singlet para-positronium p-Ps and triplet ortho-positronium o-Ps. In the case of oxide water-immersed ceramics, two channels of PAL should be considered – the positron trapping and o-Ps decaying [1]. In general, these processes are independent ones. However, if trapping sites will appear in a vicinity of grain boundaries neighbouring with free-volume pores, they can become mutually interconnected resulting in a significant complication of the measured PAL spectra. This occurs provided the input of one of the above annihilation channels will be significantly changed. In addition, adsorbed water influences on process of physical and chemical adsorption of water near grain boundaries in the MgO-Al_2O_3 ceramics.

To clarify this feature, we shall study the PAL characteristics of modified MgO-Al_2O3 ceramics affected to water sorption treatment enhancing o-Ps decaying over positron trapping modes using positron-positronium trapping algorithm [2].

The ceramic pellets were sintered in a special regime with maximal temperatures (T_s) of 1100, 1200, 1300 and 1400 °C during 2 h [1]. The PAL measurements were performed with an ORTEC spectrometer (^{22}Na source) placed between two sandwiched samples. PAL spectra were fitted on four components with positron lifetimes t_1, t_2, t_3 and corresponding unity-normalized intensities I_1, I_2, I_3. The third components in the measured lifetime spectra are due to "pick-off" annihilation of o-Ps atoms in ceramics nanopores filled with adsorbed water. It is established that the τ_3 lifetime increases with T_s, while its intensity I_3 decreases. These changes correspond to the increased nanopore size and smaller amount of nanopores. In all water-immersed samples, the intensity of third component I_3 significantly increases as compared with dried samples indicating a large content of absorbed water present in ceramics.

To apply positron-positronium trapping algorithm it was shown that the chemical-adsorbed water vapor modifies structural defects located at the grain boundaries in a vicinity of pores, this process being accompanied by void fragmentation during water adsorption and agglomeration during water desorption after drying. The physical adsorbed water not modified grain boundaries in oxide MgO-Al_2O_3 ceramics located only in nanopores.

[1] H. Klym, A. Ingram, I. Hadzaman, O. Shpotyuk, Evolution of porous structure and free-volume entities in magnesium aluminate spinel ceramics, *Ceramics International* **40** (2014) 8561–8567.

[2] O. Shpotyuk, J. Filipecki, A. Ingram, R. Golovchak, M. Vakiv, H. Klym, V. Balitska, M. Shpotyuk, A. Kozdras, Positronics of subnanometer atomistic imperfections as high-informative characterization tool in nanomaterials science, *Nanoscale Research Letters* **10**:77 (2015).

Destructive Metallic Nanoclusterizaion in Oxide and Chalcogenide Glassy Media

M. Shpotyuk

Lviv Polytechnic National University, 12 Bandera Str., 79013 Lviv, Ukraine

Plasmonic nanocomposite materials like glasses containing metallic nanoparticles (NPs) are of high practical importance in view of their excellent nonlinear optical properties such as increased high-order nonlinearities [1]. Ion implantation (***highly destructive*** method) is one the widely used methods to ensure agglomeration of ***guest*** NPs in ***host*** glassy matrix. The degree of destruction being strongly dependent on the atomic compactness [2]. In relatively dense matrices, which are proper for glassy oxides containing great amount of silica SiO_2 [2] or chalcogenide glasses (ChGs) of mixed Ge/As-S/Se systems [3], the intrinsic interatomic linking of a glass structure should be significantly destroyed to accommodate the embedded NPs. In such case, agglomeration occurs under tight chemical interaction between NPs and destructed glass components, the preferential character of this interaction being decisive in the finalized properties of NPs-embedded glassy system. So principal difference between oxide- and chalcogenide-type glassy matrices should be examined quantitatively to clarify possible consequences resulting from expected diversity in the destructive clustering for the embedded NPs. In this work, it was tried to accomplish this from point of mean bond energies.

The principal difference in the origin of optical nonlinearities caused by metallic NPs (Cu, Ag, Au) embedded destructively in oxide- and chalcogenide glasses was shown. The energetic barriers of bond disproportionality for implanted atoms occur to be different for oxide and chalcogenide environment. This finding is in full agreement with numerous evidences exploring destructive and non-destructive mechanisms of NPs embedding.

[1] A. Zakery and S.R. Elliott, *Optical nonlinearities in chalco-genide glasses and their applications*, Springer-Verlag, Berlin-Heidelberg, 2007.

[2] A.L. Stepanov, *Ion-synthesis of metal nanoparticles and their optical properties*, Nova Sci. Publ., New York, 2011.

[3] A. Feltz, *Amorphous inorganic materials and glasses*, VCH Publ., New York, 1993.

Influence of the TiO_2 Additives on Hydrogen Sorption/Desorption Properties of Mg-Based Composites

I.Yu. Zavaliy*, V.V. Berezovets, R.V. Denys, P.Ya. Lyutyy, A.B. Riabov

Physico-Mechanical Institute, NAS Ukraine, 5 Naukova Str., 79060 Lviv, Ukraine
* zavaliy@ipm.lviv.ua

Practical use of magnesium and its alloys in hydrogen storage systems is limited by slow kinetics and elevated temperatures (>300 °C) of hydrogen absorption/desorption. A lot of recent studies were devoted to the enhancement of these parameters, including preparation of magnesium by reactive ball milling in hydrogen medium (RBM) and modification by different additions, e.g. oxides, intermetallic compounds, graphite etc [1]. In our previous work we have studied the properties of Mg-based composite materials with $Ti_4Fe_2O_x$ suboxide as catalytic additive [2]. Substantially improvement of hydrogen absorption-desorption properties were demonstrated also for the Mg–$Zr_4Fe_2O_x$ composites prepared by RBM [3]. Our further studies were devoted to the combination of graphite and IMC additives in the same Mg-based composite materials. This report will be devoted to the influence of Ti and TiO_2 oxide in different dispersive states on the hydrogenation properties of Mg-based composites.

Mg-based hydride composites were prepared by reactive ball milling of Mg and Ti or TiO_2 additive (with and without graphite) under 1 MPa H pressure. It has been shown that composites have H storage capacity of 1.8-2 wt.% at room temperature and 5.5-7.0 wt.% at 200-300 °C. Hydrogen desorption from the hydrides was studied by means of thermodesorption spectroscopy (TDS) with linear heating of specimens (2 K/min) in dynamic vacuum from room temperature to 620–670 K. Thermal desorption from the selected hydrides was also studied by *in situ* XRD. Powder XRD patterns were measured during heating (2 K/min heating in 1 bar argon from 25 to 650 °C) using Bruker C2 Discover powder diffractometer at the X-ray Crystallo-graphic Center, University of Maryland, USA. The observed TDS curves demonstrated onset temperature for hydrogen release. Compared to convenient $MgH_{\sim 2}$ hydride, much lower temperatures of hydrogen desorption peaks were observed for the synthesized composites. The comparison of the hydrogenation/dehydrogenation properties will be discussed for the Mg-based composites with the Ti and TiO_2 additives in different dispersive state. The cycling stability will be compared for the composite materials with and without carbon additives.

[1] B. Sakintuna, F. Lamari-Darkrim, M. Hirscher, *Int. J. Hydrogen Energy* **32** (2007) 1121–1140.
[2] I.Yu. Zavalii, R.V. Denys, V.V. Berezovets, *Materials Science* **45** (2009) 248-257.
[3] V.V. Berezovets, R.V. Denis, I.Yu. Zavaliy, V. Paul-Boncour, *Powder Metall. Met. Ceram.* **53** (2014) 335–342.

Transport and Relaxation of Charge in Organic-Inorganic Nanocomposites

I. Olenych[1], O. Aksimentyeva[1], B. Tsizh[2,3], Yu. Horbenko[1]

[1]*Ivan Franko National University of Lviv, Lviv, Ukraine*
[2]*Stepan Gzytsky Lviv National University of Veterinary Medicine and Biotechnologies, Lviv, Ukraine*
[3]*Kazimierz Wielki University, Bydgoszcz, Poland*

Hybrid nanocomposites on the base of conjugated polymers reinforced with inorganic nanoparticles of different nature are in the focus of increased attention as composite materials for sensing and optoelectronics applications [1–3]. Incorporation of ZnO and silicon nanoclusters give a possibility to use electrochemical properties of conjugated polymers, size effects and large area surface of semiconductor nanoparticles. Comprehensive study of the electrical parameters of organic-inorganic nanocomposites improves functionality and extends prospect of practical application of the hybrid materials.

Present work focuses on the studying the processes of charge transport in nanocomposites based on poly(3,4-ethylenedioxythiophene) abbreviated hereafter as PEDOT and mixture of porous silicon (PS) and ZnO nanoparticles for sensor electronics. PEDOT–PS–ZnO hybrid films were characterized by scanning electron microscopy. The electrical properties of the obtained nanocomposites were investigated by means impedance spectroscopy in the frequency range of 25 Hz – 1 MHz and thermally stimulated depolarization (TSD) spectroscopy.

Electrical resistance and capacitance of the PEDOT–PS–ZnO composites depend on the composition. Increasing of content of ZnO nanoparticles caused the rise in the internal resistance of the PEDOT:PSS–PS–ZnO films from 20 to 70 MOhm. The complex frequency dependence of the impedance of hybrid films can be caused by the features of transport and relaxation of charges in disordered systems. Studies of the relaxation processes in the hybrid nanocomposites were performed using TSD spectroscopy in 80–325 K temperature range. In the case of disordered systems the trap levels are distributed quasi-continuously on the activation energy. To determine the activation energy of electrically active defects in experimental films, the temperature dependencies of the depolarization current have been measured. The analysis of the TSD spectra and the calculation of the density of states energy distribution suggests that the groups of trap levels, with differences in nature and activation energies in the ranges of 0.2–0.4 and 0.5–0.7 eV are present. Such localized electron states influence the charge transport in the PEDOT–PS–ZnO composites.

We have found experimentally that the electrical characteristics of our composite films are strongly dependent on the surrounding atmosphere. In particular, increasing relative humidity results in significant decrease of the electrical resistance of the PEDOT–PS–ZnO hybrid films. The response time of the sensory elements to changing of water vapour concentration is about 20 s. The combination of the porous silicon and zinc oxide nanoparticles provides an increasing of surface area of the sensors and their high sensitivity to water molecules.

[1] I.B. Olenych, O.I. Aksimentyeva, L.S. Monastyrskii, Yu.Yu. Horbenko, L.I. Yarytska, Sensory properties of hybrid composites based on poly(3,4-ethylenedioxythiophene) – porous silicon – carbon nanotubes, *Nanoscale Research Letters* **10** (2015) 187.

[2] E. Holder, N. Tessler, A.L. Rogach, Hybrid nanocomposite materials with organic and inorganic components for optoelectronic devices, *Journal of Materials Chemistry* **18** (2008) 1064.

Characterisation and Electrical Properties of Silicon–Silicon Oxide Nanosystems

I. Olenych

Ivan Franko National University of Lviv, Lviv, Ukraine

Heterogeneous nanosystems based on silicon attract attention of researchers due to the wide range of possible applications, in particular, single electron transistors [1], memory elements [2] and gas sensors [3]. Silicon oxide is the most natural dielectric material for silicon technology. The study of electronic processes that occur in the silicon–silicon oxide nanosystems opens new technological possibilities and constructive approaches for creating a new generation of sensor devices.

Silicon–silicon oxide composites were obtained by thermal oxidation of finely dispersed silicon powder. The silicon powder was separated from colloidal aqueous solution by sedimentation. Silicon oxide nanosystems were characterized by means of scanning electron microscopy, UV-vis transmittance and FTIR spectroscopy. Due to thermal oxidation of finely dispersed silicon powder we observed an increase of transmittance in the 12000–15000 cm^{-1} wavenumbers range. Transformation of optical spectra may be associated with a change in the band gap of silicon nanocrystals due to decreasing of their size.

To study the electrical properties of nanosystems the experimental samples were formed under 200 atm pressure. By means of impedance spectroscopy in the 25 Hz – 1 MHz range it was found that experimental samples show a decrease in electrical capacitance and internal resistance with increasing the frequency. To interpret the impedance of silicon–silicon oxide composite the equivalent circuit model was constructed. According to the model, the total impedance of the sample can be represented by two RC (parallel resistor and capacitor) sub-circuits, which correspond to the process of transfer of charge carriers through the boundary and in the bulk of silicon nanocrystals.

Based on the spectra of thermally stimulated depolarization current, the localized electron states in the experimental samples were found. Trap levels with non-equilibrium carriers are distributed quasi-continuously on the activation energy and exist in the ranges of 0.2–0.3, 0.35–0.45 and 0.55–0.65 eV. Such localized electron states influence the charge transport in the nanocomposites. Obtained results suggest the complex processes of transfer and relaxation of charges in the silicon–silicon oxide nanosystems.

[1] A. Dutta, S. Oda, Y. Fu, M. Willander, Electron transport in nanocrystalline Si based single electron transistors, *Jpn. J. Appl. Phys.* **39** (2000) 4647.

[2] K. Yano, T. Ishii, T. Hashimoto, T. Kobayashi, F. Murai, K. Seki, Room-temperature single-electron memory, *IEEE Trans. Electron. Dev.* **41** (1994) 1628.

[3] I.B. Olenych, O.I. Aksimentyeva, L.S. Monastyrskii, Yu.Yu. Horbenko, L.I. Yarytska, Sensory properties of hybrid composites based on poly(3,4-ethylenedioxythiophene) – porous silicon – carbon nanotubes, *Nanoscale Research Letters* **10** (2015) 187.

Cathodoluminescence of Thermoregulating Composite Materials

V.V. Harutyunyan[1,*], E.M. Aleksanyan[1], A.H. Badalyan[1], N.E. Grigoryan[1], V.S. Baghdasaryan[1], A.A. Sahakyan[1], V.V. Baghramyan[2], A.A. Sargsyan[2]

[1]*A.I. Alikhanian National Science Laboratory, Yerevan Physics Institute, 0036 Yerevan, Armenia*
[2]*Institute of General and Organic Chemistry of Armenian National Academy of Sciences, Yerevan, Armenia*
***** *vharut@mail.yerphi.am*

Silicates and other refractory composite thermoregulating coatings (TRC) form a basis of technically important products and articles such as "solar reflectors" for space vehicles. TRC properties crucially depend on the peculiarities of their structure at the atomic level such as their chemical bond, defectiveness, and nature of defects in crystal lattices.

The work presented is aimed at the study of optical characteristics (cathodoluminescence) of zirconium silicate obtained by hydrothermal microwave synthesis.

The cathodoluminescence (CL) experiments were performed using a special installation. CL spectra (ZrO_2 and SiO_2) were measured within the temperature range of 77 - 300 K using a low temperature cryostat. CL excitation was performed using a compact electron accelerator with the following beam parameters: adjustable electron energy of 1 - 30 keV and electron current of 10 - 100 nA. When TRC are exposed to 10keV and 5keV pulsed electron beams at different temperatures, an intense luminescence is observed within the spectral range of 2.75 eV - 3.5 eV. CL spectrum at 78 K is a broad band with a maximum shifted depending on the excitation energy (2.75 eV - 3.5 eV). With increasing temperature (300 K), a decrease of CL intensity is observed, and the maximum of luminescence band becomes 3.0 eV. Excitation of CL in TRC within the spectral range of 1-5 eV by pulsed electron beams of different energies has revealed that the intensity of the CL spectra depends strongly on the excitation energy. 2.75eV, 3.0eV and 3.25eV bands observed in the CR spectra of the studied TRC (ZrO_2 and SiO_2) are characteristic of luminescence of many silicates and are usually associated with radiation of defect centers. Zirconium ions may be located in tetrahedral surrounding in the form of (OH) - $Zr-(OSi)_3$ or $Zr-(OSi)_4$ and $[SiO_4]^{4-}$ groups due to the presence of zirconium ions and local distortions of silicon- oxygen tetrahedra. $[SiO_4]^{4-}$ center occurs in the case of violation of the symmetry of silicon-oxygen tetraedra because of a nearby defect. In the formation of above centers and their metastable states, impurities can play an important role: as charge compensators or as the factors of change in electron density distribution of the tetrahedra. The fact that CL luminescence of defect centers is efficiently excited at low temperatures testifies to the possible transfer of the excitation energy from excitons and, thus, to the formation of specific excited states in distorted lattices. The emission band at 3.0 eV is apparently related to an intermediate stage of the formation of exciton-defect complexes or short-living defects in the form of vacancies V_{Zr}^- and interstitial ions Zr^+ formed at bond breaking - the optical transitions in V_{Zr}^- center.

Luminescent Properties of Composite Materials in the VUV Region

V.V. Harutyunyan[1,*], E.M. Aleksanyan[1], A.H. Badayan[1], N.E. Grigoryan[1], V.S. Baghdasaryan[1], A.A. Sahakyan[1], V.B. Gavalyan[1], V.V. Baghramyan[2], A.A. Sargsyan[2]

[1]*A.I. Alikhanian National Science Laboratory, Yerevan Physics Institute, 0036 Yerevan, Armenia*
[2]*Institute of General and Organic Chemistry of Armenian National Academy of Sciences, Yerevan, Armenia*
***** *vharut@mail.yerphi.am*

Photo- and radiation resistances of white powders used as pigments for reflective thermoregulating coatings (TRC) are fundamental characteristics that determine their quality. The change in the diffuse reflection and luminescence spectra due to the formation of the absorption bands induced by light quanta in the solar spectrum range or by charged cosmic particles leads to an increase in the proportion of energy absorbed and increase in temperature of the objects with such coatings.

Spectroscopic characteristics of zirconium silicate ($ZrO\ nSiO_4$): luminescence excitation and luminescence properties were investigated over a wide spectral range of 2-20eV at different temperatures.

Doping was performed during hydrothermal microwave synthesis of zirconium silicate. The luminescent properties of the ($ZrO\ nSiO_4$) TRC were studied at HASYLAB laboratory using SUPERLUMI station. The station provides ample opportunities for research within the luminescence VUV spectroscopy region with time and energy resolution. The experiments were performed at 300 and 10 K. 2.78eV, 4.96eV, 6.52eV, 2.88eV, 3.65eV, 4.13eV, 4.96eV, 6.2eV, 11.0eV broad bands observed in the excitation and luminescence spectra of the studied $ZrSiO_4$ are characteristic of many silicates and are usually associated with the radiation of defect impurity centers and $[SiO_4]^{4-}$ which are due to impurity ions and local distortions of silicon-oxygen tetrahedra. $[\ ZrO_4]^{4-}$ center can be formed when in the regular tetrahedral position zirconium atom substitutes silicon atom. $[SiO_4]^{4-}$ center occurs in the case of violation of the symmetry of silicon-oxygen tetraedra because of a nearby defect. Violation of regular bonds in zirconium and silicon sublattices may cause short-living optically active defects such as anionic vacancy luminescence centers of F and F^+ type within UV and VUV spectral regions. Electrons are trapped by anion vacancies which always are present in the synthesis of zirconium silicate, and thus F and F^+ color and radiation centers or emission arise with maxima in UV and VUV excitation and luminescence spectra. The reason for the shift of radiation maxima in the excitation and luminescence spectra is that the generation of excitonic excitation takes place directly in those lattice sections distorted by the presence of a defect, and its non-radiative relaxation is carried out mainly with the participation of local oscillations of the defect center.

In conditions of low-temperature (T = 10 K) experiments, radiative relaxation is dominated, and the probability of non-radiative transitions is practically equal to zero.

Thus, the luminescence of silicates in the case of photoexcitation (with the photon energy in the region of interband transitions) of said optically active centers is effectively excited in UV –VUF regions, and their relaxation process includes the step of forming multicomponent defect complexes.

Nanoscale Structural Features, Phase Relationships and Thermoelectric Properties of Melt Spun and Spark Plasma Sintered Filled Skutterudites

S. Nichkalo[1], Iu. Kogut[1,2], V. Ohorodniichuk[2], A. Dauscher[2], C. Candolfi[2], P. Masschelein[2], A. Jacquot[3] and B. Lenoir[2]

[1]*Department of Semiconductor Electronics, Lviv Polytechnic National University, 12 Stepana Bandery Street, 79013 Lviv, Ukraine*
[2]*Institut Jean Lamour, UMR 7198 CNRS – Université de Lorraine, Parc de Saurupt, 54011 Nancy, France*
[3]*Fraunhofer-Institut für Physikalische Messtechnik IPM, Heidenhofstrasse 8, 79110 Freiburg, Germany*

The reduction of thermal conductivity remains a main approach to improvement of figure-of-merit of most state-of-the-art thermoelectric materials. In thermoelectric skutterudites it is achieved either by multiple filling of large lattice voids [1] or by developing of nanoscale spatial features in the material's structure. Nanostructuring by means of melt spinning (MS) combined with spark plasma sintering (SPS) has been shown to be prospective for rapid fabrication of fine-grained skutterudites with greatly reduced thermal conductivity and improved thermoelectric performance [2]. However, upon such non-equilibrium high-temperature processing the $CoSb_3$-based skutterudites, in particular, Fe-substituted p-type compounds, are prone to decompose into multiple phases, including lower antimonides and pure Sb, which may further deteriorate their thermoelectric performance. In this research we used X-ray diffractometry (XRD) and scanning electron microscopy (SEM) in order to evaluate the phase and microstructural relationships in the melt-spun filled Co_4Sb_{12} and $Fe_{4-x}Co_xSb_{12}$, as well as their change upon subsequent SPS. Our studies have shown that upon melt-spinning the skutterudites of both types decompose into multi-phase polycrystalline compounds and the nominal major phase is weakly preserved in them after rapid solidification. Surprisingly, larger amounts of skutterudite phase were found in melt-spun filled $Fe_{4-x}Co_xSb_{12}$ p-type materials as compared to their iron-free n-type counterparts. Whole profile fitting of XRDs, including Rietveld refinement and Williamson-Hall plot method, and SEM studies indicated in substantial reduction of grains to sizes below 100 nm for all phases developed upon MS. Furthermore, SPS of both conventional and melt spun skutterudites resulted in even further reduction of crystallites. Upon short annealing and sintering directly in SPS the multi-phase n-type materials were easily restored into single-phase filled $CoSb_3$ with nanoscale features preserved. Abundant secondary phases of $FeSb_2$ and pure Sb remained in the MS-SPS filled $Fe_{4-x}Co_xSb_{12}$ though. Relatively high and improved figure-of-merit ZT_{max} reaching 0.9 at $T \approx 700K$ has been gained in n-type $Yb_xCo_4Sb_{12}$ as compared to a conventional material with same nominal composition. However, the reduction in lattice thermal conductivity was not significant and comparable to that gained via multiple-filling approach. Development of abundant impurity phases in filled $Fe_{4-x}Co_xSb_{12}$ has unfortunately led to drastic drop in their thermoelectric performances, which even further deteriorated upon thermal cycling. In addition to these insights, some effects of filler atoms on phase relationships and nanoscale features in $CoSb_3$ and $Fe_{4-x}Co_xSb_{12}$ skutterudites are considered in the paper.

[1] E. Alleno, D. Bérardan, C. Godart, M. Puyet, B. Lenoir, R. Lackner, E. Bauer, L. Girard, D. Ravot, Double filling in skutterudites: A promising path to improved thermoelectric properties, *Physica B* **383** (2006) 103.
[2] G. Tan, W. Liu, S. Wang, Y. Yan, H. Li, X. Tang, C. Uher, Rapid preparation of $CeFe_4Sb_{12}$ skutterudite by melt spinning: rich nanostructures and high thermoelectric performance, *J. Mater. Chem. A.* **1** (2013) 12657.

Nanocomposite CdS:Au NPs

V.V. Kusnezh, H.A. Il'chuk, R.Yu. Petrus', F.I. Tsyupko[2]

Lviv Polytechnic National University, [1]Physics Department, [2]Analytical chemistry Department, 12 S. Bandery Str., 79013 Lviv, Ukraine

The nanoparticles (NPs) of Au and Ag noble metals can be used as light scattering elements for enhancing the solar cell energy conversion efficiencies. It is known that light can induce a localized surface plasmon resonance (i.e. a collective oscillation of the conduction electrons) in the metal particles of sub-wavelength size. These plasmonic nanoparticles have very strong interaction with light near the resonance frequency. Incident light can be either absorbed or scattered and the contribution from each mechanism depends on the size and shape of the particle. The inclusion of metallic nanoparticles in solar cells (SC) can enhance the absorption of the light by two mechanisms: an increasing of the forward scattering crossection and a near-field enhancement.

Cadmium sulfide thin films were deposited on the glass and ITO surfaces with geometry 16×8×0.7 mm by magnetron RF-sputtering method. The Au NPs array was chemically deposited from a mixture of $AuCl_3$, CH_2O and Na_2CO_3 aqueous solutions on the cadmium sulfide thin films. The substrate was covered by 300 µl of working solution for 0.5–2 min and rinsed in distilled water to prevent precipitation of NP growth in solution volume. Post deposition (400°C, 1 h) annealing was performed to evaporate water residuals and improve NPs adhesion.

The surface morphology was investigated by atomic force microscope XE-70 Park System (Park, South Korea). Transmission T(λ) and reflectivity R(λ) spectra of the samples in the wavelength range from 300 to 1100 nm with 5 nm step were measured by the spectrophotometer Bentham PVE 300 (Bentham, UK).

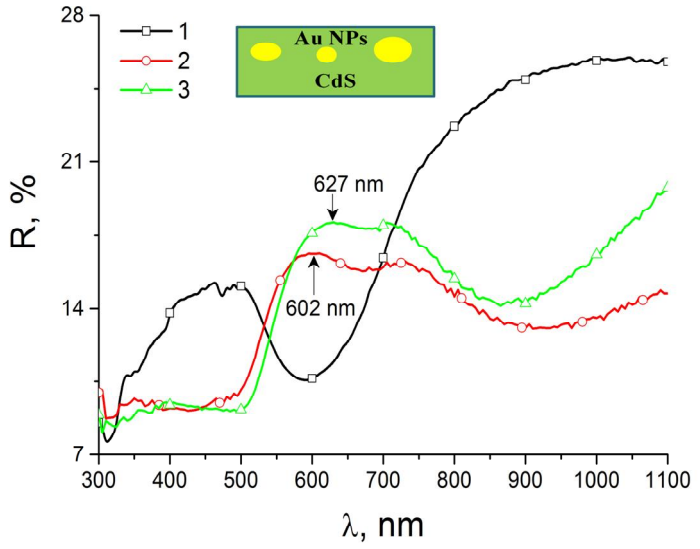

Fig. Reflectivity spectra of the as deposited CdS thin film (1) and with Au NPs array decorated on top (a) and inside (b) the CdS thin films with 60 (2) and 90 s (3) deposition time

Formation of Silver Nanoparticles in $Li_2B_4O_7$-Ag_2O and $Li_2B_4O_7$-Gd_2O_3-Ag_2O Borate Glasses

V.T. Adamiv[1], R.V. Gamernyk[2], I.M. Teslyuk [1]

[1]*O.G.Vlokh Institute of Physical Optics, Dragomanov Str. 23, Lviv 79005, Ukraine*
[2]*Ivan Franko National University, Kyrylo and Methodiy Str. 8, Lviv 79005, Ukraine*

Nanocomposite materials, whose basis is consisted of metallic nanoparticles (MNPs) of noble metals (Au, Ag, Pt) in dielectric media, are the object of significant attention in recent years. This is caused by large influence of MNPs on linear and nonlinear susceptibilities of dielectric matrix [1], radiative recombination and giant surface enhanced Raman scattering.

Borate glasses, the basis of which is boron anhydride B_2O_3 with its tendency to polycondensation, can be prospective for MNPs formation. The borate glasses structurally consist of boroxole groups, which are joined by the bridge oxygen atoms that makes their structure enough open. These boroxole groups make the borate glass structure more open near the glass transition temperature T_g [2] that simplifies the process of MNPs formation.

The formation of metallic (silver) nanoparticles (AgNPs) in the near-surface layer of $98.0Li_2B_4O_7$–$2.0Ag_2O$ ($Li_2B_4O_7$:Ag) and $97.0Li_2B_4O_7$–$1.0Gd_2O_3$–$2.0Ag_2O$ ($Li_2B_4O_7$:Gd,Ag) glasses at the annealing in vacuum or in air has been reported. The proposed mechanism of AgNPs growth in the near-surface layer of $Li_2B_4O_7$:Gd,Ag glass during its annealing in air belongs to the "bottom-up" class. On the other hand, if the specimen is annealed in vacuum, the process of formation of neutral Ag^0 atoms on the surface substantially dominates over the reduction with the participation of gadolinium ions in bulk. As a result, the processes of AgNPs nucleation and formation run more intensively on the specimen surface. A conclusion is drawn that the annealing in vacuum does not necessarily require the presence of reducing ions, where as the formation of nanoparticles at the annealing in air is impossible without reducing agents. Structural defects play a crucial role in the AgNPs nucleation process. In the absorption spectra of glass samples $Li_2B_4O_7$:Ag, annealed in a vacuum, revealed an intense plasmon band characteristic for silver atoms. At the same time, for $Li_2B_4O_7$:Gd,Ag intensive similar plasmon bands detected in samples annealed in a vacuum and in air.

The radii AgNPs calculated by us on the basis of the plasmon band half-width $Li_2B_4O_7$:Gd,Ag glasses falls within the interval of 1.0–1.5 nm and well correlate with radii of 2.8–6.0 nm obtained for AgNPs in various glasses by other authors [3,4]. However, our previous AFM researches of AgNPs formed by annealing in the reducing atmosphere of H_2 [5] or in vacuum (in this work) on the surface of $Li_2B_4O_7$:Ag glass showed that the value of R falls within the limits from 7 to 25 nm, with a maximum near 15 nm. For samples $Li_2B_4O_7$:Gd,Ag, annealed in vacuum, the size of AgNPs on the surface was evaluated also by small-angle X-ray scattering. The average size of AgNPs was found to be $d \approx 26.0$ nm. Such a spread in the dimensions of AgNPs obtained using different methods in $Li_2B_4O_7$:Ag and $Li_2B_4O_7$:Gd,Ag glasses can be explained by the fact that different techniques of radius determination may give rise to nonidentical results.

[1] V.A. Markel, V.M. Shalaev, *Phys. Rev. B* **53** (1996) 2437.
[2] R.E. Youngman, J.W. Zwanziger, *J. Non-Cryst. Sol*. **168** (1994) 293.
[3] J. Fernández Navarro, J. Toudert, Y. Rodríguez-Lazcano et al., *Appl. Phys. B* **113** (2013) 205.
[4] I.S. Sinev, M. Petrov, A.K. Samasev et al., *Nanoscale Research Letters* **8** (2013) 260.
[5] I.M. Bolesta, O.O. Kushnir, I.I. Kolych et al., *Adv. Sci. Eng. Med.* **6** (2014) 326.

SECTION 4

RESISTIVITY SWITCHING AND TRANSPORT PHENOMENA

New Nm Oxide Films for Quantum Tunnelling Effect

E. Hristoforou

Laboratory of Electronic Sensors, School of Electrical & Computer Engineering, National Technical University of Athens, Zografou Campus, Athens 15780, Greece

We propose a new non-volatile random access memory (NVRAM), based on the control of the quantum tunnelling effect of a metal-insulator-metal tri-layer. The first implemented arrangement is aluminium-alumina-aluminium tri-layer, where the ~1 nm thick alumina's quantum tunnelling coefficient depends on its crystalline or amorphous state. In case of crystalline structure the tunnelling coefficient permits the electron transport from the one aluminium layer to the other, while for the case of amorphous state the tunnelling coefficient does not permit such electron transport. The control of the phase is achieved by passing proper current waveforms from the two or the one of the metal conductors of the arrangement, while the reading of the 1/0 information, corresponding to crystalline/amorphous phase respectively can be transmitted by a single FET transistor. The advantage of this tri-layer with respect to the chalcogenide NVRAM state of the art is that reducing dimensions, the quantum tunnelling effect is enhanced instead of becoming more uncertain as it is for the case of the resistive NVRAMs. This way, dimensions of our quantum tunnelling NVRAM can go as low as the focused ion beam lithography permits, allowing also for lower current density to observe repeatable phase transformation in lower dimensions.

Tuning the High-Temperature Properties of Perovskite-Related Oxides for Electrochemical Applications

S.Ya. Istomin

Department of Chemistry, Moscow State University, Moscow, Russia

Complex transition metal oxides with mixed electronic and oxide-ion conductivities attract substantial interest due to their potential application in high-temperature electrochemical devices such as solid-state sensors, oxygen permeation membranes and solid oxide fuel cells (SOFCs). Oxides with the perovskite-related structures are considered as best materials for use in such devices. This is especiallytrue for cathode material in intermediate temperature solid oxide fuel cell (IT-SOFC). Major requirements for cathode material in IT-SOFC include high electronic and oxide-ion conductivity, catalytic activity for oxygen reduction, thermal expansion coefficient (TEC) close to that ofthe electrolyte and inertness toward chemical interaction with the electrolyte [1]. In the present work influence of the crystal structure and chemical composition on the properties of perovskite-related cobalt and copper oxides important for their use as cathode materials for IT-SOFC is discussed.

Complex perovskite-related cobaltates with Co^{3+} fit perfectly to the majority of the requirements for cathode materials for IT-SOFC listed above. However, they possess high TEC due to thermally activated transition between low (LS) and high-spin (HS) state of Co^{3+}. Influence of this transition on high-temperature thermal expansion properties of perovskite-related oxides is discussed using an example of layered $(Pr,Sr)_2(Ni,Co)O_4$ oxides [2]. One of the ways to decrease TEC of cobaltatesis to stabilize HS Co^{3+} in the ground state. Such compounds can be found among cobaltates with the brownmillerite-type structure. We have recently discovered the presence of HS Co^{3+}in the ground state in CoO_6octahedra of $Sr_2Co_{1.2}Ga_{0.8}O_5$with the brownmillerite structure [3]. This cobaltate is found to possess as low TEC as 13.1 ppm K^{-1} (298-1073K).

R_2CuO_4, R – rare-earth cation oxides with layered crystal structures having perovskite slab alternating with rock-salt slab (R=La, so called T-phase) or fluorite slab (R=Nd-Gd, so called T'-phase) are considered as prospective cathode materials for IT-SOFC due to their low TEC (~12 ppm K^{-1}) and moderate high-temperature electrical conductivity (>100 S/cm for Pr_2CuO_4). Correlation between the presence of the particular structural slab in the crystal structure of layered cuprates and their high-temperature oxide-ion conductivity is discussed.

Acknowledgement. This work was financially supported by the Russian Science Foundation (project number 16-13-10327).

[1] S.Ya. Istomin, E.V. Antipov, *Russian Chemical Reviews* **82** (2013) 686-700.

[2] S.Ya. Istomin, O.M. Karakulina, M.G. Rozova, S.M. Kazakov, A.A. Gippius, E.V. Antipov, I.A. Bobrikov, A.M. Balagurov, A.A. Tsirlin, A. Michau, J.J. Biendicho and G. Svensson, *RSC Advances* **6** (2016) 33951-33958.

[3] S.Ya. Istomin, O.A. Tyablikov, S.M. Kazakov, E.V. Antipov, A.I. Kurbakov, A.A. Tsirlin, N. Hollmann, Y.Y. Chin, H.-J. Lin, C.T. Chen, A. Tanaka, L.H. Tjeng, Z. Hu, *Dalton Transactions* **44** (2015) 10708-10713.

Ionic Conductance in Multiphase Lithium-Germanium Oxides

O.O. Nesterov[1], M.P. Trubitsyn[1], S.G. Nedilko[2], M.D. Volnianskii[1], S.M. Plyaka[1], Ya.O. Rybak[2]

[1]*Solid state physics and optoelectronics dept., Oles' Honchar Dnipropetrovsk National University, 72 prosp. Gagarina, 49010 Dnipro, Ukraine*
[2]*Faculty of Physics, Taras Shevchenko National University of Kyiv, 4 Acad. Glushkov Ave., 01360 Kyiv, Ukraine*

Electrical properties of amorphous, nano- and microcrystalline phases of the Li_2O-$x(GeO_2)$ (x=2.7, 7, 11.5 and 18) compounds were studied. It was shown that on heating Li_2O-$x(GeO_2)$ amorphous phases crystallize in several stages through intermediate nanocrystalline state with high electroconductivity σ [1, 2]. Mechanism of charge transfer in amorphous and multiphase Li_2O-$x(GeO_2)$ compounds was investigated by spectroscopy of complex impedance ρ*(ω) (Fig.1) [3].

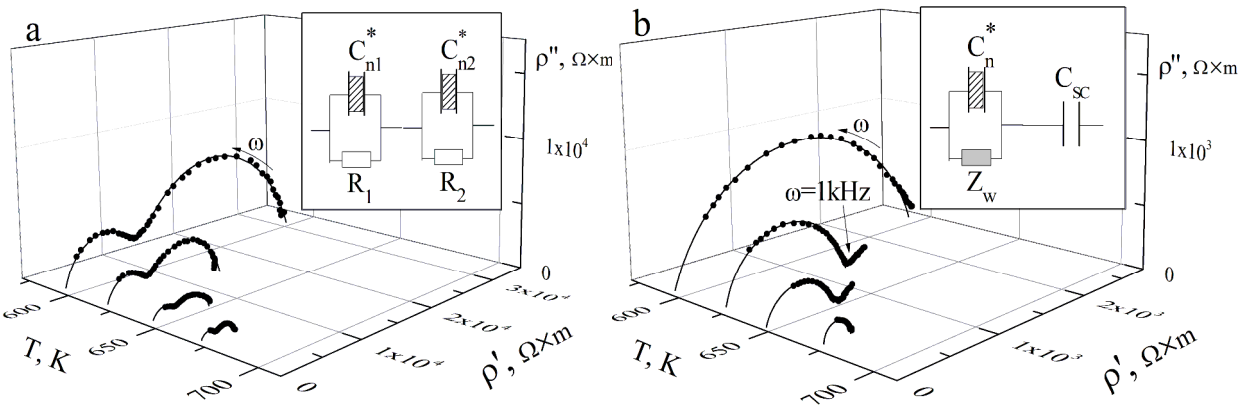

Fig.1. Hodographs (ρ'-ρ'') for intermediate nanocrystalline phases of Li_2O-$x(GeO_2)$, x=7 (a) and x=11.5 (b). Circles represent experimental data, solid lines were calculated by using equivalent circuits approach (see the insets).

It was shown that high conductivity of the intermediate state was the result of Li ions high mobility which caused by nanometer size of crystalline nuclei. On subsequent thermal treating the nuclei size increased to micrometer range that led to sharp decrease of carrier mobility and conductivity. It was demonstrated that creating nano-dispersed media can be an effective approach to increase ionic conductance in dielectrics.

[1] M. Volnyanskii, O. Nesterov, M. Trubitsyn, Devitrification of the Li_2O–$x(GeO_2)$ glass, *Ferroelectrics* **462** (2014) 126-130.
[2] O. Nesterov, M. Trubitsyn, D. Volnyanskii, Metastable state of the Li_2O-$11.5GeO_2$ glass-ceramics with a high electrical conductivity, *Phys. of the Solid State* **57** (2015) 683–688.
[3] O. Nesterov, M. Trubitsyn, S. Plyaka, D. Volnyanskii, Spectra of complex impedance of Li_2O−$11.5GeO_2$ glass and glass ceramics, *Phys. of the Solid State* **57** (2015) 1715-1719.

The Electrical Switching Properties of $Ge_{10}Se_5Sb_{85}$ Chalcogenide Glass

S. Abouelhassan*

Jazan University, KSA
* sayd1959@gmail.com

Bulk ingot material of the ternary mixture $Ge_{10}Se_5Sb_{85}$ was prepared by direct fusion of high purity constituent elements in vacuum sealed silica tube. The glassy nature of the prepared sample was confirmed by the X-ray diffraction (XRD) technique. Current - Voltage characteristics of the investigated glass have been carried out at different thicknesses and temperatures. Switching phenomenon at the turn-over point (TOP) froma high-resistance state (OFF state) to a negative-differential resistance-state (NDRS) was detected where the threshold parameters such as threshold dissipated power (P_{th}), threshold voltage (V_{th}),threshold current (I_{th}), threshold electric field (E_{th}) and threshold resistance (R_{th}) were determined at different thicknesses and ambient temperatures of the investigated samples. At the turn-over point, the activation energies (ΔE_p, ΔE_v, ΔE_i ,ΔE_r and ΔE_f) caused by the threshold dissipated powers, threshold voltages, threshold currents, threshold resistances and threshold electric fields respectively, were deduced at different thicknesses of the samples. The increasing in the ambient temperature of the investigated material (ΔT_J), the temperature of the conduction path ($T^{\backslash}$) and the Poole-Frenkel coefficient (β_{PF}) were determined at different ambient temperatures and thicknesses of the samples on the basis of the Joule heating effects. The activation energy of hopping (W), the activation energy of conduction ΔE_σ(eV), the hopping distance (d) of the charge carriers and the density of localized states N(E) were carried out due to Poole-Frenkel effect.

The Study of the Charge Transport across the CVD Diamond/Silicon Heterojunction

Kazimierz Paprocki*

Institute of Physics, Kazimierz Wielki University, Powstańców Wielkopolskich 2, 85-090 Bydgoszcz, Poland
* paprocki@ukw.edu.pl

The undoped diamond layers were synthesized by the hot filament chemical vapor deposition method (HFCVD) at total pressures in the reactor in the range of 20 -100 mbar and at the fixed concentration (2.6%) of the hydrocarbon diluted in (97.4%) hydrogen.

The films were polycrystalline in nature having an average sizes of crystallites ranging from 0.5 μm to 1μm, and thicknesses in the range from 4.7 μm to 7.9 μm as it estimated from SEM picture.

From the dc-electrical characteristics recorded for diamond layers have been determined the following parameters: saturation current (JS), the potential barrier height (Φ_b), the thermal activation energy (E_t) and the density of trap states (Ns(t)). Changes in these parameters in correlation with structural change, prove the existence of two mechanisms of charge transport in the studied structures. This statement is confirmed by AC measurements.

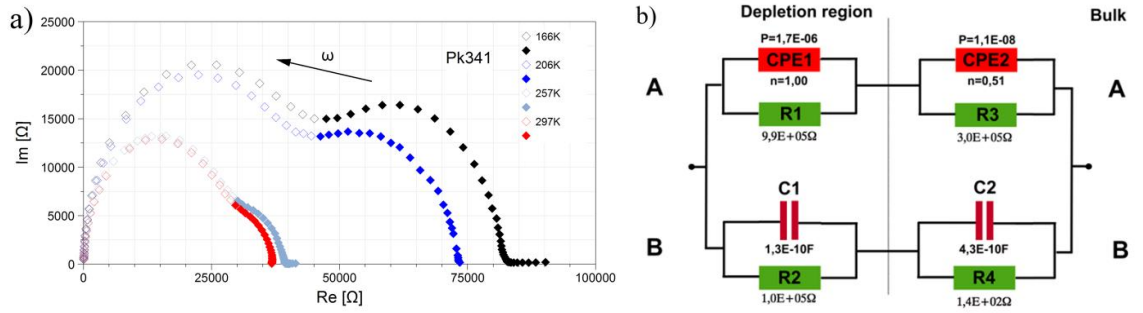

Fig. 1. Cole-Cole plots for Pk341 sample, b) Scheme and the numerical fitting of the equivalent circuit to sample of Pk271. A-A - microcrystal circuit, B-B - grain boundary circuit.

The proposed model describes well the conductivity of respondents undoped diamond films. The dominant conduction mechanism is the transport of charge along the grain boundaries, strictly associated with the presence of hydrogen atoms [1].

Problem of conductivity mechanism in undoped diamond films is complex and requires further study. As can be seen strongly depends on the parameters of diamond layers synthesis. At relatively low reproducibility, obtain undoped layers of an appropriate electrical properties, may be difficult.

[1] P. Reichart et al., Three-Dimensional Hydrogen Microscopy in Diamond, *Science* **306**(5701) (2004) 1537-1540.

Resistivity Switching in Binary and Complex Transition-Metal Oxides

E. Zhitlukhina[1,2], M. Belogolovskii[1]

[1]*Vasyl' Stus Donetsk National University, 021021 Vinnytsia, Ukraine*
[2]*O.O. Galkin Donetsk Institute for Physics and Engineering, 03028 Kyiv, Ukraine*

Oxygen vacancies which are intrinsic to transition-metal oxides play a major role in electronic and magnetic properties of the strongly correlated systems and just now are the subject of intensive research due to the increasing complexity from the fundamental point of view and ever growing activities for practical applications [1]. In this work, we discuss the role of oxygen vacancies for modulating the physical states of correlated oxides at the mesoscale level. We focus on nanoscale resistance-switching cells that operate via the formation and disruption of conducting filaments that bridge metallic electrodes and are among the most promising devices for post-CMOS electronics. Despite their importance, the key mechanisms governing the change-over properties are not well identified and at present we have a limited understanding of how device size and operating frequency affect the processes, especially for nanoscale devices operating at ultrafast rates.

Our theoretical analysis of the switching events under the application of ac electric fields to oxide-based heterostructures is focused on yttrium-barium cuprate $YBa_2Cu_3O_{7-x}$ (YBCO) famous for displaying high-temperature superconductivity and therefore studied and characterized in detail for different oxygen deficiencies by various physical and chemical techniques. In particular, it relates the compound conductivity which dependence on the vacancies content x has been well known [2]. Experimentally, [3,4] it was found that double-valued current-voltage curves typical for memristive trilayers with metallic electrodes and a binary-oxide nanometer-thick interlayer can be realized in direct contacts formed by a metallic counter-electrode, a film or an STM tip, with a YBCO film. We show that this observation can be understood in terms of a minimalist one-dimensional model, whose major ingredient is the drift of doubly positive oxygen vacancies across regions of high electric field. The key relation describing the oxygen subsystem is the conventional mass balance equation, a consequence of the conservation of the number of vacancies. We have reproduced pinched hysteretic *I-V* curves for YBCO-based planar junctions and point contacts measured at Comenius University, Bratislava [3,4]. Our results suggest that the electric field produced by the current bias modifies the vacancies profile shape and thus can radically reconfigure the physical properties of conducting filaments through the near-interface region of the YBCO film. The data obtained for complex transition-metal oxides are attracted for the analysis of experimental characteristics for related binary compounds.

Our numerical simulations predict the ultrafast switching in such memristive devices. At higher frequencies, the theory predicts the degeneracy of the hysteresis effect, resulting in a straight line typical for a linear resistor. We show also that the very substantial changes in dielectric properties of a nanometer-thick binary-oxide layer should be enough to create and destroy self-aligned conductive filaments in superconducting Josephson junctions and point contacts providing a means for controlling the McCumber-Stewart parameter in the first case and measuring the energy gap values in superconducting electrodes in the second case.

The work was supported by the Ministry of Education and Science of Ukraine.

[1] Z.-t. Xu et al., *Small* **8** (2012) 1279.
[2] K. Yamamoto et al., *J. Appl. Phys.* **69** (1991) 7189.
[3] T. Plecenik et al., *J. Appl. Phys.* **111** (2012) 056106.
[4] M. Truchly et al., *J. Appl. Phys.* **120** (2016) 185302.

Negative Dynamic Resistance and Memristive Effects in Zincite-Tungsten Semiconductor Junction

M. Nowicki[1,*], P. Nowak[2,*], R. Szewczyk[1,*]

[1]*Institute of Metrology and Biomedical Engineering*
Warsaw University of Technology
Boboli 8, 02-525 Warsaw, Poland
* *m.nowicki@mchtr.pw.edu.pl*, * *r.szewczyk@mchtr.pw.edu.pl*
[2]*Industrial Research Institute for Automation and Measurements PIAP*
Al. Jerozolimskie 202, 02-486 Warsaw, Poland
* *pnowak@piap.pl*

The zinc oxide, with its unique physical and chemical properties, such as high chemical stability, high electro-chemical coupling coefficient, broad range of radiation absorption and high photostability, is a truly multifunctional, or 'smart' material. The piezo- and pyroelectric properties of ZnO mean that it can be used as a sensor, converter, energy generator and photocatalyst in hydrogen production. In materials science, zinc oxide is classified as a semiconductor in group II-VI, whose covalence is on the boundary between ionic and covalent semiconductors. A broad energy band (3.37 eV), high bond energy (60 MeV) and high thermal and mechanical stability at room temperature make it attractive for potential use in electronics, optoelectronics and laser technology. Because of its hardness, rigidity and piezoelectric constant it is an important material in the ceramics industry, while its low toxicity, biocompatibility and biodegradability make it a material of interest for biomedicine and in pro-ecological systems [1,2]. The crystallized form of ZnO is called the zincite. Zincite crystals can be grown artificially, and synthetic zincite crystals are available as a unwanted by-product of zinc smelting. Synthetic crystals can be colourless or can range in colour from dark red, orange, or yellow to light green.

The measurement stand for real-time voltage-current characteristics of two -terminal devices was designed and built. The experimental crystal zincite-metallic tungsten semiconductor junctions were prepared, and their characteristics presented. Some of the samples are notable for hysteretic behaviour, other for distinct S-type negative resistance area. The differences are due to the random orientation of the crystal structure in the junction point of contact. It was shown, that the nonlinearity of the devices response is a function of the operating frequency, and changes dramatically. For 10 Hz it may operate like s-type tunnel diode, for 100 Hz like DIAC, and for 1 kHz it is similar to memristor.

The proposed methodology is especially convenient for students, during the classes on functional materials or semiconductors. The measurement stand may be used for other two terminal devices as well, such as resistors, diodes, inductors and capacitors, presenting their respective I(V) curves in real-time.

[1] A. Kołodziejczak-Radzimska, T. Jesionowski, Zinc Oxide—From Synthesis to Application: A Review, *Materials* **7**(4) (2014) 2833-2881.
[2] Ü. Özgür, Y.I. Alivov, C. Liu, A. Teke, M.A. Reshchikov, S. Dođan, V. Avrutin, S.J. Cho, H. Morkoç, A comprehensive review of ZnO materials and devices, *J. Appl. Phys.* 98 (2005).

Microstructure and Thermoelectric Properties of $Ca_3Co_4O_9$/SiC Thermoelectric Composites

K. Park[1], A. Iqbal[1], J.S. Cha[1], D.A. Hakeem[1], J. Kim[2]

[1]*Faculty of Nanotechnology and Advanced Materials Engineering, Sejong University, Seoul 143-747, Korea*
[2]*Department of Advanced Materials Engineering, Hoseo University, Asan 336-795, Korea*

Thermoelectric energy conversion has received considerable attention for the production of electrical energy from waste heat. The key to realize an efficient thermoelectric generator is to develop a thermoelectric material with high thermoelectric performance and high thermal stability in air. To improve the performance of thermoelectric materials, one effective way is to increase the Seebeck coefficient and to reduce the thermal conductivity by adding nanoparticles into the matrix. In this study, $Ca_3Co_4O_9$/SiC thermoelectric compositeswith various amounts of SiC particles were fabricated by solid state reaction method. The effects of SiC particles on the microstructure and thermoelectric properties were investigated. XRD patterns, FE-SEM, and EDS were used for the characterization of crystal structure, microstructure, and composition, respectively. The transport properties were mainly discussed, based on the microstructural properties. It was found that the SiC particles were evenly distributed in the $Ca_3Co_4O_9$ matrix. Both the electrical conductivity and the Seebeck coefficient of the $Ca_3Co_4O_9$/SiC composites became larger with increasing temperature. The introduction of SiC into the $Ca_3Co_4O_9$ matrix led to a decrease in the electrical conductivity and an increase in the Seebeck coefficient. The power factor was significantly improved by the SiC addition. The thermal conductivity of the composites was suppressed by enhanced phonon scattering, improving the figure-of-merit. We believe that the introduction of SiC particles into the $Ca_3Co_4O_9$ matrix is an efficient strategy for improving thermoelectric properties.

The Properties of NiO Thin Film as an Anode Buffer Layer in P_3HT:PCBM Bulk Hetero-Junction Solar Cell

Jwayeon Kim[1], Youngkyu Ko[1], Kyeongsoon Park[2]

[1]*Dept. of Materials Engineering, Hoseo University, Asan, Chungnam 336-795, Korea*
[2]*Faculty of Nanotechnology and Advanced Materials, Sejong University, Seoul 143-747, Korea*

Organic photovoltaic cells are very attractive recently because of advantages of low cost, large area and light weight fabrication. A PEDOT:PSS layer has been used between the ITO anode electrode and P_3HT:PCBM layers in organic solar cells based on the bulk hetero-junction structure. However, PEDOT:PSS has been reported to have problems using a buffer layer between ITO anode electrode and P_3HT:PCBM bulk hetero-junction layers. In the present work, we have studied the effect of the NiO anode buffer layer between photoactive and ITO anode layers in the P_3HT:PCBM bulk hetero-junction solar cell. NiO anode buffer layer was deposited with RF sputtering on ITO substrate. The photoactive area was $0.04cm^2$, and its thickness was 100nm deposited by spin coating in glove box and annealed at150^oC for 20 minutes at hot plate (N_2 ambient). Al electrode (100nm) was deposited by thermal evaporation in ~10^{-6}torr. Device electrical properties of device was measured under $100mW/cm^2$(AM1.5G). $3.4X10^{-1}$ Ωcm of NiO film resistivity was obtained at 80nm thickness with control of substrate temperature and O_2 partial pressure during sputtering, and annealing conditions. The electrical and optical properties of this film were depended on the O_2 partial pressure and substrate temperature during deposition, and duration time at room temperature in O_2 vacuum ambient. Power conversion efficiency (PCE) value (4.7%) of the P_3HT:PCBM bulk hetero-junction solar cell fabricated with NiO anode buffer layer was higher than that (3.0%) of the P_3HT:PCBM bulk hetero-junction solar cell fabricated with a conventional PEDOT:PSS anode buffer layer under AM1.5G illumination. These results have been described with improvement of charge transport across the interface between the photoactive layer and ITO anode electrode.

[1] H.-L. Yip, S.K. Hau, N.S. Baek, A.K.-Y. Jen, *Appl. Phys. Lett.* **92** (2008) 193313-1-193313-3.
[2] B.C. Thompson, J.M.J Frechet, *Chem. Int. Ed* **47** (2008) 58-77.
[3] H.-K. Park, J.-W. Kang, S.-I. Na, D.-Y. Kim, H.-K. Kim, *Sol. Energy Mater. Sol. Cells* **93** (2009) 1994-2002.
[4] F.C. Krebs, T. Tromholt, M. Jorgensen, *Nanoscale* **2** (2010) 873-886.

Rapid Fabrication and Thermoelectric Properties of Bi_2Te_3-Related Nanocomposites for Energy Applications

S. Nichkalo[1], Iu. Kogut[1,2], J. Krasinski[2]

[1]*Department of Semiconductor Electronics, Lviv Polytechnic National University, 12 S. Bandery Str., 79013 Lviv, Ukraine*
[2]*Helmerich Advanced Technology Research Center, Oklahoma State University - Tulsa, 700 N Greenwood Ave, Tulsa OK 74106, U.S.A.*

Due to relatively low efficiency of thermoelectric energy converters and high cost of their fabrication, the economic viability of current thermoelectric technology for "green power" applications remains an important issue. The existing methods for production and improvement of thermoelectric devices are usually complex, power and time consuming, sometimes hazardous for environment, thus, resulting in weak effect of introduction of state-of-the-art thermoelectrics on an everyday market. The cost efficiency of thermoelectric technology is to a great extent affected at the stage of materials development. In this regard, a self-propagating high-temperature synthesis (SHS), or in other words, combustion synthesis, appears to be a promising and economically feasible approach. It requires minimum external power supply and no sophisticated equipment, and allows for exceptionally fast synthesis of virtually any advanced thermoelectric material at a rate of several grams per second [1, 2]. In this report, on the example of doped $Bi_2Te_{3-x}Se_x$ n-type compounds, we present a fast fabrication method based on a combustion synthesis, allowing for development of high-ZT thermoelectric materials. High electronic transport properties were inherent for as-synthesized and sintered samples, resulting in substantially higher power factor, but due to relatively high thermal conductivity the maximum values of figure-of-merit ZT were lower and shifted towards higher temperatures, when compared to conventionally synthesized $Bi_2Te_{3-x}Se_x$. Nevertheless, nanostructuring by fine grinding and multiple re-sintering of SHS-developed samples resulted in significant reduction of their thermal conductivity and up to 20% increment in ZT of $Bi_2Te_{3-x}Se_x$ without loss in power factor. This improvement yielded thermoelectric performance of SHS $Bi_2Te_{3-x}Se_x$ comparable to that of currently commercialized materials on the basis of bismuth telluride for room temperature applications. Substantially better thermoelectric properties were observed for Cu-doped bismuth telluroselenide in comparison with their silver-doped counterparts. The presented research results infer that an SHS-based method combined with multiple re-sintering is a promising simple approach relevant to cost and time efficient technology of advanced thermoelectrics.

[1] X. Su, F. Fu, Y. Yan et al., Self-propagating high-temperature synthesis for compound thermoelectrics and new criterion for combustion processing, Nat. Commun. **5**, Art. № 4908 (2014).
[2] G. Zheng, X. Su, T. Liang, Q. Lu, Y. Yan, C. Uher, X. Tang, High thermoelectric performance of mechanically robust n-type $Bi_2Te_{3-x}Se_x$ prepared by combustion synthesis, *J. Mater. Chem. A.* **3** (2015) 6603.

Application of the Thermal Pulse Method for Nondestructive Evaluation of Embedded Piezoelectric Transducers

G.Suchaneck, A. Eydam, G. Gerlach

TU Dresden, Solid State Electronics Lab, 01062 Dresden, Germany

Structural components with embedded piezoelectric sensors and actuators find application in structural vibration suppression and noise reduction, energy harvesting, structural health monitoring, precision positioning, etc.. During fabrication, piezoelectric transducers are supposed to mechanical and thermal depolarization, microcrack formation, etc. Therefore, non-destructive evaluation of the polarization state is required for quality inspection.

A periodic thermal excitation of the piezoelectric material gives rise to a pyroelectric current which carries information on the polarization profile. In frequency domain, the Laser Intensity Modulation Method (LIMM) is well-established [1]. Thereby, thermal oscillations are generated by a periodically modulated laser beam. When thermal pulses are applied with a pulsed laser, the signal is recorded in time domain, but it can be Fourier-transformed and analyzed in the frequency domain similar to LIMM [2].

Recently, we have demonstrated that thermal methods are promising for the non-destructive evaluation of the polarization state and thermal interfaces of piezoelectrics embedded into low temperature co-fired ceramics (LTCC), epoxy resin and polyimide, polyamide 6 as well as high-pressure die-casted Al [3, 4]. At low modulation frequencies, the pyroelectric response of PZT is governed by thermal losses to the embedding layers. In this case, the sample behaviour can be described by a harmonically heated piezoelectric plate exhibiting heat losses to the environment characterized by discrete relaxation times or by their continuous distribution. Thermal relaxation characterizes the thermal contact and, thus, enables locating lamination failures. For Al die-casted piezoceramic modules, the pyroelectric current spectrum allows to distinguish centre-positioned from an off-centre positioned transducers [4].

In this work, we present analytical and FEM (finite element method) models to describe the time dependence of the pyroelectric current of embedded piezoelectrics generated by a laser pulse. Analytical solutions of the one-dimensional heat transfer equation consider a two-layer model, account for the experimentally derived heat pulse shape and the heat loss to the environment. They serve as a proof of the more complex FEM models which allow the consideration of three-layer models. The FEM model provides an understanding of the heat transfer in structurally complex devices excited by laser pulses. However, it underestimates the heat extraction process at the bottom transducer interface. Problems with accuracy of FEM are well known to occur near interfaces exhibiting steeply changing properties. Nevertheless, they are usually ignored in textbooks and manuals. When proved by simplified analytical solutions, FEM modelling provides a useful tool for the understanding of heat transfer processes in such complex devices as embedded piezoelectric transducers.

[1] S.B. Lang and D.K. Das-Gupta, *J. Appl. Phys.* **59** (1986) 2151-2160.
[2] A. Mellinger, R. Singh, R. Gerhard-Multhaupt, *Rev. Sci. Instrum.* **76** (2005) 013903.
[3] G. Suchaneck et al., *IEEE Tran. Ultrason. Ferroelectr. Freq. Control* **59** (2012) 1950-1954.
[4] A. Eydam et al., *Adv. Appl. Ceram.* **114** (2015) 226-230.

Design of an Intelligent Control System to Prevent the Ferroresonance Effect in Current Transformers

H. Zenk[1], A. Altinkok[2]

[1,2]*Department of Electrical-Electronics Engineering, Giresun University, Turkey*

Current transformers used for measurement and protection are one of the most used elements of the power system. The B-H characteristic of the current transformers provides electromagnetic energy conversion in a linear region with a high efficiency. With the current transformer's ferromagnetic core saturating, the energy conversion efficiency begins to fall. Nonlinear inductance of the current transformer and elements such as resistance and capacitance in the nonlinear loads of the power system connected to the current transformer has the potential to interfere suddenly and cause a ferroresonation phenomenon. In this study, it has been determined that current transformers, especially those operating in high voltage systems and compensation plants, produce destructive electrical parameters in the system due to the fact that they work together with the continuous closing-opening switches. It has been determined that it is possible to remove randomly operated switch-off openings which cause this destructive condition by means of a control system operating at appropriate times using semiconductor switches.

Comparison of Electrical Performances of Power Electronics Switches and an Effective Switch Selection Algorithm

H. Zenk

Department of Electrical-Electronics Engineering, Engineering Faculty, Giresun University, Turkey

Electronics switches commonly used in power electronics circuits, are the part of the electronics system depends on energy efficiency, circuit topology, switching matrix design, interaction with filter elements, and many other parameters [1]. For the first new switch design prototype to identify of electrical efficiency of the semiconductor switch working with a system, it is very important that estimation of the variables saving time, labor and economical resources. In this study, the new algorithm is proposed and applied to circuit estimate efficiency of power electronics switches (PES) [2]. The current-voltage-power capacities, switching rates, power losses, physical dimensions, heating levels of power electronics switches used in the circuit are investigated and algorithmically estimated according to the result of experimental performance switches.

[1] Muhammad H. Rashid, *Power Electronics Handbook*, Academic Press, 2001.
[2] Ned Mohan et al., *Power Electronics Converters, Applications And Design*, John Wiley & Sons, 2003.

SECTION 5

MATERIALS FOR QUANTUM AND OPTOELECTRONICS AND DETECTORS OF RADIATION

Emergency OSL/TL Dosimetry with Components of Mobile Phones and other Personal Items

S. Sholom, S.W.S. McKeever

Radiation Dosimetry Laboratory, Department of Physics, Oklahoma State University, Stillwater, OK 74075, USA

In case of anypotential large-scale radiological accident (like the accident at the Chornobyl Nuclear Power Plant on April 26, 1986 in Ukraine or the Fukushima Daiichi nuclear disaster on March 11, 2011 in Japan) or a possible nuclear terrorist attack, hundreds of thousands of people may be exposed to different radiation doses, and it will be necessary to triage them in order to separate the so-called "worried well", who have not been exposed to potentially dangerous levels of radiation, from those for whom medical assistance is urgently required. General population usually doesn't carry the personal dosimeters, and some fortuitous materials, in combination with some biological or physical measurement techniques, should be used to reconstruct the emergency doses of potential victims.

Many different techniques have been developed and proposed for emergency dose reconstruction. Theyall may be divided into two categories, namelybiodosimetry techniques, which exploit the biological effects in tissues exposed toionizing radiation doses, and physical techniques, which deal with some radiation-induced markers in both biological and non-biological materials[1]. Examples of physical techniques include the electron paramagnetic resonance dosimetry with teeth and nails as well as different luminescent techniques with items that arelocatedon/near to the body of an individual at the time of exposure and therefore may be used to assess the emergency dose of this individual. Examples of such items include mobile phones, clothing, shoes, different plastic and business cards, paper bills and coins.

In the present study, both optically-stimulated and thermo-stimulated luminescence (OSL and TL) techniques were applied to several commonplace materials to test their ability as potential emergency dosimeters. Main attention was given to components of the mobile phones, namely the surface mount resistors (SMR) and integrated circuits (ICs), which demonstrated the prominentradiation-induced OSL signals after stimulation with the blue color light, as well as both display and protective glasses, which could be used for dose reconstruction with TL or phototransferred TL (PTTL) techniques. Basic dosimetric characteristics (dose response dependences, values of minimum measurable doses, fading of the signal with time after exposure) have been tested and are discussed in details in the presentation. Other tested materialswere clothes, shoes and different plastic cards and paper banknotes; they have been studied just withthe OSL technique. For all tested materials, dose reconstruction protocols have been proposed and corresponding dose recovery exploratory exercises have been performed.

[1] I.K. Bailiff, S. Sholom, S.W.S. McKeever, Retrospective and emergency dosimetry in response to radiologicalincidents and nuclear mass-casualty events: A review, *Radiat. Meas.* **94** (2016) 83-139.

Transparent Ceramics for Photonic Applications

A.V. Tolmachev, R.P. Yavetskiy

Institute for Single Crystals of NAS of Ukraine, 60 Nauki Ave., 61001 Kharkov, Ukraine

Development of functional optical ceramics by nanotechnology methods is one of the most promising trends in the modern material science. Concepts of advanced ceramics engineering start with nanocrystalline powders followed by their consolidation into the bulk ceramic materials [1]. Transparent ceramics find application in photonics, quantum electronics, scintillation technique, lighting, etc.

The aim of this work is to present the progress in processing of advanced ceramics in Ukraine and worldwide. The report covers a wide range of technological issues of $Y_3Al_5O_{12}$:RE (RE=Nd^{3+}, Yb^{3+}, Cr^{4+}) optical ceramics by reactive sintering method [2], [3]. This technology could be successfully used to obtain the highly-doped $Y_3Al_5O_{12}$:RE (RE=Nd^{3+}, Yb^{3+}, Cr^{4+}) ceramics with homogenous distribution of dopant in the ceramics' volume. Utilizing nanopowders with different particle sizes allows one to reduce the sintering temperature, while phase transformation during densification provides excellent diffusion activity of nanopowders in a wide temperature range. The established relationships between the processing conditions and laser characteristics of optical ceramics will be presented.

Synthesis approaches of RE_2O_3:Eu^{3+} (RE=Y, Lu) rare-earth sesquioxides by vacuum sintering [4] and transformation-assisted consolidation of nanopowders at high-pressures [5] will be described. Possible ways to improve optical homogeneity of sintered materials and perspectives of their practical use will be discussed.

[1] G. L. Messing and A. J. Stevenson, Toward pore-free ceramics, *Science (80)* 322 (2008) 383–384.

[2] R. P. Yavetskiy, D. Y. Kosyanov, A. G. Doroshenko, S. V. Parkhomenko, P. V. Mateychenko, I. O. Vorona, A. V. Tolmachev, A. V. Lopin, V. N. Baumer, and V. L. Voznyy, Microstructure evolution of SiO_2, ZrO_2-doped $Y_3Al_5O_{12}$:Nd^{3+} ceramics obtained by reactive sintering, *Ceram. Int.* (2015).

[3] D. Y. Kosyanov, R. P. Yavetskiy, V. N. Baumer, Y. L. Kopylov, V. B. Kravchenko, I. O. Vorona, A. I. Cherednichenko, V. I. Vovna, and A. V. Tolmachev, Effect of Nd^{3+} ions on phase transformations and microstructure of 0-4 at.% Nd^{3+}:$Y_3Al_5O_{12}$ transparent ceramics, *J. Alloys Compd.* **686** (2016).

[4] Y. L. Kopylov, V. B. Kravchenko, N. A. Dulina, A. V Lopin, S. V Parkhomenko, A. V Tolmachev, R. P. Yavetskiy, and O. V Zelenskaya, Fabrication and characterization of Eu^{3+}-doped Lu_2O_3 scintillation ceramics, *Opt. Mater.* **35**(4) (2013) 812–816.

[5] R. P. Yavetskiy, V. N. Baumer, M. I. Danylenko, A. G. Doroshenko, I. N. Ogorodnikov, I. A. Petrusha, A. V. Tolmachev, and V. Z. Turkevich, Transformation-assisted consolidation of Y_2O_3:Eu^{3+} nanospheres as a concept to optical nanograined ceramics, *Ceram. Int.* **40**(2) (2014).

Development of the Novel Hybrid Film-Crystal Scintillators Based on the Garnet Compounds

Vitaliy Gorbenko[1,2], Sandra Witkiewicz[1], Kazimierz Paprocki[1], Tetyana Zorenko[1,2], Yuriy Zorenko[1,2], Pavlo Arhipov[3], Sergii Tkachenko[3], Iaroslav Gerasymov[3], Borys Grynyov[3], Oleg Sidletskiy[3], Alexander Fedorov[4], Jiri Mares[5], Martin Nikl[5]

[1]*Institute of Physics, Kazimierz Wielki University in Bydgoszcz, Powstańców Wielkopolskich Str. 2, 85090 Bydgoszcz, Poland*
[2]*Department of Electronics, Ivan Franko National University of Lviv, Gen. Tarnavskiy Str. 17, 79017 Lviv, Ukraine*
[3]*Institute for Scintillation Materials, National Academy of Sciences of Ukraine, Nauki Ave. 60, 61001 Kharkiv, Ukraine*
[4]*SSI Institute for Single Crystals, National Academy of Sciences of Ukraine, Nauki Ave. 60, 61178 Kharkiv, Ukraine*
[5]*Institute of Physics, AS Czech Republic, Cukrovarnicka Str. 10, 16253 Prague, Czech Republic*

The report presents our last achievement in the development of multilayer hybrid scintillators (HS) based on single crystalline films (SCF) and single crystals (SC) of garnet compounds for effective transformation and registration of different types of ionizing radiations and microimaging. HS have been made in the form of multilayer epitaxial structures containing one or two scintillators in the form of SCFs grown by liquid-phase epitaxy (LPE) method onto substrates from SC scintillators. In principle, the developed HS can possess the improved functionality in comparison with the known analogues for registration of γ-quanta and α-particles, and visualization of X-ray images with spatial resolution in the submicron range. Functional parts of HS in the form of SC and SCF have been fabricated from effective scintillation materials with signficantly different luminescent spectra or scintillation decays on the basis of Ce^{3+}, Pr^{3+} and Sc^{3+} doped $A_3B_5O_{12}$ garnets, where A= Lu, Gd, Tb; B= Al, Ga.

The report presents the results on fabrication of scintillators based on the materials under study in the form of SC, SCF and HS as well as the results of comprehensive investigation of their luminescent and scintillation characteristics. The report provides also establishment of the peculiarities of luminescent and scintillation characteristics of Sc^{3+}, Pr^{3+}, Sc^{3+} doped garnets, prepared in the SCF form in comparison with their bulk SC counterparts.

We have also performed testing of the developed HS in the detectors for radiation monitoring of different components of mixed ionizing fluxes as well as screens in the detectors for microimaging.

Acknowledgements. The work was performed in the framework of NCN 2016/21/B/ST8/03200 and NANOLUX2014 No 286 projects and also supported by the Ministry of Education and Science of Ukraine in the framework of SF-20 F project and Czech Science Fondation no. 16-15569S project.

Study of Luminescence Properties of Yb^{3+} - Doped Oxides Using High Hydrostatic Pressure

A. Kaminska[1,2]

[1]*Institute of Physics, Polish Academy of Sciences, Aleja Lotnikow 32/46, PL-02668 Warsaw, Poland*
[2]*Cardinal Stefan Wyszynski University, College of Science, Department of Mathematics and Natural Sciences, Dewajtis 5, 01-815 Warsaw, Poland*

Rare earths (RE) doped oxides are attracting a lot of attention due to their advantageous optical properties and high potential in new optical device applications. Among RE ytterbium is an attractive dopant for obtaining effective luminescence at a wavelength of about 1 μm, related to the intra-configurational electronic transitions of the Yb^{3+} ion. A simple energy level scheme of Yb^{3+} ions ($4f^{13}$ electron configuration), which consists of two states only (the ground $^2F_{7/2}$ and excited $^2F_{5/2}$) excludes excited state absorption and all related energy losses. From this point of view, and because of the development of high brightness InGaAs-based laser diodes emitting near 980 nm, where the Yb^{3+} has a strong absorption peak, this ion may compete with Nd^{3+} as an active lasing center emitting in the same range of emission wavelength [1-4].

One of the most important issues in a deep understanding of the mechanisms of RE active ion luminescence is to determine the energy levels of the dopant, the location of these energy levels with respect to the valence and conduction bands of the host crystal, as well as a detailed investigation of the involved energy transfer processes.

Application of high pressure reduces the ion-ion distances causing the increase of the crystal field strength experienced by the dopant ion and changing the energetic structure of the band states of the crystal matrix. Thus the high-pressure spectroscopy is a very efficient tool for investigating the energy structure of RE ions and their interaction with the lattice.

In this work we present the study of the influence of hydrostatic pressure on the radiative intra-configurational $4f \rightarrow 4f$ transitions of Yb^{3+} ions doped to several oxide materials, witch differ in energy gap values and crystal structures. A thorough analysis of ambient pressure spectra and the pressure behaviour of the Yb^{3+} luminescence lines in $LiNbO_3$, YPO_4, $GdPO_4$ and $Gd_3Ga_5O_{12}$ allowed for determining the ambient pressure positions and pressure dependence of the Yb^{3+} energy levels in crystal fields of different strengths and symmetries. The comparison of decay times of Yb^{3+} luminescence in different crystal matrices and their pressure dependencies has been also performed.

The results revealed a high thermal and pressure stability of Yb^{3+} emission in the examined crystals, and also the significant effect of the local symmetry of ytterbium dopant on its radiative transition rate, which are the important factors from the point of view of potential applications of ytterbium as an optically active ion in different crystal hosts.

[1] E. Montoya, J. Capmany, L.E. Bausa, T. Kellner, A. Diening, G. Huber, *J. Appl. Phys.* **87** (2000) 4056-4062.
[2] A. Brenier, G. Boulon, *J. Alloys Compd.* **323-324** (2001) 210-213.
[3] S. Chénais, F. Druon, F. Balembois, P. Georges, A. Brenier, G. Boulon, *Opt. Mater.* **22** (2003) 99-106.
[4] G. Boulon, *J. Alloys Compd.* **451** (2008) 1-11.

Effect of Sintering Temperature on Dosimetric Properties of BeO Ceramic Pellets Synthesized Using Precipitation Method

V. Altunal[1,*], V. Guckan[1], A. Ozdemir[1], K. Kurt[2] and Z. Yegingil[1]

[1]*Cukurova University, Art Sciences Faculty, Department of Physics, 01330 Adana, Turkey*
[2]*Mersin University, Science and Letter Faculty, Physics Department, 33343 Mersin, Turkey*
* *valtunal@student.cu.edu.tr*

The precipitation method not only has the advantages of being a simple process, suitable for doping and low production cost, but also achieves production of uniform particles with small sizes. This is because of the precipitants being formed slowly and uniformly throughout the solution during the precipitation process [1]. For this reason, in this study, BeO powders synthesized with precipitation method and prepared as pellets. In order to compress and shape a solid mass of material, sintering temperatures were chosen as 1200^{o}C, 1400^{o}C and 1600^{o}C.

Effect of sintering temperature on OSL decay curves, beta dose response, minimum detectable doses (MDD) and reusability of BeO ceramic pellets were investigated using Optically Stimulated Luminescence (OSL) signals. Furthermore, short time light and dark fading properties were carried out.

According to results of experiments, one can say that the higher sintering temperature is suitable to obtain bright and stable OSL signals.

Acknowledgement. This project has been supported by NATO in the frame of the NATO Science for Peace and Security (SPS) Programme under the project number SfP984649 and by Cukurova University under the project numbers FUA-2015-4300 and FYL-2015-3944. The authors want to thank NATO and Cukurova University Rectorate for their support.

[1] J. Azorin, Preparation methods of thermoluminescent materials for dosimetric applications: An overview, *Applied Radiation and Isotopes* **83** (2014) 187–191.

The Equipment Setup for Luminescence Spectrum with X-Ray Excitation

K. Kurt,T. Çavdar

Mersin University, Faculty of Science and Letters, Department of Physics, Mersin, Turkey

The objective of this study is to set up equipment that is capable of determining the emission spectrum from luminescence and dosimetric materials. Spectral of emission is important for thermoluminescence reader, optical stimulated luminescence reader,and synthesized dosimetric materials. Monitoring the luminescence spectrum allows choosingthe filter for reader and dopant for luminescence and dosimetric materials.

The basic agreement of system is to capture the emission of luminescence spectrum with“high sensitive spectrometer and low level light application” Ocean optics model QE Pro by f/2 collimator in front of fibre optic cable throughout the CCD detector while irradiating by from 4kV up to 40kV mini x-ray source. Spectral range of spectrometer is from about 200nm to 1100nm and resolution is about 1.63nm. Mini x-ray source has tuneable power from 4keV to 40keV. Spectra have been recorded from dosimetric materials at the room temperature. Natural quartz and some oxide samples are measured by x-ray luminescence equipment.

Acknowledgements: This research is supported by NATO through the project SfP 984649 Weacknowledge gratefully the financial supports of NATO.

Materials Based on Oxide Compounds for Composite Scintillators

Ia. Gerasymov, T. Nepokupnaya, A. Boyarintsev, O. Sidletskiy, D. Kurtsev, O. Voloshyna, Yu. Onufriyev, T. Grynko, O. Trubaeva, V. Pedash

Institute for Scintillation Materials of National Academy of Sciences of Ukraine, 60 Nauky Ave., 61001 Kharkov, Ukraine

Single crystals, optical ceramics, Cherenkov glasses, plastic scintillators are commonly used as sensitive elements of scintillation detectors. These scintillation materials have both undeniable advantages and a number of disadvantages and application limitations. The main disadvantage of bulk single crystals of a good optical quality is a complex and expensive technology for their production. Using of composite scintillators manufactured from fine granules distributed in a binder medium [1] enables to avoid the stage of bulk single crystal growth. The granules can be obtained by solid-state synthesis, by crushing of solidified melts, or by sol-gel method. Another advantage of composite scintillators is the possibility of detectors production on their basis of any size and shape.

This work is focused at search for optimal process to produce composite scintillation detectors manufactured on the base of Y_2SiO_5:Ce (YSO:Ce) and $Gd_3(Al_xGa_{1-x})_5O_{12}$:Ce (GAGG:Ce) scintillators. YSO:Ce is a standard oxide scintillator used in various types of scintillation detectors, including HEP experiments. GAGG:Ce is a new promising material which outperforms all known oxide single crystals by the light yield.

In this study YSO:Ce and GAGG:Ce materials were obtained in the form of powders synthesized by solid-state method, fragments after crushing of single crystal, as well as in the form of fragments after solidified melt crushing. Composite scintillators on their basis were manufactured using radiation-resistant polysiloxane elastomer as a binder medium [2]. Luminescent and scintillation properties of the obtained composite samples were studied and compared with those of standard bulk YSO:Ce and GAGG:Ce single crystals. The scintillation and luminescence characteristics of the composite scintillators and single crystals are similar. It was shown that composite scintillators are promising for application in HEP calorimeters and medical X-ray sensitive screens.

[1] Nikolai Z. Galunov, Boris V. Grinyov, Natalya L. Karavaeva, Yaroslav V. Gerasymov, Oleg Ts. Sidletskiy, and Oleg A. Tarasenko, Gd-Bearing Composite Scintillators as the New Thermal Neutron Detectors, *IEEE Transactions on Nuclear Science* **58**(1) (2011) 339-346.

[2] A.Yu. Boiaryntsev, N.Z. Galunov, N.L. Karavaeva, A.V. Krech, I.V. Lazarev, L.G. Levchuk, T.A. Nepokupnaya, V.D. Panikarskaya, V.F. Popov, P.V. Sorokin, O.A. Tarasenko, Study of radiation-resistant gel bases for composite detectors, *Functional Materials* **20**(4) (2013) 471-476.

Composite Scintillators Based on $ZnWO_4$

V. Zvereva[1], I. Tupitsyna[1], A. Yakubovskaya[1], S. Tretiak[1], S. Abashin[2]

[1]*Institute for Scintillation Materials NAS of Ukraine*
[2]*National aerospace university "Kharkov Aviation Institute"*

Recently, much attention is paid to the development of composite organic and inorganic scintillators preparation methods [1]. Mentioned materials have several advantages as compared with single crystals, such as: high uniformity of scintillation parameters, no restrictions of the linear sizes, high technology of production. However, the preparation of composite scintillators are often involves grinding of bulk single crystals, which determines their greater costs. According to the aim of this work it was obtained composite scintillators based on microcrystalline $ZnWO_4$, prepared by solid-phase synthesis.

Optimal conditions of the synthesis of microcrystalline zinc tungstate were determined by the results of DTA, SEM and X-ray analysis of obtained microcrystalline powders prepared from initial oxides mixture (ZnO and WO_3). It was shown the complete conversion of the starting components in a certain phase ($ZnWO_4$) occurs for 50 hours at a temperature of 950°C.

The influence of mineralizers - lithium salts as a function of their concentration in a solid-phase reaction was investigated. The positive effect of $LiNO_3$ was observed: accelerating the chemical reaction and the grain growth, reducing of the synthesis time up to 30 hours (fig.1).

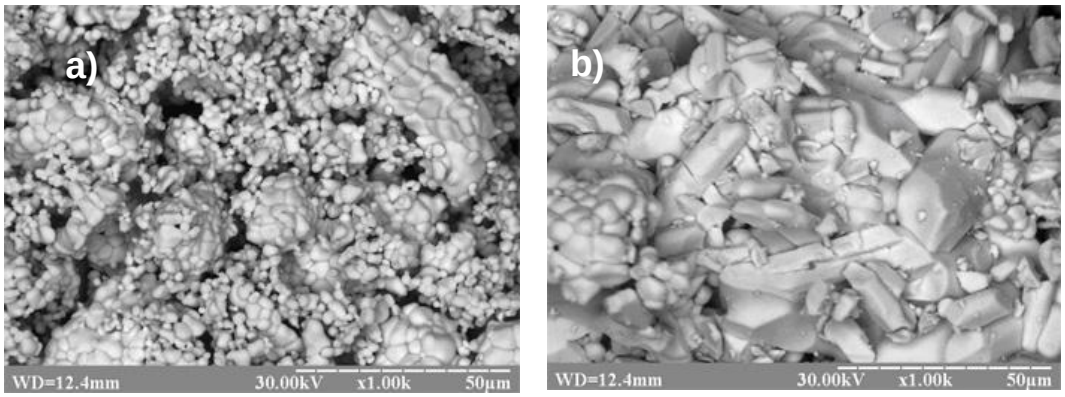

Fig. 1. SEM of $ZnWO_4$ microcrystalline powders prepared by:
a) 50 h, 950°C; b) adding of $LiNO_3$ (0,1 %), 30 h, 950°C

The number of samples of size Ø30×2 mm was produced from prepared under different synthesis conditions powders. Silicone rubber was used as the polymer binder. Scintillation characteristics of the samples were measured. The light output (was determined by the current method with X-ray excitation source IRI - U_α =100 kV, i_a = 1 mA) of the best samples of the composites was at bulk crystals and above: sample based on A -155% as compared to the bulk crystal, sample based on B – 273 %.

[1] Patric Büchele, Moses Richter, Sandro F. Tedde et al, X-ray imaging with scintillator-sensitized hybrid organic photodetectors, *Nature Photonics* (published online: 9 November 2015), doi: 10.1038/nphoton.2015.216.

Low Background $CdWO_4$ Scintillation Detector

D.V. Kasperovych, F.A. Danevich, V.V. Kobychev, B.N. Kropivyansky, A.I. Tymoshenko

Institute for Nuclear Research, Kyiv, Ukraine

Researches of rare nuclear processes play an important role in particle and nuclear physics, because they allow to explore properties of the neutrino, to test the Standard Model of particles and properties of the weak interaction. BALOO (BAsement LOw background scintillatiOn setup) was designed and built in the Lepton Physics Department of the Institute for Nuclear Research (Kyiv, Ukraine) to investigate radiopurity level of scintillators and materials screening, to carry out small scale low counting experiments. Cadmium tungstate crystal scintillator ($CdWO_4$, ∅70×70 mm) is viewed through ∅100×162 mm high purity quartz light guide by a low background photomultiplier tube. The detector is shielded by 6-12 cm of oxygen free high conductivity copper and 15 cm of old lead. A plastic scintillator counter 100×100×12 cm is placed above the set-up to veto cosmic muons, while a home designed electronics allow to reject pile-ups of fast Cherenkov signals in the quartz light guide. The background of the $CdWO_4$ detector is reduced by 3 orders of magnitude in the energy interval 0.5 – 2.6 MeV and by one order of magnitude above 3 MeV in comparison with unshielded detector at the Earth surface. Advancement of the set-up is progress, particularly by using a transient digitizer to discriminate particles by pulse-shape, and by time-of-events assay to analyze fast decay chains in the uranium and thorium families. Besides, additional plastic scintillation detectors will be installed around the setup to reduce the residual cosmic muons background.

YSO:Ce Powder for Composite Scintillators

T. Nepokupnaya, A. Boyarintsev, Yu. Onufriyev, T. Grynko, V. Pedash, O. Trubaeva, T. Ponomarenko, A. Rebrov

The Institute for Scintillation Materials of National Academy of Sciences of Ukraine, 60 Nauky Ave., 61001 Kharkov, Ukraine

The usage of the large-sized bulk single crystals of the oxide materials is limited by their scarcity. Composite scintillators based on fine powders placed in the coupling optical medium can be used as material for production of the cheap detection devices with high overlap surface. A sol-gel method for the production of such materials is an alternative to the complicated technologies of growing bulk single crystals.

The purpose of the current work consisted in the development of the methods of obtaining of scintillation powders for the production of the composite scintillators with the registration efficiency comparable with that of the single crystals of the same materials. The fine powders of the Y_2SiO_5:Ce (YSO:Ce) composition were chosen for the current research because of the application of the current scintillation material in different types of detectors, such as the detectors of the γ-radiation and the HEP experiments.

The powders of the YSO:Ce compositions were synthesized via sol-gel process. The granular and phase composition of the obtained materials were studied. The composite scintillators based on the mentioned powders were manufactured with the usage of the radiation-resistant polysiloxane elastomer as the coupling medium [1]. The spectral-kinetic and scintillation parameters of the produced composite samples were studied. The obtained data were compared with parameters for YSO:Ce single crystals. The scintillation efficiency of the composite scintillators produced from the powders obtained by a sol-gel method is appropriate for their application in the counting detectors and the detectors for the HEP experiments.

[1] A.Yu. Boyaryntsev, N.Z. Galunov, N.L. Karavaeva, A.V. Krech, I.V. Lazarev, L.G. Levchuk, T.A. Nepokupnaya, V.D. Panikarskaya, V.F. Popov, P.V. Sorokin, O.A. Tarasenko, Study of radiation-resistant gel bases for composite detectors, *Functional Materials* **20**(4) (2013) 471-476.

High-Performance Single Crystalline Film Scintillators Based on the Pr^{3+} Doped Solid Solution of $Lu_3Al_{5-x}Ga_xO_{12}$ Garnet

V. Gorbenko[1,2,*], T. Zorenko[1,2], K. Paprocki[1], B. Maglowany[1], B. Mazalon[2], A. Fedorov[3], Ya. Zhydachevskyy[4,5], A. Suchocki[1,5], Yu. Zorenko[1,2]

[1]*Institute of Physics, Kazimierz Wielki University in Bydgoszcz, 85-090 Bydgoszcz, Poland*
[2]*Department of Electronics, Ivan Franko National University of Lviv, 79017 Lviv, Ukraine*
[3]*SSI Institute for Single Crystals, National Academy of Sciences of Ukraine, Kharkiv, Ukraine*
[4]*Lviv Polytechnic National University, 79646 Lviv, Ukraine*
[5]*Institute of Physics, Polish Academy of Sciences, 02-668 Warsaw, Poland*
* vhorbenko@gmail.com

The high-performance UV emitting scintillating screens based on the single crystalline films of $Lu_3Al_{5-x}Ga_xO_{12}$:Pr garnet were developed using liquid phase epitaxy (LPE) growth method onto $Y_3Al_5O_{12}$ (YAG) substrates using the lead-free BaO based flux. The absorbance, luminescence and scintillation properties of these SCFs were investigated depending on Ga content. We have found that the shape of CL spectra, scintillation light yield (LY) and decay kinetics of Pr^{3+} ions in $Lu_3Al_{5-x}Ga_xO_{12}$ SCFs are non-linearly affected by the total gallium concentration **x** due to preference in the distribution of Ga^{3+} ions between the tetrahedral and octahedral position of the garnet host. The best scintillation properties of $Lu_3Al_{5-x}Ga_xO_{12}$:Pr SCF are achieved at the nominal Ga content x=1.5 in melt-solution. The LY $Lu_3Al_{3.5}Ga_{1.5}O_{12}$ SCF is comparable with the LY of the best reference LuAG:Pr single crystal counterpart and significantly (up to 3 times) overcome the LY of LuAG:Pr and $Lu_3Al_{3.5-3}Ga_{1.5-2}$ SCFs, grown on the YAG substrates from the conventional $PbO\text{-}B_2O_3$ flux.

Acknowledgements. The work was performed in the frameworks of Ministry of Education and Science of Ukraine SF-20F project and Polish NCN 2016/21/B/ST8/03200 and NANOLUX 2014 ID 286 projects.

Zinc Oxide Films Implanted with Rare Earth (RE) for Optoelectronic Applications

I.N. Demchenko[1], Y. Melikhov[2], P. Konstantynov[1], R. Ratajczak[3], A. Turos[4] and E. Guziewicz[1]

[1]*Institute of Physics, Polish Academy of Sciences, Aleja Lotników 32/46, 02-668 Warsaw, Poland*
[2] *School of Engineering Cardiff University, Cardiff, CF24 3AA, United Kingdom*
[3]*National Centre for Nuclear Research, Soltana 7, 05-400 Otwock, Poland*
[4]*Institute of Electronic Materials Technology, Wolczynska 133, 01-919 Warsaw, Poland*

RE-ion doped semiconductor materials are particularly interesting for infrared (IR) emitting optoelectronic devices due to their intra-4*f* shell transitions in the 1.4-1.7 μm range [1-2]. In addition, with visible emission from higher excited levels (green for Er, Yb), they potentially can be used in devices such as optical amplifiers, lasers and optically pumped glass fibers [3]. For this, it is important to understand the RE ions fundamental properties in wide band gap semiconductors, such as their lattice site locations and surroundings, and the optical ion activation mechanisms and emission properties.

The resonant photoemission (ResPES) experiment was used in this project to investigate the ytterbium electronic states and their hybridization with valence electrons of zinc oxide. The measurements were performed at Elettra synchrotron facility (Trieste, Italy). The obtained data were used to establish the correlation between the optical properties and the electronic structure. Both commercial single ZnO crystals and epitaxial ZnO films grown at IP PAS by Atomic Layer Deposition (ALD) technique were under investigations. Ytterbium ions were incorporated into the ZnO matrix via ion implantation and subsequent annealing. We investigated samples containing different quantity of (co-)doped RE atoms (implantation of Yb at the level of 10^{15} and 10^{16} cm^{-2}). Prior to photoemission experiments, Ar^+ sputtering and annealing of the investigated samples up to ~573 K were performed. Photoemission spectra were taken for the photon energy range 180-190 eV i.e. across the *Yb4d – Yb4f* photoionization threshold which allows observation the Fano resonance enhancement from the *Yb4f* electron shell.

In ResPES the photon energy is tuned to the inter-ion absorption resonance (in our case Yb $N_{5,4}$) providing an interfering channel for a classical photoelectron excitation. As a result, the photoemission intensity dramatically increases or decreases, depending on the relative amplitudes and phases of the interfering channels. This effect is applied to derive the contributions of the *Yb4f* electron states to the valence band of the measured system. We found a inconsiderable but clear resonant enhancement of *Yb4f* states to the ZnO:Yb valence band at binding energy about 7.5 eV below the Fermi level. A weak Fano resonance is consistent with a large $4f^{14-\delta}$ occupancy. It was also found that ytterbium 4*d* level shows an extended multiple structure instead of a simple spin-orbit doublet for metallic ytterbium, which allows concluding that majority of ytterbium atoms are bonded to oxygen and indicates that one of the $4f^{14}$ electrons has been promoted to the valence level. This multiple structure can be attributed to $4f^n \leftrightarrow 4d^9$ interaction.

The obtained results enhance our general understanding of RE ions fundamental properties and are of great importance to the development of optical devices as well as devices used in short-range high speed networks operating in the IR.

Acknowledgements. The work was supported by the Polish National Centre for Research and Development (NCBiR) through the project PBS2/A5/34/2013.

[1] M. Llusca et al., *Thin Solid Films* **562** (2014) 456.
[2] M. Ishii, S. Komuro, *J. Appl. Phys.* **89** (2001) 3679.
[3] A. Polman, *J. Appl. Phys.* **82** (1997) 1.

Optical Properties of $BaWO_4$:Ce Crystals

D. Wlodarczyk[1], M. Berkowski[1], M. Głowacki[1], S. Kaczmarek[2], Z. Kowalski[2], A. Wittlin[1], H. Przybylinska[1], Ya. Zhydachevskyy[1], A. Suchocki[1,3]

[1]*Institute of Physics, Polish Academy of Sciences, Aleja Lotnikow 32/46, PL-02668 Warsaw, Poland*
[2]*Institute of Physics, Faculty of Mechanical Engineering and Mechatronics, West Pomeranian University of Technology in Szczecin, Al. Piastów 17,70-310 Szczecin, Poland*
[3]*Institute of Physics, Kazimierz Wielki University, Weyssenhoffa 11, 85-072 Bydgoszcz, Poland*

Barium tungstate crystals are interesting and relatively new medium for stimulated Raman scattering for applications in Raman shifters of laser radiation [1]. Good quality $BaWO_4$ crystals can be grown by Czochralski technique and doped with rare-earth ions. Doping with trivalent ions require charge compensation which may be provided, for example, by structural defects or proper codoping with alkaline metal ions. Crystals posses sheelite structure with the space group $I4_1/a$.

Results of studies of $BaWO_4$:Ce crystals and crystals codoped with Na are presented in this work. Optical absorption in the vis-UV and infrared range and Raman spectra have been studied. In the UV range the crystals shows typical absorption for Ce^{3+} with two bands peaked at 320 nm and 285 nm, which are associated with lowest energy 4f-5d transitions. However no Ce^{3+} luminescence is observed at room temperature, in spite of some reports on this subject [2].

In the mid-infrared range several absorption bands are visible with use of Fourier-Transform spectroscopy which may be associated with lattice absorption. Besides of lines associated with single phonon modes in the range up to 1000 cm^{-1} the additional lines appear around 1700 cm^{-1} and around 2600 cm^{-1}. Origin of these lines is discussed in this work.

Raman spectra at room temperature show very sharp lines with the highest energy line at 927 cm^{-1}. Some additional much broader lines are observed above 1200 cm^{-1} [3]. Their origin is most probably associated with combination of various phonon modes.

In addition to that very sharp lines due to the 4f-4f transitions in the Ce^{3+} ions are visible around 2200 cm^{-1} and 2350 cm^{-1}. There are at least four of these lines in each group which is most probably related to the multisite structure of RE doping in these crystals. The crystal field analysis allows identifying nature of these lines. The lines associated with Ce^{3+} ions are very strongly coupled with the lattice and they undergo very important broadening with increase of temperature.

Acknowledgements. This work was supported by the Polish National Science Center (project 2015/17/B/ST5/01658).

[1] Pavel Cerný, Helena Jelínková, Tasoltan T. Basiev, and Peter G. Zverev, *IEEE J. Quantum Electronics* **38** (2002) 1471.
[2] K.V. Dabre, S.J. Dhoble, Jyoti Lochab, *J. Luminescence* **149** (2014) 348.
[3] Donggang Ran, Hairui Xia, Shangqian Sun, Peng Zhao, Fengqin Liu, Zongcheng Ling, Wenwei Ge, Huaijin Zhang, Jiyang Wang, *Cryst. Res. Technol.* **41** (2006) 1189.

Giant Increase of Photoinduced Reflectivity in $LiNa_5Mo_9O_{30}$

M. Rudysh[1,2], M. Chrunik[3], A. Majchrowski[3], I. Kityk[4], M. Piasecki[1]

[1]*Institute of Physics, Jan Długosz University, 13/15 Armii Krajowej Str., 42-201 Czestochowa, Poland*
[2]*Faculty of Physics, Ivan Franko National University of Lviv, 8 Kyryla i Mefodia Str., Lviv, Ukraine*
[3]*Institute of Applied Physics, Military University of Technology, 2 Kaliskiego Str., 00-908 Warsaw, Poland*
[4]*Institute of Electronic and Control System, Faculty of Electrical Engineering, Czestochowa University of Technology, 17 Armii Krajowej Str., 42-200 Czestochowa, Poland*

$LiNa_5Mo_9O_{30}$ single crystals are promising nonlinear optical material with excellent transparency in wide spectral range from 0,357 to 5,26 μm [1]. Previously $LiNa_5Mo_9O_{30}$ was examined in both forms as the singe crystal and polycrystalline material. To explain and understood the relation between crystal structure and electronic properties of the $LiNa_5Mo_9O_{30}$, complex approach which includes experimental studies of X-ray with photoinduced reflectance spectroscopy, and the first principles band structure techniques within a framework of electron density functional theory (DFT) were used.

Synthesis of $LiNa_5Mo_9O_{30}$ micropowders by means of sol-gel method through the citrate way was performed. The DFT band structure calculations for obtained compound were carried out. Calculations of structural, electronic and optical properties of $LiNa_5Mo_9O_{30}$ microcrystals were performed in the framework of density functional theory (DFT) using the pseudopotentials plane-wave basis set CASTEP (Cambridge Serial Total Energy Package) [2] module of Biovia Materials Studio 8.0.

It is found that maximal dispersion of band structure is observed for Brillouine zone (BZ) directions Γ-Z and X-Y both for LDA and GGA functional. The top of the valence band is situated in the point Γ(0;0;0) of the BZ. Generally, dispersion $E(k)$ is higher for the conduction band states. Single maxima of PDOS near -60 eV and -35 eV are formed by 4s and 4p states of Mo, respectively, while its 4d electrons give contributions at -18 eV and -5 eV÷-2 eV. The oxygen is presented by two bands within -18 eV÷-15 eV (2s electrons) and within -6 eV÷0 eV (4p electrons). Following the reasons presented above one can conclude that the upper valence band is formed by bands originated from 4p(O) and 2s(Li) states and the conduction band originates from combination of the s(Li), d(Mo) and some contribution of p(O).

Following the performed calculations investigations of real and imaginary parts of the dielectric dispersion functions were carried out.

The giant increase of reflectivity was discovered for $LiNa_5Mo_9O_{30}$ crystal by illumination using the 371 nm nanosecond nitrogen laser. It was shown that the illumination at 532 nm does not cause any changes.

Basing on calculations of the optical functions we performed the photoinducing treatment of the samples near and outside the first UV spectral maximum using the radiation of photoinducing UV nanosecond laser at 337 nm and second harmonic generated 532 nm signal originated from Nd:YAG laser emitting 1064 nm radiation. The changes of reflectivity within the spectral range covering this maximum were investigated. Huge sensitivity to the wavelength of photoinducing radiation was found.

[1] W. Zhang, H. Yu, J. Cantwell, H. Wu, K.R. Poeppelmeier, P. S. Halasyamani, *Chem. Mater.* **28** (2016) 4483–4491.
[2] S.J. Clark, M.D. Segall, C.J. Pickard, P.J. Hasnip, M.J. Probert, K. Refson, M.C. Payne, *Z. Kristallogr.* **220** (2005) 567–570.

Ultraviolet Photoluminescence of the Gd^{3+} Centres in Borate Glasses

B.V. Padlyak[1,2], A. Drzewiecki[1], T.B. Padlyak[2], V.T. Adamiv[2], I.M. Teslyuk[2]

[1] *University of Zielona Góra, Institute of Physics, Division of Spectroscopy of Functional Materials, 4a Szafrana Str., 65-516 Zielona Góra, Poland*
[2] *Vlokh Institute of Physical Optics, Department of Optical Materials, 23 Dragomanov Str., 79-005 Lviv, Ukraine*

The Gd-doped borate glasses of high optical quality with $Li_2B_4O_7$, CaB_4O_7, $LiCaBO_3$ basic compositions have been investigated in details using electron paramagnetic resonance (EPR) and optical spectroscopy techniques. The $Li_2B_4O_7$:Gd, CaB_4O_7:Gd, and $LiCaBO_3$:Gd glasses were obtained by standard glass synthesis method using technological conditions described in [1]. The Gd impurity was introduced into the glass compositions as Gd_2O_3 compound in amounts 0.5 and 1.0 mol. %. In all obtained Gd-doped borate glasses has been observed at room temperature characteristic EPR spectrum of the paramagnetic Gd^{3+} ($^8S_{7/2}$, $4f^7$) ions. The observed EPR spectrum of the Gd^{3+} centres practically is independent of the basic glass compositions and is typical for glassy (vitreous) materials [2,3].

The optical absorption and photoluminescence (emission and excitation) spectra as well as luminescence decay curves of the $Li_2B_4O_7$:Gd, CaB_4O_7:Gd, and $LiCaBO_3$:Gd glasses were registered and analysed. In all investigated Gd-doped borate glasses at room temperature is observed the strong and sharp UV emission band at 311 nm under excitation with 273 nm and 252 nm. The emission band at 311 nm is extremely efficient at excitation with 273 nm. Analysis of electronic levels of the rare-earth ions and referenced data [4,5] clearly shows that the emission band at 311 nm corresponds to the $^6P_{7/2} \rightarrow {}^8S_{7/2}$ intraconfiguration $4f - 4f$ transition of the Gd^{3+} ions. Observed in emission spectrum weak band at 305 nm belongs to the $^6P_{5/2} \rightarrow {}^8S_{7/2}$ transition of the Gd^{3+} ions, whereas the weak band around 325 nm most probably is related to the vibronic sideband. In the photoluminescence excitation spectrum of the Gd^{3+} centres are well observed three characteristic groups of bands, which correspond to transitions from the ground state to higher excited states: $^8S_{7/2} \rightarrow {}^6P_J$, ^6I_J, and ^6D_J [4,5]. The emission band at 311 nm is dominant under the excitation with 273 nm ($^8S_{7/2} \rightarrow {}^6I_{7/2}$ transition) and 252 nm ($^8S_{7/2} \rightarrow {}^6D_{9/2}$ transition). The observed excitation bands show good correlation with the Gd^{3+} absorption bands, which are revealed as weak features on the background of the fundamental absorption edge of the glass host.

Luminescence decay curves of the Gd^{3+} emission band at 311 nm in the investigated glasses have been described in the framework of single exponential approximation with lifetimes ~ 4 ms. The obtained results show that the investigated borate glasses, activated with Gd^{3+} ions, are very promising materials for sources of UV radiation including solid-state UV lasers with working wavelength 311 nm ($^6P_{7/2} \rightarrow {}^8S_{7/2}$ channel).

[1] B.V. Padlyak, S.I. Mudry, Y.O. Kulyk, A. Drzewiecki, V.T. Adamiv, Y.V. Burak, I.M. Teslyuk, *Mater. Sci. Poland* **30** (2012) 264.
[2] D.L. Griscom, *J. Non-Cryst. Solids* **40** (1980) 211.
[3] J. Kliava, I.S. Edelman, A.M. Potseluyko, E.A. Petrakovskaja, R. Berger, I. Bruckental, Y. Yeshurun, A.V. Malakhovskii, T.V. Zarubina, *J. Phys.: Condens. Matter* **15** (2003) 6671.
[4] R.T. Wegh, H. Donker, A. Meijerink, R.L. Lamminmaki, J. Holsa, *Phys. Rev. B: Condens. Matter* **56** (1997) 13841.
[5] A.J. Vries, M.F. de Hazekamp, G. Blasse, *J. Lumin.* **42** (1988) 275.

Mechanisms of Impact on Luminescent Properties of Thermoregulating Materials

V.V. Harutyunyan[1,*], E.M. Aleksanyan[1], A.H. Badalyan[1], N.A. Hakobyan[1], N.E. Grigoryan[1], V.S. Baghdasaryan[1], A.A. Sahakyan[1], V.V. Baghramyan[2], A.A. Sargsyan[2]

[1] *A.I. Alikhanian National Scienc Laboratory, Yerevan Physics Institute, 0036 Yerevan, Armenia*
[2] *Institute of General and Organic Chemistry of Armenian National Academy of Sciences, Yerevan, Armenia*
* *vharut@mail.yerphi.am*

Study of the luminescence of thermoregulating coatings (TRC) or the pigments obtained by different methods not only allows obtaining ideas of the composition and structure of these materials, but also has practical importance when developing light sources, fluorescent biosensors, solar energy devices, space materials science, etc.

The luminescent properties of TRC were investigated using LUMEN pilot installation. The installation provides ample opportunities for research in the field of luminescent UV-visible spectroscopy with energy resolution at different temperatures. The power of the radiation spectrum of xenon lamp as the source of radiation within 240-360 nm was 1000 watt.

The work was aimed at the influence of various factors (annealing, electron irradiation, impurities) on the photoluminescence (PL) excitation mechanisms of TRC.

Study of photoluminescence (PL) of TRC containing zirconium (ZrO nSiO2) and zinc (ZnO_2SiO_2) has revealed two broad bands of radiation, UV and visible, in them.

When acting on TRC (ZrO $nSiO_2$) treated at various temperatures by UV photons (having excitation energy E_{exc} = 3.5eV), an intense luminescence within the spectral range of 1.8 eV - 2.6 eV is observed with the emission band maxima shifted depending on the treatment temperature, which confirms the possibility of various mechanisms of excitation for radiation centers. With an increase in the treatment temperature, a decrease in the PL intensity takes place, and the luminescence band maximum is observed at 1.9 eV. 2.2eV, 2.4eV and 2.6eV bands observed in the PL spectra of the studied TRC (ZrO $nSiO_2$) are characteristic of luminescence of many silicates and are usually associated with radiation of, for instance, $[SiO_4]^{4-}$ defect centers which are due to local distortions of silicon- oxygen tetrahedra. Zirconium ions may be located in tetrahedral surrounding in the form of (OH) - Zr – ($OSi)_3$ or Zr – $(OSi)_4$ groups. The position of $[SiO_4]^{4-}$center is more beneficial and occurs in the case of violation of the symmetry of silicon-oxygen tetraedra because of a nearby defect. When the studied TPC contains zirconium and zinc ions, 5 MeV electron irradiation leads to a shift of maxima in PL spectra as a result of redistribution of the defective emission centers formed during the heat treatment: short-living defects in the form of V_{Zr}^- vacancies and Zn^+ interstitial ions formed at bond breaking - the optical transitions in V_{Zr}^- center. The changes in the PL spectra of (ZnO $nSiO_2$) TRC samples after heat treatment can be explained if we assume that the observed maxima at 1.7 – 2.6eV are due to the creation of intrinsic defects in the tetrahedral structure. In the formation of the impurity centers and their metastable states, the impurity concentration can play an important role in view of possible changes in the electron density distribution of ZnO $nSiO_2$ tetrahedron.

Thus, photoluminescence in silicate TRC is due to the multicomponent defect centers inherent in silicate materials and is efficiently excited within the UV radiation region.

Spectroscopic Properties of $Y_4Al_2O_9$:Ce Crystals under High Pressure

Yongjie Wang[1], A. Suchocki[1,2], M. Ciesielska[3], A. Kaminska[1], Ya. Zhydachevskii[1], S. Turczyński[4], D.A. Pawlak[4], M. Malinowski[5]

[1] *Institute of Physics, Polish Academy of Sciences, Al. Lotników 32/46, 02-668 Warsaw, Poland*
[2] *Institute of Physics, Kazimierz Wielki University, Weyssenhoffa 11, 85-072 Bydgoszcz, Poland*
[3] *Cardinal Stefan Wyszynski University, College of Science, Department of Mathematics and Natural Sciences, Dewajtis 5, 01-815 Warsaw, Poland*
[4] *Institute of Electronic Materials Technology, Wólczynska 133, 01919 Warsaw, Poland*
[5] *Institute of Microelectronics and Optoelectronics, Warsaw University of Technology, ul. Koszykowa 75, 00-662 Warsaw, Poland*

$Y_4Al_2O_9$ crystals, abbreviated here as YAM (monoclinic yttrium aluminate), are difficult to grow in a bulk form by the Czochralski method since they undergo structural phase transition under cooling. However they may be manufactured by the micro-down pulling method. YAM:Ce crystals with various concentrations up to 1% of Ce, grown by this technique were studied in this work.

The crystal structure has been accurately determined by XRD on single crystal samples. The obtained crystals were characterized by various spectroscopic techniques, such as FT-IR, absorption, Raman, luminescence, luminescence decay kinetics, and photoluminescence excitation. FT-IR absorption in the spectral region of 4f→4f transitions of Ce^{3+} ions reveals existence of several Ce^{3+}-related centres in this compound, in agreement with its crystallographic structure. Absorption spectra consist of several bands in the UV region associated with optical transition between 4f and 5d states of Ce^{3+} ions. Luminescence of this material, which appears in a blue spectral region between 430 and 540 nm, undergoes strong temperature quenching, which begins already at temperature of about 20 K. The luminescence quenching is thermally activated with activation energy equal to about 21 meV.

We associate this quenching with position of the 5d state of Ce^{3+} close to the bottom of the conduction band [1]. High pressure luminescence experiments, performed in diamond anvil cell confirm this hypothesis. Due to pressure induced increase of the separation energy between the 5d states of Ce^{3+} ions and a bottom of the conduction band the temperature of the luminescence quenching is increased. Meanwhile the increase of pressure causes the red shift of luminescence spectra. Furthermore, pressure induces large red shift of the luminescence at pressure of above 70 kbar - at lower energies, which might be a fingerprint of phase transition. To verify our hypothesis about pressure-induced phase transition, Raman spectra of the YAM have been measured under high pressure up to 172 kbar.

For better understanding of the nature of processes associated with Ce^{3+} luminescence quenching in YAM we investigated Ce^{3+} luminescence kinetics as function of pressure and temperature. It was found that for all considered pressures and temperatures the luminescence decays exhibit two-exponential behaviour. The PL lifetime decreases with the increase of temperature , whereas it increases with increasing pressure for pressure range up to 120 kbar.

[1] G. Cunningham, Y. R. Shen, K. L. Bray, *Phys. Rev. B* **65** (2001) 024112.

Temporal and Spatial Characteristics of the Diffusion Processes in $LiNbO_3$ Crystals Caused by Thermo-Chemical Treatment

D.Yu. Sugak [1,2], O.A. Buryy[1], I.I. Syvorotka[2], U.V. Yakhnevych[1], K.-D. Becker[3], S.B. Ubizskii[1]

[1]*Semiconductor electronics department, Lviv Polytechnic National University, Lviv, Ukraine*
[2]*Scientific Research Company "Carat", Lviv, Ukraine*
[3]*Technical University Braunschweig, Braunschweig, Germany*

High-temperature annealing of lithium niobate ($LiNbO_3$) in reduction-oxidation atmospheres in presence of metal ions or hydrogen is the technological method used for obtaining of $LiNbO_3$-based acousto- and optoelectronic elements. Firstly, such treatments change optical and electro-physical properties of lithium niobate. Obviously, these changes are caused by diffusion processes influencing on the chemical composition of crystal as well as on the state of its defect subsystem. In this paper the time characteristics of processes taking place during redox treatment of $LiNbO_3$ are investigated by means of *in-situ* optical spectroscopy and the spatial distribution of coloration changes are determined by measuring of optical absorption along X, Y, Z directions. The peculiarities of diffusion and redox processes were also revealed by XRD, IR-spectroscopy and other techniques.

The reversibility of the optical properties changes observed after consequent redox treatment allows assuming that the oxygen vacancies diffusion plays the main role in coloration/decolouration processes of lithium niobate. The observed spectra of additional absorption can be divided on three bands with the maxima in regions 350…410, 500…520 and 700…750 nm. The 'green' band at 500…520 nm is caused by bipolaron absorption and the 'red' band at 700…750 nm – by bound polarons in accordance with known interpretations. The absorption in short-wave ('violet') band is probably connected with the defects of anion sublattice capturing the electrons after oxygen out-diffusion.

Experimentally obtained distribution of depth-dependent additional absorption in reduced crystals was successfully approximated basing on the oxygen vacancies diffusion model and solution of differential equations set describing the quasichemical reaction of bipolarons formation due to the oxygen loss in $LiNbO_3$ crystal. On the other hand, this model does not allow to describe precisely the depth-dependent discoloration after oxidizing annealing of previously reduced lithium niobate.

Presence of Oxygen in Ti-Al-C MAX Phases-Based Materials and their Stability in Oxidizing Environment at Elevated Temperatures

T. Prikhna[1], V. Sverdun[1], T. Basyuk[1], M. Karpets[1], O. Ostash[2], Th. Cabioc`h[3], L. Javorska[4], P. Chartier[3], A. Ivasyshyn[2], V. Moshchil[1], A. Kalinka[4], J. Cyboroń[4], S. Dub[1], V. Podhurska[2], V. Kovylaev[5], A. Starostina[1], T. Serbenyuk[1]

[1]*Institute for Superhard Materials of the National Academy of Sciences of Ukraine, 2 Avtozavodskaya Str., 04074 Kiev, Ukraine*
[2]*Physico-Mechanical Institute of the National Academy of Sciences of Ukraine, 5 Naukova Str., 79060 Lviv, Ukraine*
[3]*Universite de Poitiers, CNRS/ Laboratoire PHYMAT, UMR 6630 CNRS Universite de Poitiers SP2MI, BP 30179, F-86962 Chasseneuil Futuroscope Cedex, France*
[4]*The Institute of Advanced Manufacturing Technology, ul. Wroclawska 37A, 30-011 Krakow, Poland*
[5]*EDL «Proton 21», 48a Chernovola Str., Kiev's region 08132, Vishnevoe, Ukraine*

MAX-phases or nanolaminated ternary complex carbides and nitrides were firstly classified by M. W. Barsoum and can be characterized by general formula $M_{n+1}AX_n$, where n = 1, 2 or 3; M – early transition metals (in our case Ti and Nb); A – elements of A-group (in our case Al) and X is C or N. They have perovskite-like crystal structures and the most abundant stoichiometries are M_2AX (211), M_3AX_2 (312) and M_4AX_3 (413), which in fact differ by the amount of carbide or nitride layers in the unit cells separated by layers of A-group metal elements. These compounds have attracted extensive attention due to their extremely high thermal shock and mechanical damage tolerance, as well as a combination of metallic and ceramic properties. They have self-healing abilities because of oxidation. MAX-phase based materials are promising for application in different industries: power electrical, hydrogen, nuclear industries; aviation; cosmonautics; mechanical and chemical engineering, etc.

Incorporation of O was first observed in the Ti_2AlC. An initial study showed experimental indications of O substituting C while still retaining the MAX phase structure [1], suggesting O as a potential *X* element besides C and N. Subsequent calculations indicated that O prefers the C site under oxygen-lean conditions and high temperature [2] and that up to at least 50% of C may be replaced by O.

The testing at 600 ^oC for 1000 h in air of (I) Ti_3AlC_2 –based material (89 wt.% of Ti_3AlC_2; 6 wt.% of TiC and 5 wt.% of Al_2O_3), (II) $(Ti,Nb)_3AlC_2$-based (60 wt.% $(Ti,Nb)_3AlC_2$, 37 wt. % TiC, 3 wt.% Al_2O_3), and (III) Ti_2AlC-based (73 wt.% Ti_2AlC, 10 wt. % $AlTi_3$, 7 wt.% TiO, 10 wt.% Al(N,C,O) showed that all tested materials turned out to be more resistant in such conditions than Crofer JDA steel, but the amounts of oxygen absorbed by the materials for 1000 h were different. Marterial III demonstrated the lowest oxygen uptaken, material II absorbed a somewhat higher amount and the highest amount is absorbed by material I. SEM and Auger study showed that amounts of oxygen in the MAX phases before the exposure in air was as well different: main matrix phases in material I was $Ti_{3.1\text{-}3.2}AlC_{2\text{-}2.2}$, II - $Ti_{1.9\text{-}4}Nb_{0.06\text{-}0.1}AlC_{1.6\text{-}2.2}O_{0.1\text{-}1.2}$ and material III contained two main phases with near $Ti_{3.6}AlC_{1.9}O_{0.6}$ and $Ti_{2.3}AlCO_{0.2}$ stoichiometries (before the study the surfaces of the materials were etched by argon ions in the chamber of microscope JAMP-9500F to remove the oxidized layer). So, oxygen present in the MAX phases did not liberate during long-tem heating and provides higher resistance against oxidation. Material III was prepared using Al with high amount of oxides at the surface.

[1] J. Rosen, P.O.Å. Persson, M. Ionescu, A. Kondyurin, D.R. McKenzie, and M.M.M. Bilek, Oxygen incorporation in Ti_2AlC thin films, *Appl. Phys. Lett.* **92** (2008) 064102.

[2] T. Liao, J. Wang, M. Li, and Y. Zhou, First-principles study of oxygen incorporation and migration mechanisms in Ti_2AlC, *J. Mater. Res.* **24**(10) (2009) 3190-3196.

Growing and Properties of $BiV_{(1-x)}Nb_xO_4$ Crystals

K.V. Agarkov, M.D. Volnianskii, L.Ya. Sadovskaya, I.V. Pozdeyev

Oles Honchar Dnipropetrovsk National University, 49010 Dnipro, Ukraine

Bismuth vanadate compound currently known due to its various applications. This is the pigment with excellent weather fastness and high opacity [1] and one of the most promising photoanodes for solar power devices [2] and super-ionic conductor [3]. Optical and acousto-optical properties of the material are not widely known. At the present time, single crystals with high birefringence ($\Delta n > 0.2$) are widely used in optoelectronic devices. One of the outstanding examples is a crystal of yttrium vanadate which has a number of unique physical properties such as high value of birefringence ($\Delta n = 0.204$), high hardness, wide transparency range (0.4 – 6 μm). All these features make yttrium vanadate crystals very attractive objects for optical components of fiber optic communication systems. In addition, these crystals doped with Nd-ions have other wide fields of application – they already are used as elements of solid state lasers. However, the technology of growing of YVO_4 is still far from perfect. The manufacturers of yttrium vanadate produce crystals which are suitable for commercial use. But the size of such crystals is quite small, not more than 2.5 centimetres in diameter.

Crystals of yttrium vanadate and bismuth vanadate belong to the same structural type $A^{3+}B^{5+}O_4$. In comparison with yttrium vanadate, bismuth vanadate has a much greater birefringence ($\Delta n = 0.45$ at $\lambda = 0.6$ μm), the optical transmission range 0.5 – 6.5 μm. At the same time bismuth vanadate has lower melting point 1210 K (in comparison with 2100 K of yttrium vanadate) and such has technological advantage over yttrium vanadate.

Bismuth vanadate has a structural phase transition at ~ 520 K. We have made an attempt to reduce the temperature of phase transition by creation $BiVO_4 – Nb_2O_5$ solid solutions. Crystals $BiV_{(1-x)}Nb_xO_4$ were grown by Czochralski method with x = 0.02, 0.04, 0.05, 0.08. Obtained crystals were 1 – 2.5 cm^3 in volume and of satisfactory optical quality. Optical transmission and temperature dependence of the dielectric permittivity were measured. It was observed that the phase transition temperature decreased with increase of niobium oxide concentration.

[1] Rangadhar Nayak, A. Suryanarayana, S. Bhanojee Rao, Synthesis, Characterisation and testing of Bismuth Vanadate - an eco-friendly yellow pigment, *Journal of Scientific & Industrial Research* **59** (2000) 833.

[2] Yiseul Park, Kenneth J. McDonald, Kyoung-Shin Choi, Progress in Bismuth Vanadate photoanodes for use in solar water oxidation, *Chemical Society Reviews* **42** (2013) 2321.

[3] I. V. Golosovsky et al., Crystal structure and phase transition in the doped super-ionic conductor Bismuth vanadate $Bi_4(V,Fe)_2O_{11}$ revealed by neutron diffraction, *Physica Status Solidi B* **250** (2013) 1345.

Impact of Annealing on Carbon Doped YAG and YAG:Ce Crystals

P. Arhipov[1], S. Tkachenko[1], O. Sidletskiy[1], S. Vasyukov[1], I. Gerasymov[1], K. Lebbou[2]

[1]*Institute for Scintillation Material NAS of Ukraine, 60 Lenin Ave., 61001 Kharkiv, Ukraine*
[2]*Institut Lumière Matière, Lyone, France*

$Y_3Al_5O_{12}$ (YAG)-based crystals are used in different applications due to the favorable combination of their properties, such as thermal conductivity, hardness, chemical stability, transparency. Doped with Ce, or Pr ions, YAG possesses attractive luminescent properties. The production cost is another important criterion in the material choice.

In the present work optical properties of YAG and YAG:Ce crystals grown in Mo crucibles under Ar+CO atmosphere are compared to those grown in Ir crucibles by the conventional technology. Effect of thermal annealing on YAG optical properties was studied on samples fabricated from the crystals grown in Ir crucible (YAG_{Ir}) under weakly oxidizing atmosphere and in Mo crucible (YAG_{Mo}) under reducing conditions. In the both cases the same batches of Al_2O_3 and Y_2O_3 powders with the purity 99.99 % were taken as the raw materials. Then, the samples fabricated from the $YAG_{\mathbf{Ir}}$ and $YAG_{\mathbf{Mo}}$ crystals were annealed under the reducing or oxidizing conditions. The absorption spectra of polished samples were registered. In parallel we measured the admixture content in crystals, including carbon, and element composition of the ~50 μm thick surface layer.

Following the growth under reducing conditions, $YAG_{\mathbf{Mo}}$ crystals have a deficiency by oxygen and aluminum. As-grown YAG_{Mo} crystals also contain carbon admixture, which affects their optical properties. Physico-chemical processes at the crystal surface, especially under the reducing conditions, should be accounted for as well at consideration of defects in garnet crystals [1].

Optimized post-growth annealing of such crystals provides irreversible discoloration of crystals and high transparency in the 200 – 1100 nm spectral range. The obtained results open new possibilities to optimization of properties of doped garnet crystals. The presence of active electron traps associated with carbon makes it possible to transfer an activator (for example, Ce, Pr, or Nd) into the optically active lower valence state by the reducing annealing thereby increasing a quantity of luminescence centers without loss of the crystal transparency.

[1] P. Arhipov, S. Tkachenko, S. Vasiukov, K. Hubenko, Ia. Gerasymov, V. Baumer, A. Puzan, P. Mateychenko, K. Lebbou, O. Sidletskiy, Features of YAG crystal growth under Ar+CO reducing atmosphere, *J. Cryst. Growth* **449** (2016) 104-107.

Synthesis of Mg^{2+}, Cr^{4+}:YAG Optical Ceramics for Passive Q-switch Lasers

M. Chaika[1], K. Chernomorets[1], A. Doroshenko[1], S. Parkhomenko[1], A. Tolmachev[1], I. Vorona[1], R. Yavetskiy[1], M. Greculeasa[2], C. A. Brandus[2]

[1]*Institute for Single Crystals of National Academy of Sciences of Ukraine, 60 Nauky Ave., 61001 Kharkiv, Ukraine*
[2]*National Institute for Laser, Plasma and Radiation Physics, Laboratory of Solid-State Quantum Electronics, Magurele, 077125, Ilfov, Romania*

The general trend of modern microelectronics to decrease the size of electronic and optoelectronic devices is now imposing strict requirements on solid-state lasers. At the same time demands on the laser beam quality also increase. Progress in fabrication of compact solid-state lasers implies the development of new type of highly-doped active media containing high concentration of functional ions [1].

$Y_3Al_5O_{12}$ (YAG) optical ceramics is a promising material for obtaining of laser materials with high doping concentration of active ions. Ceramics synthesis occurs in accordance with the corresponding equilibrium phase diagrams of binary or ternary systems, whereas non-stationary processes on the crystallization front play significant role during single crystals growth. Nowadays there are a lot of reports on the synthesis of high-quality Nd^{3+}:YAG ceramics [2], but fabrication peculiarities of Cr^{4+}:YAG optical ceramics are insufficiently covered [3]. The aim of this work is to establish fabrication pathway of Mg^{2+},Cr^{4+}:YAG optical ceramics as a model system prospective for passive Q-switches.

Mg^{2+},Cr^{4+}:YAG optical ceramics were synthesized by solid-state reaction sintering in vacuum. The effect of magnesium and chromium ions concentration on the structural-phase state and optical properties of Mg^{2+},Cr^{4+}:YAG ceramics was studied. The concentration of magnesium ions was optimized resulting in Mg^{2+},Cr^{4+}:YAG ceramics with optical transmission of 80% at λ=1064 nm. Mg^{2+} ions incorporated into YAG matrix create oxygen vacancies, which increase the effective diffusion coefficient of constituent ions and accelerate pore removal from the ceramic volume. It was shown that for highly chromium doped ceramic samples, an enhancement of the concentration of Cr^{4+} ions in the samples occurs, due to the increased probability of forming [$Mg^{2+}Cr^{4+}$] pairs.

The possibility of using Mg^{2+},Cr^{4+}:YAG optical ceramic as passive Q-switch was tested. Quasi-continuous wave diode pumping of 0.3 at.% Nd^{3+}:YVO_4 single crystal that was passively Q-switched with Mg^{2+},Cr^{4+}:YAG saturable absorber ceramic results in the generation of laser pulses with 3.1 μJ pulse energy and 45 ns pulse width.

[1] S. Zhu et al., *Journal of Laser Applications* **26**(3) (2014) 032009.
[2] I. O. Vorona et al., *Quantum Electronics* **45**(9) (2015) 819.
[3] Z. Tianyuan et al., *Journal of the American Ceramic Society* **98**(8) (2015) 2459.

Spectroscopy of the Yb^{3+} Ions in the $PbWO_4$ Crystals

O. Chukova*, S.G. Nedilko

Physics Faculty, National Taras Shevchenko University of Kyiv,
4-b acad. Hlushkov Ave., 03680 Kyiv, Ukraine,
* chukova@uni.kiev.ua

The lead tungstate crystals ($PbWO_4$) are successfully applied for many years as scintillator materials and host matrices for Raman lasers. The RE doping of these crystals is a very important for the both applications. For lasers, the RE dopants are used as activator ions. As for the $PbWO_4$ scintillators, adding of the RE impurities is used for decreasing of lead and oxygen vacancies concentrations, because such vacancies are the most probable defects in the $PbWO_4$ crystals grown by Czochralsky method. Therefore, study of luminescence mechanisms and excitation energy transfer between the RE impurities and matrix is very important for the $PbWO_4$ crystals. Luminescence properties of the Yb^{3+} ions in the $PbWO_4$ matrix were reported previously only episodically and poorly [1-3]. In the present work, we have carried out an investigation of luminescence properties of the impurity Yb^{3+} ions in the $PbWO_4$ matrix and search of mutual correlations in behaviour of matrix emission and impurity emission.

The $PbWO_4$:Yb^{3+} crystals were grown by the Czochralski method using the "Crystal-617" installation. The blend was synthesized from lead, tungsten and ytterbium oxides. Concentration of the impurity in the blend was $5x10^{-2}$ wt %. Our analysis showed that impurity concentrations in the grown samples were reduced. The rectangular 5x10x10 mm bricks used for the investigation were cut from the central part of the crystal bulk.

Luminescence emission of the Yb^{3+} ions was observed in the 970 – 1040 nm spectral range. At room temperature, emission is presented by weakly structured band. Experiments carried out at 10 K with fine spectral slits of spectrometers reveal that this band consists of 16 narrow spectral lines. The observed spectrum of linear emission is caused by *f-f* $^2F_{5/2} \rightarrow {}^2F_{7/2}$ transitions in the Yb^{3+} ions. The $^2F_{7/2}$ level in crystal field can be split on 8 Stark components maximally. Observed 16 spectral components can be easily divided on two groups by dependence of their relative intensities on excitation wave length. The group of more intensive lines (975, 978, 996.5, 998, 999.5, 1001, 1023 and 1032 nm) was assigned to the first type of emission. These lines are intensive in the spectra obtained at 300 – 340 nm excitations. Their intensities significantly fall down at excitations with $\lambda_{ex} < 300$ nm, whereas intensity of rest lines assigned to the second type of emission does not depend on excitation wavelength. The relative contribution of the Yb^{3+} emission to the matrix emission is also strongly depended on excitation wavelength. The distinctive raise of the first type of lines intensity correlates with the shift of maximum position of the wide band visible emission from 445 – 455 nm at $\lambda_{ex} < 300$ nm to 510 nm at $\lambda_{ex} = 309$ nm.

Structure of the Yb^{3+} emission centres is discussed. The observed significant differences between spectral properties of two types of centres formed by the Yb^{3+} ions in the $PbWO_4$ crystal lattice are explained by different ways of the impurity ions incorporation on Pb and W sites for the first and second types of centres, respectively. These two types of centres have different symmetry of the Yb^{3+} ions (C_s and D_2) and crystal field strength due to differences between ionic radii of lead, tungsten and ytterbium ions. Correlations in behaviour of the Yb^{3+} emission and matrix emission are analyzed.

[1] Y. Huang, K. Jang, H.J. Seo, L. Zhao, *J. of the Korean Physical Society* **49** (2006) 227-232.
[2] Y. Huang, W. Zhu, X. Feng, G. Zhao, G. Huang, S. Li, Z. Mana, *Materials Letters* **58** (2003) 159-162.
[3] O. Antonenko, O. Chukova, Yu. Hizhnyi, S. Nedilko, V. Scherbatskyi, *Optical Materials* **28** (2006) 643-648.

Optical and Magnetic Investigation of Eu^{2+} Ions in Strontium Metaborate Single Crystals

M. Głowacki[1], P. Aleshkevych[1], P. Solarz[2], I.R. Martín[3], R. Diduszko[1,4], W. Ryba-Romanowski[2], M. Berkowski[1]

[1]*Institute of Physics, Polish Academy of Sciences, Al. Lotników 32/46, 02-668 Warsaw, Poland*
[2]*Institute of Low Temperature and Structure Research, Polish Academy of Sciences, ul. Okólna 2, 50-422 Wrocław, Poland*
[3]*Departamento de Física, Instituto de Materiales y Nanotecnología (IMN),Universidad de La Laguna, Av. Astrofísico Francisco Sánchez, s/n E-38206 La Laguna, Tenerife, Spain*
[4]*Tele and Radio Research Institute, Ratuszowa 11, 03-450 Warsaw, Poland*

Strontium metaborate belong to a large family of compounds that are suitable for use as matrices for luminescent dopant ions. Similarities of ionic radii of strontium and divalent europium makes it a good candidate to host Eu^{2+} ions. Despite this mainly trivalent europium is observed during optical measurements. It was shown for the first time [1] that emission of divalent europium ions can be observed in SrB_2O_4 single crystals but co-doping with alkali ions weakens this emission [2].

The magnetic ground state of Eu^{2+} ions allowed us to use the electron paramagnetic resonance technique in order to check how the co-dopant influences the oxidation state of europium in the SrB_2O_4 matrix and to study the local symmetry of Eu^{2+} centers. In this presentation the results of EPR measurements will be shown. The optical and magnetic measurements will be compared and discussed.

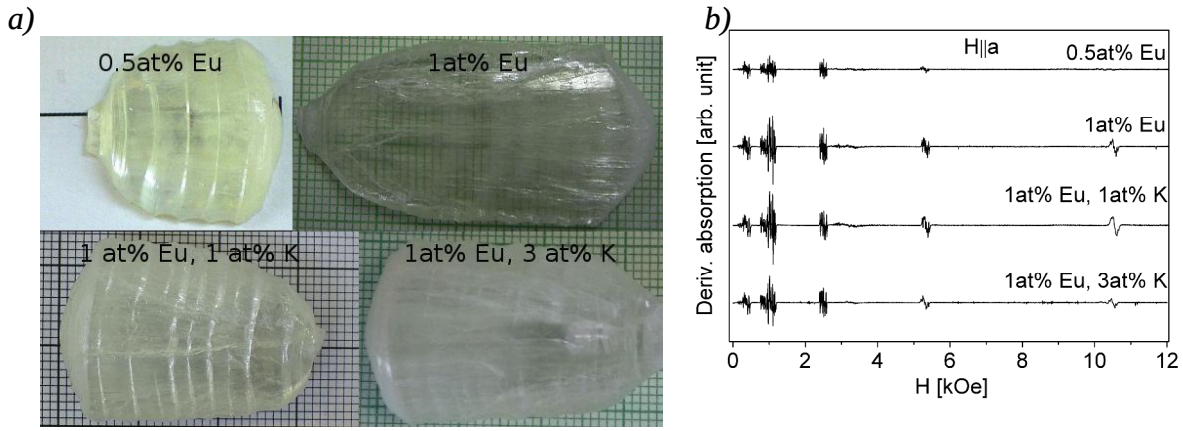

Figure 1. As-grown SrB_2O_4 single crystals (a) and EPR spectra recorded at H || to *a* axis (b)

Acknowledgements. The work was funded by the Polish National Science Center (NCN) on the basis of the decision number DEC-2013/09/D/ST5/03878.

[1] M. Głowacki, W. Ryba-Romanowski, R. Lisiecki, R. Kowalski, M. Berkowski, P. Solarz, *J. Lumin.* **169B** (2016) 807-810, doi: 10.1016/j.jlumin.2015.02.051.

[2] M. Głowacki, P. Solarz, W. Ryba-Romanowski, I.R. Martín, R. Diduszko, M. Berkowski, *J. Cryst. Growth* **457** (2017) 107–111, doi: 10.1016/j.jcrysgro.2016.07.007.

Recombination Luminescence in $Ca_{3-x}Cd_xGa_2Ge_3O_{12}$ Garnets Doped with Eu^{3+} Ions

L. Kostyk*, A. Luchechko, S. Novosad, M. Panasyuk, M. Rudko, O. Tsvetkova

Ivan Franko Lviv National University, 107 Tarnavskogo Str., 79017 Lviv, Ukraine
* kostyk@electronics.lnu.edu.ua

The calcium gallium germanium garnet $Ca_3Ga_2Ge_3O_{12}$ doped with Nd^{3+} ions are interesting materials for solid state lasers with diode pumping [1]. These crystals doped with various RE^{3+} ions can be also used as optical pressure sensors, phosphors with near-infrared and long-lasting luminescence properties, etc. [2, 3]. Nevertheless, the role of intrinsic and impurity defects in radiative recombination processes are not sufficiently studied so far. The earlier research results of spectral-luminescent properties of Eu^{3+} -doped $Ca_3Ga_2Ge_3O_{12}$ garnet under photo-excitation have been presented in [4]. This report is continuation of these investigations and is focused on the analysis of received results by joint consideration of X-ray luminescence spectra, TSL curve and influence of IR-irradiation (λ>700 nm) on TSL properties with the aim to define the trap centers origin and understanding the mechanism of recombination luminescence in Eu^{3+} -doped $Ca_{3-x}Cd_xGa_2Ge_3O_{12}$ (x=0–3) polycrystals.

The samples of pure and activated with Eu^{3+} ions $Ca_{3-x}Cd_xGa_2Ge_3O_{12}$ garnet system were prepared by the method of solid state reaction at ~1150 ^{0}C using high purity starting materials. The analysis XRD patterns showed that all samples are homogeneous and belong to a cubic garnet single phase. We can assume that incorporated Eu^{3+} impurity ions occupy a lattice site with D_2 symmetry by replacing Ca^{2+} or ions Cd^{2+} in distorted dodecahedral positions.

The steady-state X-ray luminescence (XRL) spectra of nominally pure $Ca_3Ga_2Ge_3O_{12}$ crystals at 85 K are characterized by complex wide matrix band peaked at 400 nm, which is a superposition of two elementary bands with the maxima nearly 380 and 430 nm [3]. With growing the temperature up to 200-250 K the 380 nm band is quenched and intensity of 430 nm is enhanced. The XRL spectrum at 300K consists of the dominant band with a maximum at 459 nm and a weak band at 550 nm. The XRL spectra of $Ca_{3-x}Cd_xGa_2Ge_3O_{12}$ samples show broad non-elementary band with the maximum at about 470 nm that is consisted of two elementary bands with the maxima at 440 and 555 nm. The relative increasing of band intensity at 550 nm was observed at 300 K. Decay kinetic of intrinsic XRL is characterized by fast and slower stages. Doping with Eu^{3+} leads to appearing of weak activator f-f emission lines peaking near 597 and 709 nm, besides intrinsic luminescence bands [4]. The thermoluminescence (TL) glow curve obtained for $Ca_3Ga_2Ge_3O_{12}$ samples with 0,01 mol. % Eu^{3+} in the region 80-450 K consists of a number peaks appearing at about 150, 180, 210, 337 and 380 K. The glow curve of $Ca_{1.5}Cd_{1.5}Ga_2Ge_3O_{12}$: Eu^{3+} shows one wide complex intense peak with main maximum at 200 K due to strong broadening and enhanced intensity of low-temperature peaks. Photostimulated luminescence (PSL) is available in this material. IR-light irradiation of preliminary X-ray irradiated sample at 90 K significant reduces low-temperature peaks near 150K and 190 K. We analyzed obtained results with the aim to define the trapping level nature and features of recombination luminescence processes in $Ca_{3-x}Cd_xGa_2Ge_3O_{12}$ garnets.

[1] M. Montes, C.de las Heras, D. Jaque, *Optical Materials* **10** (2006) 408-414.

[2] U. R. Rodrıguez-Mendoza, S. F. Leon-Luis et al., *J. of Appl. Phys.* **113** (2013) 213517-8.

[3] D. Chen , Y. Chen , H. Lu , Z. Ji, *Inorg. Chem.* **53** (2014) 8638-45.

[4] L. Kostyk, A. Luchechko, S. Novosad, O. Tsvetkova, *Proceedings of Int. Conf. on Oxide Materials for Electronic Engineering*, OMEE-2014, Lviv, Ukraine, 2014, pp.153-154.

Luminescence Investigations of $ZnGa_2O_4$ Polycrystals Co-doped with Mn^{2+} and Eu^{3+} Ions

A. Luchechko[1], O. Kravets[1], O. Tsvetkova[1], A. Vaskiv[2]

[1]*Department of Sensor and Semiconductor Electronics, Ivan Franko National University of Lviv, 107 Tarnavskogo Str., 79017 Lviv, Ukraine*
[2]*Scientific-Technical and Educational Center of Low Temperature Studies, Ivan Franko National University of Lviv, 50 Drahomanova Str., 79005 Lviv, Ukraine*

More and more attention has been paid to metal gallate spinel compounds focusing on the developing of different types of display technologies due to advantage over sulfide phosphors. Zinc gallate spinel compounds are one of the promising materials with possible applications in vacuum fluorescent displays and field emission displays [1]. Metal gallate spinel modified by doping with rare-earth ions and transition metals exhibits promising results. Spinels doped with Mn^{2+} and Eu^{3+} ions show excellent luminescent properties in "green" and "orange-red" spectral regions, respectively [2].

In this work, $ZnGa_2O_4$: 0,05 mol.% Mn^{2+} and $ZnGa_2O_4$: 0,05 mol.% Mn^{2+}, 4 mol.% Eu^{3+} ceramic samples have been synthesized via high-temperature solid-state reaction method at ~1200 ºC in air. X-ray diffraction measurements confirmed single-phase nature of all samples. The luminescence properties were investigated under different excitation wavelengths at room and liquid nitrogen temperature.

Intense Mn^{2+} ions excitation was found in 230-280 nm region of spectra. Doping with Eu^{3+} ions leads to suppression of Mn^{2+} excitation in the $ZnGa_2O_4$: Mn^{2+}, Eu^{3+}. The *f-f* excitation lines (350-550 nm) and a broad band in 250-350 nm spectral region were found on excitation spectra of $ZnGa_2O_4$: Mn^{2+}, Eu^{3+} with registration at 617 nm. The UV excitation band is asymmetrical and related with charge transfer from O^{2-} to Eu^{3+} ions.

Complex broad band in 325-475 nm spectral region corresponds to matrix luminescence and intense band peaking around 505 nm related to Mn^{2+} emission were found at 240 nm excitation. Together with above mentioned bands Eu^{3+} emission was found in 575-650 nm spectral region at 290 nm excitation. These lines correspond to $^5D_0 \rightarrow {}^7F_j$ (j= 0, 1, 2) transitions in $4f^6$ configuration of Eu^{3+} ions. Incorporation of Eu^{3+} ions leads to suppression of both kinds of luminescence.

Changing of excitation wavelength and temperature leads to the redistribution of luminescence intensities in three spectral regions corresponding to the matrix luminescence, emissions of Mn^{2+} and Eu^{3+} ions.

[1] Musa Mutlu Can et al., *J. of Alloys and Compounds* **549** (2013) 303-307.
[2] A. Luchechko et al., *Radiation measurements* **90** (2016) 47-50.

Structure and Cathodoluminescence of Thin Films Y_2O_3:Eu at Different Conditions of Obtained

I.O. Bordun, I.Yo. Kukharskyy*, Zh.Ya. Tsapovska

Ivan Franko National University of Lviv, 50 Dragomanova Str., 79005 Lviv, Ukraine
* kukharskij@electronics.lnu.edu.ua

Among the large number of materials the luminescent materials have particular importance for using in the optoelectronics. They are used for creating displays, scintillators, for the means for recording and visualizing information. The cubic yttrium oxide the Y_2O_3 is one widespread crystalline matrix of phosphors that was activated with rare earth ions. Among them the most investigated and widely used phosphor micron dispersion is the Y_2O_3:Eu phosphor with red emission region. The disadvantage of this material is unsatisfactory morphology of the particles that do not ensure a smooth and uniform the coating of screens and the high resolution. This situation has led to active investigation various of thin films and nanostructure objects based on Y_2O_3:Eu.

Thin films of Y_2O_3:Eu with thickness between 0.2 and 1.0 μm were obtained by radio-frequency ion-plasmous sputtering in oxygen or argon atmosphere. The X-ray diffraction studies showed the presence of the polycrystalline cubic structure films preferentially oriented in the plane (222). The investigation of surface morphology of thin films by the atomic-force microscopy showed that the increase of the concentration of Eu^{3+} activator lead to the significant increase the size of crystallites and the roughness of relief of Y_2O_3:Eu thin films.

The investigation spectra of cathodoluminescence (CL) of Y_2O_3:Eu thin films with different the concentrations of the activator shows that the view of spectra does not change, at least by the changing the concentration of the activator in the research region 1.0 – 7.5 mol. %. The narrow bands of emission appear in the spectra of CL of the thin films. These bands are caused the intrinsic central transitions between electron shells within Eu^{3+} activator.

These bands associated with the allowed magnetic dipole transitions $^5D_0$-$^7F_1$ (for Eu^{3+} ions in C_2 and C_{3i} lattice sites of Y_2O_3) and the allowed electric dipole transitions $^5D_0$–$^7F_2$ (for Eu^{3+} ions only in the sites C_2). It was found that the Y_2O_3:Eu thin films deposited in argon atmosphere and in oxygen atmosphere with a concentration of activator 5 mol% have the maximum yield of CL.

The dependence of the intensity of CL from the excitation energy was investigated. It is shown that when the bombarding electrons are achieved of the substrate the intensity of CL is slightly decreased, and then, with the increasing energy begins to increase. Based on the dependence the intensity of CL from the current density of excitation was concluded that the energy of electronic excitation of Y_2O_3:Eu is not fully transferred from the excited electron to center of radiation. The part of the energy spent on non-radiation processes that may be caused by the heterogeneity structures of thin films. With increasing dose of radiation the view of dependence is increasingly approaching to the directly proportional.

The dependence the intensity of CL from the radiation dose that is specified the exposure time was investigated. The Y_2O_3:Eu thin films are resistant to the actions of the electron irradiation than a number of other oxide films based on silicates of yttrium and of zinc was shown.

The Improved Electronic Structure of the $LuVO_4$ Crystal Evaluated with the Strong Electron Correlation

S.V. Syrotyuk, V.M. Shved

Lviv Polytechnic National University, 12 S. Bandery Str., 79013 Lviv, Ukraine

Due to exceptional optical properties, like wide optical transparency and large birefringence the zircon- and scheelite-type ABO4 compounds are potential candidates for optical isolators, circulators beam displacers and components for polarizing optics [1]. The zircon-type $LuVO_4$ crystal in tetragonal structure is described by space group 141 and its unit cell containes Z=4 formula units. The lutetium 4f- and vanadium 3d-electrons reveal the strong correlated behaviour, and therefore the LDA and GGA approaches in electronic structure are not adequate. So we employ the hybrid exchange-correlation functional similar to PBE0 [2] one:

$$E_{xc} = E_{xc}^{GGA} + a\,(E_x^{HF}(y_{4f}) - E_{xc}^{GGA}(r_{4f}) + E_x^{HF}(y_{4d}) - E_{xc}^{GGA}(r_{3d}))\,. \qquad (1)$$

The electronic structure (Fig. 1) has been evaluated by means of the ABINIT code.

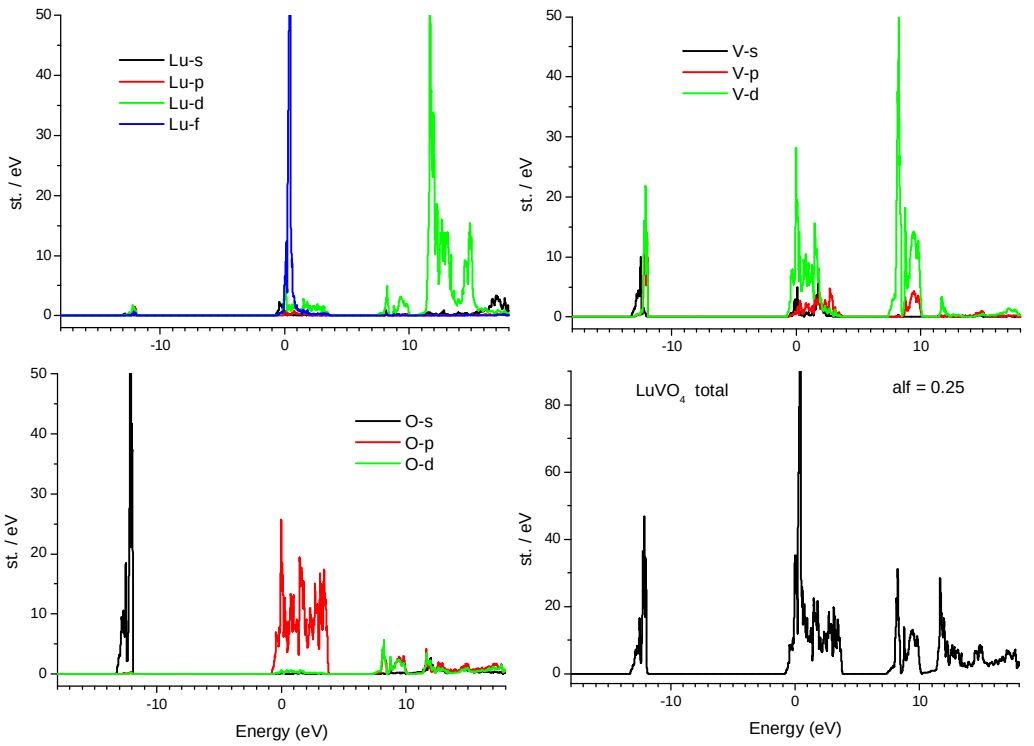

Figure 1. Partial and total DOS of the zircon $LuVO_4$ crystal found with a =0.25 value.

The obtained band gaps are: E_g = 3.05 eV (a =0), E_g = 3.46 eV (a =0.25) and E_g = 3.86 eV (a =0.45). Last calculated here value is well compared with experimental band gaps: 3.79 eV (reflectance), 3.76 eV (absorption) and 3.87 eV (emission).

[1] V. Panchal, D. Errandonea, A. Segura, P. Rodríguez-Hernandez, A. Muñoz, S. Lopez-Moreno, M. Bettinelli, *J. Appl. Phys.* **110** (2011) 043723.

[2] J. P. Perdew, M. Ernzerhof and K. Burke, *J. Chem. Phys.* **105** (1996) 9982.

The Electronic Properties of the Cubic $KMgF_3$ Perovskite under Pressure Effect

S.V. Syrotyuk, V.M. Shved, Yu.V. Klysko

Lviv Polytechnic National University, 12 S. Bandery Str., 79013 Lviv, Ukraine

Materials with perovskite crystal structure have a great potential for applications in catalysis, optoelectronics, semiconducting devices, and nonvolatile data-storage applications [1]. Fluoroperovskite KMgF3 finds applications as a vacuum-ultraviolet-transparent material for lenses in optical lithography steppers and in electrooptical applications [2, 3]. When doped appropriately, it is very promising for scintillators and radiation dosimeters [4].

The present work deals with the behaviour of electronic properties, namely, the energy band gaps, and the valence bandwidth of KMgF3 subject of hydrostatic pressures up to 30 GPa. The electronic energy bands have been evaluated here within the GGA and GWA approaches. The GWA results found here for the first time. All the calculations were carried out by means of the ABINIT code [5].

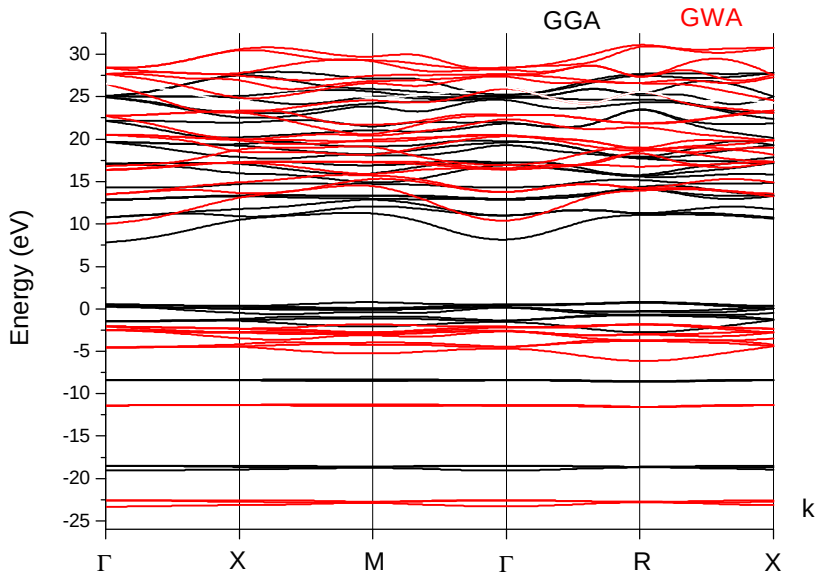

Figure 1. The electronic energy bands in $KMgF_3$ cubic crystal at ambient pressure.

We found that $KMgF_3$ has an indirect fundamental band gap Γ–R. The minimum optical gap Γ– Γ equals to 7.31 eV (GGA) and 12.04 eV (GWA). The fundamental gap equals to 6.99 eV (GGA) and 11.72 eV (GWA). The obtained here GGA band gaps are well compared with previous calculations. The measured absorption edge is 10.8 eV. So the GGA band gaps show a significant underestimation. The difference between GWA fundamental band gap and measured absorption edge equals to 0.92 eV and is found to be an exciton binding energy.

[1] G. Pilania, Vinit Sharma, *J. Mater. Sci*. **48** (2013) 7635–7641.
[2] T. Nishimatsu, N. Terakubo, H. Mizuseki, Y. Kawazoe, D.A. Pawlak, K. Shimamura, N. Ichinose, T.Fukuda, *Jpn. J. Appl. Phys.* **42** (2003) 5082.
[3] T. Fukuda, K. Shimamura, A. Yoshikawa, E.G. Villora, *Opto. Electron. Rev*. **9** (2001) 109.
[4] A.V. Gektin, M.I. Krasovitskaya, N.V. Shiran, *Radiat. Meas.* **29** (1998) 337.
[5] X. Gonze, B. Amadon, P.-M. Anglade, J.-M. Beuken et al., *Comput. Phys. Commun.* **180** (2009) 2582.

Optical Properties of GGG Epitaxial Films Grown from $PbO\text{-}B_2O_3\text{-}V_2O_5$ Flux

I.I. Syvorotka[1,2], D.Yu. Sugak[1,2], A.P. Luchechko[3], Ya.A. Zhydachevskii[2,4], S.B. Ubizskii[2]

[1]*Scientific Research Company "Carat", Lviv, Ukraine*
[2]*Lviv Polytechnic National University, Lviv, Ukraine*
[3]*Ivan Franko National University of Lviv, Lviv, Ukraine*
[4]*Institute of Physics, Polish Academy of Sciences, Warsaw, Poland*

Garnet crystals are known to be used as materials for solid-state lasers and garnets doped with transition metals for passive Q-switching in range 1…1,6 μm. Single crystalline films grown by liquid phase epitaxy (LPE) have some advantages in comparison with bulk crystals such as homogeneity, structural perfection, optical transparency, etc.

The present work is devoted to growth of the high-quality gadolinium gallium garnet $Gd_3Ga_5O_{12}$ (GGG) homoepitaxial films and investigation of the influence of technology parameters on their optical properties.

Single crystalline films of GGG were grown on (111)-oriented pure GGG substrate by LPE method from fluxes based on $PbO\text{-}B_2O_3$ and $PbO\text{-}B_2O_3\text{-}V_2O_5$. The growth temperature was in the range of 880…1010 °C. The films with thickness of 4…60 μm were grown at growth rate changing from 0.1 to 1.0 μm/min.

Optical absorption spectra of grown films were measured in the range of 200…1500 nm. The absorption band at 280 nm which correspond to electron transition ($6s^2$) $^1S_0 \rightarrow {}^3P_1$ of Pb^{2+} ions [1] were observed in all films grown from both fluxes. Besides the wide absorption band with maximum around 345 nm is observed in films grown from $PbO\text{-}B_2O_3$ (Fig. 1*a*). This absorption can be connected with the hole O^- centers which localized near Gd^{3+} in octahedral position [2]. The additional absorption bands were observed (Fig. 1*b*) in films grown from $PbO\text{-}B_2O_3\text{-}V_2O_5$ flux. The first one with maximum at 322 nm corresponds to charge transfer from the oxygen to Pb^{4+} ($O^{2-}+Pb^{4+}+h\nu \rightarrow Pb^{3+}+O^-$) and the second one with maximum at 550 nm is due to intervalence pair-wise transitions in Pb^{2+} and Pb^{4+} ions ($Pb^{2+}+Pb^{4+}+h\nu \rightarrow Pb^{3+}+Pb^{3+}$) [1]. Moreover, any absorption peaks which correspond to ions V^{3+} or V^{4+} ions were not detected.

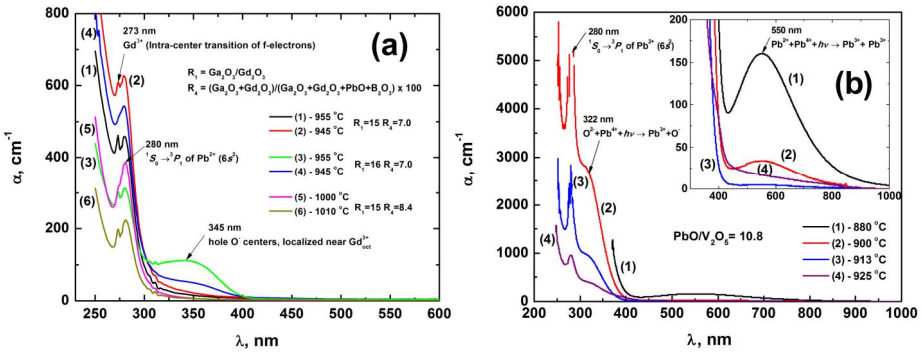

Fig. 1. Optical absorption spectra of the homoepitaxial GGG films grown from $PbO\text{-}B_2O_3$ (*a*) and $PbO\text{-}B_2O_3\text{-}V_2O_5$ (*b*) fluxes at different temperatures.

Influence of flux composition contained V_2O_5 on optical properties of GGG epitaxial films are discussed.

[1] G. B. Scott and J. L. Page, Pb valence in iron garnets, *Journal of Applied Physics* **48** (1977) 1342-1349.
[2] A. Matkovskii, P. Potera, D. Sugak, L. Grigorjeva, D. Millers, V. Pankratov, and A. Suchocki, Stable and transient color centers in $Gd_3Ga_5O_{12}$ crystals, *Crys. Res. Technol.* **39**(9) (2004) 788-795.

Ultraviolet to Near-Infrared Down-Conversion in Bi^{3+} - Yb^{3+} Co-Doped YAM Phosphor

Ya. Zhydachevskyy[1,2], V. Tsiumra[1], M. Baran[3], L. Lipińska[3], J. Barzowska[4], A. Suchocki[1,5]

[1]*Institute of Physics, Polish Academy of Sciences, Al. Lotników 32/46, Warsaw 02-668, Poland*
[2]*Lviv Polytechnic National University, 12 Bandera, Lviv 79646, Ukraine*
[3]*Institute of Electronic Materials Technology, 133 Wólczyńska Str., Warsaw 01-919, Poland*
[4]*Institute of Experimental Physics, Gdańsk University, Wita Stwosza 57, Gdańsk 80-952, Poland*
[5]*Institute of Physics, University of Bydgoszcz, Weyssenhoffa 11, Bydgoszcz 85-072, Poland*

Recently a number of papers appears showing application potential of Bi^{3+}–Yb^{3+} co-doped materials for solar spectrum modification by means of down-conversion (cutting one high energy photon into two low energy ones) and in such a way for possible enhancement of efficiency of silicon solar cells (see [1] and references here). In particular, down-conversion properties due to cooperative energy transfer (CET) were shown for Bi^{3+}–Yb^{3+} co-doped Y_2O_3, Gd_2O_3, YVO_4, $Y_3Al_5O_{12}$ (YAG), $CaTiO_3$ and other related materials. Here near-infrared emission around 1 μm from Yb^{3+} ($^2F_{5/2}\rightarrow{}^2F_{7/2}$) is observed under ultraviolet excitation of Bi^{3+} ion ($^1S_0\rightarrow{}^3P_1$ transitions).

The down-conversion quantum efficiency of the Bi^{3+}–Yb^{3+} co-doped materials is usually estimated from shortening of luminescence decay time of Bi^{3+} ions. To our best knowledge, there are no reports showing absolute measurements of external quantum efficiency of the down-conversion luminescence for any of Bi^{3+}–Yb^{3+} co-doped phosphor.

To get better insight into the down-conversion mechanisms in Bi^{3+}–Yb^{3+} co-doped phosphors, in the present work, direct measurements of external quantum yield (QY) were applied to a down-converting phosphors combined with measurements of photoluminescence (PL), photoluminescence excitation (PLE) and photoluminescence decay kinetics. The monoclinic yttrium-aluminum oxide (YAM) was chosen for the Bi^{3+}–Yb^{3+} co-doping because it provides additional broadening of absorption of Bi^{3+} ions due to their multisite structure in this host.

It was revealed that the energy transfer occurs mainly from one of four types of Bi^{3+} centers in YAM, namely Bi^{3+}(I), having the excitation maximum at 278 nm and the emission maximum at 360 nm. The absolute measurements of QY shows large discrepancy between the measured quantum efficiencies of the UV to near-IR down-conversion process and the efficiencies estimated from a shortening of the Bi^{3+} luminescence decay time. Obtained results testify the conversion ratio (which should be 2.0 for an ideal quantum cutting mechanism) to be no more than 1.0 for the studied material.

The procedure used in this study can be also applied to the other systems proposed for quantum cutting since it provides a method for checking the real efficiencies of this process instead of estimation derived from the decay kinetics of the energy donor (i.e. Bi^{3+} in this case) alone. Such a procedure is much more reliable.

Acknowledgements. The work was supported by the Polish National Science Center (project 2015/17/B/ST5/01658) and by the Ministry of Education and Science of Ukraine (project DB/KMON), and by the EU within the European Regional Development Fund through the Innovative Economy grant (POIG.01.01.02-00-108/09).

[1] Ya. Zhydachevskii et al., *Mat. Chem. Phys.* **143** (2014) 622-628.

Optical Investigation of the Cu-Ions Diffusion into Lithium Niobate Crystal

U. Yakhnevych[1], D. Sugak[1,2], I.I. Syvorotka[1,2], O. Buryy[1], N. Martynyuk[1], S. Ubizskii[1]

[1]*Lviv Polytechnic National University, Lviv, Ukraine*
[2]*Scientific Research Company "Carat", Lviv, Ukraine*

The diffusion of Cu ions is used for photorefractive elements formation as well as for modification of refractive index in lithium niobate ($LiNbO_3$ – LN) single crystal near-surface layers for obtaining of integral optics structures [1]. The point of this paper is a determination of peculiarities of Cu ions incorporation into LN crystal in different valence states and different crystal-physics directions. The samples of LN (7(X) × 15(Y) × 32(Z) mm) with polished surfaces were prepared from the optical quality congruent crystal. These samples were placed into CuO powder and annealed additively (3h + 6h + 12h) in air at 1073 K. After each stage the samples were cooled and their transmission spectra were registered in Z direction (300…1500 nm range). After annealing the shift of the LN absorption edge to longer wavelengths and formation of a weak broad band with a maximum at 1000 nm region are observed. These data, in general, coincides with the results of [2]. For measuring of optical absorption changes perpendicularly to the direction of Cu diffusion, the polished 1 mm-thick plates were cut from the central part of annealed samples. The special designed unit was used for measuring of the plates absorption spectra through the 100 μm diameter aperture with the step of 20 μm.

The sequential difference spectra (in relation to the optical absorption of the central part of the plates) were obtained at different points of the plates during scanning from their centers to the edges. Two absorption bands with maxima at 1000 nm and 400 nm were observed in these spectra. In accordance with [2, 3] they are associated with the intra-center transition in Cu^{2+} ion and the inter-valence transition $Cu^{+} \rightarrow Nb^{5+}$, respectively. The values of the absorption in these bands maxima vary with the distance from the edges to the center and characterize the changes of concentration of copper ions in different valence states.

The spatial distributions of copper ions concentration in different crystal-physics directions in $LiNbO_3$ were calculated in accordance with Smakula-Dexter formula [4] based on the oscillators strengths of corresponding optical transitions indicated in [3]. It was found that after annealing the Cu^{2+} ions concentration achieved the value of $3.3 \cdot 10^{19}$ cm^{-3} in its maxima, whereas the maximal concentration of Cu^{+} ions is about 4.8×10^{18} cm^{-3}. The maxima of Cu^{2+} ions concentration is observed at the distances from 200 to 240 μm from the plate edge and weakly depends on the crystal-physics direction. The position of Cu^{+} ions concentration maximum depends more strongly upon the crystal-physics direction: it is located near 320 μm for X-, near 340 μm for Y-, and near 440 μm for Z-one, so the incorporation of Cu into LN crystal has got the anisotropic character. The presence of copper ions in two valence states as well as the presence of maxima on their spatial distributions indicates that the incorporation of Cu into LN is a complex process involving diffusion of ions and quasi-chemical reactions of their recharging. The possible mechanisms of copper ions incorporation are discussed.

[1] F. Caccavale, C. Sada, F. Segato et al., Copper-lithium ion exchange in $LiNbO_3$, *J. Mater. Res.* **15** (2000) 1120–1124.
[2] S. Kar, K.S. Bartwal, Cu^{2+} ion in-diffusion in congruent $LiNbO_3$ single crystals, *Mater. Lett.* **62** (2008) 3934–3936.
[3] E. Krätzig, R. Orlowski, Light induced charge transport in doped $LiNbO_3$ and $LiTaO_3$, *Ferroelectrics* **27** (1980) 241–244.
[4] D.L. Dexter, Absorption of light by atoms in solids, *Phys. Rev.* **101** (1956) 48–55.

Optical Investigation of Co Ions Diffusion in $Gd_3Ga_5O_{12}$ Single Crystals

D. Sugak[1,2], I.I. Syvorotka[1,2], U. Yakhnevych[1], O. Buryy[1], Ya. Zhydachevskii[1,3], A. Suchocki[3,4], M. Vakiv[1,2], S. Ubizskii[2]

[1]*Lviv Polytechnic National University, Ukraine*
[2]*Scientific Research Company "Carat", Lviv, Ukraine*
[3]*Institute of Physics, Polish Academy of Science, Warsaw, Poland*
[4]*Institute of Physics, Kazimierz Wielki University, Bydgoszcz, Poland*

Absorption of light on the $^4A_2 \rightarrow {}^4T_1(^4F)$ transition in tetrahedrally coordinated Co^{2+} dopant ions reveals non-linear dependence on the incident light intensity. This phenomenon of Co^{2+} ions saturable absorption is used in practice for Q-switching of solid state lasers of 1.2...1.7 μm spectral range [1]. One of the materials used for Q-switching is $Gd_3Ga_5O_{12}$ (GGG) crystals doped by Co^{2+}. Both the bulk crystals grown by Czochralski method and the LPE GGG:Co^{2+} single crystalline films grown on a GGG substrate can be used for this application [2, 3]. Besides the incorporation of metal ions into some complex oxides crystals can be achieved by high-temperature annealing in the presence of their compounds, particularly the metal oxides [4].

This work presents the results of GGG doping due to diffusion of cobalt ions from the surfaces of the crystals. Two different GGG samples were used for investigations: the first one in the form of plate with dimensions of 7×15×1 mm^3, the second one in the form of cylinder with 15 mm diameter and 10 mm height. The plate surface and base surfaces of cylinder were perpendicular to crystallographic directions [111]. These surfaces were polished. Samples were placed in ceramic crucibles, were covered from all sides with Co_3O_4 powder and were annealed in air in the Naberterm (Germany) oven at 1200 °C for 24 hours. The optical spectra of annealed samples were registered with a spectrophotometer Shimadzu UV3600 (Japan) in the 200...1700 nm spectral range. Transmission spectra of 7×15×1 mm^3 plate were studied when light is passed along the [111] direction, i.e. in the direction of diffusion. For determination of the cobalt ion diffusion depth the 2 mm-thick plate was cut from the cylindrical sample and polished so that its largest facet was parallel to the direction [111]. The absorption spectra were registered in the direction perpendicular to the [111] one by a special device that allowed to perform measurements in increments of 20 microns at points along [111]. The absorption spectra obtained after annealing coincides with known data about the absorption of Co^{2+} ions in tetrahedral positions. The spatial distribution of dopants was determined from the measurements of depth-depended Co^{2+} absorption changes. It is shown that the depth of Co^{2+} diffusion in GGG reaches a value about 500 μm.

The results of XRD studies are presented for surfaces that were in contact with diffusant (Co^{2+} ions) source. For plate cut out perpendicular to the (111) plane the changes of chemical composition and structural properties along the direction of diffusion were studied by electron-probe microanalysis and micro-Raman spectroscopy methods. The mechanisms of Co^{2+} ions incorporation into GGG structure are discussed.

This work supported by EMSh project of Ukrainian Ministry of Education and Sciences.

[1] K.V. Yumashev, I.A. Denisov, N.N. Posnov et al., *J. Alloys and Comp.*, **341** (2002) 366.
[2] V. Kravchenko, P. Sadovski, A. Sobolev et al., *Quantum Electronics*, **39** (2009) 1121.
[3] K. Mazur, J. Sarnecki, J. Borysiuk et al., *Thin Solid Films*, **519** (2011) 2111.
[4] W.-B. Sun, Z.-B. Zhang, H.-X. Sun et al., *J. Lumin.*, **184** (2017) 191.

Physical Properties of the $(Ga_{70}La_{30})_2S_{300}$, $(Ga_{69,75}La_{29,75}Er_{0,5})_2S_{300}$ Single Crystals

I.A. Ivashchenko[1,*], I.D. Olekseyuk[1], V.V. Halyan[2], A.H. Kevshyn[2], T.Y. Kubatska[2], V.M. Rosolovska[2], P. Tishchenko[1], A. Selezen'[1]

[1]*Department of Inorganic and Physical Chemistry, Eastern European National University, Lutsk, Ukraine*
[2]*Department of General Physics, Eastern European National University, Lutsk, Ukraine*
* *Ivashchenko.Inna@eenu.edu.ua, inna.ivashchenko@mail.ru*

The single crystals of the $(Ga_{70}La_{30})_2S_{300}$, $(Ga_{69,75}La_{29,75}Er_{0,5})_2S_{300}$ compositions were grown by solution-melt method from their primary crystallization range. The compositions and the growth conditions were selected using the Ga_2S_3 – La_2S_3 phase diagram [1]. The supercooling of the solid solution was 70 K as determined from the cooling thermograms of the samples. The synthesis of the starting alloy at maximum temperature 1200 K and the crystal growth was performed in the same evacuated quartz container with a conical bottom. The growth process was performed in a vertical two-zone furnace. The temperature gradient at the solid-melt interface was 20 K/cm. After melting the batch, the ampoule was lowered at a rate of 5 mm/day. Immediately after the crystallization of 10 mm along the ampoule, we followed by remelting 6.0-8.0 mm of the crystallized portion. Then the ampoule was annealed for 100 hours. After that, the crystal growth was performed at a rate of lowering of 5 mm/day. At the end of the process, both furnaces were cooled to 820 K at a rate of 50-70 K/day, and then cooled to room temperature with the furnaces switched off. The grey-yellow single crystals with a diameter of 15 mm and a length of 24 mm were obtained. Both samples were indexed in the monoclinic structure, S.G. $P2_1/c$, a=1,5168(4) nm, b=1,0555(4) nm, c=1,283(3) nm, β=137,60° for $(Ga_{70}La_{30})_2S_{300}$, with good agreement with [2] and a=1,5175(3) nm, b=1,0564(2) nm, c=1,289(2) nm, β=137,70° for $(Ga_{69,75}La_{29,75}Er_{0,5})_2S_{300}$.

Photoluminescent properties of the single crystal $(Ga_{69.75}La_{29.75}Er_{0.5})_2S_{300}$ were investigated. The excitation by 400 mW laser at 810 nm wavelength led to photoluminescence (PL) in the spectral range 510–560 nm. PL spectrum consists of two peaks at 525 and 545 nm, with the ratio of the intensity at their maxima being $I_{545/I525}$=4.2. Characteristic narrow maxima and PL absence in the $(Ga_{70}La_{30})_2S_{300}$ crystal means that the emission in the $(Ga_{69.75}La_{29.75}Er_{0.5})_2S_{300}$ single crystal is caused by the intra-center transitions in Er^{3+} ions, namely $^2H_{11/2} \rightarrow {}^4I_{15/2}$ and $^4S_{3/2} \rightarrow {}^4I_{15/2}$ for 525 and 545 nm, respectively. The absorption of IR quanta (810 nm) yields green luminescence, with higher energy quanta. Such a phenomenon (so called up-conversion photoluminescence) is especially common in erbium-doped chalcogenide glasses [3]. This can occur by sequential absorption of two photons with 810 nm wavelength; or when one erbium ion is in excited $^4I_{9/2}$ state, energy is transferred to another $^4I_{9/2}$-excited ion nearby: $^4I_{15/2} + h\nu_{810} \rightarrow {}^4I_{9/2} + h\nu_{810} \rightarrow {}^2H_{9/2}\ {}^4I_{9/2} + {}^4I_{9/2} \rightarrow {}^4I_{15/2} + {}^2H_{9/2}$. The next step is non-radiative relaxation of erbium ions to the lower energy states or cross-relaxation involving $^2H_{11/2}$ and $^4S_{3/2}$ states. Thus, a high concentration of erbium ions in the $^2H_{11/2}$ та $^4S_{3/2}$ states is obtained through which PL radiation is emitted. This type of radiation is particularly promising for the manufacture of up-converters from infrared to visible light.

[1] J. Flahaut, M. Guittard, A. M. Loireau-Lozac'h, Rare earth sulphide and oxysulphide glasses, *Glass Technology* **24** (1983) 149 – 156.

[2] M. Julien-Pouzol, S. Jaulmes, C. Dagron, Structure du trisulfure de lanthane et de gallium, *Acta Crystallogr. B* **38** (1982) 1566 – 1568.

[3] V.V. Halyan, I.V. Kityk, A.H. Kevshyn, I.A. Ivashchenko, G. Lakshminarayana, M.V. Shevchuk, A. Fedorchuk, M. Piasecki, Effect of temperature on the structure and luminescence properties of $Ag_{0.05}Ga_{0.05}Ge_{0.95}S_2$-$Er_2S_3$ glasses, *Journal of Luminescence* **181** (2017) 315-320.

Global Maxima of the Acousto-Optic Effect in $CaWO_4$ Crystals

O.A. Buryy[1], A.S. Andrushchak[2]

[1]*Semiconductor electronics department, Lviv Polytechnic National University, Lviv, Ukraine*
[2]*Department of Electronic Devices, Lviv Polytechnic National University, Lviv, Ukraine*

Acousto-optic effect, i.e. the diffraction of the electromagnetic wave on the acoustic one, is widely used in science and technique. Particularly, acousto-optic devices – modulators, deflectors, filters allow to control and process of light beam, to characterize of electromagnetic or acoustic waves, etc. The effectiveness of these devices strongly depends on the geometry of interaction, i.e. on the propagation directions of electromagnetic and acoustic waves. In general, the optimal geometry of acousto-optic interaction can be determined by extreme surfaces method proposed by in [1–2] as well as by its modification elaborated by authors of [3]. Here we use this method for optimization of the acousto-optic interaction (Bragg diffraction) geometry in $CaWO_4$ crystal interesting for applications in near-UV acoustooptic filters and Q-switching modulators for high-power solid-state lasers [4]. All calculations were carried out for the electromagnetic wavelength of 633 nm and the acoustic wave frequency of 100 MHz.

As it is shown, the maximal value of the acousto-optical figure-of-merit M_2 is equal to $8.9 \cdot 10^{-15}$ s^3/kg achieved in the case of isotropic diffraction of the ordinary light wave on the slow quasi-transversal acoustic wave. At that the incident light wave propagates along the direction determined by the angles $\theta = 2^o$, $\varphi = 72^o$ of the spherical coordinate system. The corresponding acoustic wave propagates in the direction determined by the angles $\theta_a = 92^o$, $\varphi_a = 104^o$ and polarized along ($\theta_f = 88^o$, $\varphi_f = 19^o$) direction. The velocity of this wave is equal to 2043 m/s and the effective elastooptic coefficient p_{ef} is about 0.11 for this type of diffraction.

[1] O. Buryy et al., *Journal of Applied Physics* **113** (2013) 083103(12p.).
[2] O. Buryy et al., *Apllied Optics* **56** (2017) 1839 – 1845.
[3] J. Pfeiffer and K. Wagner, *Physics Procedia* **70** (2016) 762 – 765.
[4] D. Vynnyk et al., *Proceedings of the XIIIth International Conference TCSET'2016*, Lviv–Slavske, Ukraine, 2016, pp. 373 – 375.

Structure and Thermally Stimulated Luminescence of β-Ga_2O_3 Thin Films

O.M. Bordun*, B.O. Bordun, I.I. Medvid

Ivan Franko National University of Lviv, 50 Dragomanova Str., 79005 Lviv, Ukraine
* bordun@electronics.lnu.edu.ua

Recently, the thin films of β-modification of gallium oxide (β-Ga_2O_3) are widely used in various optoelectronic devices. Particularly, the pure and doped thin films are used as a phosphors, cathode phosphors, electroluminescent phosphors, UV-detectors and gas sensors. The luminescent properties of β-Ga_2O_3 thin films are strongly dependent from the method as well as from the conditions of preparation. The efficiency of the transfer excitation energy from the basic material to the luminescent centers is largely determined by the presence trapping centers (TC), which manifest themselves in thermally stimulated luminescence (TSL). This led to investigation the TC of charge carriers and the determining of their parameters by the thermal activation methods.

β-Ga_2O_3 thin films with thickness from 0.2 to 1.0 μm were obtained by radio-frequency ion-plasmous sputtering. The deposition of thin films was occurred in the spraying argon atmosphere. The heat treatment of thin films was performed after deposition in oxygen atmosphere. X-ray diffraction studies showed the presence of the polycrystalline structure of thin films that preferentially oriented in the planes (400), (002), (111) and (512). The investigation of surface morphology of thin films by the atomic-force microscopy showed that the diameter of the grains on the surface of thin films without heat treatment is average equal to 30 nm and the average roughness of thin films is about 7 nm. The treatment of thin films in oxygen atmosphere leads to the increase size of grains through the processes of growth and sintering, thus, the average diameter of grains is increased to 45 nm. The surface roughness of thin films after annealing increases more than twice, the average to 15 nm.

The investigation of thermally stimulated luminescence (TSL) of β-Ga_2O_3 thin films after annealing in oxygen atmosphere and X-ray excitation showed 4 different of the TC in the temperature range 50-300 K. Meanwhile, the property the storage of light appears in the bands of the TSL with maxima at 77, 135, 178 and 235 K.

The analysis of the luminescence spectra of the TSL of β-Ga_2O_3 thin films shows that the radiative recombination at the termination TC passes through the same centers as in stationary regime luminescence. As in the spectra of stationary luminescence [1], the spectra of TSL of the films are well simulated by two independent Gaussians (the model linear electron-phonon coupling) with maxima at 2.95 and 3.14 eV. Thus, for the band with the maximum at 77 K in the spectrum of luminescence the dominant is the band with maximum at 3.14 eV and for more high-temperature bands are predominant the bands with maximum at 2.95 eV.

On the basis of several methods was defined the thermal activation energy of TC E_T and frequency factor of trapping centers p_0 that characterizes the frequency of effective collisions which capable of vacate the localized charges.

Based on the deviations the dependence of $E_T(T)$ was done the hypothesis about the presence of remote diffuse-controlled tunnel mechanism of luminescence. The diffuse nature of migration of the electron excitations with the possible intermediate localization is confirmed also low values the defined factor of frequency p_0 of the processes of relaxation.

[1] O.M. Bordun, B.O. Bordun, I.Yo. Kukharskyy, I.I Medvid, *Zh. Prikl. Spektr.* **84** (1) (2017) 56-62.

Optical Properties of Epitaxial ZnO-ALD Films Implanted with Rare Earth

E. Guziewicz[1], R. Ratajczak[2], M. Stachowicz[1], T.A. Krajewski[1], D. Snigurenko[1], A. Turos[3]

[1]*Institute of Physics, Polish Academy of Sciences, Warsaw, Poland*
[2]*National Centre for Nuclear Research, Świerk, Poland*
[3]*Institute of Electronic Materials Technology, Warsaw, Poland*

Rare Earth (RE) doped semiconductor materials have been widely investigated because of their optical properties and possible application as fiber lasers and amplifiers, plasma displays, phosphors in fluorescence lamps and solar cells. The *RE4f* electron shell is highly localized, so the intra-shell transitions of *4f* electrons are only slightly affected by the host material, therefore the radiative efficiencies are almost temperature independent. Wide bandgap semiconductors are especially interesting as host materials, because they are expected to overcome the temperature quenching observed in other materials (e.g. in Si) and to promote effective resonant pumping of the *f* shell [1]. GaN and ZnO have been the most investigated semiconductors in this field. Both materials have a similar bandgap (about 3.4 eV at RT) and nowadays they compete with each other as the most promising new materials for optoelectronics. However, important advantages of ZnO are much higher exciton binding energy (60 meV vs. 24 meV) and availability of single crystal ZnO substrates. Additionally, the ZnO based technology is expected to be much cheaper than the GaN technology.

Epitaxial ZnO films were grown by Atomic Layer Deposition which is an inexpensive growth technology that can be applied in industry. The films were implanted with Yb, Pr or Dy ions to a fluence of $1x10^{15}$ at/cm^2. A considerable crystal lattice damage has been observed in the Rutherford Backscattering spectra and microscopic images after the implantation process [3-4]. As a result only a weak photoluminescence (PL) signal from ZnO:Yb, ZnO:Dy and ZnO:Pr layer was observed. It was found that annealing under oxygen or under ambient atmosphere at 800°C leads to ZnO crystal lattice recovery and activation of the band-edge and defect-related PL from the ZnO lattice as well as the RE-related emission. It is concluded that the intensity of the observed PL signal strongly depends not only on crystal lattice recovery, but on RE ions location in the ZnO lattice as well. Therefore, the parameters of used annealing processes play a crucial role in the obtained optical response from ZnO:RE films.

Acknowledgements. The work was supported by the Polish National Centre for Research and Development (NCBiR) through the project PBS2/A5/34/2013 and project by Helmholtz Zentrum Dresden-Rossendorf (HZDR) in the frame of the program Access to Infrastructure (16000696-ST).

[1] A.J. Kenyon, *Prog. Quntum El.* **26** (2002) 225.
[2] P.N. Favennec, H. L'Haridon, D. Moutonnet, M. Salvi, M. Gauneau, Rare Earth Doped Semiconductors, in: Pomrenke, Klein, Langer (Eds.), MRS Symposia Proceedings, Materials Research Society, Pittsburgh, PA, vol. 31, 181 (1993).
[3] R. Ratajczak, S. Prucnal, E. Guziewicz, C. Mieszczynski, D. Snigurenko, M. Stachowicz, W. Skorupa and A. Turos, *J. Applied Phys.* (in print).
[4] E. Guziewicz, R. Ratajczak, M. Stachowicz, D. Snigurenko, T.A. Krajewski, C. Mieszczynski, K. Mazur, B.S. Witkowski, P. Dluzewski, K. Morawiec, A Turos, *Thin Solid Films* (under consideration).

Effect of HRT ZnO Film on Optical Spectra of Transmission and Absorption in CdS/CdTe Solar Elements

A. Danylov, H. Ilchuk, R. Petrus'

Lviv Polytechnic National University, 12 S. Bandera Str., 79013 Lviv, Ukraine

CdS/CdTe heterojunction is one of the most promising photovoltaic systems for solar energy conversion. Theoretical limit of CdTe solar cell efficiency approaches to 30 %, but maximal efficiency of experimental cells up to date is 21 %. The main energy losses are caused by solar light reflection at solar element layer interfaces, propagation of radiation through the element without absorption, recombination losses and high value of series resistance in the element. The thinner is buffer layer of CdS, the higher is irradiance at CdS/CdTe interface and as a result the higher is photogeneration in CdTe active layer. Technological regimes of solar element formation include CdS/CdTe annealing. The structure annealing even for gentle temperature conditions leads to pinhole formation into thin CdS film. The film becomes discontinuous that leads to shunting junction formation between transparent conductive oxide (TCO) and CdTe active layer. To avoid the effect and prevent diffusion of undesirable impurities into active layer the additional high resistive transparent (HRT) layer can be deposited between TCO and buffer layer.

ZnO is transparent n-type direct bandgap (3.36 eV) metal oxide semiconductor that has diverse application as electrodes in optoelectronic devices, window and buffer layers in solar cells and can be used as TCO supplying high shunting resistivity of solar element. In the present work we performed comprehensive analysis of optical spectra in the working range of CdTe solar element for structure with ITO as TCO, inorganic oxide ZnO as HRT and CdS/CdTe heterojunction. As a basic we chose the structure ITO(25 nm)/ZnO(270 nm)/CdS(50 nm)/CdTe(800 nm) and explored the tendencies of changes in optical spectra of absorption and transmission caused by different layer thickness variation. Transmission spectra for upper layers of solar element including light reflection from the interface CdS/CdTe but without considering light propagation through CdTe substrate were calculated. The spectra showed distinct interference nature. We determined optimal thickness of ZnO layer which supplies minimum of interference in reflection geometry for the basic structure. For ZnO layer thickness equal to 230 nm mean transmittance of light to CdS/CdTe interface in wavelength range 400-800 nm becomes the highest and approaches to 77 %. Mean transmittance of the structure increases with buffer layer thickness decrease and from technological aspects the thickness of buffer layer 50 nm can be optimal for solar element with HRT layer. Variation of ITO thickness in the range 25-100 nm showed the highest transmission for thinnest layer also.

Protective glass superstrate can be fruitful for structure with upper layer of ZnO because of at least threefold decrease of reflection from the structure in the whole, but when ITO is first film in the stack reflection significantly increases in the range 600-800 nm in comparison with structure without top glass plate and total transmission into active layer decreases.

Calculated spectra for structure with textured top surface in the shape of set of random triangle pyramids revealed essential rise of transmission in the region of CdS absorption range (from 400 to 500 nm) and 5-% gain in the rest region as compared with planar structure. But the texturing profit becomes negligible for the case of glass texturing. Therefore, as findings, additional thin ZnO level deposition at the top of ITO with further glass surface protection application could be useful. The experimental verification of the theoretical predictions comes to the end.

Thermochromic Effect in Doped $Bi_{12}SiO_{20}$ Crystals

A. Dyachenko, T. Panchenko

Oles Honchar Dnipropetrovsk National University, 49010 Dnipro, Ukraine

By now, thermochromic effect (TCE) attracts attention of researches because of the urge to learn its physical nature in inorganic crystals and interrelation between TCE and photochromic effect (PCE) as well as owing to the usage of availability in heat-indicating devices and thermochromic display units.

Results of TCE experimental studying in photorefractive crystals of complex oxides $Bi_{12}SiO_{20}$ (BSO), doped by Al and Ga ions (BSO:Al and BSO:Ga correspondingly) are presented.

Crystals BSO:Al, BSO:Ga were grown by Czochralski method along the crystallographic direction [001]. The Al and Ga content in crystals according to data of spectral-emission analysis was 0.5 mass.%. The samples were prepared as a set of polished plates with thickness d = 4.8 ÷ 5.5 mm with large planes (001).

The procedure was as follows. Thermal influence on stationary absorption spectra $\alpha(h\nu, T)$ in the range $h\nu$ = 0.5 ÷ 3.4 eV were carried out in cycles "heating - cooling" in the temperature range T = 300 – 600 K. Moreover, stationary $\alpha(T)$ and photoinduced absorption $\alpha^{ph}(T)$ temperature dependences for the different spectral range (IR-, visible and nearby UF) and the so-called curves of PCE thermal erasing $\Delta\alpha^{ph}(T) = \alpha^{ph}(T) - \alpha(T)$ were carried out.

The results obtained are reduced to the follows. Difference spectra $\Delta\alpha(h\nu, T = 300\ K) = \alpha^{T}(h\nu, T = 300\ K) - \alpha_0(h\nu, T = 300\ K)$, which were taken after the cycle "heating – cooling" passing, have a close similarity for BSO:Al and BSO:Ga crystals. Corresponding curves with a complex structure indicate TCE occurrence and several types of thermo induced defects. Temperature dependences $\alpha(h\nu, T)$ in the nearby UF- range ($h\nu$ = 3.1 – 3.4 eV) close to exponential, obey to Uhrbach rule and indicate a significant temperature shift of the fundamental absorption edge of the researched crystals. Stationary absorption is small in visible and IR-ranges and any temperature peculiarities are observed, curves of the photoinduced absorption have a complicated structure with maxima in the nearby IR- range ($h\nu$ = 0.5 – 1.25 eV). Thermal fading curves have a stepped form, which denote a thermal destruction of photoinduced centers. Temperature, which correspond to the absorption sharp decrease in the "step" on curves $\Delta\alpha^{ph}(T)$ assign a thermal activation energy of the PCE erasing process. All received curves are characterized by a hysteresis.

Obtained results analyzed within the framework of the model for redistribution of electrons over donor and acceptor levels of the band gap involving spectral and thermal data of the photoconductivity for BSO:Al and BSO:Ga crystals [1, 2].

[1] A.A. Dyachenko, T.V. Panchenko, Excitation and erasure of photochromic effect in the $Bi_{12}SiO_{20}$ crystals doped with Al, Ga and Sn, *Ukrainian Journal of Physical Optics* **16**(3) (2015) 127 – 133.

[2] A.A. Dyachenko, T.V. Panchenko, Optical and thermal erasing photochromic effect in Al doped $Bi_{12}SiO_{20}$ crystals, *Functional materials* **23**(2) (2016) 197 – 201.

Linear Electro-Optic Effect in $La_3Ga_5SiO_{14}$ Crystals

N. Ftomyn[1,*], Y. Shopa[2], I. Sudak[1]

[1]*Ivan Franko National University of Lviv, 8 Kyrylo and Mefodiy Street, 79005 Lviv, Ukraine*
[2]*Cardinal Stefan Wyszyński University in Warsaw ul. Dewajtis 5, 01-815 Warszawa, Poland*
* nazar.ftomyn@gmail.com

The $La_3Ga_5SiO_{14}$ (LGS) crystals remain promising for practical use in quantum electronics, high temperature sensors etc. These materials have the space group symmetry *P*321. Furthermore, the investigations of the optical properties described by third-rank tensors are very interesting for this system. There is linear electro-optic (Pockels) effect or e.g., electrogyration phenomenon. Because of the LGS crystals have a point group symmetry 32 (as well as α-quartz) only linear electro-optic r_{11} and r_{41} coefficients of the $\hat{\mathbf{r}}$ tensor are non zero for these materials[1].

The aim of our work is to determine the electro-optic coefficients of LGS crystals using the computation method based on so-called DES (DES – dipole electron shifting) model [2, 3]. According to DES the $\hat{\mathbf{r}}$ tensor is calculated using equations [3]:

$$a_{ij}\left(E_k^{Ext.}\right) - a_{ij}\left(0\right) = r_{ijk}E_k^{Ext.}. \qquad (1)$$

were $\mathbf{E}^{Ext.}$ – external electric field which shifts the atomic nuclei by the distance proportional to the polarizability of atoms, a_{ij} – polarization tensor ($a_{ij} = \varepsilon_{ij}^{-1}$). In addition, the effective relative dielectric constant ε' is still needed for calculations.

On the other hand, the electro-optic effect is experimentally investigated in langasite single crystal. The experiment is performed with the aid of a computer-controlled laser polarimeter. The optical scheme of the polarimeter includes a minimal quantity of optical components: a polarizer, specimen and analyzer, thus forming the PSA system. The method involves the measuring the optical transmission of the PSA system.

Finally, the computations based on dipole electron shifting model applied to determining the electro-optic tensor components of langasite crystals will allow to compare the experimental results with theoretical calculations.

[1] O.G. Vlokh, *Spatial dispersion phenomena in parametric crystal optics*, Vyshcha Shkola, Lviv, 1984, p. 156.
[2] V. Devarajan, A. Glazer, Theory and computation of optical rotatory power in inorganic crystals, *Acta. Cryst.* **A 42** (1986) 560-569.
[3] W. Kaminsky, Experimental and phenomenological aspects of circular birefringence and related properties in transparent, *Rep. Prog. Phys.* **63** (2000) 1575-1640.

Electric Transport Properties of Sn-Dopped Bi_2Te_2Se Topological Insulators

P. Iwanowski[1], A. Hruban[1], K. Piotrowski[1], R. Diduszko[1,2]

[1]*Institute of Physics, Polish Academy of Sciences, Al. Lotników 32/46, 02-668 Warsaw, Poland*
[2]*Tele and Radio Research Institute, Ratuszowa 11, 03-450 Warsaw, Poland*

Topological insulators are new states of quantum matter. In these materials surface states resides in the bulk insulating gap and they are protected by time-reversal symmetry. Bi_2Te_2Se are topological insulators with resistivities twice order of magnitude higher than in Bi_2Te_3 or Bi_2Se_3.

In this work we described influence of Sn-dopping on transport properties. Bi_2Te_2Se and $Bi_{1.99}Sn_{0.01}Te_2Se$ were grown using modified Bridgman method. The temperature dependent of bulk resistivities, carrier densities and Hall resistivity for both crystals will be compared and discussed.

Figure 1. As-grown Bi_2Te_2Se and $Bi_{1.99}Sn_{0.01}Te_2Se$ single crystals

Application of Combined Molten Salts for Tailoring Crystal Growth of Indium Phosphates

D.V. Kyselov, K.V. Terebilenko, M.S. Slobodyanik

Taras Shevchenko National University of Kyiv, Chemistry Department, Ukraine

The quest for novel oxide materials containing tetrahedral groups has brought forward manifold promising materials, including indium containing oxides [1-2]. Among their various representatives, the ternary In-P-O and quaternary M-In-P-O compounds (M – alkaline metal) excel through their versatile chemical and physical properties [3]. In particular, $K_3In(PO_4)_2$, $K_3In_3(PO_4)_4$ and $KInP_2O_7$ have attracted considerable research attention due to its excellent performance as luminescence hosts for rare-earth metals doping with enhanced emitting under visible light irradiation [4]. Whereas the structural peculiarities of indium phosphates are known for most of them, structural substitution and solid solution formation that can influence band structure, charge-transfer and the morphological properties of the respective material are rarely studied. Herein, the unified method for indium phosphates preparation has been applied for tailoring crystal growth of a number of M-In-P-O crystalline compounds in a pure and doped with europium phases.

As a key reagent molybdate component has been used as a reaction media and a phosphate one as a direct reagent. Indium oxide or indium fluoride has been applied as a source of indium. The crystallization trends has been explored for K –In – P – Mo – O molten system in details. Generally, the melt with a certain composition has been cooled to reach a solidified mixture, whereas crystalline product has been leached out by washing in water. The crystals obtained in this way have been studied by IR spectroscopy and X-Ray powder diffraction. The crystal structure of $KInP_2O_7$ has been verified by single crystal X-Ray diffraction. The crystallization trends for the compounds mentioned above and their mixtures have been explored depending on the K/Mo and K/P ratios in the initial melt. As it was shown, there is a relationship between the indium polyhedral condensation and the basic properties of the melt applied. Thus, the most basic melt containing K_2MoO_4 and $K_4P_2O_7$ after cooling leads to the full separation of InO_n polyhedral in the framework of $K_3In(PO_4)_2$, while more acidic ones give a corner-sharing groups In_3O_n in case of $K_3In_3(PO_4)_4$. The complicity of molybdate component role is also followed by the change of the crystallization area of different phosphates and the presence of phosphates, which are not common for pure M-In-P-O melts.

Consequently, addition of molybdate salts through MoO_3 and K_2MoO_4 is a challenging multi-parameter process and leaves room for further investigations that are now in progress. The present systematic study demonstrates that the combination of the inert and direct salts is a promising approach towards the construction of new compounds with different crystalline blocks aggregation.

[1] E. Fabbri, A. Habereder, K. Waltar, R. Kötz and T. J. Schmidt, *Catal. Sci. Technol.* **4** (2014) 3800-3821.
[2] K.-H. Lii, *J. Chem. Soc., Dalton Trans.* (1996) 815-818 .
[3] X.-H. Lin, Y. Wang, Y.-H. Su, C.-S. Yang, *J. Chin. Chem. Soc.* **54** (2007) 1123-1128.
[4] O. Gomenyuk, S. Nedilko, N. Slobodyanyk, N. Stoos, V. Scherbatskiy, *Ukr. J. Phys.* **50** (2005) 1168-1174.

Criterion for Determining the Dipole-Center

N.Yu. Pavlova[1], V.Ya. Degoda[2], M. Alizadeh[2], B.V. Kozhushko[3]

[1]*National Pedagogical Dragomanov University, 9 Pyrogova Str., 01601 Kyiv, Ukraine*
[2]*Taras Shevchenko National University of Kyiv, 64 Volodymyrs'ka Str., 01601 Kyiv, Ukraine*
[3]*Institute of Physics of NAS of Ukraine, 46 Nauky Ave., 03028 Kyiv, Ukraine*

One of the dominant X-ray spectra in the ZnSe crystals is non-elementary broad band luminescence with maxima at 630 nm. In the light-induced centers, which cause the emission band realized two simultaneous recombination mechanism: electronic (recombination at the heart of a free electron) and hole (recombination of free holes) [1]. This luminescence (630 nm) can be due either to the two centers with different recombination mechanisms that have almost the same emission band or due to one-stop centers (Dipole-center), which are implemented at the same time both of the recombination mechanism. Dipole-center can locate the first in their environment (on the ligands) as an electron and a hole. The Luminescence was observed only after the localization on it of free charge carriers of the opposite. At the same time, there is an intermediate exciton-impurity the excited state of the centre. Further, there is a spontaneous transition to the ground state with the emission of a photon of light.

In the two kinetic models of crystals considered: different recombination centers and Dipole-center. Also, in both models include one of the recombination luminescence center with electronic recombination mechanism (in ZnSe crystals it causes the emission band with a maximum emission at 970 nm) and deep traps for electrons. Consideration of these two models is necessary to obtain for experimental criteria by which it can be concluded that causes emission band of 630 nm, Dipole-center, or two different center. For this model have to analyze and obtain both characteristics for comparison, i.e. to make a clear choice between one- and two-center model that describes the mechanisms of recombination band of 630 nm.

The results of the analysis of these two models were obtained crystalline phosphor solutions for all luminescence parameters for the stationary states. It was found that the dependence of luminescence intensity of the excitation does not allow the choice of the appropriate model.But, if you change the excitation temperature varies the number of deep traps by changing the probability of thermal delocalization of charge carriers. As a result, a change in temperature changes the ratio of the intensities of the different bands (J_{630}^{-}/J_{630}^{+}, J_{630}^{-}/J_{970}^{-}, J_{630}^{+}/J_{970}^{-}). Moreover, these changes the intensity ratio of the bands happen in different ways for these models of crystal. As a result, we obtain a criterion for determining which model adequately describes the luminescence centers in crystals of ZnSe.

[1] V.Ya. Degoda, N.Yu. Pavlova, G.P. Podust, A.O. Sofiienko, Spectral structure of the X-ray stimulated phosphorescence of monocrystalline ZnSe, *Physica B: Condensed Matter* **465** (2015) 1-6.

Optical Properties of ZnCrO Layer Obtained by PVD Method

P. Potera[1], I. Virt[2,1]

[1]*Faculty of Mathematics and Natural Sciences University of Rzeszow, Rzeszow, Poland*
[2]*Drogobych State Pedagogical University, Drogobych, Ukraine*

ZnO is example of wide band gap semiconductors which have been used for light emitting diodes and laser diodes. ZnO is mostly chosen for its better excitonic properties compared to GaN, with an excitonic binding energy of 60 meV at room temperature [1].

Doping non-magnetic semiconductors with transition metals (e.g., Ti, V, Cr, Mn, Fe, Co, Ni and Cu) lead to the production of diluted magnetic semiconductors (DMS) which are regarded as important materials for spintronic and photonic devices.

However, most DMS have low Curie temperature, which limits their practical applications. The Curie temperature of p-type DMSs based on wide-band gap semiconductors, i.e., ZnO should be increased above room temperature with stable ferromagnetism [2].

In this work we are study the absorption spectra of ZnCrO thin films obtained by PVD method in sapphire substrate at room temperature from $Zn_{0,96}Cr_{0,04}O$ target. The influence of annealing in air after growth on the transmission spectra as well as band-gap energy will be discussed.

[1] K.-H. Bang, D.-K. Hwang, and J.-M. Myoung, *App. Surf. Sci.* **207** (2003) 359.
[2] X. Pang, J. Zhang, K. Gao, A.A. Volinsky, *Materials Letters* **65** (2011) 2728–2730.

Conductivity Effects in Bi_2TeO_5 Single Crystals

L.Ya. Sadovskaya, K.V. Agarkov

Oles Honchar Dnipropetrovsk National University, 49010 Dnipro, Ukraine

The tellurites of metals have attracted the attention as useful materials for acousto-optical devices. The physical properties of the compositions $Bi_{1-x}TeO_{(3+x)/2}$, where $0{,}33 \le x \le 0{,}50$, were studied and improper ferroelectric behavior of these compositions were revealed [1,2]. Bismuth tellurite (Bi_2TeO_5) is one of the most stable forms among the numerous compositions identified in the phase diagram of the Bi_2O_3 – TeO_2 system. Bi_2TeO_5 crystallizes in an orthorhombic structure with space group Abm2 and have layer type structure along c-axis. The nonlinear crystal of bismuth tellurite became an interesting material when its photorefractive properties were discovered [3].

In this report, we present the results of investigations of the electrical conductivity and dielectric parameters for the Bi_2TeO_5 single crystals over wide range of temperatures (20 – 400 °C) and frequencies ($2\cdot10^2$ – $5\cdot10^7$ Hz). The dielectric parameters and ac–conductivity of Bi_2TeO_5 have been measured along three crystallographic directions corresponding to the rhombic lattice axes. dc-conductivity ($\sigma_=$) has been measured along c-axis only.

The features of the dielectric parameters as a function of the temperature and frequency are discussed. It was found that the frequency dependence of $\sigma_\sim$ can be described by relation of $\sigma_\sim \sim w^s$, where s depends from frequency and changes from 0,4 to 2. There are relaxation maxima of the $\sigma_\sim$ in temperature dependence.

The dc–conductivity increases with the temperature increase up to 150 °C with activation energy $\Delta E \approx 0{,}2$ eV and $\sigma_=$ increases exponentially at higher temperature with $\Delta E \approx 1{,}0$ – 1,1 eV.

Voltage-current curves of the Bi_2TeO_5 single crystals are typical for the space charge limited currents [4]. From these characteristics, the effective mobility of carriers and concentration of the equilibrium-trapped charge at different temperatures have been determined. Low values of the mobility (10^{-7} $cm^2/V\cdot s$ at 100 °C) obtained for the carriers and its exponential increase with temperature are characteristics for hopping conductivity model.

The conductivity stimulation effect was observed in Bi_2TeO_5 single crystals at the fields corresponding to nonlinear ranges of voltage-current curves. If it is assumed the hopping conductivity model for Bi_2TeO_5 single crystals then the conductivity stimulation can be explained by increase of carrier mobility due to the shift of the Fermi level to range with higher density of states. The latter is the result of the occupation of the state levels by injected carriers.

[1] V.A. Dolgikh, L.A. Demina, S.Yu. Stefanovich, B.A. Popovkin, O.I. Vorobeva and S.I. Kucheryavenko, *Inorg. Mater*. **21** (1985) 399.
[2] K.V. Domoratsky, E.F. Dudnik, V.F. Katkov, L.Ya. Sadovskaya, Condensed Matter Physics **2** (1999) 591.
[3] I. Foldvari, H. Liu, C. Powell and A. Peter, *J. Appl. Phys.* **71** (1992) 5465.
[4] M.A. Lampert and P. Mark, *Current injection in solids*, Academic Press, New York and London, 1970.

Size Effect Caused by Incommensurate Superstructure in $[N(CH_3)_4]_2Zn_{0,58}Cu_{0,42}Cl_4$ Crystals

S. Sveleba, I. Karpa, I. Katerynchuk, I. Kunyo

Ivan Franko National University of Lviv, 107 Tarnavsky Str., UA–79017 Lviv, Ukraine
incomlviv@gmail.com

Surfaces in the crystal physics is considered as a two-dimensional defect, in particular, as a special state of a crystal where the crystallography and the energy structure differs from those in a bulk crystal.

A distorted surface structure cannot jump to the ordered structure of the bulk crystal, so there is some transition zone. Therefore the surface is considered as the surface phase, which physicochemical properties differ from the bulk part of the crystal. Such surface makes influence on the lattice and electronic subsystem of the crystal. It changes spectra of elementary excitations that are sensitive to changes in symmetry and boundary conditions.

It is suggested that the thickness of the surface defect layer in the direction of the incommensurate modulation axis for crystals with incommensurate phase is about a wavelength of incommensurate modulation. Superstructure period increases with decreasing temperature of the crystal increasing the impact of surface energy on the crystal volume.

In this work, an influence of the surface layer on the crystal volume when the wavelength of the incommensurate modulation increases was studied.

The period modulated superstructure in $[N(CH_3)_4]_2MeCl_4$ (Me=Cu, Co, Zn, Mn) crystals is about 100 unit cells, namely 1500-800 angstroms. Hence the size effect related to the size of the crystal of proportion to the wavelength of incommensurate modulation in micron diapason be expected, crystal size is commensurate to the incommensurate wavelength.

Based on the obtained temperature dependences of optical birefringence of $[N(CH_3)_4]_2Zn_{0,58}Cu_{0,42}Cl_4$ crystal the shift of phase transition temperature parent-incommensurate phase (T_i) toward low temperatures is observed, the thickness of the crystal measured along the axis of incommensurate modulation is $d_c = 35 \div 40$ microns. Under the same conditions a similar bias value phase transition temperature incommensurate-commensurate phase of long-seen in the $d_c = 75 \div 80$ microns, and the phase transition to the incommensurate-commensurate ferroelectric phase (T_c) at $d_c = 95 \div 100$ microns.

So increasing the thicknesses of the crystal in which there is a size effect caused by increasing wavelength incommensurate modulation. Note, the incommensurate modulation wavelength increasing with crystal temperature growing from T_i to T_c.

Nature of Intrinsic Luminescence of the Undoped Borate Glasses

I.I. Kindrat[1], B.V. Padlyak[1,2], S. Mahlik[3], B. Kukliński[3], R. Lisiecki[4]

[1] *University of Zielona Góra, Institute of Physics, Division of Spectroscopy of Functional Materials, 4a Szafrana Str., 65-516 Zielona Góra, Poland*
[2] *Vlokh Institute of Physical Optics, Sector of Spectroscopy, 23 Dragomanov Str., 79-005 Lviv, Ukraine*
[3] *University of Gdańsk, Institute of Experimental Physics, Condensed Matter Spectroscopy Division, 57 Wita Stwosza Str., 80-952 Gdańsk, Poland*
[4] *Institute of Low Temperature and Structure Research Polish Academy of Sciences, Division of Optical Spectroscopy, 2 Okólna Str., 50-422 Wrocław, Poland*

The intrinsic luminescence of a series of the undoped borate glasses has been investigated by optical spectroscopy (absorption, photoluminescence, decay kinetics, time-resolved luminescence) as well as electron paramagnetic resonance (EPR) and thermally stimulated luminescence (TSL). The undoped nominally-pure borate glasses of high chemical purity and optical quality with $Li_2B_4O_7$ (Li_2O–$2B_2O_3$), $LiKB_4O_7$ ($0.5Li_2O$–$0.5K_2O$–$2B_2O_3$), CaB_4O_7 (CaO–$2B_2O_3$), and $LiCaBO_3$ ($0.5Li_2O$–CaO–$0.5B_2O_3$) compositions were obtained from corresponding polycrystalline compounds in the air atmosphere using standard glass synthesis technology described in [1].

The optical absorption spectra show that investigated undoped borate glasses are high transparent in the 330 – 2500 nm spectral region. Three types of the intrinsic luminescence have been observed in the investigated borate glasses at room temperature under UV excitation. Possible nature and mechanisms of the intrinsic luminescence are considered and discussed.

The investigated borate glasses upon excitation at 310 – 340 nm (3.6 – 4 eV) exhibit luminescence band with maximum in the 360 – 400 nm (3.1 – 3.4 eV) spectral range. The position and shape of excitation band well correlates with the edge of fundamental absorption. The luminescence decay curves are satisfactory described in the framework of single exponential approximation with lifetimes about 30 ns. Basing on obtained results it is concluded that first type of intrinsic luminescence is related to band-to-band electron-hole recombination process.

The intrinsic luminescence of second type is exited about 380 nm (3.2 eV) and emits about 440 nm (2.8 eV). The energy of excitation bands shows very good correlation with optical band gaps. The luminescence lifetimes, which approximately equal 1 and 4 ns were obtained in the framework of two-exponential approximation. Basing on experimental results, one can propose that the second type of intrinsic luminescence belongs to the luminescence of excitons.

The undoped borate glasses upon excitation about 260 – 270 nm (4.6 – 4.7 eV) exhibit broadband intrinsic luminescence with extended maximum in the 470 – 490 nm (2.5 – 2.6 eV) spectral range. The luminescence decay curve of this band is strongly non-exponential and can be satisfactory described by decay kinetics of the hyperbolic type. The average lifetime value equals about 130 μs. The EPR spectra and TSL glow curves of the *X* - and γ - irradiated undoped borate glasses show presence of the O^- hole centres, which are stable at room temperature and characterised by trap depth about 1.0 eV. The third type of intrinsic luminescence is caused by recombination of electrons with O^- hole centres, which are created upon the UV excitation. In this case, electrons before recombination were trapped and re-trapped by shallow electronic traps at room temperature that result in luminescence kinetics of the second order.

[1] B.V. Padlyak, S.I. Mudry, Y.O. Kulyk, A. Drzewiecki, V.T. Adamiv, Y.V. Burak, I.M. Teslyuk, *Mater. Sci. Poland* **30** (2012) 264–273.

Defect-Related Effects in the Modified Chalcogenide Glasses Caused by Gamma-Irradiation

H. Klym[1], O. Shpotyuk[2,3], A. Ingram[4], L. Calvez[5]

[1]*Lviv Polytechnic National University, 12 Bandera Str., 79013 Lviv, Ukraine*
[2]*Vlokh Institute of Physical Optics, 23 Dragomanov Str., 79005 Lviv, Ukraine*
[3]*Jan Dlugosz University, 13/15 al. Armii Krajowej, Czestochowa 42201, Poland*
[4]*Opole University of Technology, 75 Ozimska Str., Opole 45370, Poland*
[5]*Equipe Verres et Céramiques, UMR-CNRS 6226, Institute des Sciences chimiques de Rennes, Université de Rennes 1, 35042 Rennes Cedex, France*

Ge-Ga-S/Se chalcogenide glasses have shown many advantages for potential applications in optical modulators or frequency converters, as efficient laser host materials and for fiber-optical amplifiers in the IR spectral region. Their structural and electronic modification by thermal annealing processes and irradiation results in changes of their functional properties [1].

The process of crystallization in $80GeSe_2$-$20Ga_2Se_3$ glasses influences their optical transmission spectra. Non-annealed glassy samples show maximum optical transmittance at the level of 65 %. Annealing at 380 °C decreases this transmittance and shifts optical transmission edge towards long-wave side. The appearance of growing of Ga_2Se_3 and $GeGa_4Se_8$ nanocrystals inside the glassy matrix induces light scattering at shorter wavelengths. Generally, this phenomenon shows the presence of large crystals that deteriorate optical transparency of the material rapidly, leading progressively to its complete opacity in the IR range.

The influence of gamma irradiation on optical properties of Ge-Ga-S/Se glasses was investigated using Co^{60} source. The dose of gamma-irradiation was near 0.8 MGy and the total duration of this procedure was 2 months [2].

The slight long-wavelength shift of the fundamental optical absorption edge and the decrease in transmission are observed in $80GeS_2$-$20Ga_2S_3$ glasses after irradiation. This indicates possible formation of additional defects in $80GeS_2$-$20Ga_2S_3$ glasses and their observed darkening. After irradiation, nanovoids with different size are created as intrinsic structural defects associated with topologically uncoordinated negative-charged centers. These defect centers form additional energy levels both near the bottom of the conduction band and in the vicinity of the valence band, as well as additional intrinsic electric fields. The mechanism of irradiation-induced darkening of $80GeS_2$-$20Ga_2S_3$ glasses is connected with oxidation processes most probably related with the appearance of GeS_2 phase at the surface of the glasses.

Gamma irradiation practically does not alter the optical transmission spectra in the modified $80GeSe_2$-$20Ga_2Se_3$ glasses. The position of optical transmission edge and the spectra profiles in the saturation region coincide before and after irradiation. Such radiation stability of $80GeSe_2$-$20Ga_2Se_3$ glasses allows their use as radiation-stable optical sensors in the visible and IR spectral region.

[1] P. Masselin, D. Le Coq, L. Calvez, E. Petracovschi, E. Lepine, E. Bychkov, X. Zhang, CsCl effect on the optical properties of the $80GeS_2$–$20Ga_2S_3$ base glass, *Appl. Phys. A* **106** (2012) 697-702.

[2] H. Klym, A. Ingram, O. Shpotyuk, O. Hotra, A.I. Popov, Positron trapping defects in free-volume investigation of Ge-Ga-S-CsCl glasses, *Radiation Measurements* **90** (2016) 117-121.

Excitonic Quasimolecules in Nanoheterosystems Containing Semiconductor and Dielectric Quantum Dots: Theory

Sergey I. Pokutnyi*

Chuiko Institute of Surface Chemistry, National Academy of Sciences of Ukraine,
*17 General Naumov Str., 03164 Kyiv, Ukraine, * pokutnyi_sergey@inbox.ru*

The Ge/Si heterostructures promising to create new elements silicon infrared optoelectronics are self-assembled structures with Ge/Si nanoislands. Ge/Si heterostructures with quantum dots (QDs) of Ge are heterostructures II type. In this nanosystem the lowest electronic level is in matrix, and the lowest hole level is within volume of QD. A large shift of the valence band (610 meV) generates the localization of holes in the volume of QD. A significant shift of the conduction band (about 340 meV) is a potential barrier for electrons. The electrons move in the matrix and do not penetrate in the volume of QD [1].

In [2] we show that the biexciton formation in a nanoheterosystems made up of aluminum oxide QDS synthesized in a dielectric matrix is of threshold character and can occur in a nanosystem where the distance D between the surfaces of QD is given by the condition $D_c^{(1)} \leq D \leq D_c^{(2)}$. We also demonstrate that in such nanoheterosystems acting as "exciton molecules" (or biexciton) are the quantum dots of aluminum oxide with excitons localizing over their surfaces. The position of the biexciton state energy band is shown to depend both on the mean radius of quantum dots, and the distance between their surfaces, which enables one to purposefully control it by varying these parameters of the nanoheterosystems. It is established that at constant concentrations of biexcitons at temperatures T below a certain critical temperature T_c due to the radiative annihilation of one of the excitons forming a biexciton one can expect a new spectral band of luminescence shifted relative to the exciton band by the biexciton binding energy E_B. This new luminescence band disappears at temperatures above T_c. At a constant temperature $T < Tc$ the growth of exciton concentration brings about weakening of the exciton band and strengthening of the biexciton band of luminescence. As follows form the results of the variational calculations, the major contribution to the biexciton binding energy is from the energy of exchange interaction of electrons and holes, which by far surpasses that from their Coulomb interaction (i.e. the ratio ≤ 0.11).

A review devoted to the theory of excitonic quasimolecules (formed of spatially separated electrons and holes) in a nanosystems that consists of semiconductor and dielectric QDS synthesized in a dielectric (or semiconductor) matrix [1, 2]. It is shown that exciton quasimolecule formation is of the threshold character and possible in nanosystem, in with the spacing between the QDs surfaces is larger than a certain critical spacing. It was found that the binding energy of singlet ground state of exciton quasimolecule, consisting of two semiconductor QDs is a significant large values, larger than the binding energy of the biexciton in a semiconductor single crystal almost two orders of magnitude [1, 2]. Such an effect opens up the possibility of using the exciton quasimolecules as active medium in nanolasers emitting in the infrared region and operating on exciton transitions at room temperatures in the elementary base of quantum nanocomputers. The presented results demonstrate the fundamental possibility of creating novel quasiatomic nanosystems in the form of exciton quasimolecules, including natural systems with new physical characteristics. On their basis it is possible to construct new nanosystems or quasicrystals in which control of the symmetry and lattice constant will make it possible to realize unique physical effects and phenomena and to create new principles in materials behavior.

[1] S.I. Pokutnyi, *Semiconductors* **47** (2013) 1626; [2] S.I. Pokutnyi, *J. Nanophoton.* **10** (2016) 036008.

Comparative Studies of Crystal Field Effects in $YbCoGaO_4$ and $YbMgGaO_4$ Single Crystals

I. Radelytskyi[1], T. Zajarniuk[1], A. Szewczyk[1], M. Gutowska[1], H.A. Dabkowska[2], J. Fink-Finowicki[1], P. Aleshkevych[1], Ya. Zhydachevskyy[1], V. Tsiumra[1], H. Szymczak[1]

[1]*Institute of Physics PAS, al.Lotnikow 32/46, 02-668 Warsaw, Poland*
[2]*The Department of Physics and Astronomy, McMaster University, Hamilton, Ontario, Canada*

Spin geometrically frustrated systems attract a lot of attention because of specific magnetic properties like spin glass and spin liquid materials. The $YbMgGaO_4$ single crystal is a good quantum spin liquid candidate with two-dimentional and special isotropic magnetic triangular-lattice [1, 2]. In contrast the $YbCoGaO_4$ single crystal presents a unique three-dimensional Ising-like spin glass behavior. These single crystals were grown using the optical floating zone image furnace technique [3]. In this paper the properties of the ground-state Kramers doublet of Yb^{3+} have been investigated to assess their influence on the electronic structure of both crystal. We plan to solve following problems:

1. Differences in mechanisms responsible for randomness in both crystals. These differences should be seen in low temperature linewidths of optical absorption transitions $^2F_{7/2} \rightarrow {}^2F_{5/2}$ [4].

2. Differences in g-factors in the ground-state Kramers doublet of Yb^{3+} in both crystals [5,6].

Acknowledgement. This study was partially supported by the National Center for Research and Development, research project no. PBS2/A5/36/2013.

[1] Joseph A. M. Paddison, Marcus Daum, Zhiling Dun, Georg Ehlers, Yaohua Liu, Matthew B. Stone, Haidong Zhou and Martin Mourigal, *Nature Physics* **13** (2017) 117.
[2] Yuesheng Li, Haijun Liao, Zhen Zhang, Shiyan Li, Feng Jin, Langsheng Ling, Lei Zhang, Youming Zou, Li Pi, Zhaorong Yang, Junfeng Wang, Zhonghua Wu & Qingming Zhang, *Scientific Reports* **1** (2015).
[3] H. A. Dabkowska, B. D. Gaulin, in International School on Crystal Growth of Technologically Important Electronic Materials, Ed. K. Byrappa, Allied Publishers, 2003.
[4] Yuesheng Li, Devashibhai Adroja, Robert I. Bewley, David Voneshen, Alexander A. Tsirlin, Philipp Gegenwart, and Qingming Zhang, *Phys. Rev. Lett.* **118** (2017) 107202.
[5] Y. Xu, J. Zhang, Y. S. Li, Y. J. Yu, X. C. Hong, Q. M. Zhang, and S. Y. Li, *Phys. Rev. Lett.* **117** (2016) 267202.
[6] I. Radelytskyi, PhD thesis (2016).

Eight Channel Optical Add Drop Multiplexer Based on Ring Resonator Using LNOI Channel Waveguides

Harsh Kumar[1], Vijay Janyani[1], Buryy Oleh[2], Ubizskii Serhij[2], Sugak Dmytro[2], Ghanshyam Singh[1]

[1]*Department of Electronics and Communication Engg. MNIT Jaipur, India*
[2]*Inst. of Tele. Radioelectronics and Electronic Engg., Lviv Polytechnic National University, Lviv, Ukraine*

In this paper we report on an eight channel optical add drop multiplexer based on ring resonator using Lithium Niobate on Insulator (LNOI) channel waveguides. The PIC of 8-channel OADM is made of eight cascaded ring resonators and the free spectral range (FSR) of each is 6.4 nm. The OADM drops every eighth channel of the DWDM system with the channel spacing of 100 GHz (0.8 nm) in C-band. The insertion loss at the drop port is maximum 1.2 dB and the Q-factor is 1636. The data rate is 10 Gbps and hence this pic can be used in DWDM-GPON network to enhance the performance.

The OADM is designed and simulated using mode-solver tool and the PIC is designed using s-parameters and simulated using Interconnect tool by Lumerical. The block diagram of PIC is shown in figure, it has input port, through port and 8 add and drop ports. It can be used as Multiplexer as well as Demultiplexer in 8 channel DWDM systems.

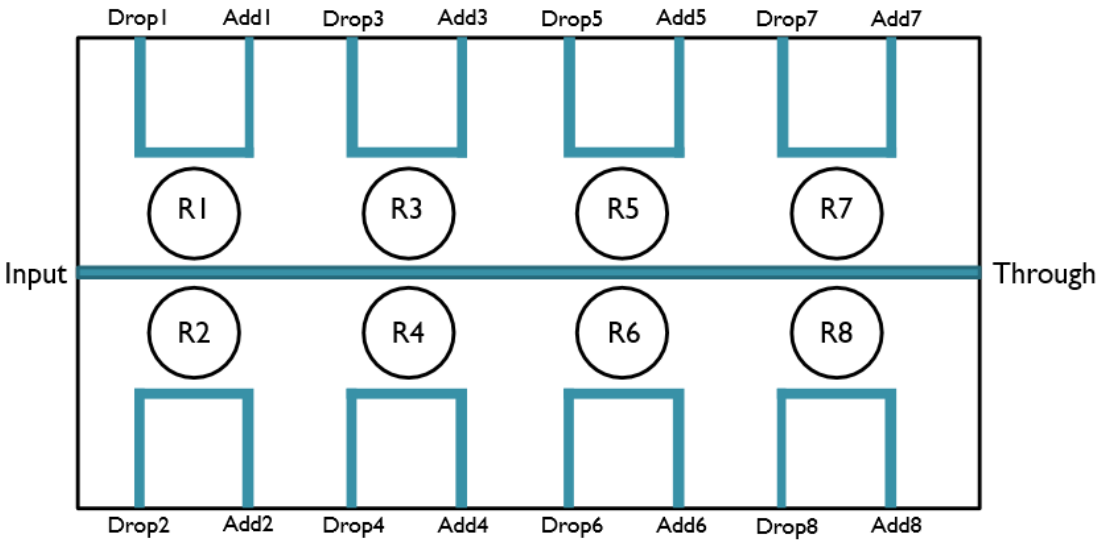

Figure: The block diagram of 8 channel OADM

Acknowledgement. The authors are grateful to India–Ukraine inter-governmental science & technology cooperation programme between the MNIT Jaipur (India) and the Lviv National Polytechnique Institute, Lviv (Ukraine) for technical support. Project sanction no: INT/RUS/UKR/P-15/2015.

[1] Wu, Danning, et al., Four-channel optical add-drop multiplexer based on dual racetrack micro-ring resonators, *Optics Communications* **354** (2015) 386-391.

[2] Kumar, Harsh, et al., Ring Resonator based Optical Add Drop Multiplexer Using Lithium Niobate on Insulator Channel Waveguides, *Proc. of International Conference on Fibre Optics and Photonics*, Optical Society of America, 2016.

[3] Godbole, Abhishek, et al., Microring resonator based all optical XOR and XNOR logic gates, *Proc. of International Conference on Computational Techniques in Information and Communication Technologies,* ICCTICT, IEEE, 2016.

Highly Nonlinear Multi-Material Chalcogenide Spiral Photonic Crystal Fiber for Supercontinuum Generation

Shruti Kalra[1,*], Sandeep Vyas[2], ManishTiwari[3], Buryy Oleg[4], Ghanshyam Singh[5]

[1]*Dept. of ECE, Jaipur Egineering College & Research Centre, Jaipur, India*
[3]*Dept. of ECE, Manipal University, Jaipur, India*
[4]*Inst. of Tele. Radioelectronics and Electronic Engg., Lviv Polytechnic National University, Ukraine*
[2,5]*Dept. of ECE, Malaviya National Institute of Technology, Jaipur, India*
* shrutikalra.ece@jecrc.ac.in

In this paper, we have investigated a highly nonlinear multi-material chalcogenide photonic crystal fiber. The photonic crystal fiber is designed with borosilicate and As_2S_3 glass, where borosilicate is doped in a spiral shape in the cladding. The designed fiber was investigated carefully for effective refractive index, effective mode area, and dispersion and nonlinearity coefficients. The estimated parameters are satisfactory and suitable. This motivates the idea to further investigate the design for broadband supercontinuum generation.

Photonic crystal fibers have attracted attention of researchers since their inception due to the higher design flexibility and their enormous applications in field of communication, sensing and biomedical science. Photonic crystal fibers commonly also known as microstructured optical fibers and holey fibers are special class of photonic crystals with core surrounded by a micro-structure of air-hole arrangement in a lattice forming the cladding.The geometry of the photonic crystal fibers offers greater degree of freedom to tailor its optical properties. The advancement in fabrication technology it is now possible to fabricate the photonic crystal fibers with different materials other than only silica.

Supercontinuumcan be simply defined as a pulse broadening. It can be well explained as nonlinear phenomena where an intense ultra-short (narrow) laser pulse undergoes a spectral broadening during its propagation in nonlinear medium results in a super-wide continuous optical spectrum. The parameters which greatly affect the generation of supercontinuum include chromatic dispersion, peak power of the pulse, pump wavelength, pulse duration and length of the of nonlinear fiber.

In the paper presented here a multi-material photonic crystal fiber with hexagonal lattice arrangement of air-hole is investigated for its characteristics like effective refractive index, effective area, dispersion and nonlinear coefficients. The range for flat dispersion of the proposed photonic crystal fiber design is from 1.8 µm to 8 µm. The nonlinear coefficient (γ), effective area (A_{eff}) and dispersion at the wavelength (λ) 2.8 µm are 1052 W^{-1} km^{-1}, 8.53242 μm^2 and 4.903392 ps/km/nm, respectively for the design of the fiber. The results of the investigation are satisfactory and it can be further investigated for broadband supercontinuum generation.

Photoluminescence and Thermoluminescence of the Oxygen-Deficient YAG, YAP and YAM Phosphors

Ya. Zhydachevskyy[1,2], I. Kamińska[1], M. Glowacki[1], A. Twardak[3], S. Ubizskii[2], P. Bilski[3], M. Berkowski[1], K. Fronc[1], D. Elbaum[1], A. Suchocki[1,4]

[1] *Institute of Physics, Polish Academy of Sciences, Warsaw, Poland*
[2] *Lviv Polytechnic National University, Lviv, Ukraine*
[3] *Institute of Nuclear Physics, Polish Academy of Sciences, Kraków, Poland*
[4] *Institute of Physics, University of Bydgoszcz, Bydgoszcz, Poland*

Application potential of the carbon-doped $Y_3Al_5O_{12}$ (YAG:C) for radiation dosimetry using the thermoluminescence (TL) or the optically stimulated luminescence (OSL) techniques has been shown recently [1]. In particular, the OSL sensitivity of the non-optimized YAG:C to β-radiation ($^{90}Sr/^{90}Y$, 10 mGy) was found to be about 0.1 of the commercial α-Al_2O_3:C.

The present work was aimed to check the photoluminescent and thermoluminescent properties of YAG:C phosphor and to compare them with other yttrium-aluminum oxides of $YAlO_3$ (YAP) and $Y_4Al_2O_9$ (YAM).

For this purpose, the nominally pure compounds of YAG, YAP and YAM in the form of nanopowders have been synthesized by the solution combustion method using urea as a fuel, as described in [2]. The solid ceramic samples have been prepared from the obtained nanopowders at 1000-1500 °C in strongly reducing conditions (pure N_2 gas atmosphere + graphite equipment). Besides, doping with carbon (from 1 to 5 wt.%) was used. Similar ceramic samples, however without carbon doping and prepared in oxidizing conditions (in air), were studied for comparison as well. The obtained powder and ceramic materials were controlled by the X-ray powder diffraction (XRD) and scanning electron microscopy (SEM) techniques.

The work presents results on photoluminescence, photoluminescence excitation, TL and OSL properties of the materials after exposure to UV- (250-400 nm) or ionizing γ- (^{60}Co) and β- ($^{90}Sr/^{90}Y$) radiations. The observed luminescent properties of the materials are related to the F-type centers created on the basis of oxygen vacancies, antisite (Y_{Al}) defects and uncontrolled Tb^{3+} impurity ions.

Acknowledgements. The work was supported by the NATO Science for Peace and Security Program (Project G4649) and by the European Regional Development Fund (Innovative Economy grant POIG.01.01.02-00-108/09).

[1] M.S. Kulkarni et al., Carbon doped yttrium aluminum garnet (YAG:C) – A new phosphor for radiation dosimetry, *Radiat. Meas.* **43** (2008) 492-496.

[2] Ya. Zhydachevskii et al., Thermoluminescent properties of Mn-doped $YAlO_3$ synthesized by the solution combustion method, *Opt. Mater.* **37** (2014) 125-131.

Effect of Lutetium Co-Doping on the Main Dosimetric Peak of YAP:Mn^{2+} TL Detectors

Ya. Zhydachevskyy[1,2], M. Glowacki[1], N. Martynyuk[2], S. Ubizskii[2], M. Berkowski[1], A. Suchocki[1,3]

[1] *Institute of Physics, Polish Academy of Sciences, Warsaw, Poland*
[2] *Lviv Polytechnic National University, Lviv, Ukraine*
[3] *Institute of Physics, University of Bydgoszcz, Bydgoszcz, Poland*

Application potential of Mn^{2+}-doped $YAlO_3$ (YAP) for thermoluminescent (TL) dosimetry of ionizing radiation has been shown previously (see [1] and references herein). For this purpose, one of two types of detectors can be used. The first type produces green emission near 530 nm (caused by Mn^{2+} ions) in the main TL peak at 200 °C, whereas the second type produces an orange emission around 640 nm in the TL peak near 350 °C.

Main features of the $YAlO_3$:Mn^{2+} detectors are as following: high thermochemical and time stability, high resistance to radiation damage, high sensitivity to ionizing radiation (up to 40 relative to TLD-100 for ^{60}Co), extremely wide range of linearity (from few μGy up to few kGy), high effective atomic number (Z_{eff} = 31.4) and consequently high energy response (about 40 for photon radiation of 55 keV/^{60}Co), low thermal fading of single crystalline detectors (≤20%/year for 200 °C peak and ≤5%/year for 350 °C peak). In such a way the material is a good candidate for wide-range dose measurements, especially when tissue equivalence is not required, as well as for a purpose of the radiation quality determination if used alongside with other low-Z materials.

The TL peak at 200 °C is related most likely to Y_{Al} antisites in $YAlO_3$ structure [2, 3], therefore it can be expected that substitution of yttrium ions by smaller lutetium ions can effect on this TL peak.

The Mn^{2+}-doped (Lu-Y)AP single crystals with Lu content of 0, 5, 10 and 20% (with respect to Y) were grown by the Czochralski technique as it was described before [2]. The studied crystals were characterized by photoluminescence and thermoluminescence techniques.

Mn^{2+} ions in (Lu-Y)AP crystals reveal the same as in YAP crystal the broad emission band with maximum at 530 nm (caused by the transition $^4T_1$ (^4G) → $^6A_1$ (^6S) in Mn^{2+}). However the maximum of the TL peak at 200 °C was found to be shifted towards higher temperatures (from 200 °C for YAP:Mn to 230 °C for (Lu-Y)AP:Mn at 4 °C/s heating rate). Herewith this shift is not monotonous with increasing of Lu content. The TL peak shifts all at once for the crystals with the Lu content more than 5%. At the same time the position of the second TL peak near near 350 °C remains unchanged.

Acknowledgements. The work was supported by the NATO Science for Peace and Security Program (Project G4649) and by the European Regional Development Fund (Innovative Economy grant POIG.01.01.02-00-108/09).

[1] Ya. Zhydachevskii et al., Energy response of the TL detectors based on $YAlO_3$:Mn crystals, *Radiat. Meas.* **90** (2016) 262-264.

[2] Ya. Zhydachevskii et al., Technological approaches for improving thermoluminescent properties of the Czochralski-grown $YAlO_3$:Mn crystals, *J. Cryst. Growth* **310** (2008) 3219–3223.

[3] M. Baran et al., Sol–gel synthesis and luminescent properties of nanocrystalline YAP:Mn, *Opt. Mater.* **34** (2012) 604-608.

Luminescence Spectrum with X-Ray Excitation of $CaSO_4$:REE

T. Çavdar[1], K. Kurt[1], V. Güçkan[2], V. Altunal[2], A. Özdemir[2], T. Deptçi[3], Z. Yeğingil[2]

[1]*Mersin University, Faculty of Science and Letters, Department of Physics, Mersin, Turkey*
[2]*Çukurova University, Faculty of Science and Art, Department of Physics, Adana, Turkey*
[3]*İnönüUniversity, Faculty of Engineering, Department of Mining Engineering, Malatya, Turkey*

Luminescence spectrum of doped with REE and undoped$CaSO_4$have been studied under x-ray excitation at room temperature. The broad band luminescence emission of undoped $CaSO_4$is situated from 500nm to 900nm. Emissions of doped $CaSO_4$ are extended from UV to IR region. 385nm is dominant and suppressed the green to IR region which is about 588nm, 610nm and 690nm belong toEu^{+3}transition from $^5D_0 \rightarrow {}^7F_1$, $^5D_0 \rightarrow {}^7F_2$, $^5D_0 \rightarrow {}^7F_4$ respectively. The emission of 385nm might be attributed to Eu^{+2} transition $^6P_{7/2} \rightarrow {}^8S_{7/2}$.

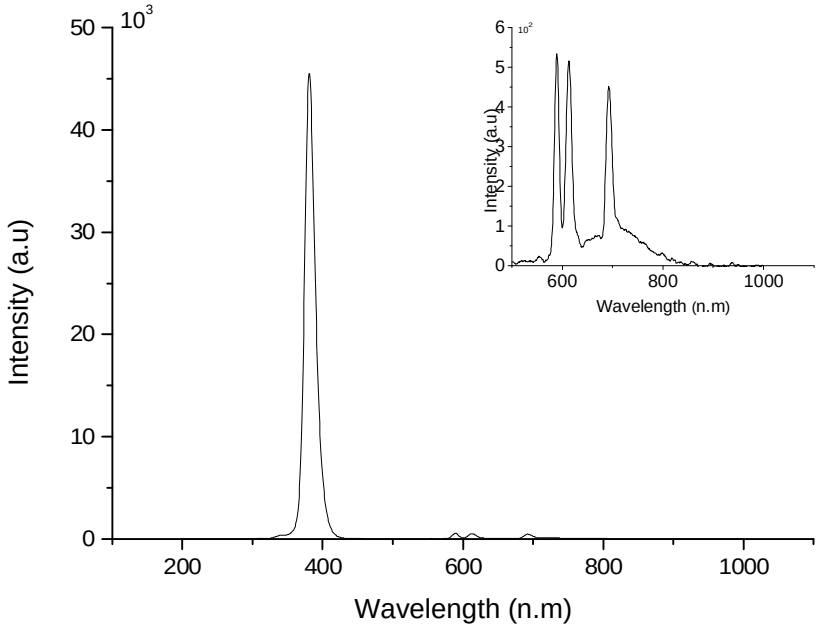

Fig. Luminescence of spectra of $CaSO^4$:REE^{+3} under x-ray exitation

Acknowledgements. This research is supported by NATO through the project SfP 984649 and byCukurova University Rectorate through the Projects FDK-2017-6833, FAY-2016-6410 and FBA-2016- 6000. We acknowledge gratefully the financial supports of NATO and Cukurova University.

[1] G.H. Dieke, *Spectra and energy levels of rare earth ions in crystals*, New York: Interscience, 1968.
[2] K. Binnemans, Interpretation of europium(III) spectra, *Coordination Chemistry Reviews* **295** (2015) 1–45.

New Hybrid Scintillator Based on the $Lu_{1.5}Gd_{1.5}Al_{1.5}Ga_{3.5}O_{12}$ Single Crystalline Films and $Gd_3Al_{2.5-2}Ga_{2.5-3}O_{12}$ Crystals for Simultaneous Registration of α-Particles and γ-Quanta

S. Witkiewicz[1], V. Gorbenko[1,2], K. Paprocki[1], T. Zorenko[1], Yu. Zorenko[1], Ia. Gerasymov[3], O. Sidletskiy[3], A. Fedorov[4], J.A. Mares[5], M. Nikl[5]

[1]*Institute of Physics, Kazimierz Wielki University in Bydgoszcz, Powstańców Wielkopolskich Str. 2, 85090 Bydgoszcz, Poland*
[2]*Department of Electronics, Ivan Franko National University of Lviv, Gen. Tarnavskiy Str. 17, 79017 Lviv, Ukraine*
[3]*Institute for Scintillation Materials, National Academy of Sciences of Ukraine, av. Nauki 60, 61001 Kharkiv, Ukraine*
[4]*SSI Institute for Single Crystals, National Academy of Sciences of Ukraine, av. Nauki 60, 61178 Kharkiv, Ukraine*
[5]*Institute of Physics, AS CR, Cukrovarnicka Str. 10, 16200 Prague, Czech Republic*

This work presents the results of creation of hybrid film-crystal scintillators based on the Ce^{3+} doped $Lu_{1.5}Gd_{1.5}Al_{1.5-2}Ga_{3.5-3}O_{12}$ single crystalline films (SCF), grown by liquid phase epitaxy (LPE) onto substrates prepared from undoped and Ce^{3+} doped $Gd_3Al_{2.5}Ga_{2.5}O_{12}$ (GAGG) single crystal (SC) from the super-cooling melt solution based on the $PbO\text{-}B_2O_3$ flux. We have found that the SCFs of the $Lu_{1.5}Gd_{1.5}Al_{1.5-2}Ga_{3.5-3}O_{12}$ mixed garnets can be grown onto GAGG substrates with a misfit of about 0.88-1.31%. We have also determined the segregation coefficients of Gd, Lu, Ga cations and Ce^{3+} impurity at LPE grown of these SCFs onto GAGG substrates.

We have shown that the best scintillation properties are observed in $Lu_{1.5}Gd_{1.5}Al_{1.5}Ga_{3.5}O_{12}$:Ce SCF. The light yield (LY) of these SCFs under α– particles excitation by Pu^{239} source (5.15 MeV) is comparable with the LY of reference YAG:Ce SCF. This SCF scintillator possesses also relatively fast scintillation response with $t_{1/e}$=105 ns and $t_{1/20}$=1078 ns. Such scintillation response is significantly faster in the 0-500 ns range than in the GAGG:Ce SC substrate. For this reasons the epitaxial structures based on the $Lu_{1.5}Gd_{1.5}Al_{1.5}Ga_{3.5}O_{12}$:Ce SCFs, grown onto GAGG:Ce SC substrates, can be used as hybrid scintillators for simultaneous registration of the components of mixed ionizing fluxes, specifically α– particles and γ– quanta, respectively. The separation of the signals from SCF and SC components of hybrid scintillator can be realized by the way of registration of the difference in the scintillation decay kinetics of SCF and substrate scintillators. Namely, the separation of the response from SCF and substrate can be achieved at large (>2) ratio K= $t_{1/e}$ (SCF) / $t_{1/e}$ (substrate). Taking into account that the scintillation decay times of $Gd_3Al_{2-2.5}Ga_{3-2.5}O_{12}$:Ce substrates are within $t_{1/e}$=248-418 ns and $t_{1/20}$=837-1543 ns ranges, the K ratio is equal to 4 and 2.36 for hybrid scintillators based on the $Lu_{1.5}Gd_{1.5}Al_{1.5}Ga_{3.5}O_{12}$:Ce SCF, grown onto $Gd_3Al_{2.5}Ga_{2.5}O_{12}$:Ce and $Gd_3Al_2Ga_3O_{12}$:Ce substrates, respectively.

Acknowledgements. The work was performed in the framework of NCN 2016/21/B/ST8/03200 and NANOLUX2014 No 286 projects and also supported by the Ministry of Education and Science of Ukraine in the frame of SF-20 F and FK 64/34 projects and Czech Science Foundation in frame of no. 16-15569S project.

BeO+MgO as a Mixture Dosimeter: Its Luminescence Mechanism

V. Altunal[*1], A. Ozdemir[1], V. Guckan[1], K. Kurt[2] and Z. Yegingil[1]

[1]*Cukurova University, Art Sciences Faculty, Department of Physics, 01330 Adana, Turkey*
[2]*Mersin University, Science and Letter Faculty, Physics Department, 33343 Mersin, Turkey*
* valtunal@student.cu.edu.tr

Beryllium oxide (BeO) has attracted significant attentions since about 1950, because it possesses high heat conductivity (as high as that of aluminium), high chemical and thermal stability, hardness, a wide energy gap of about 10.6 eV, high radiation stability to different forms of photon and corpuscular radiation, high melting point (2570 ^{o}C) [1,2,3]. Special interest in BeO as a material for personal dosimetry is determined by its effective atomic number (Z_{eff} =7.13), which is close to biological tissue (Z_{eff} =7.42). MgO is also an interesting material for radiation dosimetry, because it has simple cubic lattice structure, high chemical stability (melting point of 2800 °C) and wide band gap (7.8 eV), a low effective atomic number (Z_{eff} = 10.8) [4,5,6].

In this study, BeO phosphors synthesized using precipitation method and mixed with MgO phosphors. Using mixture of BeO+MgO, some dosimetric pellets were prepared with evacuable dies. Luminescent signals of produced mixture ceramic pellets were studied using OSL technique. Some dosimetric experiments, such as the beta dose response, minimum detectable dose, reusability and the effect of Thermoluminescence (TL) measurement on OSL signals, were carried out with comparing the results obtained from commercial used BeO chips (Thermalox995).

It can be concluded from the experimental results that BeO+MgO mixture pellets have nearly linear dose response in the range 0.1-10 Gy and OSL decay curves in accordance with the literature.

Acknowledgement. This project has been supported by NATO in the frame of the NATO Science for Peace and Security (SPS) Programme under the project number SfP984649 and by Cukurova University under the project numbers FUA-2015-4300 and FYL-2015-3944. The authors want to thank NATO and Cukurova University Rectorate for their support.

[1] V.Yu. Ivanov, V.A. Pustovarov, A.V. Kruzhalov et al., *Nucl. Instr. Meth. Phys. Res. A* **282** (1989) 559.
[2] E. Bulur, H.Y. Göksu, *Radiat. Meas.* **29** (1998) 639-650.
[3] M. Sommer, J. Henniger, *Radiat. Protect. Dosim.* **119** (2006) 394-397.
[4] G. Pacchioni, *The Chemical Physics of Solid Surfaces*, ed. D. P. Woodruff, Vol. 9, pp. 94–135, Elsevier, 2001.
[5] W. Las, & T. Stoebe, TL mechanisms and luminescence characteristics in MgO, *Radiat. Prot. Dosim.* **8** (1984) 45–67.
[6] S. H. Tamboli, R. Patil, S. Kamat, V. Puri, & R. Puri, Modification of optical properties of MgO thin films by vapour chopping, *J. Alloys Compd*. **477** (2009) 855–859.

Preliminary Study for Optically Stimulated Luminescence Characterization of BeO+SiO_2 as a Mixture Dosimeter

V. Guckan[1,*], V. Altunal[1], A. Ozdemir[1], K. Kurt[2] and Z. Yegingil[1]

[1]*Cukurova University, Art Sciences Faculty, Department of Physics, 01330 Adana, Turkey*
[2]*Mersin University, Science and Letter Faculty, Physics Department, 33343 Mersin, Turkey*
* *veysiguckan@gmail.com*

Oxide materials have been used in many applications including radiation measurements. In this study, after BeO phosphors were synthesized using precipitation method, SiO_2 (Sand) powders were mixed to BeO using solid state synthesis method. The mixture of BeO+SiO_2 were prepared and sintered. Morphological and structural analysis, X-ray Diffractometer (XRD) and Scanning Electron Microscopy (SEM), were performed.

Luminescence characteristics of BeO+SiO_2 were studied using OSL technique and blue stimulation light were used. OSL decays were obtained from irradiated pellets and the life times were found. Dose response of the OSL signals were performed and found to be nearly linear for personal dosimetry applications. On the other hand, since the OSL measurements must be reproducible for the dosimetric applications, reusability of the signals was carried out. Furthermore, short time light and dark fading of the signals were studied and compared with the results obtained from well-known commercial BeO chips (Thermalox995).

Considering the results of this study, one may say that BeO+SiO_2 pellets have promising OSL properties in general to be used in personal and environmental dosimetry applications as an OSL dosimeter.

Acknowledgement. This project has been supported by NATO in the frame of the NATO Science for Peace and Security (SPS) Programme under the project number SfP984649 and by Cukurova University under the project numbers FUA-2015-4300 and FYL-2015-3944. The authors want to thank NATO and Cukurova University Rectorate for their support.

Optically Stimulated Luminescence Properties of $BeO+TiO_2$ as a Mixture Dosimeter

V. Guckan[1,*], V. Altunal[1], A. Ozdemir[1], K. Kurt[2] and Z. Yegingil[1]

[1]*Cukurova University, Art Sciences Faculty, Department of Physics, 01330 Adana, Turkey*
[2]*Mersin University, Science and Letter Faculty, Physics Department, 33343 Mersin, Turkey*
* veysiguckan@gmail.com

This study presents the Optically Stimulated Luminescence (OSL) characterization of $BeO+TiO_2$ as a mixture dosimeter. BeO is the one of the most important material for the radiation dosimetry, because of its chemical and physical properties, to be the tissue equivalent material. Interest in titanium oxide-based ceramics has increased significantly in recent years as possible Thermoluminescence (TL) dosimeters which could be used in applications of ionizing radiation dosimetry.

In this study, in order to investigate the effect of the two materials together in radiation measurements, BeO material was synthesized using precipitation method and mixed with TiO_2 using solid state synthesis method. This mixture was examined for its usefulness as an OSL dosimeter.

OSL technique was used to investigate the dosimetric characteristics of $BeO+TiO_2$ mixed ceramic dosimeters, after the pellets were exposed to beta source ($^{90}Sr/^{90}Y$). Dosimetric characteristic of $BeO+TiO_2$ pellets were investigated by performing basic dosimetric experiments such as dose response, minimum detectable dose, reusability and the effect of TL measurement on OSL signals. These results compared with that of commercially available BeO chips (Thermalox995).

Acknowledgement: This project has been supported by NATO in the frame of the NATO Science for Peace and Security (SPS) Programme under the project number SfP984649 and by Cukurova University under the project numbers FUA-2015-4300 and FYL-2015-3944. The authors want to thank NATO and Cukurova University Rectorate for their support.

Synthesis and Optically Stimulated Luminescence (OSL) Characterization of $BeO+Al_2O_3$ a Mixture Dosimeter

V. Altunal[1,*], V. Guckan[1], A. Ozdemir[1], K. Kurt[2] and Z. Yegingil[1]

[1]*Cukurova University, Art Sciences Faculty, Department of Physics, 01330 Adana, Turkey*
[2]*Mersin University, Science and Letter Faculty, Physics Department, 33343 Mersin, Turkey*
* valtunal@student.cu.edu.tr

Oxides are the most important inorganic substances in nature and have numerous industrial applications. Since BeO and Al_2O_3 have been widely used for dosimetric applications, in this study, BeO was synthesized using precipitation synthesis method and then mixed with Al_2O_3 powder. Using the solid state synthesis method, a mixture pellet dosimeter was prepared and sintered at high temperature.

In order to investigate crystal structure and surface morphology, *X-ray Diffractometer (XRD)* and *Scanning Electron Microscopy (SEM)* analysis were performed. Luminescence properties of the mixture pellet dosimeters were investigated by OSL techniques. OSL decays for 1 Gy irradiated $BeO+Al_2O_3$ mixture dosimeters were recorded and the decay life times of the signals were found as 4.84 and 41.95 s. On the other hand, the beta dose response was found to be nearly linear in the range 0.1-10 Gy. Reusability and short time fading of the signals were investigated.

The information obtained in this study may help to understand the nature of the mixture dosimeters and to create a new application area in radiation dosimetry.

Acknowledgement. This project has been supported by NATO in the frame of the NATO Science for Peace and Security (SPS) Programme under the project number SfP984649 and by Cukurova University under the project numbers FUA-2015-4300 and FYL-2015-3944. The authors want to thank NATO and Cukurova University Rectorate for their support.

Investigation of Double Beta Decay of ^{116}Cd with the Help of Enriched $^{116}CdWO_4$ Crystal Scintillators

O.G. Polischuk[1], A.S. Barabash[2], P. Belli[3,4], R. Bernabei[3,4], F. Cappella[5,6], V. Caracciolo[7], R. Cerulli[7], D.M. Chernyak[1,8], F.A. Danevich[1], S. d'Angelo[3,4,+], A. Incicchitti[5,6], D.V. Kasperovych[1], V.V. Kobychev[1], S.I. Konovalov[2], M. Laubenstein[7], V.M. Mokina[1,5], D.V. Poda[1,9], V.N. Shlegel[10], V.I. Tretyak[1], V.I. Umatov[2], Ya.V. Vasiliev[10]

[1]*Institute for Nuclear Research, Kyiv, Ukraine*
[2]*NRC "Kurchatov Institute", Institute of Theoretical and Experimental Physics, Moscow, Russia*
[3]*Dipartimento di Fisica, Universita di Roma "Tor Vergata", Rome, Italy*
[4]*INFN sezione Roma "Tor Vergata", Rome, Italy*
[5]*INFN, sezione di Roma, Rome, Italy*
[6]*Dipartimento di Fisica, Università di Roma "La Sapienza", Rome, Italy*
[7]*INFN, Laboratori Nazionali del Gran Sasso, Assergi (AQ), Italy*
[8]*Kavli Institute for the Physics and Mathematics of the Universe (Kavli IPMU), The University of Tokyo, Japan*
[9]*CSNSM, Univ. Paris-Sud, CNRS/IN2P3, Universite Paris-Saclay, Orsay, France*
[10]*Nikolaev Institute of Inorganic Chemistry, Novosibirsk, Russia*
[+] *deceased*

Neutrinoless double beta decay ($0\nu2\beta$) is considered as a powerful tool to check physics beyond the Standard Model of particles. The nucleus ^{116}Cd is one of the most promising for $0\nu2\beta$ experiments thanks to the high energy of the decay $Q_{\beta\beta}$ = 2813 keV, relatively large isotopic abundance 7.5%, availability of relatively cheap enrichment and promising theoretical calculations. The AURORA experiment aiming to search for 2β processes in ^{116}Cd with the help of two $^{116}CdWO_4$ crystal scintillators (total mass 1.16 kg) enriched in ^{116}Cd (to 82%) is in progress at the Gran Sasso underground laboratory (Italy) of INFN. High optical and scintillation properties of the crystals were obtained thanks to the deep purification of the initial materials, and the advantage of the low-thermal-gradient Czochralski technique for the crystal growth. The $^{116}CdWO_4$ scintillators are highly radiopure (~0.03 mBq/kg of ^{228}Th, < 0.005 mBq/kg of ^{226}Ra, < 0.3 mBq/kg of ^{40}K). We have also observed a strong segregation of thorium, radium and potassium in the crystal growing process, which allows to improve substantially the radiopurity level of the $^{116}CdWO_4$ scintillators. The two neutrino mode of the 2β decay of ^{116}Cd was investigated with the highest up-to-date accuracy resulting in $T_{1/2}$ = [2.69 ± 0.14(syst.) ± 0.02(stat.)] × 10^{19} yr. Limit on $0\nu2\beta$ mode has been obtained as $\lim T_{1/2} = 1.9\times10^{23}$ yr at 90% C.L., which corresponds to the effective Majorana neutrino mass limit ≤ (1.2 − 1.8) eV (depending on the nuclear matrix elements used). New limits on other double beta decay processes in ^{116}Cd (decays with majoron emission, transitions to excited levels) were also obtained.

Pile-Up Analysis of Li_2MoO_4, $ZnMoO_4$ and $CdWO_4$ Cryogenic Scintillators for Low-Counting Experiments

M.O. Nikolaichuk[1], F.A. Danevich[1], D.V. Poda[1,2]

[1] *Institute for Nuclear Research, Kyiv, Ukraine*
[2] *Centre de Sciences Nucléaires et de Sciences de la Matière, Orsay, France*

Search for neutrinoless double beta decay is considered as a powerful tool to probephysics beyond the Standard Model of particles. Cryogenic scintillating bolometers based on molybdates of zinc ($ZnMoO_4$) and lithium (Li_2MoO_4) have been proposed as promising detectors to search for neutrinoless double beta decay of ^{100}Mo [1-3], while cadmium tungstate remains the most suitable scintillator to realise double beta decay experiments to investigate double beta processes in ^{106}Cd and ^{116}Cd [4]. In addition, $CdWO_4$ bolometers can be used to study precisely the beta-spectrum shape of ^{113}Cd to refine a value of the axial vector coupling constant g_A [5]. The parameter is strongly requested by the theory to estimate neutrino mass from the double beta decay experiments. One of the main problem of low temperature bolometers is their slow response (hundreds milli-seconds) which leads to the pile-up of signals, and therefore to the background due to random coincidence of events (first of all, of the two neutrino double beta decay) [6], and eventslosses of the studied effect. Pulse-shape analysis of the low background data accumulated with Li_2MoO_4 and $ZnMoO_4$ detectors was used to reject random coincidences of events, and to correct the number of double beta events aiming at estimation the half-life of ^{100}Mo relatively to the two neutrino double beta decay. The data of low temperature measurements with a $CdWO_4$ bolometer was analysed to estimate the half-life of ^{113}Cd relatively to the beta decay and to derive the beta spectrum shape at low energies requested to estimate the g_A parameter.

[1] J.W. Beeman et al., A next-generation neutrinoless double beta decay experiment based on $ZnMoO_4$ scintillating bolometers, *Phys. Lett. B* **710** (2012) 318.
[2] T.B. Bekker et al., Aboveground test of an advanced Li_2MoO_4 scintillating bolometer to search for neutrinoless double beta decay of ^{100}Mo, *Astroparticle Physics* **72** (2016) 38.
[3] E. Armengaud et al., Development of ^{100}Mo-containing scintillating bolometers for a high-sensitivity neutrinoless double-beta decay search, arXiv:1704.01758 [physics.ins-det].
[4] A.S. Barabash et al., First test of an enriched $^{116}CdWO_4$ scintillating bolometer for neutrinoless double-beta-decay searches, *Eur. Phys. J. C* **76** (2016) 487.
[5] M. Haaranen, P. C. Srivastava, J. Suhonen, Forbidden nonunique β decays and effective values of weak coupling constants, *Phys. Rev. C* **93** (2016) 034308.
[6] D.M. Chernyak et al., Rejection of randomly coinciding events in $Li_2{}^{100}MoO_4$ scintillating bolometers using light detectors based on the Neganov-Luke effect, *Eur. Phys. J. C* **77** (2017) 3.

Solid-State Sintering and Luminescent Properties of Yb^{3+}, Er^{3+}:YAG Transparent Ceramics

I.O. Vorona[1], R.P. Yavetskiy[1], M.V. Dobrotvorskaya[1], A.G. Doroshenko[1], S.V. Parkhomenko[1], A.V. Tolmachev[1], L. Gheorghe[2], C. Gheorghe[2], S. Hau[2]

[1]Institute for Single Crystals of NAS of Ukraine, 60 Nauki Ave., 61001 Kharkov, Ukraine
[2]National Institute for Laser, Plasma and Radiation Physics, Laboratory of Solid-State Quantum Electronics, PO Box MG-36, 077125 Magurele, Bucharest, Romania

Er^{3+} and Yb^{3+} co-doped hosts have been proposed for obtaining up-conversion and down-conversion luminescence by energy transfer between Yb^{3+} and Er^{3+} ions [1, 2], as well as for active media of diode-pumped solid-state lasers operated at 1.6 μm wavelength [3]. Polycrystalline Yb^{3+}, Er^{3+}:YAG is a promising material for laser and photonics applications due to excellent solubility of dopants into garnet matrix, high optical and structural quality, which are beneficial properties for obtaining of efficient laser devices. Nowadays there is an increasing interest in obtaining of YAG-based materials via advanced ceramic technology.

Yb^{3+}, Er^{3+}:YAG transparent ceramics contained 5 at.% of Yb^{3+} ions and 0.5 to 1.5 at.% of Er^{3+} ions were produced by the solid-state reactive sintering method [4]. Influence of Yb, Er doping on shrinkage and the microstructure of reactive-sintered ceramics was investigated. Temperature conditions that are responsible for effective densification and inhibition of grain coarsening were optimized. Structural, optical and luminescence properties of ceramics, obtained under optimized condition were studied. In accordance to XRD analysis and SEM observations, the obtained ceramics have single phase garnet structure and no secondary segregated phases were observed. They have near-theoretical density (residual porosity not excess 10 ppm) and high transparency. Luminescent properties of obtained ceramics were measured under Xe-lamp and 975 nm diode excitation corresponding to up- and down-conversion modes.

The results could be used for optimization of eye-safe compact ceramic diode-pumped solid-state lasers, for range-finders, optical and communication devices, or for light convertors of semiconductor detectors and solar cells.

Acknowledgements. This work was partially supported by the Ministry of Education and Science of Ukraine and the Romanian Ministry of National Education and Scientific Research, Executive Unit for Financing Higher Education, Research, Development and Innovation (UEFISCDI), within the frame of Ukrainian-Romanian project no. M/57-2016 and 2/BM/15.06.2016, respectively.

[1] J. De Wild, J.K. Rath, A. Meijerink, W. Van Sark, R.E.I. Schropp, Enhanced nearinfrared response of a-Si:H solar cells with b-$NaYF_4$:Yb^{3+} (18%), Er^{3+} (2%) up-conversion phosphors, *Sol. Energy Mater. Sol. Cells* **94** (2010) 2395–2398.

[2] V.D. Rodriquez, V.K. Tikhomirov, J. Mendez-Ramos, A.C. Yanes, V.V. Moshchalkov, Towards broad range and highly efficient down-conversion of solar spectrum by Er^{3+}-Yb^{3+} co-doped nano-scale glass-ceramics, *Sol. Energy Mater. Sol. Cells* **94** (2010) 1612–1617.

[3] E. Georgiou, F. Kiriakidi, O. Musset, J.-P. Boquillon, 80mJ/1.64μm pulsed Er:Yb:YAG diode-pumped laser, *Proceedings of SPIE* **5460** (2004) 272-283.

[4] R.P. Yavetskiy, D.Yu. Kosyanov, A.G. Doroshenko, S.V. Parkhomenko, P.V. Mateychenko, I.O. Vorona, A.V. Tolmachev, A.V. Lopin, V.N. Baumer, V.L. Voznyy, Microstructure evolution of SiO_2, ZrO_2- doped $Y_3Al_5O_{12}$:Nd^{3+} ceramics obtained by reactive sintering, *Ceram. Int.* **41** (2015) 11966–11974.

SECTION 6

MAGNETIC MATERIALS, SUPERCONDUCTORS, MULTIFERROICS

Bose-Einstein Magnon Condensation and Bottleneck Accumulation of Magneto-Elastic Bosons in Yttrium-Iron-Garnet Films

A.A. Serga

Fachbereich Physik and Landesforschungszentrum OPTIMAS,
Technische Universität Kaiserslautern, 67663 Kaiserslautern, Germany

It is known that an ensemble of magnons, quanta of a spin wave, can be prepared as a Bose gas of weakly interacting quasi-particles with conservation of the particle number. The external pumping of magnons into the system causes an increase in the chemical potential of a thermalized magnon gas. When it becomes equal to the minimal magnon energy a magnon Bose-Einstein condensate (BEC) may form at this spectral point [1, 2]. However, magnon-phonon scattering processes can significantly modify this scenario.

Our observations of the magnon BEC in a single-crystal film of yttrium iron garnet (YIG, $Y_3Fe_5O_{12}$) [3] by means of wavevector-resolved Brillouin Light Scattering (BLS) spectroscopy [4] resulted in the discovery of a novel condensation phenomenon mediated by magneto-elastic interaction: A spontaneous accumulation of hybrid magneto-elastic bosons at the intersection of the lowest magnon mode and a transversal acoustic wave [5]. We have found that the transfer of pumped magnons toward a BEC state is almost fully suppressed near the intersection point between the magnon and phonon spectral branches. Such a bottleneck leads to a strong spontaneous accumulation of the hybrid magnon-phonon quasiparticles trapped near the semi-linear part of the magnon-phonon hybridization area. As opposed to the Bose-Einstein condensate, which is a consequence of equilibrium Bose statistics, the bottleneck accumulation is determined by varying inter-particle interactions. Furthermore, unlike the magnon BEC, the accumulated magneto-elastic bosons possess a significantly nonzero group velocity, which is determined by their position in the hybridization area. As a result, the density of these particles depends on their travel path through the thermalized cloud of the pumped magnons and consequently on the width of the pumping area.

The developed theoretical model describes the experimentally observed density peak of hybrid magneto-elastic bosons and proves the saturation effect in the accumulation process: Increase in the pumping power leads to the increase of the magnon BEC population and to the reduction of the bottleneck effect [5].

Acknowledgements. The work is supported by the Deutsche Forschungsgemeinschaft within the SFB/TR 49 “Condensed Matter Systems with Variable Many-Body Interactions”, by EU-FET (Grant In-Spin 612759), and by the Graduate School Material Sciences in Mainz (MAINZ) through DFG funding of the Excellence Initiative (GSC-266). As well, we acknowledge I.I. Syvorotka (Scientific Research Company “Carat”, Lviv, Ukraine) for supplying us with the YIG film.

[1] S.O. Demokritov et al., Bose-Einstein condensation of quasi-equilibrium magnons at room temperature under pumping, *Nature* **443** (2006) 430.
[2] A.A. Serga et al., Bose-Einstein condensation in an ultra-hot gas of pumped magnons, *Nature Commun.* **5** (2014) 3452.
[3] V. Cherepanov, I. Kolokolov, V. L’vov, The saga of YIG: spectra, thermodynamics, interaction and relaxation of magnons in a complex magnet, *Phys. Rep.* **229** (1993) 81.
[4] C.W. Sandweg et al., Wide-range wavevector selectivity of magnon gases in Brillouin light scattering spectroscopy, *Rev. Sci. Instr.* **81** (2010) 073902.
[5] D.A. Bozhko et al., Bottleneck accumulation of hybrid magneto-elastic bosons, arXiv: 1612.05925.

Defect Induced Magnetism in ZnO: a First Spintronic Device

L. Botsch, P. Esquinazi, I. Lorite, Y. Kumar

Division of Superconductivity and Magnetism, Felix-Bloch Institute for Solid State Physics, University of Leipzig, Linnéstrasse 5, D-04103 Leipzig, Germany

The appearance of a magnetically ordered state through atomic lattice defects with a concentration of roughly 5 at.% in a nominally non-magnetic material depends on the details of the lattice structure and the elements involved. This phenomenon, called nowadays Defect-Induced Magnetism (DIM), has been found in a broad spectrum of materials, like graphite [1], SiC [2] and several oxides [3]. The evidence for magnetic order obtained by different experimental methods like, e.g., Magnetization, XMCD, Electrical transport, EPR and NMR, and the sensitive magnetic impurities characterization through PIXE, leaves no doubt about its intrinsic origin in solids.

An interesting example of DIM in oxides can be found in ZnO, a large gap semiconductor that has been thoroughly studied in the last years [3]. DIM in pure ZnO is induced by increasing the concentration of Zn vacancies through, e.g., proton irradiation [4]. These defects can be stabilized in the ZnO lattice and remain above room temperature by previous doping it with Li or Na [5], for example. The Curie temperature reached in this case remains always above 300K [3,4,6].

In spite of a large amount of work, a possible application of DIM has not yet been realized. In this work we present an electron-spin filter and a magnetoresistance sensor based on ZnO nanostructures, in which magnetic order was reached by introducing atomic lattice defects following the simple procedure to produce vacancies in ZnO through low-energy plasma treatment [4,6]. The measured signals and the scalability of the phenomenon indicate that the proposed device has good potentials for applications in micro- and nanospintronics.

[1] D. Spemann and P. Esquinazi, Chapter 3 in “Basic Physics of Functionalized Graphite”, Springer Series in Material Science 244 (2016).
[2] Y. Liu et al., *Phys. Rev. Lett.* **106** (2011) 087205.
[3] P. Esquinazi, W. Hergert, D. Spemann, A. Setzer, A. Ernst, *IEEE Trans. Magn.* **49** (2013) 4668.
[4] M. Khalid, P. Esquinazi, D. Spemann, W. Anwand, and G. Brauer, *New J. Phys.* **13** (2011) 063017.
[5] E.-C. Lee and K. J. Chang, *Phys. Rev. B* **70** (2004) 115210.
[6] I. Lorite et al., *Appl. Phys. Lett.* **106** (2015) 082406.

Core-Shell Nanoparticles with Strong Magnetic Anisotropy as Potential Building Blocks for Permanent Magnets

M. Shatruk, L.A. Saucedo, D.J. Carnevale, G.F. Strouse

Department of Chemistry and Biochemistry, Florida State University, Tallahassee, FL 32306, USA

High-performance magnets are critical components in energy technologies for rotors and magnetic bearings in motors. The performance of current state-of-the-art materials relies heavily on the availability of rare-earth elements, which are the source of high magnetic anisotropy. Currently, the high demand for permanent magnets and the monopolized market of critical rare-earth elements call for new approaches in developing magnetic composites with high energy products while minimizing the content of critical elements. Our approach follows the theoretical prediction by Kneller and Hawig [1], according to which hard magnetic particles embedded into a soft magnetic matrix should demonstrate a substantial enhancement of both coercivity and remnant magnetization, the two ingredients of the energy product. To probe this prediction at the nanoscale, we carry out a systematic growth of soft-magnet shells (Fe_3O_4, Co, Ni) around a hard-magnet core (ε-Fe_2O_3, FePt, $SmCo_5$) using microwave chemistry and conventional techniques. We discovered a remarkable 4-fold enhancement in the energy product of such a core-shell assembly as compared to the energy product of bare hard-magnet nanoparticles [2]. Furthermore, the variation in the shell thickness allowed us to observe evolution of magnetic exchange regimes. At small shell thicknesses, we observe hard exchange which effectively increases the size of the core, leading to a slight increase in the coercivity and blocking temperature of the superparamagnetic nanoparticles. At the intermediate shell sizes, an enhancement in the magnetization recovery is observed, signifying an onset of the theoretically predicted exchange-spring behavior. Finally, for thicker shells we observe decoupling of the outer soft-magnet layers from the hard-magnet core which leads to the decrease in the coercivity and energy product. The demonstration of nanoscale exchange-spring magnets can lead to improved high-performance magnet design for energy applications.

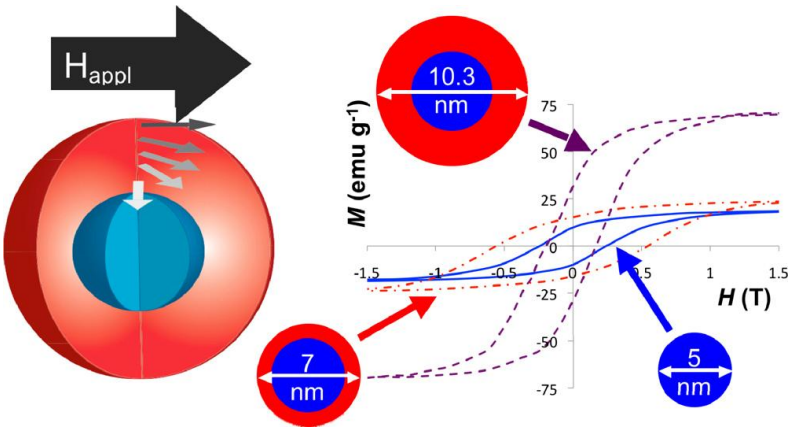

[1] E.F. Kneller and R. Hawig, *IEEE Trans. Magn.* **27** (1991) 3588.
[2] D.J. Carnevale, M. Shatruk and G.F. Strouse, *Chem. Mater.* **28** (2016) 5480.

Ferromagnetic Nanomaterials: Synthesis and Properties

A. Belous[1], A. Tovstolytkin[2], S. Solopan[1], Yu. Shlapa[1], O. Fedorchuk[1]

[1]*Vernaskii Institute of General and Inorganic Chemistry of the NAS of Ukraine*
[2]*Institute of Magnetism of the NAS of Ukraine and MES of Ukraine*

The physical and chemical properties of ferromagnetic materials significantly change during the transition to the nanoscale, which is very important, both from a scientific and practical point of view [1].

This study deals with the synthesis and investigation of three types of ferromagnetic nanomaterials: M-type barium hexaferrite, ferrites with the spinel structure and lanthanum-strontium manganites with the perovskite structure.

It was investigated the effect of the fractal structure on the phase composition and physic-chemical properties of M-type barium hexaferrite nanoparticles, synthesized by precipitation from the solutions and via sol-gel method. The conditions at which the amorphous nanoparticles form the three-level complicated fractal structure, that allow obtaining the weakly agglomerated monodisperse crystalline nanoparticles, were determined. It was shown the possibility to control the shape of Ba-hexaferrite nanoparticles (plates and rods).

AFe_2O_4 ferrite nanoparticles (*A* = Mn, Fe, Co, Ni, Zn) and based on them core/shell structures were synthesized by different methods (precipitation from diethylene glycol solution and microemulsions, criochemical method). Weakly agglomerated nanoparticles with particle size 3 – 15 nm and superparamagnetic properties were obtained. It was shown the possibility to effect on the magnetic properties of nanoparticles by the formation of the core/shell structures.

Weakly agglomerated crystalline nanoparticles of heterosubstituted $La_{1-x}Sr_xMnO_3$ manganites with the narrow size distribution and the average size 30 – 40 nm were synthesized via sol-gel method [2].

Based on the synthesized ferrite nanoparticles with the spinel and perovskite structures magnetic fluids were developed. They heat up effectively under the action of an alternating magnetic field. It was shown that obtained fluids are compatible with living organisms and are of particular interest for their possible application in medicine as the inducers of hyperthermia treatment.

The film-forming solutions for obtaining nanocrystalline thin films of M-type Ba-hexaferrite were created. Thin films with uniform distribution of Ba^{2+} and Fe^{3+} ions in the film volume with the thickness 200 nm, rod-liked grains ($d_{av.}$, $l_{av.}$= 62 nm, 320 nm, $l_{av}/d_{av.}$= 5) and high level of magnetic characteristics were obtained by "spin-coating" method.

Based on thick films of Ba-hexaferrite and Ni-ferrite with the spinel structure magnetic resonant microwave elements were developed. They include α-Al_2O_3 high-Q dielectric resonator and thick ferrite film. It was shown that obtained elements might be perspective for application in the microwave equipment.

Based on ferroelectric-semiconductors and $La_{1-x}Sr_xMnO_3$ ferromagnetic film heterostructures in which magnetic properties may be effected by the electromagnetic field, were created for the first time.

[1] A. Ito, M. Shinkai, H. Honda, T. Kobayashi, Medical application of functionalized magnetic nanoparticles, *J. Biosci. Bioeng.* **100** (2005) 1 – 11.

[2] S.O. Solopan, O.I. V'yunov, A.G. Belous, T.I. Polek, A.I. Tovstolytkin, Effect of nanoparticles agglomeration on electrical properties of $La_{1-x}A_xMnO_3$ (A = Sr, Ba) nanopowders and ceramic solid dolutions, *Solid State Sci.* **14** (2012) 501 – 505.

A New Application of Relaxor Ferroelectrics: Electrocaloric Cooling

G. Suchaneck

TU Dresden, Solid State Electronics Lab, 01062 Dresden, Germany

The electrocaloric (EC) effect is a reversible entropy change in polar dielectrics under an applied electric field. Recently, we have proposed a coefficient of performance of EC elements and a new upper bound of the EC effect which is based on the fact that only a certain energy density might be stored in a dielectric - equivalent to a limit in electrostatic pressure [1]. Correspondingly, a large EC response is expected in materials with large values of thermal diffusivity, dielectric permittivity and its temperature coefficient, as well as high dielectric strength (in order to apply large electric fields), low dielectric and hysteresis losses and a broad temperature region of high dielectric response caused, for instance, by a phase transition. With regard to these requirements, relaxor ferroelectrics (relaxors) appear to be the best choice for EC application. In fact, relaxors such as PVDF-based polymers, lead containing and lead-free perovskite provide a sufficient for practical cooling applications EC temperature changes over a broad temperature range. Data for lead-free barium titanate-zirconate is available solely for comparable low electric fields. Here, an extrapolation to comparable fields based on the 2/3 power law predicts a performance worthy for experimental examination.

Relaxors are a class of disordered crystals possessing peculiar structure and properties [2]. They exhibit frequency dispersion, i.e., the temperature T_m of the dielectric constant maximum increases with increasing frequency. In relaxor ferroelectrics, polar entities, e.g. polar nanoregions (PNR), appear at temperatures much higher than the Curie point, but below the so-called Burns temperature. These PNRs are not subjected to dielectric losses characteristic of polar domains. The huge dielectric response and the existence of a maximum of $e(T)$ is attributed to the peculiarities of the PNR behaviour: the size and number of dynamic PNRs responsible for the dielectric relaxation are believed to increase upon cooling. Above the temperature of maximum dielectric permittivity up to a temperature T^* where static PNRs disappear [3], relaxors provide a large and reversible polarization change due to contributions to polarization not present in ordinary ferroelectrics [2]. This is just required for a large EC response. In this temperature region, the dielectric response is dominated by the static dielectric susceptibility. However, to fulfil the condition that heat rejected to the sink is larger than heat absorbed from the load, relaxors must be driven at a certain temperature above the temperature of maximum dielectric permittivity.

EC relaxor materials are characterized by different time scales, two electronic ones due to (i) polarization response and (ii) polar nanoregion dynamics and two thermal ones, (iii) the thermal transit time during which the sample reaches internal thermal equilibrium (called by us the acoustic limit) and (iv) the time constant of the material´s volume during which thermal equilibrium with the environment is established. In order to provide adiabatic depolarization during the cooling step, the decay time of the applied electric field should not exceed the acoustic limit. On the other hand, the performance of EC cooling devices is limited by the thermal time constants of heat switches or by the heat transfer coefficient to the gaseous or liquid heat transfer agent of active EC regenerators.

[1] G. Suchaneck and G. Gerlach, *Mater. Today: Proc.* **3** (2016) 622-631.
[2] A. Bokov and Z.-G. Ye, *J. Adv. Dielectrics* **2** (2012) 1241010.
[3] W. Dmowski et al., *Phys. Rev. Lett.* **100** (2008) 137602.

Effect of Oxygen Distribution in the Structure of Magnesium Diboride-Based Materials on their Superconducting Characteristics

T. Prikhna

V. Bakul Institute for Superhard Materials of the National Academy of Sciences of Ukraine, 2 Avtozavodskaya Str., 04074 Kiev, Ukraine

Devices based on the superconductor MgB_2 can be envisaged for many applications, as MRI, cables, electromotors, magnetic bearings and fault current limiters, etc. There are many factors which can influence the functional properties of MgB_2, the most important ones being: critical current density, J_c, trapped magnetic field, upper critical magnetic field B_{c2}, irreversibility field, B_{irr}, ac losses, rate of superconducting-normal state (S-N) transition, density, hardness and fracture toughness.

Although MgB_2 is a nominally oxygen-free superconductor, it is practically impossible to synthesize oxygen-free MgB_2-based materials even if high purity initial components and protecting atmosphere are used. However, previous studies indicated a positive role of oxygen-containing nano-inclusions as pinning centers: MgO, $Mg(OH)_2$, $MgB_{2-x}O_x$, $MgB_{0.6-0.8}O_{0.8-0.9}$ or nanolayers $MgB_{1.2-2.7}O_{1.8-2.5}$.

The experimental X-ray, SEM and Auger results concerning oxygen incorporation into MgB_2 crystal structure are supported by *ab initio* calculations of the electronic structure, binding energy and enthalpy of formation [1, 2].

As indicated by SEM and Auger study, some oxygen is usually present in superconducting MgB_2-based materials (bulk, thin films, and wires). The matrices phases of bulk MgB_2 contain rather small amount of oxygen while the high amount of dispersed inclusions or areas with the close to MgBO composition are present in them. X-ray phase analysis with the Rietveld refinement of several highly dense magnesium diboride-based bulks (demonstrated high level of superconducting characteristics and high critical current densities, in particular) showed that the materials superconducting matrices had near $MgB_{1.75}O_{0.25}$ composition instead of pure MgB_2. Besides, a small amount of MgO was observed in the materials as well. The calculation of the enthalpy of formation proves the possibility of oxygen solubility in MgB_2 and shows that formation of $MgB_{1.75}B_{0.25}$ is favorable. The results of *ab initio* calculations of the electronic structure and stability of the MgB_2 compounds with partial oxygen substitution for boron show that it is energetically preferable for oxygen atoms to ordered replace boron forming pairs or zigzag chains.

For the bulk MgB_2-based materials critical current densities J_c(10 K)=1.2-1.0·10^6 A/cm^2 in 0-1 T field, J_c(10 K)=9 ·10^4 A/cm^2 in 4 T field and J_c(20 K)=9-7 ·10^5 A/cm^2 in 0-1 T field were registered. For the thin (140 nm) MgB_2 films in zero magnetic field of magnetometer critical current densities J_c(10 K, $B||ab$)=1.8·10^7 A/cm^2; J_c(10 K, $B||c$)=1.5·10^7 A/см^2, J_c (20 K, $B||ab$)=7.8·10^6 A/см^2 , J_c(20 K, $B||c$)=6.4·10^6 A/см^2 have been measured and B_{C2}($B||ab$)=15 T at 22 K and H_{irr}($B||a$)=15 T at 19 K were observed.

[1] *T*.A. Prikhna, A.P. Shapovalov, G.E. Grechnev, V.G. Boutko, A.A. Gusev, A.V. Kozyrev, M.A. Belogolovskiy, V.E. Moshchil and V.B. Sverdun, Formation of nanostructure of magnesium diboride based materials with high superconducting characteristics, *Low Temperature Physics* **42**(5) (2016) 486–505.

[2] T. Prikhna, V. Romaka, A. Shapovalov, M. Eisterer, V. Sokolovsky, H. Weber, G. Grechnev, V. Boutko, A. Gusev, A. Kozyrev, W. Goldacker, V. Moshchil, V. Sverdun, T. Habisreuther, Ch. Shchmidt, V. Kovylaev, V. Shaternik, M. Karpets, A. Shaternik, Structure and Properties of MgB_2 Bulks, Thin Films and Wires, *IEEE Transactions on Applied Superconductivity* (in press June 2017), doi: 10.1109/TASC.2016.2638201.

Simulation of Remagnetization in Composite Structures

V. Sohatsky, G. Parhomchuk, V. Laichuk

Taras Shevchenko National University of Kyiv, Ukraine

Composite structures, having components with the different properties (in particular, ferromagnetic and piezoelectric or magneto-electric nanolayers) are of considerable interest for use in spintronics (or straintronics) as memory or logic devices, microwave filters or integrated photonic cells. [1]. The problems of remagnetization of such structures are the difficulties of nanosized magnetic field localization and correspondent large enough energy losses; necessity of high speed magnetization switching with a reliable arrangement of logic operations, etc. The experimental investigations confirmed the possibility of effective remagnetization of YIG film crystal structures as well as the amorphous ferromagnetic Fe nanolayers under mechanical strain while they being in a rigid contact with the piezoelectric PZT [2].

The calculations of optima parameters of such structures allowed to adjust operating characteristics of composite cells for various possible applications. The performed research are based on energy balance equations method within which the 3D diagrams of the total magnetization energy vs intensities of the applied magnetic field and/or mechanical strain were plotted. The equilibrium states of magnetization in ferromagnetics were determined from the coordinates of the energy minima and correspondent remagnetization curves (magnetic hysteresis loops) were calculated and depicted according to the sequence of these coordinates. Thus obtained curves were in a good agreement with the experimental ones, taken magnetooptically by means of Faraday and Kerr effects.

The results of simulation confirmed the possibility of variation of the hysteresis loops (operating characteristics) shape from a linear to almost rectangular by changing either the external influence (in particular, the direction of the applied magnetic field or mechanical strain), or inherent parameters of the structures (e.g. the relative orientation of uniaxial anisotropy axes in the nanolayers). The plotted energy diagrams also helped to explain the origin of the "intersecting" loops (with non-monotonic change of the magnetization vector orientation) as complex exchange/magnetostatic interaction of the magnetizations in adjusted layers with differently oriented anisotropy axes. Useful evaluations of the frequency characteristics of remagnetization were also done for some another compositions of magnetic nanolayers, such as in particular, permalloy or Eu, Tm and Dy orthoferrites.

A computer program created on JS allowed to promptly observe changes of the shape of calculated magnetic hysteresis curves in dynamics for wide variety of the specified magnetic, electric and mechanical parameters of the above composite structures.

[1] X. Tang, H. Su, H. Zhang, and N.X. Sun, Voltage-impulse-induced dual-range nonvolatile magnetization modulation in metglas/PZT heterostructure, *Appl. Phys. Lett.* **109** (2016) 202903.

[2] I.V. Zavislyak, V.P. Sohatsky, M.A. Popov, G. Srinivasan, Electric-field-induced reorientation and flip in domain magnetization and light diffraction in an yttrium-iron-garnet/lead-zirconate-titanate bilayer, *Phys. Rev. B* **87** (2013) 134417.

Active LR Integrator Circuit with Ferrite Core

Piotr Gazda[1,*], Michał Nowicki[1,*], Maciej Kachniarz[2,*]

[1]*Institute of Metrology and Biomedical Engineering, Warsaw University of Technology, sw. Andrzeja Boboli 8, 02-525 Warsaw, Poland*
* *{p.gazda, m.nowicki}@mchtr.pw.edu.pl*
[2]*Industrial Research Institute for Automation and Measurements, al. Jerozolimskie 202, 02-486 Warsaw, Poland*
* *mkachniarz@piap.pl*

There are many types of magnetic fluxmeters. For the reason of flexibility of the system and low cost, the most popular implementation is search coil and integrator. The operation of this system is based on Faraday's induction law. Contemporary systems mostly use active RC integrator circuits. Fundamental difficulty connected with analog method is the integrator drift. This effect is the more inconvenient, the longer is the measurement time. It is possible to control drift by compensating it, or by resetting the circuit, but it is complicated, and requires additional subsystems.

The following paper presents the idea of the active integrator circuit based on inductive and resistance components. Such design allows to eliminate the time drift of the circuit, which is undesired phenomenon resulting from capacitive components utilized in classic constructions.

In the article research with metal oxide (ferrite) core of the inductive component was performed. The paper indicates advantages and disadvantages of such solution.

This type of integrator circuit can be used to develop the drift-free fluxmeter for investigation of ferromagnetic hysteresis phenomenon in soft magnetic materials. Moreover, the main advantage of proposed system lies in innate ability for continuous, drift-free operation, which may be useful in novel NDT methods, as well as magnetoelastic sensors transducers. The paper presents concept of the integrator circuit. The SPICE simulations were performed to validate the presented idea. Finally the developed solution was tested, and obtained results confirm the correctness of the integrator circuits operation.

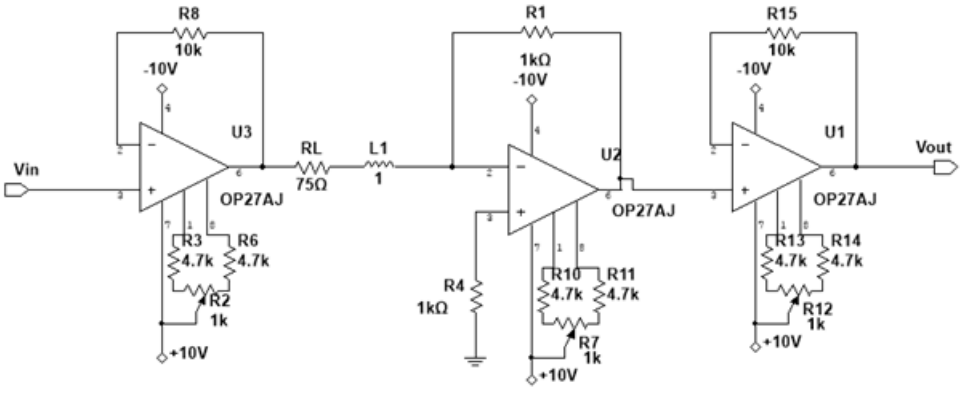

Fig. Model of the LR integrator circuit design in SPICE software

Automatic Measurement Station for Ferrite Materials Testing

T. Charubin[1,*], P. Nowak[2,*]

[1]*Institute of Metrology and Biomedical Engineering, Warsaw University of Technology, Św. Andrzeja Boboli 8, 02-525 Warsaw, Poland*
* *t.charubin@mchtr.pw.edu.pl*
[2]*Industrial Research Institute for Automation and Measurement PIAP Aleje Jerozolimskie 202, 02-486 Warsaw, Poland*
* *pnowak@piap.pl*

Many modern electronic devices are made using inductive elements. Often, the magnetic cores in these elements are made of iron oxides, such as ferrites. Selection of the right core is essential for the proper work of a device, for example switching mode power supplies, filters, chokes and transformers. Each type of material is used for different application, and the core parameters need to be examined. For this purpose an automated measurement station designed for ferrite magnetic cores testing was made.

The system is a classical hysteresisgraph, which generates alternating magnetic field in the sample and measures the sample's response, which is the change of the material's magnetization. Key parameters which result from such measurements are relative permeability curve, coercivity, saturation induction, remanence and power loss changes in the function of various parameters of magnetizing current.

The test stand consists of KEPCO BOP 36-6M high resolution U/I converter and Lakeshore Model 480 fluxmeter controlled by a PC with NI PCI 6221 National Instruments Data Acquisition Device running under LabView software.

System allows for conducting series of measurements, with variable magnetizing fields parameters such as amplitude, frequency and shape. The shape used varies depending on the sample's application. Using iteration method, the station also allows for generating linear and sinusoidal magnetic flux in the samples, which ensures lower losses than when using linear and sinusoidal magnetizing field. This in turn allows for true magnetic parameters measurements, without the eddy current disruption. The system also allows for measurements –under variable compressing force, using external press and integrated force sensor, and under variable temperature in -50˚C - +200˚C range, using additional PolyScience cryostat.

The paper presents detailed configuration of the test stand, shows the process of measurement and presents data acquired from a reference sample.

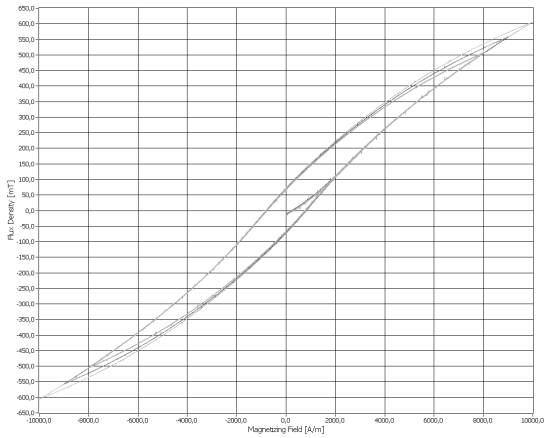

Fig.1. Reference sample hysteresis curves

Reduction of Eddy Current Losses in Multilayer Amorphous Alloys Cores with the Ribbons Surface Oxidation

P. Frydrych[1,*], P. Nowak[2,*]

[1]*Institute of Metrology and Biomedical Engineering, Warsaw University of Technology, Św. A. Boboli 8, 02-525 Warsaw, Poland*
* *p.frydrych@mchtr.pw.edu.pl*
[2]*Industrial Research Institute for Automation and Measurements PIAP, Al. Jerozolimskie 202, 02-486 Warsaw, Poland*
* *pnowak@piap.pl*

In this paper possibility of improvement of cross-layer resistivity in multilayer magnetic cores was studied. It is known, that amorphous alloys are only possible to be obtained in shape of very thin ribbons and nanowires. Due to their thickness, magnetic cores for transformers and other devices have to be made of many layers of ribbons [1]. They exhibit great magnetic properties such low hysteretic losses, high saturation induction and high magnetic permeability. Unfortunately their low resistivity causes high losses for frequencies higher than 50Hz mostly due to the eddy current phenomena. In this research ribbons surface was oxidised in order to increase multilayer impedance.

Amorphous alloys are usually made of steel with more than 50% of iron. Most common iron oxide is a rust, which can increase risk of pitting corrosion. To prevent that rust has to be reduced to FeO oxide.

Hysteresis loops of cores made of oxidised ribbons were compared with unoxidised ones for wide range of frequencies. Cross-layer resistivity was significantly improved.

[1] R. Hasegawa, A.C. Lee, L.A. Lowdermilk, Amorphous alloy core distribution transformers, *Proceedings of the IEEE*, Vol.79, Issue 11, Nov 1991.

Transverse Field Effect in GPI Ferroelectrics: Microscopic Consideration

I.R. Zachek[2], R.R. Levitskii[1], A.S. Vdovych[1], I.V. Stasyuk[1]

[1]*Institute for Condensed Matter Physics of the National Academy of Sciences of Ukraine, 1 Svientsitskii Str, 79011 Lviv, Ukraine*
[2]*Lviv Polytechnic National University, 12 Bandera Str., 79013 Lviv, Ukraine*

Glycinium phosphite (GPI) crystal belongs to the family of ferroelectrics with hydrogen bonds. It is usually supposed that the phase transition to the ferroelectric phase at T=225K is connected with ordering of protons on bonds. The corresponding model was proposed in [1]. An important feature of GPI, that was revealed experimentally [2], consists in possibility of reorientation of the local dipole moments (formed by protons and the adjacent glycine groups) by the external electric field E_z perpendicular to the ferroelectric axis OY. It manifests in the proportional to E_z^2 decrease of T_c and in the increasing with E_z anomalies of transverse permittivity ε_{zz}. The latter effect was explained in [2] assuming the smearing of phase transition in the presence of field E_z.

Starting from the model [1] we extend in this work the investigation of field effects in GPI. The approach is supplemented by allowance for piezoelectric coupling of the proton subsystem with the lattice strain. Calculations of thermodynamic, dielectric and elastic characteristics are performed in the frames of the two-particle cluster approximation. At the proper choice of the model parameters the satisfactory quantitative description of the wide set of the available experimental data has been obtained.

A separate attention is paid to the E_z influence on the permittivity ε_{zz} and polarization P_z. It is shown that the quite good description of the measured in [2] temperature dependence of ε_{zz} can be achieved, when the presence of the small longitudinal component E_y (of the order of ~$0.05E_z$) is supposed (fig.1). Such a component could appear due to incomplete reorientational relaxation of the glycine groups; one can not exclude, also, the possibility of some deflection of the applied transverse field from the OZ-axis during experiment. We have calculated also the $P_y(T)$ and $P_z(T)$ dependences at various values of E_z. The plots for $P_z(T)$ presented in fig.2 confirm the parabolic lowering of T_c under influence of E_z.

Our consideration shows, that along with the reordering of protons, the remarkable role in the field effects in GPI can be served by the glycine groups.

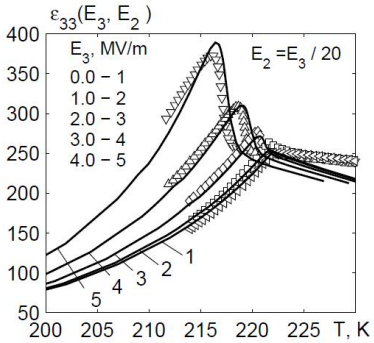

Figure 1. The temperature dependence of dielectric permittivity ε_{zz} at different values of field E_z and at field E_y=0.05E_z. Symbols are experimental data taken from [2].

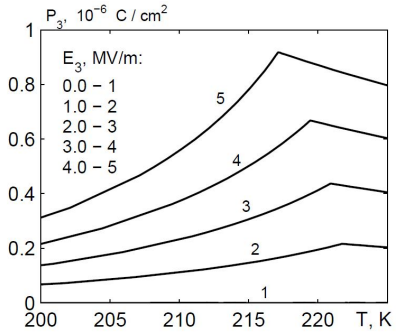

Figure 2. The temperature dependences of the P_z component of polarization of GPI crystal.

[1] I.V. Stasyuk, O.V. Velychko, *Ferroelectrics* **300** (2004) 121.
[2] I. Stasyuk, Z. Czapla, S. Dacko, O. Velychko, *J. Phys.: Condens Matter* **16** (2004) 1963.

The Effect of Alkali-Element Substitution on Structural and Magnetic Properties of Bi-2212 Superconductors

B. Özkurt[1,2]

[1] *Department of Nanotechnology and Advanced Materials, Graduate School of Natural and Applied Science, Mersin University, Mersin, Turkey*
[2] *Department of Energy Systems Engineering, Faculty of Tarsus Technology, University of Mersin, Mersin, Turkey*

In the present work, the structural and magnetic properties of Bi-2212 ceramics with both Na doped and Li-Na co-adding are summarized. All samples have been synthesized by the conventional solid state reaction method. It is clearly observed that the doping and adding of alkali elements into Bi-2212 ceramics at the appropriate values ensures positive effect on their T_c and J_c values. The automatically obtained lattice parameters from XRD measurements show that all samples have the ideal composition of 2212 phases. Additionally, SEM micrographs show that the size of grains can be increased by the presence of alkali elements at their optimal values in BSCCO superconductors, which strongly affect J_c values.

Analysis of Observed Voltage Oscillations in Silver Doped High Temperature Superconductor YBCO

A. Altinkok[1], M. Olutas[2], H. Yetis[2], A. Kiliç[2] and K. Kiliç[2]

[1]*Giresun University, Department of Electrical and Electronics, Giresun, Turkey*
[2]*Abant Izzet Baysal University, Department of Physics, Bolu, Turkey*

The influence of bi-directional square wave (BSW) current on the evolution of $V-t$ curves as functions of the amplitude and period of the BSW current were investigated at different temperatures and external magnetic fields. It was observed that slow transport relaxation measurements result in regular sinusoidal voltage oscillations. The symmetry in the voltage oscillations was attributed to the elastic coupling between the flux lines and the pinning centers along grain boundaries and partly inside the grains. This case was also correlated to the equality between flux entry and exit along the YBCO/Ag sample during regular oscillations. It was shown that the voltage oscillations can be described well by an empirical expression $V(t) \sim \sin(wt+f)$.We found that the phase angle f generally takes different values for the repetitive oscillations. We suggest that, for each cycle observed, the initial conditions of the flux lines joining the motion are determined by the distribution of flux lines formed by the former cycle and, thus, every cycle prepares new initial condition for the next cycle. Therefore, it is natural to expect such phase difference between successive oscillations. Fast Fourier Transform analysis of the $V-t$ oscillations showed that the oscillation period is comparable to that (P_I) of the BSW current. This finding suggests a physical mechanism associated with charge density waves (CDWs), and, indeed, the weakly pinned flux line system in YBCO/Ag resembles the general behavior of CDWs. At certain values of P_I, amplitude of BSW current, H and T, the YBCO/Ag sample behaves like a double-integrator, since it converts the BSW current to sinusoidal voltage oscillations in time.

Self-Shunted Josephson Junctions with Ultrathin Oxide Interlayers – Progress and Outlook

M. Belogolovskii[1], E. Zhitlukhina[1,2], V. Lacquaniti[3]

[1]*Vasyl' Stus Donetsk National University, 021021 Vinnytsia, Ukraine*
[2]*O.Galkin Donetsk Institute for Physics and Engineering, 03028 Kyiv, Ukraine*
[3]*National Institute for Metrological Research, 10135 Turin, Italy*

Conventional Josephson junction consists of two superconducting (S) electrodes coupled by a weak link, a thin oxide barrier (I) or a short section of a normal (N) metal. Dynamics of the Josephson device strongly depends on the McCumber-Stewart damping parameter β_c, a product of the characteristic Josephson frequency and the decay time $\tau = R_{sg}C$, where R_{sg} and C are subgap resistance and capacitance of the junction. Nonhysteretic current-voltage (*I-V*) characteristics needed for most applications like voltage metrology and single-flux quantum logic is achieved when β_c is less than unity. To get rid of the double-valued *I-V* curves, the subgap resistance in the operating voltage region R_{sg} should be suppressed below the junction resistance R_N in the normal state. The simplest way would be to replace an insulating weak link with an N one. Another possibility is an external shunt resistor but such procedure results in a considerable complication of the circuitry design due to additional wiring and a significant parasitic inductance which limits its high frequency operation.

In this work, we describe a new technology for realizing *internally shunted* Josephson junctions with a single-valued *I-V* trace which employs an oxide barrier containing a desired resistive component. Two possible ways are discussed, ultra-thin amorphous AlO_x oxides with very strong local fluctuations of the barrier height and thickness and comparatively thick I films with embedded metallic granules. In the first case, the main mechanism of the charge transport is direct quantum tunneling through an inhomogeneous barrier while in the second case it is based on the quantum-percolation process along resonance trajectories. We show that in both cases the distribution function of the weak-link transparency D is bimodal with a significant amount of "open" channels with $D \leq 1$ and many more "closed" channels with $D << 1$. It is demonstrated that the adequate normalization of experimental curves measured in the superconducting state permits to eliminate the only adjustable parameter and to test the feasibility of a bimodal transparency distribution in Josephson junctions *without any fitting parameters.*

The first class of intrinsically shunted Josephson junctions proposed by us are Nb/Al-AlO_x-Nb Josephson junctions fabricated using a standard Nb-technology but with an insulating barrier thinner than that in conventional tunnel Nb-AlO_x-Nb trilayers and a thick Al interlayer comparing to double-barrier Nb-AlO_x-Al-AlO_x-Nb heterostructures. The aim of introducing the Al interlayer with the thickness d_{Al} has been two-fold: (i) to protect the junction against the impact of pinholes in the ultra-thin Al-oxide barrier and (ii) to improve the temperature stability of the supercurrent at the operating temperature of 4.2 K. The second class of the self-shunted S devices are those with low-height and, hence, comparatively thick oxide interlayers. Transport across them can be dominated whether by tunneling via those configurations of localized states that permit resonant transmission of electrons or by direct transport across extremely thin filaments connecting two sides of the trilayer. We present related theoretical results that are compared with experimental data measured in the INRiM, Turin, Italy.

At last, we discuss future prospects of the superconducting heterostructures with ultra-thin oxide interlayers. in particular, possibility to form a self-aligned filament during the electrical breakdown in a transition-metal oxide.

The work was supported by the Ministry of Education and Science of Ukraine.

Nanostructured γ-Fe_2O_3: the Correlation between Physical Characteristic and Synthesis Conditions

V. Kotsyubynsky[1], A. Hrubiak[2], V. Moklyak[2], L. Mohnatska[1], S. Fedorchenko[1]

[1]*Vasyl Stefanyk Precarpathian National University, 57 Shevchenko Str., 76018 Ivano-Frankivsk, Ukraine*
[2]*Institute of Metal Physics, National Academy of Science, 36 Acad. Vernadsky Boulevard, 03680 Kyiv, Ukraine*

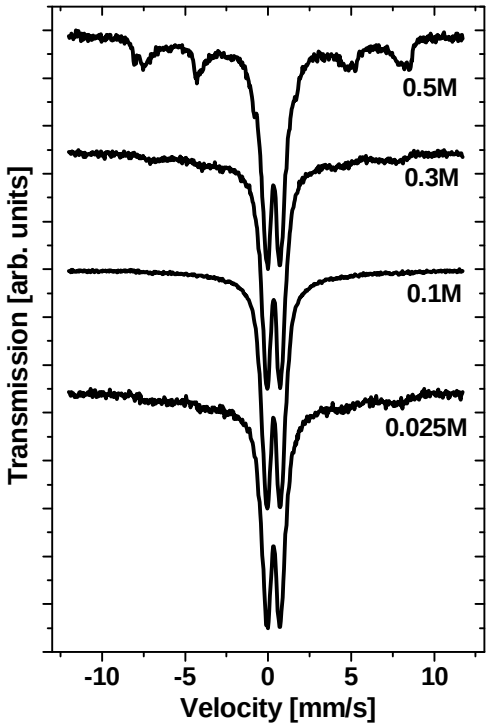

Fig.1. Mossbauer spectra of γ-Fe_2O_3 samples obtained at the different precursors molarity

Nanostructured iron oxides, in particular γ-Fe_2O_3, have numerous applications – both biomedical (magnetic hyperthermia, drug and gene delivery, magnetic resonance imaging) and technological (memristors, cathodes for lithium batteries and pseudocapacitors). The efficiency of material using in each sphere depends on the peculiarities of the crystal and magnetic microstructure, particles sizes and morphology. The investigation of synthesis conditions effect on γ-Fe_2O_3 properties is important and topical.

The samples of γ-Fe_2O_3 were obtained by slowly mixing of $Fe(NO_3)_3 \cdot 9H_2O$ and $C_6H_8O_7 \cdot H_2O$ solutions (molarity 0.025M, 0.1M, 0.3M, 0.5M) with the next iron citrate xerogel annealing at 200ºC [1]. The sizes of coherent scattering areas growth in the range 6-12 nm with the increase of initial molarity were determined (XRD data). The correlation between particles sizes and synthesis conditions was observed by Mossbauer spectroscopy as a change of Fe^{57} nuclei relative contents with different local surroundings in the inner and outer layers of particles (Fig.1). It was determined that the obtained oxides are the systems of monodomain particles with fluctuated magnetic moments. All obtained materials are characterized by porous structure (scanning electron microscopy data) as a result of organic products evaporation. The tendency to porosity increasing with the molarity enlarging was found. The frequency dependences of samples complex conductivity (impedance spectroscopy data) are typical for disordered semiconductors and explained by small polaron hopping mechanism between metal sites with the valence interchange process The dc-conductivity and charge carriers hopping frequency both despite with the particle size enlarging. Adsorption/desorption isotherms for all samples have H4 hysteresis (typical for mesoporous materials). Specific surface areas (low temperature nitrogen adsorption data) non-linear vary depending on the molarity of precursors in a range of 95-165 m^2/g with the maximum for 0.3M sample. Dependences of the pores volume on pores size are characterized by the pore sizes in the range of 3-7 nm. The contribution of small mesopores (diameter about 2-3 nm) is insignificant. For all materials optical band gap energies (optical adsorption spectroscopy data) is close to 2 eV and correspond to direct transitions. The relationship between the effective band gaps and the average particle sizes based on the Brus model was proposed

[1] V. Kotsyubynsky, V. Moklyak, A. Hrubiak, Synthesis and Mossbauer Studies of Mesoporous γ-Fe_2O_3, *Materials Science-Poland* **32**(3) (2014) 481-486.

Refinement of the Modulated Structures of Pb-Free and Pb-Doped Bi-2223 HTSC

O. Shcherban[1,2], L. Akselrud[1], E. Giannini[3], R. Gladyshevskii[1]

[1]*Department of Inorganic Chemistry, Ivan Franko National University of Lviv, Lviv, Ukraine*
[2]*Scientific Consulting Company "Structure-Properties", Lviv, Ukraine*
[3]*Département de Physique de la Matière Quantique, University of Geneva, Geneva, Switzerland*

Among the members of the high-temperature superconducting Bi-based family $Bi_2Sr_2Ca_{n-1}Cu_nO_{2n+4+\delta}$ (n = 1, 2, 3), the three-layer compound $Bi_2Sr_2Ca_2Cu_3O_{10+\delta}$ (hereafter Bi-2223) is the most attracting one, because of its high critical temperature 110 K, its better transport properties, and its potential industrial applications. However, it is difficult to synthesize the Bi-2223 phase even at the laboratory scale. Partial substitution of Pb for Bi was found to improve the stability, facilitate the synthesis, and enhance the superconducting properties. Due to oxygen off-stoichiometry and differences in the translation periods of the atom layers, the real crystal structures of these compounds are complex and exhibit incommensurate modulations [1]. The superstructures of $Bi_2Sr_2CuO_{6+\delta}$ and $Bi_2Sr_2CaCu_2O_{8+\delta}$ (Bi-2201 and Bi-2212, respectively) have been refined on single-crystal diffraction data [2, 3].

We here report refinements of the structures of Pb-free and Pb-doped Bi-2223 phases from single-crystal X-ray diffraction. Single crystals were grown by the Vapor-Assisted Travelling Solvent Floating Zone method [4, 5]. Diffraction data were collected on a Stoe IPDS II diffractometer equipped with Mo $K\alpha$ radiation, a graphite monochromator, and an imaging plate. The structures were refined by the full-matrix least-squares method based on F, using the program package WinCSD [6]. The modulation was found to be approximately commensurate with a vector $q \sim 0.2a^*$. The reflections could be indexed in a satisfactory way in large primitive orthorhombic cells, which correspond to 5-fold supercells of the conventional side-face centered orthorhombic cells.

The average structures were refined in the orthorhombic space group $A2aa$ with cell parameters a = 5.4210(7), b = 5.4133(6) and c = 37.010(7) Å for the Pb-free phase, and a = 5.3952(14), b = 5.4130(10) and c = 37.042(11) Å for the Pb-doped phase. The Bi site was split into two positions, the two partly occupied sites showing the largest difference in the x coordinates, which is in agreement with a modulation along a. The commensurate approximant superstructures were refined in the orthorhombic space group $Pnnn$, using a 5-fold supercell. An additional oxygen site within the BiO layers was identified.

Refinements of the modulated structures were performed in the (3+1)D-superspace group $A2aa(\alpha 00)000$, considering up to 2nd order satellites corresponding to a modulation vector q = (0.2, 0, 0). A longitudinal displacement modulation of the atoms, with increasing magnitude from the CuO_2 to the BiO layers, was confirmed. The transverse displacement modulation showed the largest magnitude for the Cu and Ca atoms.

[1] R.E. Gladyshevskii, Ph. Galez, *Handbook of Superconductivity*, ed. Ch.P. Poole et al., Academic Press, 1999, pp. 267-431.
[2] M. Onoda, M. Sato, *Solid State Commun.* **67** (1988) 799-804.
[3] R.E. Gladyshevskii, R. Flükiger, *Acta Cryst. B* **52** (1996) 38-53.
[4] E. Giannini, V. Garnier, R. Gladyshevskii, R. Flükiger, *Supercond. Sci. Technol.* **17** (2004) 220-226.
[5] E. Giannini, N. Clayton, N. Musolino, R. Gladyshevskii, R. Flükiger, *Frontiers in Superconducting Materials*, ed. A.V. Narlikar, Springer-Verlag, 2005, pp. 739-764.
[6] L. Akselrud, Yu. Grin, *J. Appl. Crystallogr.* **47** (2014) 803-805.

The Physical Properties of Mettalic Au-Added Bi-2212 Superconductors

B. Özkurt[1,2], U. Öztornacı[1]

[1]*Department of Nanotechnology and Advanced Materials, Graduate School of Natural and Applied Science, Mersin University, Mersin, Turkey*
[2]*Department of Energy Systems Engineering, Faculty of Tarsus Technology, University of Mersin, Mersin, Turkey*

In this study the electrical and magnetic properties of $Bi_{1.8}Sr_2Au_xCa_{1.1}Cu_{2.1}O_y$ (x=0.0, 0.05, 0.1 and 0.2) samples with added metallic gold are invesitigated. The all samples are prepared using the standart solid-state reaction method. Resistivity values obtained at 150 K significantly decrease with increasing Au content, indicating the positive effect of Au addition in low contents into Bi-2212 ceramics. M-H measurements were performed at T = 10 K and 25 K, respectively. In addition, J_c values of the samples were calculated from their magnetic hysteresis loops using the Bean's model. The highest Jc values was obtained for sample including x=0.2 Au content.

Interaction of the Components in the System Ba-Tb-Cu-O and Related Systems

O. Zaremba, R. Gladyshevskii

Ivan Franko National University of Lviv, 6 Kyryla i Mefodiya Str., UA-79005 Lviv, Ukraine

The interaction of the components in the *A*-*R*-Cu-O systems, where *A* is an alkaline-earth and *R* is a rare-earth metal, has attracted considerable interest for a long time. The compounds of these systems are usually characterized by layered structures and are first of all interesting as high-temperature superconductors. The most prominent among them is undoubtedly $YBa_2Cu_3O_7$ (*YBCO*), the crystal structure and properties of which have been studied meticulously. The interaction of the components in the system Ba-Y-Cu-O and related systems with other alkaline-earth and rare-earth metals has also been widely investigated [1]. In this work we focus on the system Ba-Tb-Cu-O, and some related systems, for which data in the literature are scarce.

Polycrystalline samples of the BaO-Tb_2O_3-CuO system were prepared by solid-state reaction of appropriate amounts of high-purity carbonates and oxides at 1173 K in air in two 24-hour stages. Firstly the reagents were mixed and heated in a corundum crucible to decompose the carbonates. Then, after cooling to room temperature, the mixtures were reground to achieve homogeneity, pressed into pellets and sintered again. Phase and structure analyses were carried out on X-ray powder diffraction data (DRON 2.0M diffractometer, Fe K_α radiation). Samples of nominal composition $A_{0.5}Tb_{0.5}TO_3$, where *A* = Ca, Sr or Ba, *T* = Ni or Zn, were prepared in similar way.

The isothermal section of the phase diagram of the BaO-Tb_2O_3-CuO system at 1173 K was constructed based on the investigation of fifteen samples. The existence of the compounds $BaTbO_3$ ($SrZrO_3$ structure type, *I*4/*mcm*, a = 0.6034(1), c = 0.8576(1) nm, R_B = 0.052) and $Ba_{44}Cu_{45}O_{90}$ (own structure type, *Im*-3*m*, a = 1.8266(3) nm, R_B = 0.237) was confirmed in the pseudo-binary BaO-Tb_2O_3 and BaO-CuO systems, respectively. It was established that the interaction of the components in the ternary region of the BaO-Tb_2O_3-CuO system is characterized by the absence of compounds. The only compound reported in the literature, $TbBa_2Cu_3O_7$ with orthorhombic $YBa_2Cu_3O_7$ structure type [2], was not observed under the conditions of our study. The $BaTbO_3$ phase is in equilibrium with the $Ba_{44}Cu_{45}O_{90}$ and CuO phases. Hence, there are three three-phase and two two-phase regions in the system. It should be noted that, during the synthesis, the initial cubic Tb_2O_3 phase with $(Mn_{0.5}Fe_{0.5})_2O_3$ structure type was oxidized into the rhombohedral Tb_7O_{12} phase with Pr_7O_{12} structure type.

$Ba_{0.5}Tb_{0.5}ZnO_3$ and $Sr_{0.5}Tb_{0.5}ZnO_3$ were found to be two-phase samples, which contained in equilibrium $BaTbO_3$ ($SrZrO_3$ structure type, *I*4/*mcm*, a = 0.6039(1), c = 0.8578(1) nm, R_B = 0.099), or $SrTbO_3$ ($GdFeO_3$ structure type, *Pnma* a = 0.5945(1), b = 0.8347(2), c = 0.5879(1) nm, R_B = 0.160), and ZnO. The investigation of the samples with nominal compositions $Ca_{0.5}Tb_{0.5}ZnO_3$ and $Ca_{0.5}Tb_{0.5}NiO_3$ showed the presence of phases that correspond to the reagents only – CaO, Tb_7O_{12} and ZnO (or NiO), in appropriate ratios.

[1] P. Villars, K. Cenzual (Eds.), Pearson's Crystal Data – Crystal Structure Database for Inorganic Compounds, ASM International, Materials Park, OH, USA, Release 2014/15.

[2] H. Ouchi, Preparation and superconducting properties of *Ln*-Ba-Cu-O ceramics, *Ferroelectrics* **95** (1989) 215-220.

Temperature Influence of the Functional Properties of Inductive Components with Metal Oxide Magnetic Cores

D. Jackiewicz[1], M. Kachniarz[2], A. Bieńkowski[1]

[1]*Institute of Metrology and Biomedical Engineering, Warsaw University of Technology, sw. A. Boboli 8, 02-525 Warsaw, Poland*
[2]*Industrial Research Institute for Automation and Measurements PIAP, Al. Jerozolimskie 202, 02-486 Warsaw, Poland*

Inductive coils and transformers are commonly used components in electronics. These elements are composed of a ferromagnetic core and windings. The most common material used for the cores of inductive components are ferrites.

Ferrites are ceramic materials, whose main component is iron oxide (Fe_2O_3). Ferrites are produced by sintering a mixture of oxides: Fe_2O_3, MnO, NiO, MgO, CuO, ZnO, SrO, BaO. They are ferrimagnetic and electrically nonconductive materials. Ferrites have a higher resistance and much lower energy losses than metallic materials.

Main functional properties of the ferrite cores are inductance and power loss. The cores are often working in environmental conditions other than normal conditions. Especially temperature is very often differing from its normal value. These changes may come from heating of the elements during work or from changes in the ambient temperature. Changes of the value of inductance may affect the parameters of the electrical circuit. The increase of the value of power losses leads to higher energy consumption.

The paper presents the results of investigation on the influence of temperature on the inductance and power loss in the ferrite cores. Special measurement system composed of hysteresisgraph, cryostat and computer was utilized to perform the experiment. The cores used during the investigation had closed magnetic circuit. In order to perform measurements of magnetic properties of the material, two sets of windings (magnetizing and sensing) were made on each core. The cores were placed in a cryostat, which was used to set the temperature value within the range from -20 to +60°C. The magnetic properties were measured by the hysteresisgraph.

The obtained results confirmed the change in the value of inductance and power loss under the influence of temperature. These results should be taken into account in the design of electronic circuits containing such elements.

[1] M. Kachniarz, J. Salach, R. Szewczyk, A. Bieńkowski, Temperature Influence on the Magnetic Characteristics of Mn-Zn Ferrite Materials, in Progress in Automation, Robotics and Measuring Techniques Volume 3 Measuring Techniques and Systems, **352** (2015) 121–127.

[2] A. Bieńkowski, K. Rożniatowski, R. Szewczyk, Effects of stress and its dependence on microstructure in Mn–Zn ferrite for power applications, *Journal of Magnetism and Magnetic Materials* **254–255** (2003) 547–549.

Demagnetizing Field in a Sample of Magnetically Ordered Medium

O. Tychko*

Taras Shevchenko Kyiv National University, Department of Radiophysics, Electronics and Computer systems, 64/13 Volodymyrska Str., 01601 Kyiv, Ukraine
* pasat@univ.kiev.ua

Spatial distribution of a magnetization vector **M** orientation in a volume of a open form sample of magnetically ordered medium depends on a local value of "internal" (Maxwellian) magnetic field $\mathbf{H_i}$. This field $\mathbf{H_i}$ does not have direct physical sense, as far as it is impossible to measure in the sample volume. However the field $\mathbf{H_i}$ can be considered as formal value connected with an external field **H** and a demagnetizing field $\mathbf{H_d}$: $\mathbf{H_i} = \mathbf{H} - \mathbf{H_d}$. The field $\mathbf{H_d}$ of a sample is proportional to medium magnetization **M** and is a function of demagnetizing factor $|\mathrm{N}|$: $\mathbf{H_d} = |\mathrm{N}|\mathbf{M}$. In general case of arbitrary shape of a sample that is placed in arbitrary oriented field **H** the demagnetizing factor is determined by sample shape and is a tensor of the second rank. Only samples in the form of ellipsoids of revolution those are made of homogeneous medium material and are placed in a uniform magnetic saturation field have homogeneous demagnetization field. For such samples it is obtained exact analytical expressions for demagnetizing factor [1]. For samples of no ellipsoidal shape the demagnetizing factor depends on not only the sample shape but also the material properties of the sample medium and magnetization distribution in the sample volume as well as supervision coordinates. The empirical values of the factor N for different forms samples are given in the form of graphs or tables [1]. In most cases the factors N are determined by experimental measurements of samples stray fields [2]. The field $\mathbf{H_d}$ in the volume of periodic domain structure was investigated only theoretically [3].

Local optical exposure by linearly polarized radiation of a magnetically ordered medium with photomagnetic properties [4] leads to formation of a magnetization nucleus in the irradiated medium volume [5]. The photoinduced nucleation in volumetric sample of magnetically ordered m3m medium with negative (cubic) magnetocrystalline anisotropy energy always takes place in the field $\mathbf{H_i}$ (at $\mathbf{H_i} = \mathbf{H_n}$, where $\mathbf{H_n}$ is a nucleation field [5]) and duration of the sample exposure is determined by the field $\mathbf{H_i}$ value. Above-mentioned dependence opens up possibilities of direct experimental measurement of local value and/or spatial distribution of the demagnetizing field $\mathbf{H_d}$ in a volume of arbitrary shape sample that is placed in arbitrary magnetic field **H** .

Local values and spatial distribution (at **H**=0) and spatial distribution (at sample saturation state) of demagnetizing field $\mathbf{H_d}$ are obtained experimentally in a volumes of the sample domain structure (at **H**=0) and uniformly magnetized sample respectively. All results where obtained at local irradiation of single crystal (110) – plates of ferrite – garnet $Y_3Fe_{4.96}Si_{0.04}O_{12}$ at $T = 77\ K$

[1] Du-Xing Chen, E. Pardo, A. Sanchez, Demagnetizing factors of rectangular prisms and ellipsoids, *IEEE Trans. on Magn.* **38**(4) (2002) 1742 – 1752.
[2] Q.M. Wang, H.F. Qin, Q.S. Liu, T. Song, Room temperature sample scanning SQUID microscope for imaging the magnetic fields of geological specimens, *Appl. Mechanics and Materials* **475-476** (2013) 3-6.
[3] S.D. Mal'ginjva, R.A. Doroshenko, N.V. Shul'ga, Static and high - frequency magnetic properties of stripe domain structure in a plate of finite sizes, *JMMM* **296**(1) (2006) 13 – 24.
[4] E.L. Nahaev, Photoinduced magnetism and conduction electrons in magnetic semiconductors, *Phisica Status Solidi (b)* **145**(1) (1988) 11 – 64.
[5] V.F. Kovalenko, O.V Tychko, Nucleatio during photoinduced spin – reorientation transition, *Functional Materials* **11**(3) (2004) 521 – 527.

Experimental Research for Domain Nucleation

O.Tychko*

Taras Shevchenko Kyiv National University, Department of Radiophysics, Electronics and Computer systems, 64/13 Volodymyrska Str., 01601 Kyiv, Ukraine
* pasat@univ.kiev.ua

As a rule the modern utilizations of magnetically ordered media is based on a change of an orientation of a magnetization vector **M** of local volume of homogeneously magnetized media in spatially non-uniform fields of various natures: magnetic, light, thermal, etc. Such **M** reorientation passes through formation of a magnetic nucleus (medium area with **M** orientation that is distinct from initial) near non-magnetic or magnetic defect of medium. These defects can exist or are formed in medium volume during external influence. Difficulties on a way of creation of the consecutive nucleation theory are caused both theoretical [1] and experimental [2] problems. They are caused by high sensitivity of formation conditions and parameters of a nucleus to the slightest variations of material properties of the medium. Exact conformity of the experimental results and theoretical dependences demands of a knowledge of local defect parameters (linear sizes, dispersion of material properties of the medium, etc.). In real media these parameters, as a rule, are unknown. Therefore the experimental researches supposing purposeful and supervised change of magnetic "activity" of defects are necessary for formation of the general representation about nucleation in magnetically ordered media. Photoinduced magnetic defect [3] satisfies these requirements.

An optical exposure by linearly polarized radiation of a magnetically ordered medium with photomagnetic properties leads to change of its initial magnetocrystalline anisotropy energy and appearance of a combine (magnetocrystalline and uniaxial photoinduced) magnetic anisotropy in the irradiated sample volume [4] that causes a formation of a photoinduced magnetic defect (irradiated region with spatially inhomogeneous distribution of magnetic energy density), an occurrence and change of a region with metastable initial magnetization state in magnetic defect volume [3] and a formation of a magnetization nucleus [5]. Linear dimensions and configuration of the photoinduced magnetic defect volume easily change by the choice of focusing degree and light spot form on the medium surface. Spatial dispersion of the magnetic anisotropy energy density in the defect volume is modified by the change of spatial distribution of an intensity of optical radiation in the cross section of light spot or orientations of a polarization vector of the linearly polarized optical radiation or duration of irradiation. Analytical expressions for above – mentioned dependencies are obtained [3].

Experimental values of nucleation fields [1] in the irradiated volume of single crystal (110) – disk of ferrite – garnet $Y_3Fe_{4.96}Si_{0.04}o_{12}$ at $T=77\,K$ are obtained at sample optical ($l=1.15\ mm$) irradiation with arbitrary orientation of polarization vector for light spot's cross-section of round and elliptic form on medium surface are presented.

[1] H. Kronmuller, T. Reininger, Micromagnetic background of magnetization processes in inhomogeneous ferromagnetic layer, *JMMM* **112**(1) (1992) 1-5.
[2] L.A. Pamyatnykh, G.A. Shmatov, G.S. Kandaurova, Nucleation of magnetic inhomogeneities in iron garnet films with mixed anisotropy, *Proc. VIII Europen magnetic materials and applictions conference*, 2000 p.285.
[3] O.V. Tychko, Photoinduced magnetic defect, *Book of Reports International Scientific Conference on Topical Problems of Solid-state Physics*, PhTT-2013, Minsk, 2013, vol.1, pp.196-198.
[4] V.F. Kovalenko, D.G. Makarov, O.V. Tychko, Photoinduced changes of magnetic anisotropy in substituted iron garnet, *J. of Alloys and Comp*. **369** (2004) 222-226.
[5] V.F. Kovalenko, O.V. Tychko, Nucleation during photoinduced spin - reorientation transition, *Functional Materials* **11**(3) (2004) 521-527.

The Power and Frequency Dependence of the Inverse Spin Hall Effect in La-YIG/Pt Heterostructures

Lichuan Jin, Yiheng Rao, Huaiwu Zhang

State Key Laboratory of Electronic Films and Integrated Devices, University of Electronic Science and Technology of China, Chengdu, 610054, China

SAMPLE FABRICATION AND EXPERIMENTAL DETAILS

La-YIG sample was fabricated by liquid phase epitaxy(LPE) with a thickness of 300 nm on gadolinium gallium garnet (GGG) substrates at temperature about 964℃. Lanthanum was used to expend the lattice parameter of YIG. The chemical formula can be written as $La_{0.07}Y_{2.93}Fe_5O_{12}$ which has better lattice match with GGG. The 10 nm Pt strip was deposited on La:YIG by DC sputtering way at growth rate of 42 nm/min. the strip has length of 3 mm and width of 200 μm. Two copper pad were deposited at the sides of Pt strip.

THE POWER AND FREQUENCY DEPENDENCE OF THE INVERSE SPIN HALL EFFECT

The measurement was carried out by flipping the La:YIG films onto a shorted co-plane waveguide. I_{SHE} voltage was measured through two pads. Agilent E8257D, SR830 lock-in amplifier, IT6153 DC power supply and Lakeshore 455 Gauss-meter are used for accurate measurement of inverse spin Hall voltage V_{ISHE}, as show in Fig. 1. The V_{ISHE} as function of microwave power are shown in Fig. 2(a)-(d). From Fig. 2, it's easily visible that the curves are nonlinear even at low power values [1]. Even so, Fig. 2(a) shows a better linear shape in low frequency range. We can see that the curvature becomes larger with the increase of frequency, as shown in Fig. 2(a)-(d). From the results, we can get the function of V_{ISHE}~F(P, f). However, both microwave power and frequency cannot directly act on magnetization $\vec{M}$. With the Kittel equation[2], frequency f can be replaced by the resonance field H_{FMR}. Considering microwave power works as a perturbation to $\vec{M}$, we replace it by the angle θ of $\vec{H}$ and $\vec{M}$ [3]. The function of V_{ISHE}~F(P, f) can be rewritten as V_{ISHE}~$F(H_{FMR}, \theta)$.

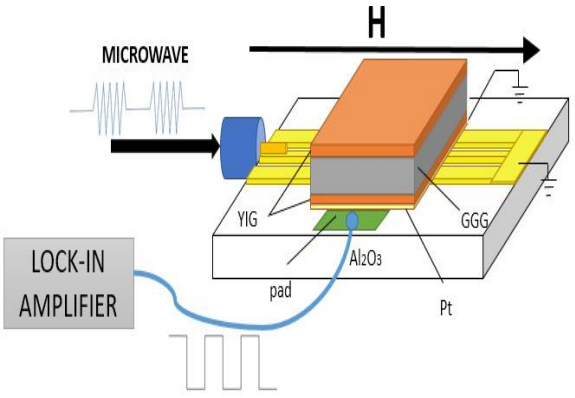

Fig. 1 Schematic illustration of the experiment setup.

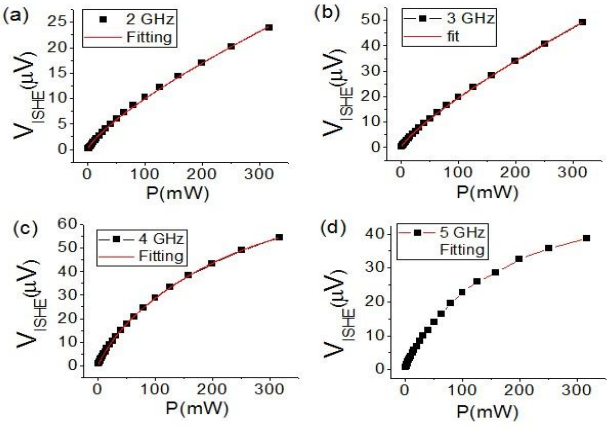

Fig. 2 V_{ISHE} as functions of microwave power measured at (a) 2GHz, (b) 3GHz, (c) 4GHz, (d) 5GHz.

[1] C. Kittel, *Phys. Rev.* **73**(2) (1948) 155.
[2] M. B. Jungfleisch et al., *Phys. Rev. B* **91**(13) (2015) 134407.
[3] Y. Guan et al., *J. Magn. Magn. Mater.* **312**(2) (2007) 374-378.

Growth of Pure YIG Epitaxial Films from Pb-Free Flux

I.I. Syvorotka

Scientific Research Company "Carat", Lviv, Ukraine

The yttrium iron garnets $Y_3Fe_5O_{12}$ (YIG) films have been shown to be a prospective material for microwave devices, magneto-optic (MO) applications as well as spintronics [1-2]. For growth garnet films by liquid phase epitaxy (LPE) method the most commonly used flux is $PbO–B_2O_3$ (PB) of Bi_2O_3-based. However, the uses of such fluxes are contaminated films of Pb^{2+}, Pb^{4+} and Pt^{4+} ions, which have negative effect on properties of garnet films. To avoid this problem, the use of Li_2MoO_4-based flux has been proposed in [3].

This work is focused on growth process by LPE method of pure $Y_3Fe_5O_{12}$ films from PbO-free flux, investigation of surface morphology and magnetic properties of grown films.

The YIG films were grown by LPE method on (111)-oriented gadolinium gallium garnet (GGG) substrate from a melts based on the $Li_2MoO_4–MoO_3$ (LM) flux. Melt compositions and molar ratios was choose to ensure garnet primary phase crystallization and remain to the binary join of $Li_2MoO_4–Y_2(MoO_4)_3$ on phase diagram (Fig. 1a). The technological experiments were carried out in a temperature range 950…1050 °C. Growth rate of YIG films was changed from 0,1 to 0,3 μm/min. Films thickness till to 9 μm.

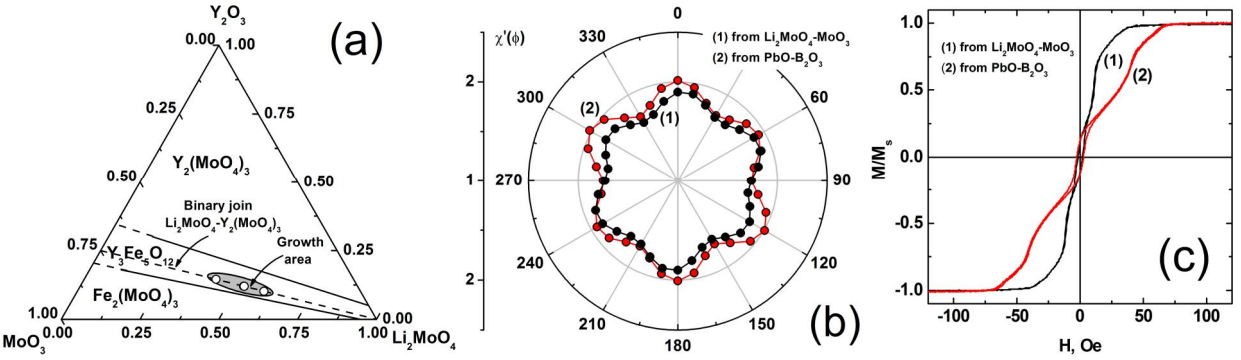

Fig.1 Y_2O_3-MoO_3-Li_2MoO_4 pseudo-ternary diagram (a); angular dependence of transverse susceptibility $\chi'(\varphi)$ in a rotating field H = 80 Oe (b) and magnetization curves (c) for YIG films grown from PbO-B_2O_3 and $Li_2MoO_4–MoO_3$ fluxes.

In the YIG films grown from LM flux, uncontrolled impurity of Pt or Pb were not detected. The composition of the grown films corresponds to pure stoichiometric yttrium iron garnet. All grown films demonstrate a mirror surface, however, with an increase of film thickness the surface roughness was observed.

The YIG films grown from LM flux demonstrate FMR linewidth ΔH around 5...6 Oe, which 6 times more than for YIG grown from PB flux (ΔH < 1 Oe).

In-plane anisotropy field for YIG films grown form LM and PB fluxes equal to 2,7 and 2,6 Oe (fig1.b). Saturation magnetisation of films grown from both fluxes close to theoretical value equal to 1750 G, but difference in magnetisation curves has been observed (fig1.c).

Such differences in the magnetic properties, apparently, connected with the peculiarities of growth mechanisms of YIG films from LM flux and require further investigation.

[1] P. Capper and M. Mauk, *Liquid Phase Epitaxy of Electronic, Optical and Optoelectronic Materials*, John Wiley & Sons Ltd, 2007, p. 441.

[2] A.V. Chumak, V.I. Vasyuchka, A.A. Serga and B. Hillebrands, Magnon spintronics, *Nature physics* **11** (2015) 453-461.

[3] W.A. Bonner, A novel non-Pb flux system for the preparation of yttrium and rare earth iron gallium and aluminum garnets, *Mat. Res. Bull.* **12** (1977) 289-298.

Structural and Vibrational Spectroscopy of Manganese Oxides

N. Mironova-Ulmane[1], A. Kuzmin[1], V. Skvortsova[1], G. Chikvaidze[1], I. Sildos[2], J. Grabis[3], A. Dindune[3]

[1]*Institute of Solid State Physics, University of Latvia, Kengaraga Str. 8, LV-1063 Riga, Latvia*
[2]*Institute of Physics, University of Tartu, W.Ostwaldi tn 1, 50411 Tartu, Estonia*
[3]*Institute of Inorganic Chemistry, Riga Technical University, P.Valdena Str. 3/7, LV-1048 Riga, Latvia*

In this study we have performed investigation of stoichiometric and non-stoichiometric manganese oxides (polycrystalline and single-crystal) using x-ray diffraction (XRD), micro-Raman and FT-IR spectroscopy.

Polycrystalline MnO and Mn_3O_4 were prepared by thermal decomposition of oxalate or manganese carbonate in vacuum and in air, respectively. Single-crystals MnO and Mn_3O_4 (hausmannite) were grown by the method of chemical transport reactions from polycrystalline sources on MgO(100) substrate. All samples were characterized by x-ray diffraction. It is known that MnO phase with a NaCl-type structure is a weak Raman scatterer. Its Raman signal consists of two broad asymmetric bands at about 530 cm^{-1} and 1050 cm^{-1}, of which only the first one has been attributed to 2TO mode.

The Raman spectrum of polycrystalline tetragonal hausmannite Mn_3O_4 consists of a narrow strong band at 660 cm^{-1} and two small bands at about 318 and 370 cm^{-1}. The contribution from hausmannite phase is well visible in mixed single-crystal MnO-Mn_3O_4 sample and is also present in a small amount in nominally pure single-crystal MnO. However, the three bands become broadened in the Raman spectrum of single-crystal Mn_3O_4/MgO(100), which corresponds to the cubic hausmannite Mn_3O_4 phase.

Infrared spectra were measured using the KBr pellet method in the energy range from 200 to 700 cm^{-1} employing vacuum Fourier transform infrared spectrometer Brucker Vertex 80v equipped with the closed circle optical helium cryostat. The low temperature (7 K) infrared spectrum of polycrystalline MnO contains one band at 285 cm^{-1}, whereas three bands at 420, 480 and 513 cm^{-1} were observed for Mn_3O_4.

The phase composition of nominally pure single-crystal MnO and mixed MnO-Mn_3O_4 samples was probed by micro-Raman and micro-FT-IR mapping techniques. The optical image of nominally pure MnO is dominated by green colour; however, reddish-brown colour can be observed in some points mostly homogeneously distributed across the sample: it is attributed to the presence of the Mn_3O_4 phase.

To conclude we have shown that the vibrational spectroscopies can be successfully used to control the presence of the hausmannite Mn_3O_4 phase in polycrystalline and single-crystal manganese oxides. However, micro-Raman spectroscopy should be used with care, since local heating of MnO phase by laser can easily induce an oxidation of manganese ions leading to a formation of Mn_3O_4 phase.

Magnetoelastic Villari Effect in Ferrite Materials for Force and Stress Sensors Working in Low Magnetizing Field Region

M. Kachniarz[1,*], A. Bieńkowski[2], R. Szewczyk[2]

[1]*Industrial Research Institute for Automation and Measurements PIAP, al. Jerozolimskie 202, 02-486 Warsaw, Poland*
[2]*Institute of Metrology and Biomedical Engineering, Warsaw University of Technology, sw. Andrzeja Boboli 8, 02-525 Warsaw, Poland*
* mkachniarz@piap.pl

Metal oxide materials known as ferrites are one of the most important groups of ferromagnetic materials in modern technology and science. They are often utilized as ferromagnetic cores for many inductive components in modern electronics including transformers, filters, chokes, etc. Ferrites are ceramic materials chemically composed of iron oxide Fe_2O_3 and one or more metallic elements [1]. They are classified as ferrimagnetics, so their atoms are organized within two crystal sub-lattices exhibiting opposing magnetic moments. These atomic moments are not equal and they do not compensate each other completely, so the material still exhibits spontaneous magnetization, unlike antiferromagnetic.

The magnetoelastic Villari effect is a physical phenomenon involving changes of the magnetic properties of the ferromagnetic (or ferrimagnetic) material under the influence of the external mechanical stress. This creates the possibility of utilization ferrite materials in measurements of mechanical force or stress. However, previous researches in this filed were performed with high magnetizing fields, in saturation region [2]. The following paper presents the results of studies on the magnetoelastic properties of ferrite materials in the region of low magnetizing fields, known as Rayleigh region, where magnetic characteristics of the material could be approximated with second degree polynomial equation.

The objects of the investigation were several ferrimagnetic materials, prepared as frame-shaped samples allowing to obtain closed magnetic circuit and almost uniform distribution of mechanical stress within the material. The magnetoelastic characteristics of the materials were investigated with special measurement system allowing measurement of magnetic parameters of the ferrite materials magnetized with low fields under the influence of the compressive stress. The obtained results indicates strong correlation between the magnetic properties of the material and applied mechanical stress, which allows to consider the development of the magnetoelastic stress or force sensor with ferrite core working in low magnetizing fields region.

[1] C.B. Carter, M.G. Norton, *Ceramic Materials: Science and Engineering*, Springer-Verlag, New York, 2013.
[2] A. Bieńkowski, R. Szewczyk, The possibility of utilizing the high permeability magnetic materials in construction of magnetoelastic stress and force sensors, *Sensors and Actuators A: Physical* **113**(3) (2004) 270-276.

Bismuth Substitution Effects in Mg_3/Al_1 Layered Double Hydroxides

A. Kareiva[1], D. Sokol[1], M. Ivanov[2], A. N. Salak[3], R. Grigalaitis[2], M.G.S. Ferreira[3], A. Beganskiene[1], J. Banys[2]

[1]*Institute of Chemistry, Vilnius University, Naugarduko 24, LT-03225 Vilnius, Lithuania*
[2]*Faculty of Physics, Vilnius University, LT-10222 Vilnius, Lithuania*
[3]*Department of Materials and Ceramic Engineering/CICECO, University of Aveiro, 3810-193 Aveiro, Portugal*

Numbers of pairs of M^{II}-M^{III} cations were experimentally used to estimate the ranges of the relative sizes of the cations that can form an layered double hydroxide (LDH) structure. In a majority of the known M^{II}-M^{III} LDHs, M^{II} is cation of magnesium or a 4th-period transition metal from iron to zinc, and M^{III} is, as a rule, Al, Ga, Fe, or Cr [1]. In such combinations, the divalent metal cation is slightly bigger than the trivalent one. It should be pointed out that Bi-containing LDH are potentially of a great interest. Bi^{III} has a stereochemically active lone pair of electrons. This feature of bismuth is associated with onset of the unusual dielectric relaxation in oxygen octahedral phases that contain Bi^{III} coordinated by twelve (8+4) oxygens [2, 3]. Besides, polar (antipolar) orderings in oxygen octahedral multiferroics is typically resulted from parallel (antiparallel) displacements of Bi^{III} [4, 5]. Although trivalent bismuth is a relatively large cation, there are compounds with Bi^{III} coordinated by six oxygens [6, 7]. In those compounds, the BiO_6 octahedra are corner-linked; moreover, they are surrounded by the octahedra with smaller-size cations. Such alternation of the octahedra allows to accommodate Bi^{III} in the structure. Phenomenon of the cation ordering in LDH is rare and little investigated [8]. Taking into account a likely deformation of the BiO_6 octahedra in the hydroxide layers and the cation displacements, a Bi^{III} -containing LDH compound could appear to be an example of a 2-D multiferroic material that combines elastic and polar order parameters.

This work was aimed at investigation of feasibility of preparation of LDH compounds with M^{III}= Bi. LDH with the nominal compositions of $Mg_3Al_{1-x}Bi_x$-CO_3 (x=0 to 0.5) were prepared using co-precipitation and sol-gel methods. The mixed oxides were obtained either by calcination of the LDH or sol-gel precursor. All the LDH products were characterized using the methods of X-ray diffraction, scanning electron microscopy coupled with energy-dispersive X-ray spectroscopy and thermogravimetry. We also present an initial study of dielectric and conductive properties of bismuth containing LDHs in this contribution.

Acknowledgements. The work has been done in frame of the project TUMOCS. This project has received funding from the European Union's Horizon 2020 research and innovation programme under the Marie Skłodowska-Curie grant agreement No 645660.

[1] A.I. Khan, D. O'Hare, *J. Mater. Chem.* **12** (2002) 3191.
[2] A.N. Salak, V.M. Ferreira, *J. Eur. Ceram. Soc.* **27** (2007) 2887.
[3] A.N. Salak, V.M. Ferreira, J.L. Ribeiro, L.G. Vieira, R.C. Pullar, N. McN. Alford, *J. Appl. Phys.* **104** (2008) 014105.
[4] D.D. Khalyavin, A.N. Salak, N.M. Olekhnovich, A.V. Pushkarev, Yu.V. Radyush, P. Manuel, I.P. Raevski, M.L. Zheludkevich, M.G.S. Ferreira, *Phys. Rev. B* **89** (2014) 174414.
[5] D.D. Khalyavin, A.N. Salak, A.B. Lopes, N.M. Olekhnovich, A.V. Pushkarev, Yu.V. Radyush, E.L. Fertman, V.A. Desnenko, A.V. Fedorchenko, P. Manuel, A. Feher, J.M. Vieira, M.G.S. Ferreira, *Phys. Rev. B* **92** (2015) 224428.
[6] W.T. Fu, R. de Gelder, R.A.G. de Graaff, *Mater. Res. Bull.* **32** (1997) 651.
[7] P.E.R. Blanchard, Z. Huang, B.J. Kennedy, S. Liu, W. Miiller, E. Reynolds, Q. Zhou, M. Avdeev, Z. Zhang, J.B. Aitken, B.C.C. Cowie, L.Y. Jang, T.T. Tan, S. Li, C.D. Ling, *Inorg. Chem.* **53** (2014) 952.
[8] D.E. Evans, R.C.T. Slade, *Structure & Bonding*, Springer-Verlag, Berlin, Germany, 2005; Vol. 119, pp. 1−87.

The Influence of Compressive Stresses on the Properties of Inductive Electronics Components

J. Salach[1,*], P. Nowak[2,*]

[1]*Institute of Metrology and Biomedical Engineering, Warsaw University of Technology, sw. A. Boboli 8, 02-525 Warsaw, Poland*
* *j.salach@mchtr.pw.edu.pl*
[2] *Industrial Research Institute for Automation and Measurements PIAP, Al. Jerozolimskie 202, 02-486 Warsaw, Poland*
* *pnowak@mchtr.pw.edu.pl*

The cores of electronic components are an important element of these devices. These are usually inductors, transformers or electromagnets, usually used as wounded ring cores made of metaloxide ceramic. The quality, precision and stability of the entire device depends mostly on the cores' parameters. Their characteristics may be influenced by a lot of factors, such as temperature, humidity and stresses. The strains can have two sources: its own internal stresses and external forces. Internal stresses are associated with the manufacturing process, mostly caused by the residual stresses in the core or winding core too tightly, and should be eliminated during the production of cores. On the other hand, external stresses can occur due to improper installation, or other incidental factors which apply a strength to the core.

The most important thing, from the users and constructors the point of view, is the knowledge about the stresses' effects on the properties of the magnetic cores of an electronic component. The impact on the ferrites in the form of frame cores has been previously reported [1]. However, so far no research have confirmed a clear impact of stresses on the ring-shaped core. The results of such research will be presented in the paper. The tests will be conducted in a way which will take ensure both the uniformity of stress distribution in the core as well as closed magnetic path. This methodology has been described for amorphous cores ring in previous publications [2], and will be adjusted to the ceramic ferrite cores tests.

[1] A. Bienkowski, R. Szewczyk, The dependence of the magnetoelastic properties of Zn-Mn ferrites on their magnetocrystalline properties, *Physica Status Solidi A - Applied Research* **189**(3) (2002) 825-828.
[2] A. Bienkowski, R. Szewczyk, New possibility of utilizing amorphous ring cores as stress sensor, *Physica Status Solidi A - Applied Research* **189**(3) (2002) 787-790.

Thermodynamic Properties of Ferroelectric Glycine Phosphite

I.R. Zachek[1], R.R. Levitskii[2], Ya. Shchur[2], A.S. Vdovych[2]

[1]Lviv Polytechnic National University, 12 Bandera Str., 79013 Lviv, Ukraine
[2]Institute for Condensed Matter Physics of the National Academy of Sciences of Ukraine, 1 Svientsitskii Str., 79011 Lviv, Ukraine

Model of ferroelectric Glycine Phosphite (GPI) crystal [1] is modified by taking into account piezoelectric coupling of proton subsystem and strains ε_i. Within the two-particle cluster approximation for short-range interactions and mean field approximation for long-range interactions we calculate the thermodynamic potential of the system. Using the appropriate equations of state, we calculate the crystal polarization (fig.1), strains ε_i, molar entropy and heat capacity, longitudinal (fig.2) and transverse dielectric permittivities, piezoelectric moduli and elastic constants of the crystal. At the proper set of parameters satisfactory description of experimental data for partially deuterated crystalls is obtained.

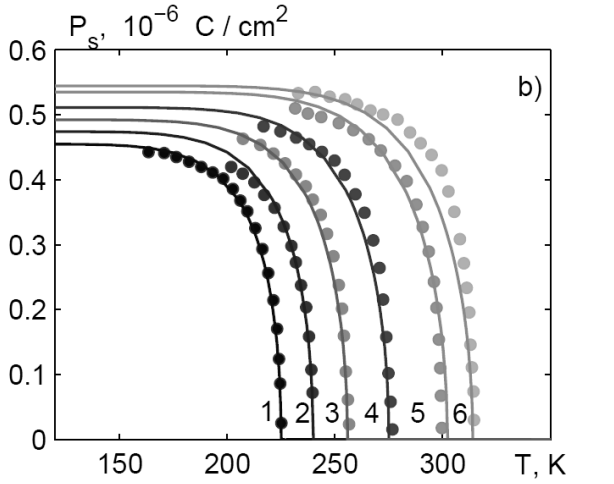

Figure 1. Temperature dependence of the spontaneous polarization of GPI crystal at different concentrations of deuterium *x*: 0.00 – 1, 0.16 – 2, 0.31 – 3, 0.47 – 4, 0.67 – 5, 0.75 – 6. Experimental points for P_s taken from [2].

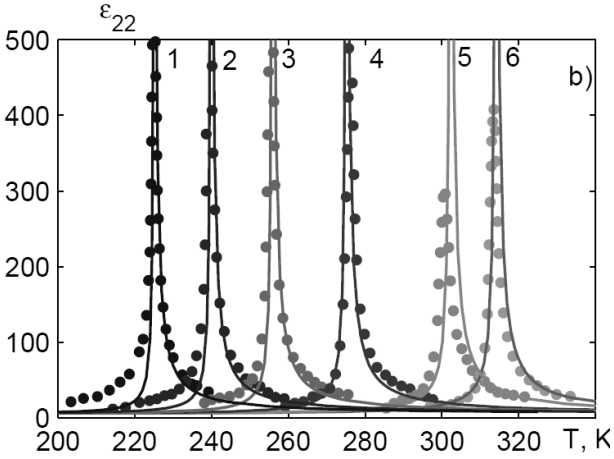

Figure 2. Temperature dependence of the longitudinal dielectric permittivity of GPI crystal at different concentrations of deuterium *x*: 0.00 – 1, 0.16 – 2, 0.31 – 3, 0.47 – 4, 0.67 – 5, 0.75 – 6. Experimental points for ε_{22} taken from [3].

[1] I. Stasyuk, O. Velychko, *Ferroelectrics* **300** (2004) 121.
[2] J. Nayeem, T. Kikuta, N. Nakatani, F. Matsui, S.-N. Takeda, K. Hattori, H. Daimon, *Ferroelectrics* **332** (2006) 13.
[3] J. Nayeem, H. Wakabayashi, T. Kikuta, T. Yamazaki, N. Nakatani, *Ferroelectrics* **269** (2002) 153.

Effect of Hydrostatic Pressure on Thermodynamic Properties of Ferroelectric GPI

I.R. Zachek[1], R.R. Levitskii[2], A.S. Vdovych[2]

[1]*Lviv Polytechnic National University, 12 Bandera Str., 79013 Lviv, Ukraine*
[2]*Institute for Condensed Matter Physics of the National Academy of Sciences of Ukraine, 1 Svientsitskii Str., 79011 Lviv, Ukraine*

On the basis of the model of ferroelectric GPI [1], modified by taking into account piezoelectric coupling of proton subsystem and lattice strains ε_i, within the two-particle cluster approximation we have calculated components of crystal polarization, components of dielectric permittivity tensor (fig.1), piezoelectric and thermal properties of the crystal at different values of hydrostatic pressure. Pressure decreases the phase transition temperature T_c (fig.2). The long-range interactions in our theory much stronger change under pressure, then short-range for nondeuterated crystal. At the proper set of parameters satisfactory description of experimental data is obtained.

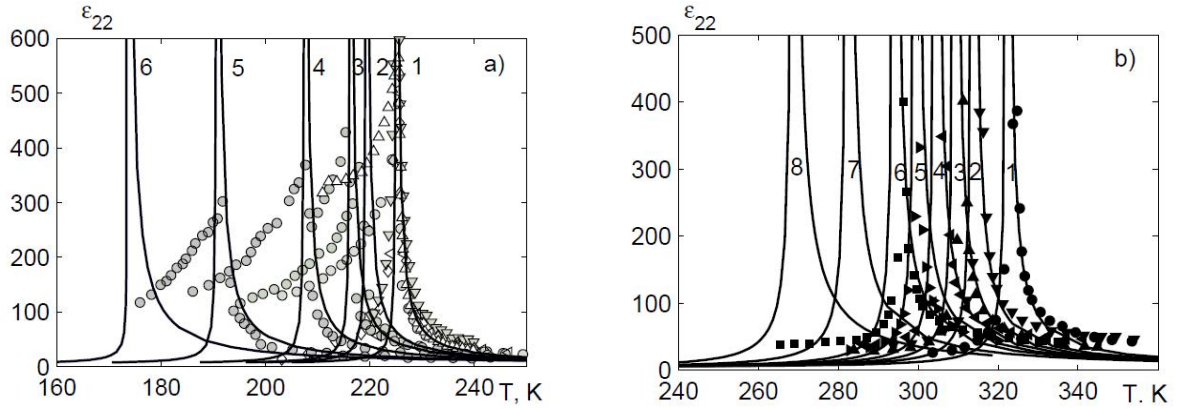

Figure 1. The temperature dependence of the longitudinal dielectric permittivity of GPI (a) crystal at different values of pressure p ($10^9 dyn/cm^2$): 0.00 – 1, ▽ [4], Δ[5], ◊[6], ○[2]; 0.6 – 2, ○ [2]; 0.9 – 3, ○ [2]; 1.7 – 4, ○ [2]; 3.0 – 5, ○ [2]; 4.0 – 6 and $GPI_{0.2}DGPI_{0.8}$ at different values of pressure p ($10^9 dyn/cm^2$): 0.0 – 1, ●[3] ; 2 – 2, ▼[3]; 3 – 3, ▲[3]; 4 – 4, ◀ [3]; 5 – 5, ▶ [3]; 6 – 6, ■[3]; 8 – 7; 10 – 8.

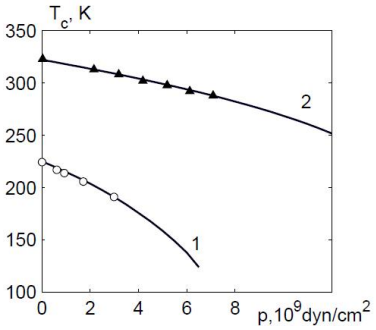

Figure 2. The pressure dependence of temperature T_c of GPI1-*x*DGPI*x* at different concentrations of deuterium *x*: 0.00 – 1, ○ [2]; 0.8 – 2, ▲ [3].

[1] I. Stasyuk, O. Velychko, *Ferroelectrics* **300** (2004) 121.
[2] N. Yasuda, T. Sakurai, Z. Czapla, *J. Phys.: Condens. Matter.* **9** (1997) L347.
[3] N. Yasuda, A. Kaneda, Z. Czapla, *J. Phys.: Condens. Matter.* **9** (1997) L447.
[4] R. Tchukvinskyi, R. Cach, Z. Czapla, S. Dacko, *Phys.stat. sol (a)* **165** (1998) 309.
[5] S. Dacko, Z. Czapla, J. Baran, M. Drozd, *Physics Letters A* **221** (1996) 217.
[6] M. Wiesner, *Phys.stat. sol (b)* **238** (2003) 68.

Relaxation Dielectric Properties of GPI Crystal

I.R. Zachek[1], R.R. Levitskii[2], A.S. Vdovych[2], O.B. Bilenka[1]

[1]*Lviv Polytechnic National University, 12 Bandera Str., 79013 Lviv, Ukraine*
[2]*Institute for Condensed Matter Physics of the National Academy of Sciences of Ukraine, 1 Svientsitskii Str., 79011 Lviv, Ukraine*

Within pseudospin model of ferroelectric GPI on the basis of Zubarev nonequilibrium statistical operator [1] we obtained kinetic equation for pseudospin operators [2]. Solving this equation we have calculated the temperature and frequency dependences of dynamic dielectric permittivity (fig.1, 2) of the crystal, relaxation time. At the proper set of parameters satisfactory description of experimental data is obtained.

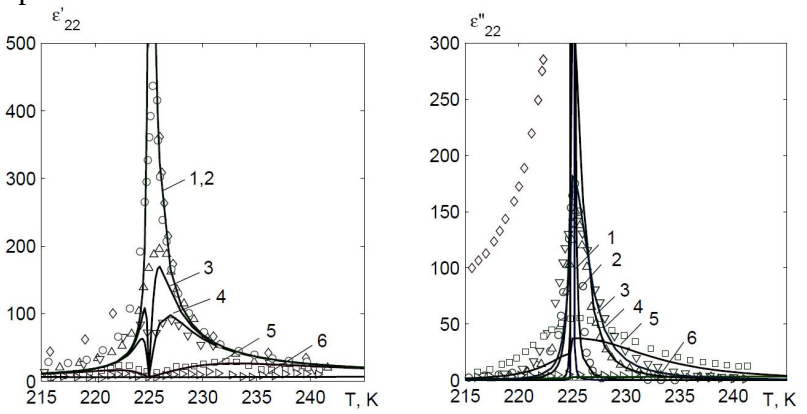

Figure 1. Temperature dependeces of e'_{33} and e''_{33} of GPI crystal for various frequencies ν (MHz): 1.0 – 1, ◊[3]; 15.0 – 2, ○[3]; 230.0 – 3, □ [3]; 610 – 4, □ [3]; 2000 – 5, □[3]; 27000 – 6, ▷[3].

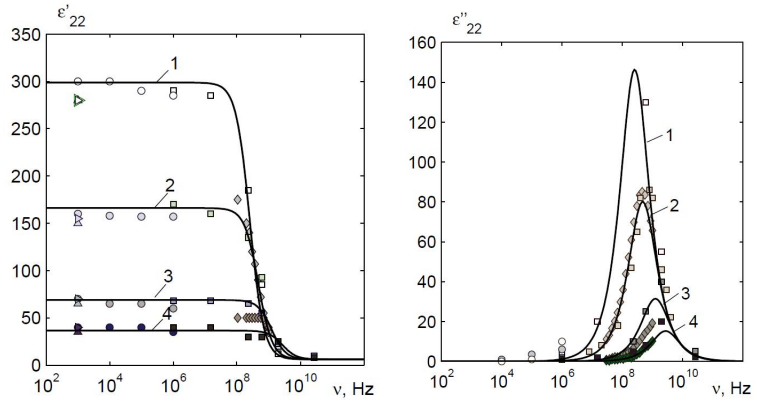

Figure 2. Frequency dependeces of e'_{33} and e''_{33} of GPI crystal for various ΔT (K): 1.0 – 1, 2.0 – 2, 5.0 – 3, 10 – 4; Symbols: ● [4], ■[3], ♦[5], ►[6], ▲[7].

[1] D.N. Zubarev, *Nonequilibrium statistical thermodynamics*, M.: Nauka, 1971, 416 p. (in Russian).
[2] G.O. Berim, A.R. Kessel, *Physica A* **101**(1) (1980) 112-126.
[3] R. Tchukvinskyi, Z. Czapla, R. Sobiestianskas, A. Brilingas, J. Grigas, J. Baran, *Acta Phys. Polonica A* **92** (1997) 1191.
[4] M. Wiesner, *Phys. Stat. Sol (b)* **238** (2003) 68.
[5] J. Baran, G. Bator, R. Jakubas, M. Sledz, *J. Phys.: Condens. Matter.* **8** (1996) 10647.
[6] J. Nayeem, H. Wakabayashi, T. Kikuta, T. Yamazaki, N. Nakatani, *Ferroelectrics* **269** (2002) 153.
[7] S. Dacko, Z. Czapla, J. Baran, M. Drozd, *Physics Letters A* **221** (1996) 217.

Electron Dynamics and High-Temperature Superconductivity in Cuprates

E.E. Zubov

Vasyl' Stus Donetsk National University, 021021 Vinnytsia, Ukraine

During the last decades the electron dynamics in cuprates has been an object of the numerous investigations. Apparently, from a knowledge of the ground state structure and contribution of the electron-electron correlations in the thermodynamic potential we can understand the mechanism of high-temperature superconductivity. It is necessary to point out that the available experimental and theoretical data reflect an extremely complicated character of the interplay between charge, spin and lattice degrees of freedom. Unfortunately, the series of observed phenomena in cuprates is not reproduced by existing theories.

In this work, in the framework of doped Hubbard model the conception of effective field with parameters of order is proposed. It is considered the most general case of relation between Coulomb repulsion U and hopping integral t, when $U \sim t$. By diagrammatic method based on the scattering matrix formalism the effective field with self-consistent parameters of order is extracted from the Hubbard Hamiltonian. This is a zeroth approximation which coincides with a known approximation Hubbard I. For a half filled band the parameters of order determine both the site electron-hole occupancy and a metal or insulator state. This approximation does not describe a phase transition metal-insulator. That's why in work one-loop diagrams were accounted for Green's functions. It allowed to calculate the spectral density and chemical potential of electron subsystem with correlations in paramagnetic state. For a half filled band the metal state is found to be stable at temperature $T=0$ and $U/W<2.1$, where W is bandwidth. Also, a step-like character of the resistivity as a function of the electron doping is observed that is in correspondence with experiment.

The next part of this work is devoted to problem of high-temperature superconductivity. The presented theory is developed as applied to BCS Hamiltonian with exchange binding J. The transformation of the Hamiltonian to real site representation from the wave subspace was made. The perturbation theory of superconductivity with account for smallness of band gap relatively Fermi energy E_F has been presented. In this case the effective self-consistent field is formed by BCS-type bond of the exchange origin and we have ordinary approximation Hubbard I. In the limit of the strongly correlated electrons there is a fundamental difference between metal and doped Mott insulator because of existence a pure hole state and different parameters of order. For the pure t-J model it has been proved that the singlet electron pairs are destroyed by a strong effective kinematic field. Indeed, in the superconductive state the chemical potential μ renormalized by electron correlations was obtained to be in a very narrow energy area, i.e. $J/4 \le m \le J/3$. This condition forbids the realization of the superconductivity by spin-fluctuation mechanisms.

It has been considered the t-J model with Holstein polaron excitations and one Einstein phonon mode. The electron-phonon interaction with binding constant g plays an important role in the correlation narrowing of the band. In this case the chemical potential is decreased. It was obtained that at $g/W=0.07$ the necessary condition on μ may be realized. For optimally doped cuprate with phonon frequency75 mV, $J/W=0.058$ and $W=4$ eV we obtained the value of the critical temperature equal to 100K. The calculated critical temperature of the superconductivity and the gap function are in a good agreement with experimental data for cuprates. Near the Fermi level along the nodal direction a strong electron-phonon binding enforces the degree of coherency of the electron-polaron excitations that is supported by ARPES data.

The work was supported by the Ministry of Education and Science of Ukraine.

Structure and Transport Characteristics of Tunnel Junctions with Hybrid Semiconductor Barriers with Quantum Dots

V.E. Shaternik[1], A.P. Shapovalov[2], T.A. Prikhna[2], O.Yu. Suvorov[1], M.A. Skorik[1], A.V. Shaternik[2], V.I. Bondarchuk[1], E.E. Zubov[3]

[1]*G.V. Kurdyumov Institute for Metal Physics, Kyiv 03142, Ukraine*
[2]*V. Bakul Institute for Superhard Materials, Kyiv 07074, Ukraine*
[3]*Vasyl' Stus Donetsk National University, Vinnytsia 021021, Ukraine*

Now the activity aimed at fabrication and investigation of semiconductor heterostructures (tunnel junctions) with quantum dots and quantum wells in the barriers is well known, and a large number of devices based on them have been designed.The use of self-organization effects is one of the most effective technological techniques for the creation of quantum dots (metal clusters) in the semiconductor barriers. At ultra-low temperatures, the semiconducting heterostructures demonstrate current-voltage characteristics with an unusual characteristic shape. A single or several current peaks caused by electron tunneling through the allowed states in the barrier were observed in such CVCs.A distinct first peak in related current-voltage curves has got a special name, Fermi-edge singularity since this feature appears when both the Fermi energy level of one electrode and that of the levels in the quantum dot are matched.

We have studied thin-film superconductor - semiconductor (with quantum dots) - superconductor MoRe–Si(W)–MoRe junctions where electrons are tunnelling through a single or several quantum dots within the Si(W) barrier.We have revealed the presence and characteristics of the tungsten clusters in silicon-based Si(W) films with a transmission electron microscope (TEM) JEM-2000FX. For the comparison, thefabricated modelSi(W) layers of a thickness about 200 nm were studied with a TEM at an accelerating voltage of 200 kV.

The results of this study are shown in Fig.1. It was found that tungsten clusters formed inside the silicon layer with a diameter of 30 -100 nm. Based on the Si(W) film diffraction patterns, see Fig.1 b), it can be concluded that both silicon and tungsten layers were amorphous – indeed, only characteristic halos are seen in the diffraction patterns in Fig. 1 b) which indicates on an amorphous state of the material. The broadening of the pattern can be understood if we consider the possibility of combining two patterns from Si and SiO phases.The TEM data indicate that, under our experimental conditions, nano-scaled 10-50 nm-thick tungsten clusters with a distance from 100 up to 1000 nm between them are formed within the amorphous silicon matrix.

Current-voltage characteristics of the MoRe–Si(W)–MoResamples were measured in a wide voltage range from -900 to 900 mV at temperatures from 4,2 K to 8 K and we have observed resonant current peaks in the CVCs at bias voltages from 40 to 300 mV that were symmetrical for positive and negative voltages. In the studied heterostructures, metal clusters inside the barrier behave as quasi-one-dimensional quantum dots, hence, the charge transport can be adequately described by scattering matrices within the quantum model of one-dimensional charge transport.

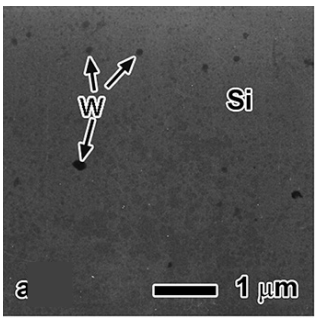

a)TEM image of Si(W) film with 200 nm thickness;

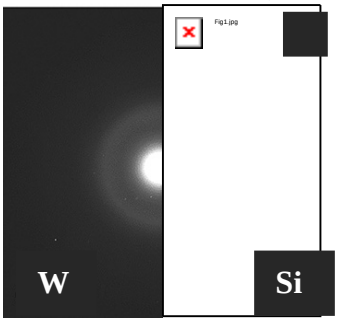

b) diffraction patterns of the Si film and W cluster in it;

Fig. 1.

Lanthanum-Strontium Manganite Nanoparticles for Magnetic Hyperthermia: Fine Tuning of Parameters by Substitutions in Lanthanum and Manganese Sublattices

A. Tovstolytkin[1], Yu. Shlapa[2], S. Solopan[2], A. Bodnaruk[3], M. Kulyk[3], V. Kalita[3], V. Zamorskyi[4], S. Ryabchenko[3], A. Belous[2]

[1]*Institute of Magnetism of the NAS of Ukraine and MES of Ukraine, 36b Vernadsky Blvd., Kyiv 03680, Ukraine*
[2]*V.I. Vernadskii Institute of General and Inorganic Chemistry, NAS of Ukraine, 32/34 Palladinaave., Kyiv 03680, Ukraine*
[3]*Institute of Physics, NAS of Ukraine, 46 Nauky Ave., Kyiv 03028, Ukraine*
[4]*Faculty of Radiophysics, Electronics and Computer Systems, Taras Shevchenko National University of Kyiv, 4G Glushkova Ave., Kyiv 03680, Ukraine*

Hyperthermia (HT) is a rapidly developing technique in cancer therapy. It takes advantage of the higher sensitivity of tumor tissue to heat and typically involves heating of the affected organ to 42 – 45 °C. Magnetic nanohyperthermia [1] allows minimizing side effects by the localized heating of only desired parts of the organism. The method involves introduction of magnetic nanoparticles (MNPs) into the desired part of the organism and heating them with an alternating magnetic field (AMF).

Magnetic fluids based on nanocrystalline Fe_3O_4, stabilized by biocompatible surfactants, are typically used as HT mediators. Unfortunately, due to impossibility to control the local temperature near the particles, there is a risk of overheating and necrosis of normal tissue. This problem could be solved with MNPs of high efficiency of AMFabsorption and a Curie temperature (T_C) of 42 – 45 °C. Thus, local temperature control can be ensured even with a nonuniform distribution of mediator particles throughout the tissue, variable AMF intensity and uneven dissipation of the evolving heat.

Substituted perovskite manganites $La_{1-x}Sr_xMnO_3$ (x = 0.2 – 0.4) are of interest in this context due to easy tunable composition-dependent $T_C$and relatively large magnetic moment at room temperature [1,2].The Curie temperature of $La_{1-x}Sr_xMnO_3$strongly depends on the chemical composition: it displays a maximum at $x\approx$ 0.3 ($T_{C\max}\approx$ 370 K) and is quite sharply reduced as x deviates from 0.3. A smoother change of the Curie temperature can be reached by additional substitutions either in manganese sublattice, or in lanthanum sublattice. Such substitutions are expected to insure reliable and controllable shift of the $T_C$towards the range, which is necessary for hyperthermia treatment.

In this work, the effects of partial substitutions in lanthanum and manganesesublattices on structural, magnetic and calorimetric properties of (La,Sr)MnO_3MNPs have been studied. Fe substitution for La, as well as Nd and Sm substitutions for Mn have been usedin the experiments. The possibility of fine control of magnetic parameters has been proved experimentally. It is demonstrated that chemical substitutions may serve as anefficient tool to “softly”tune the maximal temperature achieved during the AMF-induced heating of MNPs, which is important for application of these materials as mediators of self-controlled magnetic nanohyperthermia.

[1] V.M. Kalita, A.I. Tovstolytkin, S.M. Ryabchenko et al., *Phys. Chem. Chem. Phys.* **17** (2015) 18087.
[2] O. Kaman, T. Dedourkova, J. Koktan et al., *J. Nanopart. Res.* **18** (2016) 100.

Magnetic Properties of Ce^{3+} Ions in Nb-Doped Cerium Dioxide

O. Gornostaeva[1,2], T. Kolodiazhnyi[3]

[1]*Donetsk National University, 600-Richchya Str. 21, 21021 Vinnytsia, Ukraine*
[2]*G. V. Kurdyumov Institute for Metal Physics, National Academy of Sciences of Ukraine, 03680 Kiev, Ukraine*
[3]*National Institute for Materials Science, 1-2-1 Sengen, Tsukuba, Ibaraki 305-0047, Japan*

Dilute magnetic oxides are currently attracting much attention in view of their potential for applications in spintronics and magneto-optical devices. In particular, it relates doped cerium dioxide where we have performed theoretical and experimental studies of crystal-field effects on magnetic properties of Nb-doped CeO_2. Using the crystallographic data for the abovementioned compound and the modified crystal- field theory, a novel computational approach, we have calculated energy levels of the Ce3+ ions and g-factor values.

It was found that the Γ8 ground state is separated from the overlying Γ7 state by 173 cm-1 in good agreement with the optical transmission data. With the g-factor value and related experimental data, we calculated the Curie-Weiss constant and get a percentage of Ce3+ ions in a mole of the substance. Comparison of calculated and experimentally measured temperature dependences of the magnetic susceptibility in Nb-doped and undoped cerium dioxide allows us to estimate the contribution of Ce3+ ions to the magnetism of the dilute magnetic oxide.

Composite Synthesis Using Nanoceramic Method and Properties of $BaTiO_3$-Ni-Co-ferrite ferroic

V. Bushkova[1], A. Kopajev[1], I. Yaremiy[1], U. Tomyn[2]

[1]*Vasyl Stefanyk Precarpathian National University, 76000 Ivano-Frankivsk, Ukraine*
[2]*Ivano-Frankivsk National Medical University, 76000 Ivano-Frankivsk, Ukraine*

Volume ferroics have become very important in the design of various types of electronic devices [1]. They are characterized by high value of magnetoelectric effect coefficient – the electric field intensity upon application of a certain external magnetic field. Compared with layered magnetoelectrics they are easier to produce and mechanically stronger. However, due to the relatively low electrical resistance of the magnetic phase of composite, induced by the magnetic field electric charges rapidly annihilate. In this report a possibility of improving the fabrication technology of bulk ferroics was investigated. Ferrimagnetic ingredient of composite was obtained by milling of Ni-Co-ferrite synthesized by the ceramic technology. $BaTiO_3$ piezoelectric phase was obtained by sol-gel method. Piezoelectric particles are 50-100 times smaller and more active during sintering than the ferrite particles. The mixture of components was pressed and sintered under high temperature. Obtained product had a structure of the ferrite particles in a medium of solid piezoelectric with high electric resistance. Size of ferrite particles is very important. Large demagnetizing fields are generated around too small particles [2]. On the other hand, the larger the magnetic particles, the smaller the contact area with the piezoelectric phase. In both cases, the magnetoelectric effect decreases.

In the presented research the Mössbauer study, as well as the complex of structural studies of produced by the new technology composites were performed. Experimental results indicate that produced composites consist of spinel and perovskite phases. Spinel lattice parameter insignificantly differs from the parameter of pure Ni-Co-ferrite. $BaTiO_3$ lattice parameter corresponds to the published data for the perovskite of specified chemical composition. Mössbauer spectra of the samples indicate the presence of the characteristic magnetic order in the structure of Ni-Co-ferrite. Measurements of magnetic and electrical properties of the obtained composites were made. Data of carried out research indicate that the chemical interaction between the phases at the used synthesis modes is insignificant.

Obtained by nanoceramic method ferroics have higher parameters compared with the materials produced by the conventional technique, in which both of the composite component are produced using the same methods.

[1] G.S. Radchenko, D.A. Filippov, V.M. Laletin, *Appl. Phys. A* **121**(2) (2015) 619-623.
[2] A.V. Kopayev, B.K. Ostafiychuk, I.P. Yaremiy, I.Y. Vylka, *Journal of Surface Investigation: X-ray, Synchrotron and Neutron Techniques* **10**(10) (2007) 79-83.

Structural and Magnetic Properties of Cobalt Ferrite Nanopoweders Synthesis with Using Contact Non-Equilibrium Plasma

L.Frolova*, A. Derimova, T. Butyrina

Department of Inorganic Materials Technology and Ecology, Ukrainian State Chemical Technology University, 8 Gagarina Str., 49005 Dnepropetrovsk, Ukraine
** frolova_l.a@mail.ru*

Nanosized ferrites have been attracting extensive attention due to their wide applications, such as magnetic memory, MRI contrast agents and catalysts etc. Among these magnetic materials, spinel-type ferrite nanoparticles [1-5]. These properties of the nanoferrites are affected by the preparation conditions, chemical composition, sintering temperature and the method of preparation [6, 7]. So far, various synthetic routes have been explored for the preparation of $CoFe_2O_4$ nanoparticles, such as hydrothermal, coprecipitation, microemulsion, forced hydrolysis, reduction–oxidation route [8-9]. In order to avoid the drawbacks from this methods ferrite have been synthesized by wet-chemical method with using contact nonequilibrium plasma (CNP). Among the most promising methods of using electrical discharges, there's one based on CNP of reduced pressure contact influence on the disperse environment.

Numerous studies have shown that aqueous solutions non-equilibrium plasma treatment causes oxidation and reduction of solution components. Thus, metal ions oxidize and form insoluble or sparingly soluble compounds. The aim of this work was to study the effect of CNP on the structure and magnetic properties cobalt ferrite. To carry out the task samples were synthesized under different conditions: the ratio of cations cobalt and iron, pH, reaction time, parameters glow discharge. Synthesis conditions were varied so that it was possible to find the mechanism of glow discharge ferritization effect.

Structural identification of the samples was carried out using the method of differential thermal analysis (DTA) and differential thermogravimetric analysis (DTGA), X-ray diffraction, Fourier transform infrared spectroscopy, Scanning electron microscopy. Vibrating sample magnetometer was used for the magnetic investigation of the samples. Magnetic properties of nanoparticles show strong dependence on the phase composition. The magnetic properties increase with pH of the precipitating medium. The coercivity also increases with increasing pH, goes through a maximum, peaking at around 12. It was found that the characteristic of products depended on pH, temperature, mole ratio (x) of Co^{2+} to Fe^{3+}. The products were $Co_xFe_{3-x}O_4$ at $1 \le x \le 2$. Pure $CoFe_2O_4$ nanoparticles with uniform size were synthesized at 35 °C, pH 12 and x = 0.5-1. The maximum coercivity and saturation magnetization of $CoFe_2O_4$ prepared by the present method were 502.6 Oe and 58.9 emu/g, respectively.

[1] Y. Wang, D. Su, A. Ung, J.H. Ahn, G. Wang, *Nanotechnology* **23**(5) (2012) 055402.
[2] M. George, S.S. Nair, K.A. Malini, P.A. Joy, M.R. Anantharaman, *Journal of Physics D: Applied Physics* **40**(6) (2007) 1593.
[3] M.V. Limaye, S.B. Singh, S.K. Date, D. Kothari, V.R. Reddy, A. Gupta, S.K. Kulkarni, *The Journal of Physical Chemistry B* **113**(27) (2009) 9070-9076.
[4] M. Sangmanee, S. Maensiri, *Applied Physics A* **97**(1) (2009) 167-177.
[5] T.E. Torres, A.G. Roca, M.P. Morales, A. Ibarra, C. Marquina, M.R. Ibarra, G.F Goya, *Journal of Physics: Conference Series* **200** (2010) 072101.
[6] B. Liu, Q. Li, B. Zhang, Y. Cui, H. Chen, G. Chen, D. Tang, *Nanoscale* **3**(5) (2011) 2220.
[7] M. Rajendran, R.C. Pullar, A.K. Bhattacharya, D. Das, S.N. Chintalapudi, and C. K. Majumdar, *J. Magn. Magn. Mater.* **232** (2001) 71.
[8] C. Cannas, A. Falqui, A. Musinu, D. Peddis et al., *Journal of Nanoparticle Research* **8**(2) (2006) 255.
[9] M. A. Hamad, *Journal of superconductivity and novel magnetism* **26**(3) (2013) 669.

Influence of Magnetostriction on Localised Flux Density Distribution in Different Type of Amorphous Cores

Naim Derebasi, M. Kemal Bektas

Physics Department, Uludag University, Gorukle Bursa, 16059, Turkey

Application of a force causes a localized bending stress which results in a change in the domain structure and therefore a variation in the induced voltage in the search coils wound uniformly on this area [1, 2]. In this study, variation of localized angular flux density with applied force was concentrated on different flux density and frequency levels in amorphous toroidal transducer core made high and near zero magnetostrictive Metglas® amorphous ribbons. Investigations were carried out for high magnetostrictive Fe-based Metglas 2605SA1 and near zero magnetostrictive Co-based 2705X as-cast amorphous ribbon toroidal cores to confirm the influence of applying force and frequency on output characteristic of the transducer due to their magnetostriction. A force was applied to the toroidal core in steps of 20 g from 0 to 500 g-force. The transducer under the test were sinusoidally magnetised over the frequency range from 1 to 10 kHz and flux density levels of 1-150 mT (Fig. 1). Variation in the induced voltage of search coils located at 0º and 90º was very significant with applied stress however the induced voltage detected from the search coil located at 45º was less affected with applied stress on the Fe-based toroidal core. Although the applying force is not effective on 2705X amorphous ribbon. This investigation highlights the influence of localised bending stress on flux density in amorphous ribbon cores due to its magnetostriction.

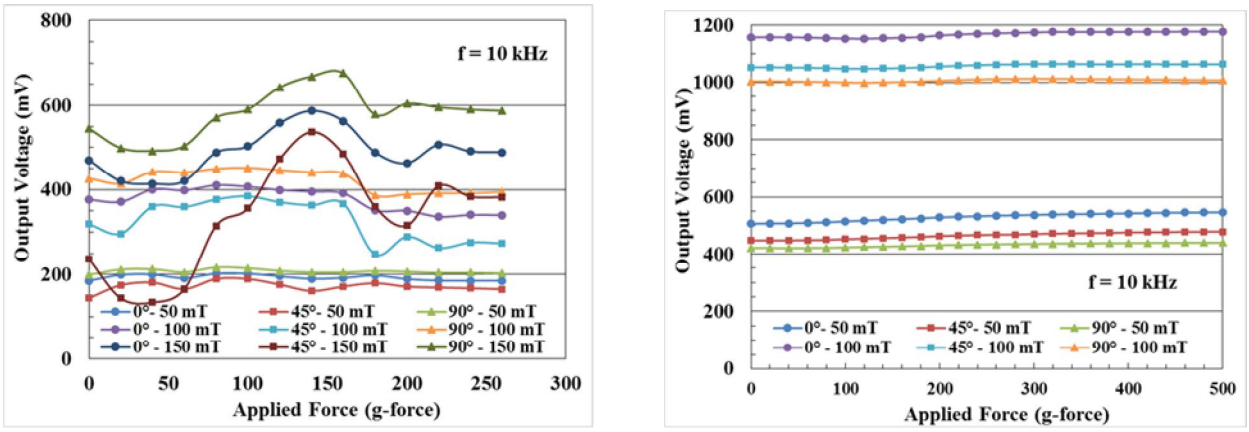

Fig. 1. Variation of localized coil output voltage with applied force on 2605SA1 and 2705X at 10 kHz

[1] T. Meydan, M. Goktepe, A. Honda, N. Derebasi, Influence of bending stress on domain motion in amorphous material based magneto elastic transducers, *J. Magn. Magn. Mater.* **112** (1992) 269-271.

[2] S. Chikazumi, *Physics of magnetism*, Robert E. Krieger Publishing Co. Inc., Chapter 13, 1986, pp. 260.

Localised Flux Density Variation Around a Different Type Holes on Electrical Steel Using Numerical Methods

Naim Derebasi

Physics Department, Uludag University, Gorukle Bursa, 16059, Turkey

Localised flux density orientations are closely related the degraded area around the cut edge or a hole. Artificial neural networks (ANN) and MATLAB® Curve Fitting Toolbox™ are useful tools in prediction and calculation of magnetic properties of electrical steels [1, 2]. A 4-node input layer and 1-node output layer model with three hidden layers, and full connectivity between nodes was developed (Fig. 1). The input parameters were hole size, cutting method, induction frequency and bulk flux density while the output parameter was localised flux density due to the search coil located at the angles 0º, 25º, 45º and 65º corresponding to the centre of hole and rolling direction. The previous data obtained was used for training the proposed ANN model. Minimum correlation coefficients and RMS error for the localised flux density were found to be 0.99 and 0.09 respectively after the network was trained. After the network was tested using untrained data minimum correlation coefficient and RMS error for localised flux density was found to be 0.98 and 0.04 respectively. A simple analytical equation as depending on experimental results has been determined by using MATLAB® Curve Fitting Toolbox™ for localised flux distributions around the hole (Fig. 2). The results obtained by using the proposed ANN model and analytical equations are in good agreement with experimental results previously reported.

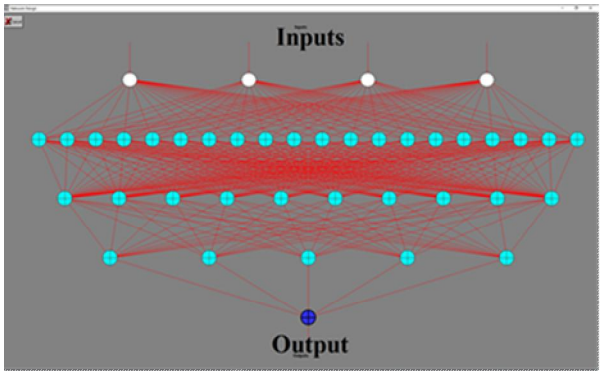

Fig. 1. Developed ANN model for the localized flux density

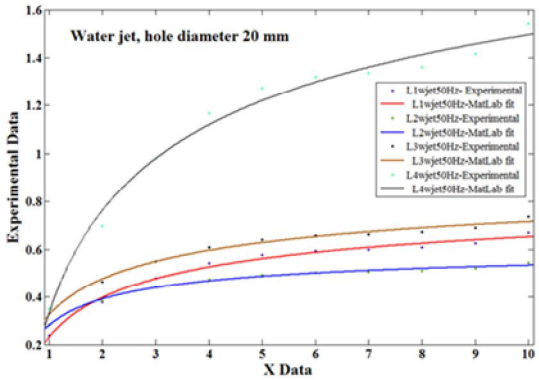

Fig. 2. Variation of localized peak magnetic flux density B_m for abrasive waterjet cut for 20 mm diameter holes at 50 Hz.

[1] G.K. Miti, A.J. Moses, N. Derebasi, D. Fox, A neural network-based tool for magnetic performance prediction of toroidal cores, *J. Magn. Magn. Mat.* **254** (2003) 262-264.

[2] N. Derebasi, Effect of geometrical factors on magnetic induction distribution of toroidal cores using numerical methods, *J. Supercond. Nov. Magn.* **28**(3) (2015) 767-771.

Utilization of Eddy Current Tomography for Testing Ferrite Rings

P. Nowak[1,2,*], M. Nowicki*

[1]*Industrial Research Institute for Automation and Measurements PIAP,*
Al. Jerozolimskie 202, 02-486 Warsaw, Poland
* *pnowak@piap.pl*
[2]*Institute of Metrology and Biomedical Engineering, Warsaw University of Technology,*
Boboli 8, 02-525 Warsaw, Poland
* *p.nowak@mchtr.pw.edu.pl*, * *m.nowicki@mchtr.pw.edu.pl*

Paper presents results of an investigation of cylindrical ferrite samples on eddy current tomography setup. Non-destructive testing (NDT) with the usage of eddy current phenomena is well-known technique of production fault selection. Reference objects (validated with other measurement method) are measured and their signature response is obtained. Then tested objects are measured and their response is compared with reference objects response. Thus selection of the defective objects can be made. On the other hand it does not allow to determine the shape of the objects' defect and is not suitable for correction of production process. This gap can be supplemented with the usage of eddy-current tomography. This method merges the well-known advantages of eddy current testing with the possibility of determination of defects' shape, size and location.

During the measurement process tested object is placed between two coaxial coils – exciting and measuring. The exciting coil is supplied with an alternating sine current, which generates alternating magnetic field. This field induces eddy currents in the tested object, which influence the magnetic field measured by the second coil. Depending on the objects' shape, the distribution of the eddy currents may significantly vary. On the other hand the measurement coil response is an implicit function of the defects' size, shape and orientation as well as from the physical parameters of the tested sample, mostly its magnetic permeability and electrical conductivity. Thus the data from the single measurement is not suitable for the objects shape reconstruction. The measurement process is based on measuring the amplitude of the inducted signal as well as the phase shift between the exciting and measured signal. The measured object is moved linearly (perpendicularly to the coils' axes) and in each linear step is rotated around its axis. The tomography setup is most suitable for axisymmetric samples so for the tests typical ferrite ring with high magnetic permeability and low electric conductivity was selected.

The measurements were conducted on the ferrite ring in a fabric state and with series of reference defects. Results confirmed the possibility of utilization of eddy current tomography for the determination of defects' shape and size. Further work shall concern development of inverse tomography transformation which may allow not only determine the size of objects' defects but also its physical properties such as magnetic permeability and electrical conductivity.

Magnetic Losses Evolution of Ferritic Fe-Si Steels Subjected to Temper Rolling at Elevated Temperature

I. Petryshynets, F. Kováč, V. Puchý, M. Šebek

Division of Metals Systems, Institute of Materials Research, Watsonova 47, 041 01 Košice, Slovakia

Non-oriented FeSi steels belong to important group of the soft magnetic materials that are typically used as core parts in a variety of electrical rotating equipments. Their good soft magnetic characteristics strongly rely on the ability to control the grain size and texture as well as chemistry of the final steel sheets products. The most appropriate texture for NO steels is "rotating cube" texture, which provides isotropic magnetic properties in all plane directions of non-oriented steels.

In the present work, we have used an adjusted temper rolling process at elevated temperature for development of coarse grained microstructure with particular cube textures in high silicon NO steels. The main idea behind the improvement of soft magnetic properties relies on deformation induced grain growth and heat transport phenomena promoting the preferable formation of coarse grains with desired orientation. The vacuum degassed NO steel with high silicon content was taken from industrial line after cold rolling with 84% of deformation. Nanohardness measurements were carried out after temper rolling, in order to evaluate local variations of work hardening as a function of crystallographic orientation as well as a material thickness. The coarse grained microstructure with pronounced intensity of cube and Goss texture components in the investigated NO steel was achieved by using deformation induced growth of ferrite grains during the continuous final annealing at dynamic conditions. This thermal treatment was carried out at the laboratory furnace with the heating rate of Vh~25ºC/s and cooling rate of Vc~7ºC/s. EBSD was used to determine the crystallographic orientations of grains with respect to individual rolling planes and rolling directions. The magnetic losses of the experimental samples were measured in AC magnetic field with the frequency 50Hz and magnetic field intensity 2500A/m on the toroid with external diameter 25mm and internal diameter 15mm. The magnetic measurements demonstrated that the coercivity of investigated steels treated by suggested approach were decreased from 218 A/m to 112 A/m.

Acknowledgements. This work was partially supported by the Slovak Grant Agency VEGA, project No. 2/0081/16 and No. 2/0120/15. Also, this work was realized within the frame of the project "Technology of preparation of electrotechnical steels possessing high permeability for high affectivity electromotors" ITMS 26220220037, the project "New materials and technologies for energetic", ITMS 26220220061 and project "Research centre for efficient integration of the renewable energy sources", ITMS: 26220220064 financed through European Regional Development Fund.

Experimental Validation of Energy Dependences of YAP TL Detectors: Irradiation to ISO Radiation Qualities

Ya. Zhydachevskyy[1,2], V. Voloskii[3], N. Denyachenko[3], O. Bakhanova[3], W. Gieszczyk[4], V. Chumak[3], S. Ubizskii[1], A. Suchocki[2]

[1] *Lviv Polytechnic National University, Lviv, Ukraine*
[2] *Institute of Physics, Polish Academy of Sciences, Warsaw, Poland*
[3] *Radiation Protection Institute ATS Ukraine, Kyiv, Ukraine*
[4] *Institute of Nuclear Physics, Polish Academy of Sciences, Kraków, Poland*

Energy dependence of the energy deposition values is an important characteristic both for scintillators and radiation storage phosphors. For low-Z materials, for which inelastic scattering (Compton interaction) of photon radiation dominates for radiation energies from about 10 keV to 10 MeV, such energy dependence is of less significance. However, for high-Z materials, for which the photoelectric effect dominates especially for lower radiation energies, such energy dependence should be considered. As it was shown recently, the energy response of YAP:Mn-based thermoluminescent (TL) detectors (Z_{eff} = 31.4) of 1 mm thickness to photon radiation is about 40 times higher for 55 keV than that for Co-60 (1.25 MeV) [1].

The present work demonstrates experimental results obtained for single crystalline YAP:Mn detectors irradiated to photon radiation of different radiation qualities modified by various metal (copper, aluminum, tin) filters of thickness from 2 to 6 mm. For this purpose the following ISO standard radiation qualities were used: X-rays of N-40 (effective energy 33 keV), N-60 (48 keV) and N-100 (83 keV), γ-radiation series S-Cs (Cs-137, 662 keV) and S-Co (Co-60, 1.25 MeV). These results are compared with results of Monte Carlo simulations of the value of energy deposition (which is assumed to be proportional to the luminescence output of the detectors) done for the same 'radiation-attenuator-detector' combinations.

The analysis shows good agreement between experimental and calculated results that testifies adequacy of the used calculation approach and their applicability to modulate an output from high-Z TL detectors exposed to radiation of different qualities.

Acknowledgements. The work was supported by the NATO Science for Peace and Security Program (Project G4649), by the European Regional Development Fund (Innovative Economy grant POIG.01.01.02-00-108/09) and the Radiation Protection Institute intramural funding.

[1] Ya. Zhydachevskii, A. Morgun, S. Dubinski, Yan Yu, M. Glowacki, S. Ubizskii, V. Chumak, M. Berkowski, A. Suchocki, Energy response of the TL detectors based on $YAlO_3$:Mn crystals, *Radiat. Meas.* **90** (2016) 262-264.

Effect of Si on the Magnetic and Mechanical Properties of Arc Melted Soft Magnetic Fe-Si-Al Alloys

A. Boulouma[1, 2], A. Drici[2], A.K. Gangopadhyay[3], A. Benaldjia[2]

[1] *ESTI of Annaba, Algeria*
[2] *LEREC laboratory, Department of physics, university of Annaba, Algeria*
[3] *Department of physics and Institute of Materials Science and Engineering, Washington University in St Louis, Mo 63130, USA*

This work aims to study the effect of silicon addition on structural, mechanical and magnetic properties of arc melted Fe-Si-Al Sundust alloys. Analysis of x-ray diffraction data on arc-melted ingots were used to calculate the lattice parameters, lattice strain and crystallite size. Scanning Electronic Microscopy analysis confirmed high-density materials synthesized by arc-melting. Vickers microhardness (HV) tests showed a significant enhancement with increasing silicon. Magnetic susceptibility, under 0.5T, showed a composition and temperature dependent behavior.

Key words: Fe-Al-Si, sendust alloys, Vickers microhardness, magnetic susceptibility, order-disorder transition, Fe solid solution, ordered DO_3 (α_1-$Fe_3Si_{0.7}Al_{0.3}$) phase.

Achieve a TE/TM Mode Conversion in an Ion-Exchanged Glass Waveguide

Mounir Bouras, Abdessalem Hocini

Department of Electronics, University of M'sila BP.166,
Route Ichebilia, M'sila 28000, Algeria

The integration of magneto-optical materials with classical technologies being still a difficult problem, Many novel materials and device designs have been proposed as photonic analogs to electrical diodes over the last four decades. This study explores the possibility to realize a mode converter TE-TM based on a hybrid structure. This hybrid device is made by coating a SiO_2/ZrO_2 layer doped with magnetic nanoparticles on an ion-exchanged glass waveguide. We have used the finite difference beam propagation method for numerical solution of the scalar wave equation. We have also used the transparent boundary condition. The mode converter TE-TM depending on the amount of nanoparticles in the composite, on the spatial distribution of the field in the guide and on the modal birefringence of the hybrid structure.

[1] F. Choueikani, F. Royer, D. Jamon, A. Siblini, J.J. Rousseau, S. Neve, J. Charara, Magneto-optical waveguides made of cobalt ferrite nanoparticles embedded in silica/zirconia organic-inorganic matrix, *Appl. Phys. Lett.* **94** (2009) 051113.

[2] N. Bahlmann, M. Lohmeyer, O. Zhuromskyy, H. Dötsch, P. Hertel, Nonreciprocal coupled waveguides forinte grated optical isolators and circulators for TM- modes, *Opt. Commun.* **161**(4–6) (1999) 330–337.

[3] H. Dötsch, N. Bahlmann, O. Zhuromskyy, M. Hammer, L. Wilkens, R. Gerhardt, P. Hertel, Applications of magneto-optical waveguides in integrated optics, *JOSA B* **22**(1) (2005) 240253.

[4] A. Hocini, M. Bouras, H. Amata, Theoretical investigations on optical properties of magneto-optical thin film on ion-exchanged glass waveguide, *Opt. Mater.* **35** (2013) 1669–1674.

Analysis and Design of Magneto-Optic Mach-Zehnder Isolator Made with a Magnetic Nanoparticles-Doped SiO_2/ZrO_2 Layer

Mounir Bouras, Abdessalem Hocini

Department of Electronics, University of M'sila BP.166, Route Ichebilia, M'sila 28000, Algeria

Magneto-optical SiO_2/ZrO_2 layer doped with magnetic nanoparticles $CoFe_2O_4$ combine high Faraday rotation, low optical losses and the full compatibility of the sol-gel coating with classical integrated technologies and especially the technology on glass. In this work, we developed an efficient monomodal waveguide with an integrated magneto-optic Mach-Zehnder (MZ) isolator. The waveguide isolator is based on a nonreciprocal phase shift in the magneto-optic branch of the MZ isolator. This last made by SiO_2/ZrO_2 layer doped with magnetic nanoparticles $CoFe_2O_4$, We considered two different types of MZI configurations, one with an S-bend and another with an angular Y-junction. We were able to determine the critical cut-off radius for the S-bend Y-junction and the critical cut-off angle for the angular Y-junction. We have used the finite difference beam propagation method for numerical solution of the full wave equation. These critical parameters, typically requiring microscale resolution, ensure minimal optical losses in the forward direction and increase return loss in the backward direction and achieved a 35 dB isolation ratio.

[1] Dibyo Sarkar, Iqbal Jamal, Sushanta K. Mitra, Analysis, design and fabrication of optical waveguides for Mach–Zehnder Interferometry, *Opt.Commun.* (2013).

[2] F. Choueikani, F. Royer, D. Jamon, A. Siblini, J.J. Rousseau, S. Neve, J. Charara, Magneto-optical waveguides made of cobalt ferrite nanoparticles embedded in silica/zirconia organic-inorganic matrix, *Appl. Phys. Lett.* **94** (2009) 051113.

[3] N. Bahlmann, M. Lohmeyer, O. Zhuromskyy, H. Dötsch, P. Hertel, Nonreciprocal coupled waveguides forinte grated optical isolators and circulators for TM- modes, *Opt. Commun.* **161**(4–6) (1999) 330–337.

[4] A. Hocini, M. Bouras, H. Amata, Theoretical investigations on optical properties of magneto-optical thin film on ion-exchanged glass waveguide, *Opt. Mater.* **35** (2013) 1669–1674.

[5] H. Dötsch, N. Bahlmann, O. Zhuromskyy, M. Hammer, L. Wilkens, R. Gerhardt, P. Hertel, Applications of magneto-optical waveguides in integrated optics, *JOSA B* **22**(1) (2005) 240253.

SECTION 7

MATERIALS FOR SENSING AND CATALYSIS

Lithium Diffusion Pathways in Modern Solid State Electrolytes

A. Senyshyn[1], M. Monchak[2], H. Boysen[3]

[1]*Heinz Maier-Leibnitz Zentrum (MLZ), Technische Universität München, Lichtenbergstr. 1, D-85748 Garching, Germany*
[2]*Karlsruher Institut für Technologie (KIT), Institut für Angewandte Materialien (IAM), Karlsruhe, Germany*
[3]*Department für Geo- und Umweltwissenschaften, Sektion Kristallographie, LMU München, Am Coulombwall 6, D-85748 Garching, Germany*

Rapid development of portable energy storage media permanently requires materials, which are cheaper, safer, more stable\robust and have better electrochemical performance compared to the existing analogues. On the other hand the concept of all solid ceramic Li ion batteries is now actively explored as potentially safer, more stable and capable to operate at higher potentials alternative to conventional Li-ion batteries based on liquid electrolytes.

To large extent the electrochemical energy storage and energy conversion are diffusion-based/limited processes, where the knowledge about underlying diffusion pathways and mechanisms is essential. However, the experimental information about preferable diffusion pathways of polycrystalline (non-cubic) materials can hardly be obtained *per see* by bulk (e.g. resistivity, impedance spectroscopy, quasielastic neutron scattering *etc*) measurements. The majority of theoretical methods typically utilized for prediction of diffusion pathways are often based on molecular dynamics simulations (either force-field or *ab initio*) and create certain challenges for the modelling of diffusion properties of new materials.

The diffusion process in a material is determined by its crystal structure and in many cases the crystal structure is a key for its understanding. At the moment there are several methods available and capable to predict the preferred ion diffusion pathways with high reliability on the basis of the underlying crystal structure, *e.g.* analysis of topology based on Voronoi-Dirichlet partitioning, Hirschfeld approach, differential bond valence method *etc*. However most of them requires accurate structural input, which, along with the fact, that modern "green energy" production and storage is based on light atoms, where conventional X-ray methods have certain limitations, makes neutron-based scattering techniques highly relevant. Neutron powder diffraction is a powerful experimental tool, well suited for the localization of Li under the presence of heavier elements, delivering accurate fractional coordinates, lattice dimensions, Debye-Waller factors etc. Probe of nuclear density distribution in lithium conducting materials by the analyses of probability density function from anharmonic refinements of powder diffraction data and/or the reconstruction of electron/nuclear densities by maximum entropy method [1] opens ample opportunities for the development of new generation solid state lithium conductors.

In the current contribution the application of differential bond valence method for the prediction and neutron diffraction-based techniques for the experimental evaluation of ion diffusion pathways in model materials [1], modern solid state lithium electrolytes [2-4] and promising materials for electrochemical energy conversion and storage [5,6] will be presented and discussed in brief.

[1] A. Senyshyn, H. Boysen, R. Niewa et al., *J. Phys. D: Appl. Phys.* **45** (2012) 175305.
[2] M. Monchak, T. Hupfer, A. Senyshyn et al., *Inorg. Chem.* **55**(6) (2016) 2941-2945.
[3] D.A. Weber, A. Senyshyn, K.S. Weldert et al., *Chem. Mater.* **28**(16) (2016) 5905-5915.
[4] H. Buschmann, J. Dolle, S. Berendts et al., *Phys. Chem. Chem. Phys.* **13** (2011) 19378-19392.
[5] O. Dolotko, A. Senyshyn, M.J. Mühlbauer et al., *Solid State Sci.* **36** (2014) 101-106.
[6] M. Monchak, O. Dolotko, M.J. Mühlbauer et al., *Solid State Sciences* **61** (2016) 161-166.

Non-Contact Luminescence Lifetime Micro-Thermometry Using Scintillation Sensors

V.B. Mykhaylyk[1], H. Kraus[2], A.Wagner[1]

[1]*Diamond Light Source Ltd, Harwell Science and Innovation Campus, Didcot, OX11 0DE, UK*
[2]*Department of Physics, University of Oxford, Keble Road, Oxford OX1 3RH, UK*

Temperature is a critical parameter that defines the state of any system in the nature. Measuring temperature accurately and reliably is thus very important when monitoring chemical, physical and biological processes. For example, knowledge of the precise sample temperature is of high importance in reducing radiation damage to protein crystals during X-ray diffraction experiments using intense synchrotron radiation. A novel technique for remote, non-contact monitoring of the protein crystal temperature has been developed for the new I23 beamline at the Diamond Light Source, a facility dedicated to macromolecular crystallography (MX) with long-wavelength X-rays [1]. Conceptually the method is based on the measurements of the variation of the decay time of a scintillation crystal with temperature. The possibility to have a submicron size sensor in the close proximity to the sample under test and the contactless readout of the signal are the main appealing features of this method.

In this talk we first describe the features of the technique starting with a brief introduction of the measurement principles. We will discuss the characteristics of the components, including choice of scintillation sensors, and practical implementation of the system in the suite of beamline instrumentation. The system performance and application examples will be described and discussed using application examples to demonstrate the potential of the developed technique for non-contact, *in situ* measurements of cryogenic temperatures.

[1] A. Wagner et al., *Acta Cryst. D* **72** (2016) 430-439.

Material Properties of $Ca_3TaGa_3Si_2O_{14}$ Resonators at Elevated Temperatures

Yu.Suhak[1], M. Schulz[1], A. Sotnikov[2], H. Schmidt[2], H. Fritze[1]

[1]*Institute of Energy research and Physical Technologies, Clausthal University of Technology, Goslar, Germany*
[2]*SAWLab Saxony, Leibniz Institute for Solid State and Materials Research (IFW Dresden), Dresden, Germany*

Langasite family crystals attract currently significant attention for high temperature piezoelectric sensors, since they do not show any phase transition up to their melting point (1300-1500 °C). Further, they exhibit good piezoelectric properties. Their crystal structure has four different cation sites and can be described by the general formula $A_3BC_3D_2O_{14}$. In langasite ($La_3Ga_5SiO_{14}$, LGS) Ga^{3+} ions fully occupy both B and C sites, and half of the D sites in a random way, which leads to the structural disorder and increase of losses. In contrast, $Ca_3TaGa_3Si_2O_{14}$ (CTGS) has the ordered structure resulting in lower conductivity and damping, compared to those of LGS [1]. However, the CTGS material properties at elevated temperatures have not been completely studied for now.

This work focuses on determination of piezoelectric coefficients of CTGS from ambient temperature to 900 °C, using the resonant method according to [2] and the ultrasonic pulse-echo method. Additionally, the piezoelectric coefficient d_{11} is determined by the laser Doppler vibrometry (LDV). The single crystalline CTGS samples used in this study are fabricated from Czochralski-grown boules, manufactured by Leibniz Institute for Crystal Growth, Berlin, Germany and by Fomos-Materials, Moscow, Russia. The application of three independent methods for determining the same coefficients is used here for validating the results. The temperature dependences of d_{11} piezoelectric coefficient are presented on Fig. 1.

In addition, the long-term properties of CTGS samples are examined by determining their conductivity and resonance frequency at 1000 °C in air. Beside crystals grown by the mentioned above manufacturers, CTGS from SICCAS, Shanghai, China, is investigated. A resonance frequency shift of approximately 0.1% is observed for investigated samples during 5000 h of thermal treatment.

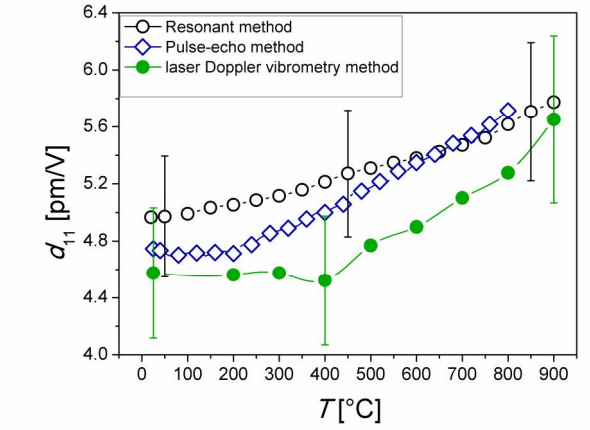

Fig. 1. Piezoelectric coefficient d_{11} as a function of temperature, determined by the resonant, LDV and pulse-echo methods.

[1] Yu. Suhak *et al*., *MRS Advances* **1** (2016) 1513-1518.
[2] IEEE Standard on Piezoelectricity. *ANSI/IEEE Standards* **176** (1987) 1-66.

$K_{1.75}[NH_4]_{0.25}SO_4$ – New Crystal with Isotropic Point

P.A. Shchepanskyi[1,2], V.Yo. Stadnyk[1], R.S. Brezvin[1], I. Kityk[3] , M.Ya. Rudysh[1,2], M. Piasecki[2]

[1]*Ivan Franko National University of Lviv, 8 Kyrylo and Mefodiy Str., 79005 Lviv, Ukraine*
[2]*Jan Dlugosz University in Częstochowa, Al. Armii Krajowej 13/15, 42-200 Czestochowa, Poland*
[3]*Institute of Electronic and Control System, Faculty of Electrical Engineering, Czestochowa University of Technology, 17 Armii Krajowej Str., 42-200 Czestochowa, Poland*

Appearance of the isotropic point (IP) or the point of birefringence sign inversion (BSI) is known to be a result of temperature–spectral deformations of the optical indicatrix at which, for each wavelength at a fixed temperature, the crystal undergoes a transition from an optically uniaxial state to an isotropic state or from an optically biaxial state to uniaxial state.

Earlier, isotropic state was found in a number of dielectric ferroic crystals of the A_2BX_4 group (K_2SO_4, $LiKSO_4$, Rb_2SO_4, $(NH_4)_2BeF_4$, $RbNH_4SO_4$, $RbKSO_4$, $LiNH_4SO_4$) [1, 2] which covers wide temperature and spectral ranges but some of them possesses IP in an inconvenient for practice region of spectrum.

Interesting is search for new crystals of this group with IP. This search aims to expand the range of practically important materials for thermometry [3] and to associate the effect of structural elements substitution on already known temperature and spectral ranges of BSI existence in the crystal. Since cationic substitution leads to insignificant changes in the optical indicatrix parameters, one can expect it will lead to changes in the spectral or temperature range of existence of isotropic state, depending on the percentage of mixing substances.

Considering that K_2SO_4 possess IP, within upper described issue, interesting for us was to investigate the influence of partial isomorphic substitution $K \rightarrow NH_4$ on the existence of BSI.

To follow that aim a representative of mixed systems with the formula $(K_x[NH_4]_{x-1})_2SO_4$ $(0 < x < 1)$, $K_{1.75}[NH_4]_{0.25}SO_4$ single crystals was chosen. Thus, in this work, spectral dependences of refractive indices and birefringence as well as temperature and pressure changes of birefringence of $K_{1.75}[NH_4]_{0.25}SO_4$ crystals on a subject of revealing isotropic points were investigated.

Birefringence dispersion at room temperature was found to be normal in *Y* and *Z* directions and abnormal in *X* direction leading to the occurring of isotropic point which corresponds to the equality $n_x = n_y$ at the wavelength $\lambda \approx 1350$ nm. Such phenomenon is not observed for K_2SO_4 single crystals and thus is caused by the presence of NH_4 ions altering the dispersion character in *x* direction. From study of temperature dependences of birefringence for the $K_{1,75}[NH_4]_{0,25}SO_4$ crystals at wavelength $\lambda = 500$ nm decreasing of birefringence values for main crystal optics directions with temperature increasing is revealed. At temperatures $T_{01} \approx 541$ K and $T_{02} \approx 589$ K two IPs which correspond to the equalities $n_z = n_y$ and $n_z = n_x$, respectively, are detected.

From the investigation of birefringence dispersion under the action of uniaxial stresses it was also showed the displacement of IP and a possibility of inducing pseudo IPs in the crystal by applying uniaxial stresses which for wavelength $\lambda = 500$ nm are equal $\sigma_x \approx 8.3$ kbar, $\sigma_x \sim \sigma_y \approx 7.5$ kbar and $\sigma_x \sim \sigma_z \approx 10.5$ kbar.

[1] M. O. Romanyuk, *Crystal Optics,* IZMN, Kiev, 1997 (in Ukrainian).
[2] V. Stadnik and V. M. Gaba, *Refractometry of Dielectric Crystals with Incommensurable Phases,* Liga Press, Lviv, 2010 (in Ukrainian).
[3] M. O. Romanyuk & M. M. Romanyuk, *Ferroelectrics* **317**, (2005).

Speciation Level Differences in the Structure of Three Mg-Al-CO_3 Layered Double Hydroxides Prepared by Alkoxide and Alkoxide-Free Sol-Gel Syntheses, and Hydrothermal Precipitation

N. Chubar[1], V. Gerda[1], M. Mičušík[2], M. Omastova[2], K. Heister[3], P. Man[4], J. Fraissard[5]

[1]*Taras Shevchenko National University of Kyiv, Faculty of Chemistry, 01601, Ukraine*
[2]*Polymer Institute, Slovak Academy of Sciences, 84541 Bratislava, Slovak Republic*
[3]*GeoLab, Faculty of Geosciences, Utrecht University, 3584 CB Utrecht, The Netherlands*
[4]*Institut des Matériaux de Paris Centre, Université P. et M. Curie, 75005 Paris, France*
[5]*Université P. et M. Curie, ESPCI- LPEM, 75005 Paris, France*

Layered double hydroxides (LDHs), called also anionic clays or hydrotalcites, are complex hydrous oxides built on the layers with a brucite-like structure carrying a net positive charge that is balanced by the anions intercalated between the positively charged layers. The chemical compositions of their layer cations and their interlayer anions can be greatly varied, and the interlayer space can be explored for many applications such as removal of target ions/molecules from water, catalysis, medicine, drug delivery, cosmetics etc. However, after being discovered more than 170 years ago, in two major applications based on the interfacial phenomena, adsorption and catalysis, the application of LDHs at the industrial scale have not been found. The main producing companies of LDHs sell them as plastic additives and PVC stabilizers [1-2]. To explain this phenomenon, the structure, surface chemistry, and anion adsorptive properties of the three Mg-Al LDHs produced by different (yet advanced) methods of synthesis have been compared in [3]. The studies were conducted on the speciation level to demonstrate how different the properties of LDHs are if prepared by various synthetic methods.

Application of greater than usual number of research tools for characterisation of the structure, surface chemistry and mechanism of adsorption demonstrated that the three Mg-Al-CO_3 LDHs differed in their porous/layered structure (N_2 adsorption, CO_2 sorption,) crystallinity (XRD), speciation of Al (NMR) and Mg (XPS), thermal stability (TGA), hydration (TGA, FTIR), the interlayer carbonate (FTIR), morphology (SEM) and Mg/Al ratio on the surface and in bulk. Commercial LDH (Sasol company, Germany) [2] produced by traditional alkoxide sol-gel method had poor speciation parameters, the lowest surface area and hydration. Hydrothermally precipitated LDH had an intermediate structure/surface properties desired for adsorbents. Alkoxide-free sol-gel generated LDH (a purely fine inorganic synthesis) had the highest surface area and CO_2 sorption, hydration, variety of ionic carbonate and Al/Mg species. These differences were reflected in their adsorptive performance and stability in water solutions comparing to the materials shown in the literature. In addition to exceptional adsorptive removal properties towards toxic anions (target anions for water industry) the LDH prepared by the original alkoxide-free sol-gel method [4-7] produces unique material which is the only LDH that keeps its layered structure after thermal treatment until 600 ^oC while all other LDHs shown in the literature lose their layered structure at 300 ^oC. This unique property (when double oxide produced from layered double hydroxide is still layered material) in combination with rich speciation can open new avenues in many industrial applications of LDHs if prepared by this synthetic approach.

[1] http://kyowa-chem.jp [2] http://www.sasolgermany.de [3] N. Chubar, V. Gerda, O. Megantari, M. Mičušík, M. Omastova, K. Heister, M. Man, F. Fraissard, *Chem. Eng. J.* **234** (2013) 284-299. [4] N. Chubar, *J. Colloid Interface Sci.* **357** (2011) 198-209. [5] N. Chubar, *Water Sci. Tech.: WS* **5**(11) (2011) 505-515. [6] N. Chubar, *J. Mat. Chem. A* **2** (2014) 15995–16007. [7] N. Chubar, M. Szlachta, *Chem. Eng. J.* **279** (2015) 885–896.

Determination of Surface Reactivity of Inorganic Anion Exchangers Based on Complex Metal Hydrous Oxides Using EXAFS Simulation

N. Chubar[1], V. Gerda[1], G. Yablokova[2], D. Banerjee[3]

[1]*Taras Shevchenko National University of Kyiv, Faculty of Chemistry, 01601, Ukraine*
[2]*KU Leuven, Department of Materials Engineering, 3001 Leuven, Belgium*
[3]*Dutch-Belgian Beamline (DUBBLE), ESRF – The European Synchrotron CS 40220, Grenoble, France*

Many emergent functions have been discovered at the interfaces of complex metal oxides, including such promising compositions as hydrous oxides of d-metal + lanthanide, Fe-Ce, and their composites. Success in applications of these materials in adsorption and catalysis depends on their structural and electronic properties which can be fully investigated by synchrotron-based techniques, such as EXAFS (X-ray absorption fine structure)/XANES (X-ray absorption near edge structure) that covers both crystalline and amorphous phases and provide new insight into the structure of complex oxide-based materials.

To gain deeper insight on adsorptive reactivity of Fe-Ce oxide-based composites (hydrothermally precipitated at Fe-to-Ce dosage ratios of 1:0, 2:1, 1:1, 1:2, and 0:1) their atomic-scale properties at synthesis [1] as well as their reconstruction processes upon treatment at 300°C [2] were investigated by EXAFS/XANES, XRD, XPS and FTIR. The structural changes were correlated with the adsorptive removal of arsenate, phosphate, fluoride, bromide, and bromate which are the target anions for water treatment industries. In spite of general awareness of the importance of surface area in adsorptive removal, the increase in surface area upon thermal treatment did not increase adsorption of the studied anions. However, EXAFS simulations and the adsorption of most of the anions provided evidence of regularities between local structures around Fe atom in composites treated at 80 and 300°C. The best adsorption of most anions was demonstrated by adsorbents whose simulated outer Fe shells resulted from oscillations from both O and Fe atoms. In contrast, the loss of extended local structures at >4 Å was correlated with the decrease of adsorptive removal, Fig. 1 [1-2].

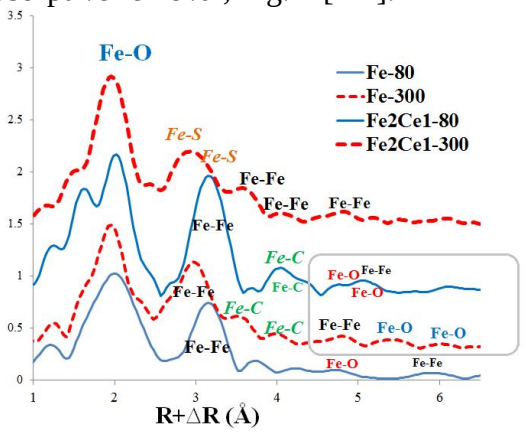

Radial structure around Fe, obtained from Fourier transforms of Fe K-edge EXAFS oscillations of the samples and fitting results.

For the first time, the utilization of EXAFS to obtain an extended local structure has been suggested as a methodological approach to estimate the surface reactivity of inorganic materials based on metal hydrous oxides intended for use as anion exchange adsorbents and possibly catalysts.

[1] N. Chubar, V. Gerda, D. Banerjee, Influence of 300 °C thermal conversion of Fe-Ce hydrous oxides prepared by hydrothermal precipitation on the adsorptive performance of five anions: Insights from EXAFS/XANES, XRD and FTIR (companion paper), *J. Colloid Interface Science* **491**(1) (2017) 111-122.

[2] N. Chubar, V. Gerda, D. Banerjee, G. Yablokova, Effect of Fe(II)/Ce(III) dosage ratio on the structure and anion adsorptive removal of hydrothermally precipitated composites: Insights from EXAFS/XANES, XRD and FTIR, *J. Colloid Interface Science* **487**(1) (2017) 388-400.

Hydrogen Evolution Reaction on the Oxidized Surfaces of the Fe-Based Amorphous Alloys

O.M. Danyliak[1], L.M. Boichyshyn[1,*], N.L. Pandiak[2]

[1] *Faculty of Chemistry, Ivan Franko National University of Lviv, 6 Kyryla and Mefodia Str., 79005 Lviv, Ukraine, * lboichyshyn@yahoo.com*
[2] *The National Forestry and Wood-Technology University of Ukraine, 103 Gen. Chuprynka Str., 79057 Lviv, Ukraine*

Different amorphous and nanocrystalline metallic alloys have been studied as electrocatalysts for hydrogen evolution reaction (HER) in alkaline aqueous solutions. The highly defects microstructure of the nanocrystalline materials and the coordinatively unsaturated surface atoms in the amorphous metallic alloys (AMA) are prerequisites for attractive catalytic properties [1]. Characteristics of amorphous and nanocrystalline metallic electrodes can be modified by changing elements composition and geometric surface area [2].

The aim of this study was to investigate the influence of the oxide-hydroxide layers formed by different conditions on the electrocatalytic activity of the $Fe_{82}Nb_2B_{14}RE_2$ (RE = Y, Gd, Tb, Dy) AMA-electrodes for HER. The object of this study were Fe-Nb-B-RE amorphous ribbons produced by melt spinning (Physics of Metals Institute, NAS Ukraine, Kyiv) with the following compositions: $Fe_{84}Nb_2B_{14}$, $Fe_{82}Nb_2B_{14}Y_2$, $Fe_{82}Nb_2B_{14}Gd_2$, $Fe_{82}Nb_2B_{14}Tb_2$ and $Fe_{82}Nb_2B_{14}Dy_2$. The oxidation of the AMA has been received by different conditions: immersion AMA in the KOH 4 M solution for 24 hours; annealing of AMA for 1 h in air atmosphere at the first phase transition. The oxide-hydroxide layers formed at different conditions was studied by the atomic force microscopy (AFM) and scanning electron microscopy (SEM) methods. The identification of oxide on the surface of the AMA was studied voltammetric method. Due various treatment of the AMA oxide-hydroxide layers of the alloys have different nature. The electrocatalytic activity layer was formed on the surface of the AMA consists mainly of iron oxide and hydroxide compounds with the inclusion of niobium and rare earth metals (Fig. 1).

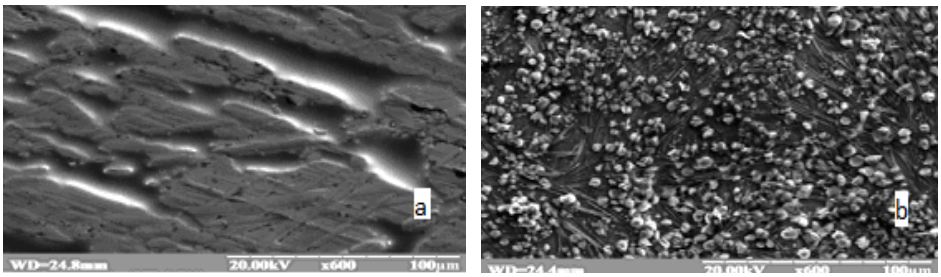

Fig. 1 SEM of the initial (a) and oxidized (b) $Fe_{84}Nb_2B_{14}$ amorphous alloys in the 4 M solution KOH

The oxidation of the $Fe_{82}Nb_2B_{14}RE_2$ (RE = Y, Gd, Tb, Dy) alloys (thermal treatment and maintaining AMA in the KOH 4 M solution for 24 hours) changed the structure of the surface. The surface oxide-hydroxide layer which appeared caused changes in electrochemical activity of the oxidized AMA-electrodes due to the enhancement of roughness of electrode surface of alloys.

Doping by 2 at. % RE base alloy $Fe_{84}Nb_2B_{14}$ increases the catalytic activity of amorphous alloys $Fe_{82}Nb_2B_{14}RE_2$ for HER in an alkaline solution. It is caused by the formation of oxides of rare earth metals on the surface of investigated alloys, which are not soluble in alkaline solutions.

[1] L. Mihailov, T. Spassov and M. Bojinov, *International journal of hydrogen energy* **37** (2012) 10499–10506.
[2] M.A. Domínguez-Crespo, M. Plata-Torres, A.M. Torres-Huerta et al., *Materials Characterization* **55** (2005) 83–91.

Catalytic Properties of Iron Oxides in the Reaction of Low-Temperature Ozone Decomposition

A.S. Truba*, T.L. Rakitskaya, A.A. Stoyan, V.Y. Volkova

Faculty of Chemistry, Odessa I.I. Mechnikov National University, 2 Dvoryanskaya Str., 65082 Odessa, Ukraine
* truba@onu.edu.ua

Iron oxides show low activity as catalysts of redox reactions at ambient temperature and normal pressure. However, the significant attention paid to them lately is caused by the possibility to obtain the desired phase composition, physicochemical properties and, as a result, maximum catalytic activity by varying the nature of their precursors, the ratio of their components, the temperature of their calcination and other factors. The work presents the results of determination of the catalytic activity shown by maghemite (γ-Fe_2O_3) synthesized by coprecipitation of $FeSO_4 \cdot 7H_2O$ with $FeCl_3 \cdot 9H_2O$ (sample I) or with $Fe_2(SO_4)_3 \cdot 9H_2O$ (sample II) in non-protected medium followed by thermal treatment of coprecipitation products at 200, 300, and 500 °C. The samples thus synthesized were characterized by X-ray phase analysis, IR spectroscopy, water vapor ad/desorption, DTG-DTA, pH-metry and also tested in the reaction of ozone decomposition. The both samples calcinated at 200 °C contained maghemite as a dominant phase and minor amounts of magnetite (Fe_3O_4), hematite (α-Fe_2O_3), and goethite (α-FeOOH) as impurity phases. The calcination of the samples at 300 and 500 °C led to a change in the ratio of the phases with domination of hematite as indicated by a prevalence of reflexes corresponding to it.

The testing of the samples in the reaction with ozone depicted in Figure (*a*, *b*) was carried out at its initial concentration of 1 mg/m^3 which was by an order of magnitude greater than the maximum permissible ozone concentration, MPC_{O_3}. Since a half-conversion time, $t_{1/2}$, is one of the mostly used parameters characterizing the reactivity substances in the reaction with ozone, all tests were finished when a final ozone concentration became equal to 0.5 mg/m^3.

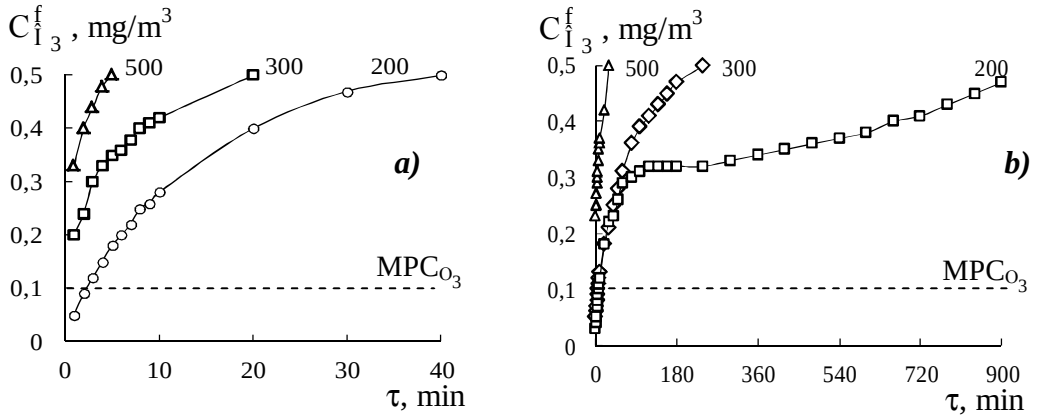

Figure. Time dependences of a final ozone concentration in the course of ozone decomposition by the synthesized samples calcinated at different temperatures: sample I (a) and sample II (b)

Analyzing the kinetics of ozone decomposition, some conclusions can be drawn. Samples II prepared from Fe(II) and Fe(III) sulfates are much more active than samples I: their $t_{1/2}$ values and the amount of ozone entered into the reaction up to a moment of experiment termination are many times higher than those for samples I. Both samples I and samples II lose their activity with the increase in the calcination temperature due to the following phase transformation: γ-$Fe_2O_3 \rightarrow \alpha$-$Fe_2O_3$.

Catalytic Compositions Based on Copper(II) and Iron(III) Chlorides and Bentonite for Low-Temperature Sulfur Dioxide Oxidation with Air Oxygen

T.A. Kiose*, T.L. Rakitskaya, K.O. Golubchik

*Faculty of Chemistry, Odessa I.I. Mechnikov National University, 2 Dvoryanskaya Str., 65082 Odessa, Ukraine, * kiose79@mail.ru*

Sulfur dioxide is one of the most widespread environmental impurities which demands great efforts for its removal from air. The work presents some results of our investigation of chemisorption-catalytic behavior of natural bentonite (N-Bent) based compositions containing copper(II) or iron(III) chloride or both these salts in the process of air purification from sulfur dioxide. Both N-Bent and the compositions were characterized by X-ray phase analysis, FT-IR spectroscopy, DTG-DTA, water vapor ad/desorption, pH-metry and also tested in the reaction with sulfur dioxide contained in the air. Figure shows kinetic curves (1-5) representing the time dependences of a final sulfur dioxide concentration ($C^{f}_{SO_2}$) in the gas-air mixture (GAM) passing through the fixed bed of each composition under study. N-Bent (1) containing montmorillonite as a dominant phase and minor amounts of iron(III) oxide, silicon oxide (α-quartz), calcite, and kaolinite as impurity phases totally absorbs sulfur dioxide for 10 min. Then the sulfur dioxide final concentration rapidly increases and, in 170 min, becomes equal to the initial sulfur dioxide concentration, $C^{in}_{SO_2}$, in the GAM (150 mg/m^3). The kinetics of the process for $CuCl_2$/N-Bent (**2**) and $FeCl_3$/N-Bent (**3**) compositions is similar to that shown by N-Bent, however, the amount of sulfur dioxide absorbed is much higher, probably, due to SO_2 chemisorption by the metal ions. The kinetic curves drastically change their profiles for bimetallic compositions $CuCl_2$-$FeCl_3$/N-Bent (**4**) and $CuCl_2$-$FeCl_3$-KCl/N-Bent (**5**): periods of time when SO_2 absorption is total are much longer, $C^{f}_{SO_2}$ increases up to the initial one much slower (**4**) and the amounts of sulfur dioxide entered into the reaction up to a moment when $C^{f}_{SO_2}$ became equal to $C^{in}_{SO_2}$ (**4**) and a moment of experiment termination (**5**) are much higher than those for monometallic compositions. Analyzing the fact that these SO_2 amounts many times exceed the amount calculated taking into account the stoichiometry of SO_2 reactions with Cu(II) and Fe(III) and also the fact that the times of protective action for bimetallic compositions are many times longer than the sum of protective times for both monometallic compositions, one can conclude that there is a certain synergism in the action of supported $CuCl_2$ and $FeCl_3$ in the case of their simultaneous presence. The true catalytic process takes place for the bimetallic composition (**5**) containing additional chloride ions (C = 1.0×10^{-6} mol/g) which are supposed to form a coordination sphere of Cu(II) and/or Fe(III) optimal for ascertainment of a closed catalytic cycle confirmed by the steady-state mode of SO_2 oxidation with air oxygen.

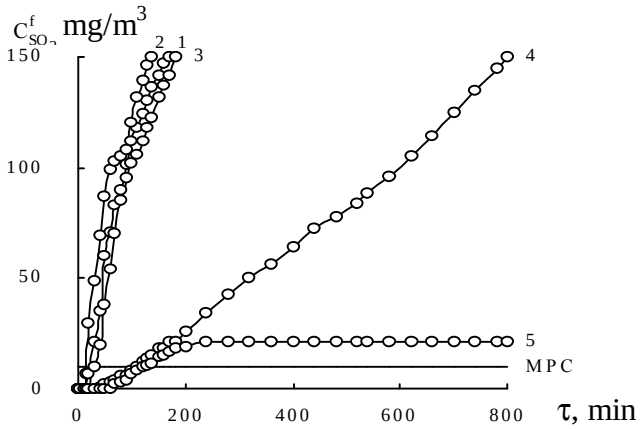

Figure. Time dependences of $C^{in}_{SO_2}$ in the course of chemisorption-catalytic oxidation of SO_2 by compositions 1-5
$C_{Cu(II)}$ = 5.9×10^{-5}, $C_{Fe(III)}$ = 1.0×10^{-6} mol/g; t = 20 °C.
$C^{in}_{SO_2}$ = 150 mg/m^3

The Impact of the Phase Composition of Ni - Fe Catalytic Systems on their Activity in the Reaction of CO_2 Methanation

R. Meshkini Far[1,*], A. Dyachenko[1], O. Bieda[1], M. Filonenko[2], O. Ischenko[1]

[1]*Taras Shevchenko Kyiv National University, 64 Volodymyrs'ka Str, 01601 Kyiv, Ukraine*
[2]*National Pedagogical Dragomanov University, 9 Pirogova Str, 01601 Kyiv, Ukraine*
* *r.meshkinifar@gmail.com*

The catalytic properties of Ni-Fe system were investigated in concentrations interval of 100 - 65 wt. % Ni. Synthesis of the catalysts was carried out by dissolving the proper amount of metal in nitric acid with subsequent precipitation by ammonia, and subsequent drying, and reducing the obtained oxides to metals by the gas mixture (50 vol % H_2 - 50 vol % He) at atmospheric pressure at the temperature of 300°C for 1 hour. The final step of the synthesis is a run of a catalyst in the reaction mixture (about 2 vol. % CO_2 - 55 vol. % H_2 – 43 vol. % He). - up to 350°C.

As a result, the most active samples are in the concentration range of 60-70 wt. % Ni and 80-100 wt. % Ni. It is consistent with the literature data [1], because in 72-77 wt. % Ni we observe the formation of $FeNi_3$ intermetallide at 493 °C.

For the active $Ni_{80}Fe_{20}$ sample, a CO_2 conversion starts after 150 °C, while the maximum amount of CH_4 (60%) is formed at 300 °C. The amount of CO formed after 200 °C remains low and does not exceed 7%. For the inactive $Ni_{75}Fe_{25}$ sample, the transformations start at a higher temperature (250 °C), while the reaction products (basic CH_4 and secondary CO) are produced approximately in equal amounts (up to 8%) in the temperature range 350 - 370 °C.

Studying the structure of the samples by X-ray analysis before and after catalytic action showed that the samples before the recovery exist as NiO and Fe_3O_4 phases. After using samples in methanation reaction, the diffraction pattern shows a cubic face-centered crystalline phase with cell parameters a bit smaller than in γ-solution iron in nickel. It corresponds to the Fe-Ni intermetallides of variable composition with the same crystal structure as in Ni (see Table). For comparison: unit cell parameter of pure Ni is approximately 3.520, for pure Fe – approximately 3.568.

Table. XRD data of the Ni-Fe catalysts

Sample	T, ^{0}C	Phase	Cell parameter, A	Crystallite size (Scherrer), nm
$Ni_{80}Fe_{20}$ before reaction	300	NiO	4,182	5-7
	300	Fe_3O_4	8.367	12-19
$Ni_{80}Fe_{20}$ after reaction	300	Ni/Fe	3.537	9-13
	500	Ni/Fe	3.542	10-13
$Ni_{75}Fe_{25}$ before reaction	300	NiO	4.186	5-8
	300	Fe_2O_3	8.338	5-8
$Ni_{75}Fe_{25}$ after reaction	300	Ni/Fe	3.561	18-23
	500	Ni/Fe	3.556	18-20

[1] N.V. Grum-Grjimailo, *Chemistry bounds in the metals alloys*, Moscow: NA of USSR, 1960 (in Russian).

Catalytic and Structural Properties of Co-Fe Systems in the Reaction of CO_2 Methanation

A. Dyachenko[1], M. Zhludenko[1], O. Bieda[1], S. Gaidai[1], M. Filonenko[2], O. Ischenko[1]

[1]*Taras Shevchenko Kyiv National University, 64 Volodymyrs'ka Str, 01601 Kyiv, Ukraine*
[2]*Dragomanov National Pedagogical University, 9 Pirogova Str, 01601 Kyiv, Ukraine*

Many research studies has been devoted to explore the process of carbon dioxide recycling into high energy content fuels or industrially important compounds. Among these, methanation processes have been proposed to be an effective method for the utilization of CO_2.

The catalytic properties of Co-Fe system were investigated in concentrations range of Co 0-100 wt. % in the reaction of CO_2 methanation. Synthesis of the catalysts was carried out by dissolving the proper amount of metal in nitric acid with subsequent precipitation by ammonia and subsequent drying, and reducing the obtained oxides to metals by the gas mixture (50 vol % H_2 - 50 vol % He) at atmospheric pressure, at the temperature of 300°C for 1 hour. The final step of the synthesis is a run of a catalyst in the reaction mixture (about 2 vol. % CO_2 - 55 vol. % H_2 – 43 vol. % He) - up to 350°C.

The catalytic activity of Co-Fe systems grows with the increasing of Co concentration: for the range of 0-10 Co wt. % - CH_4 yield is about 3 %; 14-50 wt% - CH_4 yield is increased up to 40%; 70-80 wt. % - CH_4 yield is about 60 % and 85-93 wt. % - CH_4 yield is reached its maximum amount (100 %). The sample of pure cobalt demonstrates 57 % of CH_4 yield.

Formation of carbon monoxide, as a co-product of CO_2 methanation, was observed for the samples with a low–middle Co wt.%. and also for the pure Co. The catalysts with 85-93 wt. % of Co demonstrated high activity with 100% CH_4 selectivity at the 150-300 ^{0}C. It could be explained by the heterogenous state of these samples.

XRD analysis of the samples with high Co wt.% ($Co_{75}Fe_{25}$, for example) before catalytic reaction has shown the presence of substituted spinel phase $Co_{3-x}Fe_xO_4$. After catalytic process α-Fe solid solution (cell parameter 2,842 Å) and α-Co solid solution (cell parameter 3,558 Å) were observed. Calculated crystallite size for these samples was 20 nm.

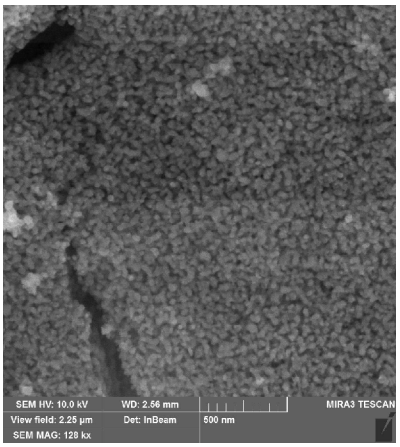

Analysis with SEM-EDX method showed the next averaged elemental composition (at. %) of the $Co_{75}Fe_{25}$ sample after the catalytic run: Fe:Co = 27:73, (Fe+Co):O = 85:15 (which corresponds to $Me:Me_3O_4$ ratio of 95:5, indicating that sample is in the metallic state). These samples consist of spherical particles with a size of 15-20 nm (see figure).

Fig. Scanning electron micrograph of $Co_{75}Fe_{25}$

It could be concluded that the high catalytic activity of Co-Fe materials enriched with Co is determined by specifics of their structure.

Oxygen Electrocatalysis by Electrolytically Doped Manganese (IV) Oxides

G. Sokolsky[1], L. Zudina[1], O. Miroshnikov[1], E. Boldyrev[2]

[1]*National University of Food Technologies*
[2]*Institute of General and Inorganic Chemistry of NASU*

Manganese (IV) oxides are among the most effective O_2 electrocatalysts. The phase composition and structure defects have profound influence on this material activity. The purpose of this work was to study influence of induced by dopant ions changes in phase composition and disorder of surface states on ability of manganese(IV) oxides to be oxygen electrocatalyst.

Manganese (IV) oxide obtained on the platinum anode (with current density, *i*, of 10 A/dm^2) using the vitreous carbon plate as an auxiliary electrode. The pristine fluorine-containing electrolyte consisted of 0.1 M HF + 0.7 M $MnSO_4$ and the dopant additives in the electrolyte were: 0.01 M Fe^{2+}, 1.5 M NH_4^+ [1]. XRD was performed on a DRON 4 instrument (Cu*K*α-radiation). The cyclic voltammetry (CVA) experiment was carried out in a standard three electrode cell and 0.3 M LiOH electrolyte saturated with O_2 on IPC-PRO potentiostat–galvanostat at the potential scan rate to within 0.001–0.5 V/s. Carbon paste electrode (CPE) was a thoroughly grounded mixture of doped manganese oxide : graphite in the ratio 70:30 and polytetrafluoroethylene (PTFE) emulsion loaded into PTFE-tube.

The XRD phase analysis showed the following main phase components depending on dopants added: α-MnO_2 (hollandite, I4/m) — NH_4^+; γ-MnO_2 (ramsdellite, Pbam) — Fe^{2+}. These results are in agreement with thermodynamics of hollandite phase since foreign ions like NH_4^+ in structure channels decrease its free energy significantly [2] as a result of influence of entropic factor. Both samples have nanorod shape of crystallites with diameter of about 10—20 nm as shown by TEM. The high activity in oxygen reduction(oxidation) reaction ORR (OOR) of α-MnO_2 nanorods among other MnO_2 polymorphs [3] can be attributed to availability of structure tunnels to small O_2 and H_2O molecules. The broadened nature of ORR (OOR) peaks on α-MnO_2 unlike Fe-doped γ-MnO_2 sample confirms the latter hypothesis. The high activity of Fe^{2+}-doped MnO_2 indicates the positive role of Fe^{3+}/Fe^{2+} redox pairs as active sites of surface states. The ORR (OOR) CVA effects in literature are uncertain. ORR electrode potential range based on rotating disk electrode (RDE) and RDE with ring electrode is too negative because thermodynamically the ORR starts at higher potentials as two weak waves. CVAs of doped MnO_2 CPE in 0.30 M LiOH solution saturated with ambient oxygen are demonstrated at V=20 mV·s^{-1}, **Figure**. MnO_2 CPE 1 exhibit two reduction peaks (–0.75 V and –1.05 V) and two oxidation peaks (–0.35 V and –0.1 V) with slightly resolved shoulder of the third one (0.2 V) that were ascribed to manganese redox behaviour. Graphite electrode has by the order of magnitude lower currents of the same processes that are shifted due to polarisation effects. Peaks observed at higher electrode potentials were ascribed to the four-electron redox processes of O_2 with HO_2^- as the intermediate, Fe^{3+}/Fe^{2+}.

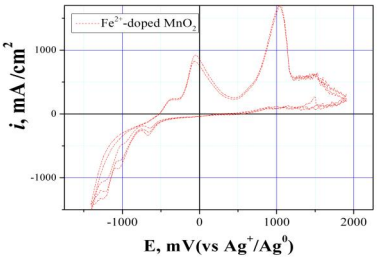

Fig. CVA of Fe-doped γ-MnO_2 sample CPE in O_2 saturated 0.3M LiOH (V = 20 mV·s^{-1})

The electrolytic doping procedure makes the number of available structure states of electrodeposited materials broader and improves the prospective of practical application of electrodeposited manganese(IV) oxides as electrocatalyst.

[1] G.V. Sokolsky, S.V. Ivanov, E. I. Boldyrev et al., *Solid State Phenom.* **230** (2015) 85. [2] S. Fritsch, E. J. Post, A. Navrotsky, *Geochim. Cosmochim. Acta.* **61**(13) (1997) 2613. [3] P.-C. Li, C.-C. Hu, et al., *Journal of Power Sources* **298** (2015) 102-113.

Methods and Ways of Piezoelectric Accelerometers Fastening on the Objects of Research

I. Korobiichuk[1], O. Bezvesilna[2], M. Koshovyj[3], M. Kachniarz[1]

[1]*Industrial Research Institute for Automation and Measurements PIAP, Warsaw, Poland*
[2]*National Technical University of Ukraine "Kyiv Polytechnic Institute", Kyiv, Ukraine*
[3]*National Aerospace University named after N.E. Zhukovsky "KhAI", Kharkiv, Ukraine*

The piezoelectric measuring converters (PMC) are most often used for measurement of dynamic processes [1], mechanical parameters (efforts, pressure, accelerations, deformations) [2], thermal devices (sensors of thermal streams), devices to control the structure and concentration of gases. In many cases, PMC surpass the sensors made on other physical principles in the accuracy and scopes of usage. PMC are used in mechanical engineering, medicine, industrial systems of measurement and management, inertial systems of navigation, aircraft, geological researches, telecommunication and in many other spheres of human life. The PMC sensitive element is single-crystal or polycrystalline materials with piezoelectric properties. The principle of operation is based on the physical phenomenon of a direct piezoeffect, i.e. the ability of piezoelectric materials to generate electric charge under the impact of mechanical forces [1].

PMC for measurement of mechanical oscillations and impacts are most widely used. The piezoelectric accelerometers (PA) differ from other types of sensors of acceleration and vibration by the wide operating frequency band and dynamic ranges, small sensitivity to the influence of magnetic fields, linear characteristics in these wide ranges, reliability of a design and rather long-term stability of parameters. As PA are active sensors which generate the electric signal proportional to mechanical oscillations, so at their operation the power supply isn't required. Lack of mobile elements of the design excludes the possibility of wear-out and guarantees durability of PA. Besides, the signal which an accelerometer gives, can be integrated for the purpose of measurement and analysis of speed or shift of mechanical oscillations. Piezoelectric accelerometers are sensors of a contact type, they have a mechanical contact with the object of research. The peculiarity of such connection is the fact that the object immediately has an influence on the output signal of the accelerometer. Therefore, study of methods and ways of PA fastening on the objects of research is, undoubtedly, topical [3].

The modern stabilization systems, using the spring, string, quartz, magnetic, and gyroscopic accelerometers cannot provide the required speed of response and accuracy [4]. Therefore, the urgent scientific and technical challenge is to improve the accuracy and speed of response when measuring the acceleration values by increase precision of a piezoelectric sensor for the automatic weapons stabilization system.

[1] I. Korobiichuk, O. Bezvesilna, A. Tkachuk, T. Chilchenko, M. Nowicki, R. Szewczyk, Design of piezoelectric gravimeter for automated aviation gravimetric system, *Journal of Automation, Mobile Robotics & Intelligent Systems* **10**(1) (2016) 43-47, doi:10.14313/JAMRIS_1-2016/6.

[2] G.-P. Wang, Y. Hong, J.-J. Lee, D.-P. Hong, Y.-M. Kim, J.-Y. Kim, Quantitative estimation of the fastening condition of a bolt with using piezoceramic (PZT) sensors, *Key Engineering Materials* **353-358**(4) (2007) 2436-2440.

[3] Z. Jiang, Y. Takeuchi, Health monitoring technique for truss structure with PZT patches (estimation of fastening condition of bolts and damage indices), *Nippon Kikai Gakkai Ronbunshu, C Hen/Transactions of the Japan Society of Mechanical Engineers, Part C* **69**(3) (2003) 586-593.

[4] I. Korobiichuk, Mathematical model of precision sensor for an automatic weapons stabilizer system, *Measurement: Journal of the International Measurement Confederation* **89** (2016) 151-158, doi: 10.1016/j.measurement.2016.04.017.

Improving the Accuracy of Piezoelectric Gravimeter Using New Materials

I. Korobiichuk

Industrial Research Institute for Automation and Measurements PIAP, Warsaw, Poland

Piezoelectric gravimeters currently have the highest measurement accuracy gravitational field of the Earth [1]. The quality of piezo materials that used to construct the sensor of the piezoelectric gravimeters has an impact on the accuracy and sensitivity of measuring gravity anomalies [2, 3].

Piezoelectric gravimeters currently have the highest measurement accuracy of gravitational field of the Earth [1]. The quality of piezo materials that are used to construct the sensor of the piezoelectric gravimeter has an impact on the accuracy and sensitivity of gravity anomalies measurement [2, 3].

Design of the piezoelectric gravimeter of the aviation gravimetric system (AGS) should provide maximum sensitivity. The piezo package is usually formed into mounting bracket with high elasticity. The bending of the element is transformed into the electrical signal due to the piezoelectric effect itself. The material used for the piezoelectric gravimeters construction is quartz [1]. This sensor provides a measurement of the gravity acceleration in the only one direction - along the axis perpendicular to the plane of piezoelectric installation. Thus the gravimeter sensitivity to transverse vibrations and cross velocities is reduced, and therefore the measurement accuracy of the gravity acceleration is increased.

Nowadays there are many other piezoelectric materials that meet the above requirements, but there is no analysis of the use of other types of materials in the gravimeters construction [4]. Analysis of other types piezo materials will reduce measurement error of piezoelectric gravimeters and increase gravimeter sensitivity.

[1] I. Korobiichuk, O. Bezvesilna, A. Tkachuk, R. Szewczyk, M. Nowicki, Piezoelectric gravimeter of the aviation gravimetric system, *Advances in Intelligent Systems and Computing* **440** (2016) 753-763, doi: 10.1007/978-3-319-29357-8_65.

[2] I. Korobiichuk, O. Bezvesilna, A. Tkachuk, T. Chilchenko, M. Nowicki, R. Szewczyk, Design of piezoelectric gravimeter for automated aviation gravimetric system, *Journal of Automation, Mobile Robotics & Intelligent Systems* **10**(1) (2016) 43-47, doi: 10.14313/JAMRIS_1-2016/6.

[3] R.P. Middlemiss, A. Samarelli, D.J. Paul, J. Hough, S. Rowan, G.D. Hammond, Measurement of the Earth tides with a MEMS gravimeter, *Nature* **531**(7596) (2016) 614-617.

[4] *Piezoelectric and Acoustic Materials for Transducer Applications*, Ahmad Safari, E. Koray Akdo˘gan (Editors), 2008, p.478.

SECTION 8

BIOMEDICAL APPLICATIONS OF OXIDES AND RELATED MATERIALS

Glasses for Bioscaffold Applications

Roman Golovchak

Department of Physics and Astronomy, Austin Peay State University, Clarksville, TN 37044, USA

Ability to regenerate (replace) lost structures was always a dream of human beings. There are some living species in nature capable of regeneration, like for example salamander which is able to regenerate its lost limb in about 7-10 weeks. Therefore, one can ask a natural question: if it is possible for salamander, why it shouldn't be possible for human? It is known that salamander possesses the specific genes, which upon activation start the regenerative process and the special type of proteins, which control these genes activity. For a human it might seem a hopeless task, since we don't know if humans even have all the genes necessary for the regeneration, though it is known that certain cells, such as liver cells or red blood cells, can self-renew.

Alternative and more realistic approach relies on substitution of lost structures by implants or scaffolds made of biocompatible materials. Modern trends in tissue engineering and regenerative medicine yield application of biodegradable scaffolds made of engineered biomaterials to restore diseased or damaged tissues. The goal is to provide biodegradable three-dimensional (3D) substrate that facilitates generation of natural tissue, degrades gradually in human body, and finally is replaced by the natural tissue completely. In this regard, bioactive glasses (BG) and ceramics have been widely studied and already developed (45S5 BG composition is even FDA approved) as implants to replace hard tissues of the musculo-skeletal system, such as bones and teeth. The idea on the use of BG-derived bioscaffold for tissue regeneration has generated much interest recently [1,2]. Existence of interconnected pores is an important characteristic of bioscaffolds, which makes them distinct from bulk materials, where the lack of developed pore structure is a reason for slower degradation kinetics and, as a result, the implant may remain in the human body for a long time. The macropores are needed for new tissue ingrowth and blood vessel formation while the nanopores determine degradability of bioscaffold in vivo and enhance cell response. The surface area, which controls the degradation of scaffold can be tuned by changing the nanopore size. The structure and, therefore, bioactivity of BG also can be modified via phase separation at the nanoscale (droplet-like or spinodal), which originates from liquid-liquid immiscibility and can be controlled by synthesis conditions.

Influence of the above factors is analyzed at the example of 45S5 BG (24.4 mol% Na_2O – 26.9 mol% CaO – 2.6 mol% P_2O_5 – 46.1 mol% SiO_2), which appears to be the most promising candidate for hard-tissue bioscaffold applications.

[1] L.L. Hench, *J. Mater. Sci: Mater. Med.* **17** (2006) 967-978.
[2] L.-Ch. Gerhardt, A.R. Boccaccini, *Materials* **3** (2010) 3867-3910.

New Generation of Fluorescent Markers for Application in Medicine

Michal M. Godlewski[1,2], Jaroslaw Kaszewski[1,2,3], Anna Szal[1,2], Anna Slonska[1,2], Malgorzata A. Domino[2], Zdzislaw Gajewski[2], Marek Godlewski[3,4]

[1]*Department of Physiological Sciences, Faculty of Veterinary Medicine, Warsaw University of Life Sciences – SGGW, Nowoursynowska 159, 02-776 Warsaw, Poland*
[2]*Veterinary Research Centre, Centre for Biomedical Research, Department of Large Animals Diseases with Clinic, Faculty of Veterinary Medicine, Warsaw University of Life Sciences – SGGW, Nowoursynowska 100,02-797 Warsaw, Poland*
[3]*Institute of Physics, Polish Acad. of Sci., Al. Lotników 32/46, 02-668 Warsaw, Poland*
[4]*Dept. Math. & Natural Sciences College of Science, Cardinal S. Wyszynski Univ., Warsaw, Poland*

A new generation of fluorescent markers (FMs) for application in biology and medicine is based on oxides nanoparticles doped with rare earth ions. Oxides (ZnO and ZrO_2) were selected due to their bio-neutrality. Rare earth doping of the markers results in an efficient photoluminescence (PL) in a visible light spectral region. PL shows a good stability, the absence of blinking and photo-bleaching. Importantly, the possibility of X-ray stimulated fluorescence was demonstrated for selected markers. This, after functionalization of markers surface with porphyrin, will allow their use for not only detection, but also for cancer treatment – for a photodynamic therapy of tumors.

An innovative method of introducing those markers to living organisms, via ingestion (intra-gastric gavage (IG)), was demonstrated by us. After IG introduction FMs are quickly absorbed by the duodenal epithelium and rapidly (within 24 h) distributed through the organism. IG introduction results in FMsdistribution into the blood-stream and later from the blood into the tissues and organs. In the consequence, majority of the blood-organ barriers within organism are permeable for FMs. The only exception being the blood-lung barrier for a healthy organ.

FMs can penetrate and gradually accumulate in tumors, including the difficult to diagnose and treatmetasthases to the lungs. Our observations show effective trafficking of FMs to the areas of lung cancer growth, whereas surrounding tissue was impermeable for nanoparticles. This shows a high potential of studied FMs in direct tracing of the extent of cancer spread in lungs.

In the talk FM properties will be discussed and compared with those used by other groups.

Acknowledgements. The research was partially supported by the National Centre for Research grants “Maestro” 2012/06/A/ST7/00398 and “Sonata-Bis” UMO 2012/05/E/NZ4/02994.

Biominerals, Challenging Functional Composites

U. Bismayer

University of Hamburg, Mineralogical-Petrological Institute, Hamburg, Germany

Material science is challenged by excellent biological, physical and chemical properties of the hard tissue of organisms which build for instance skeletons, masticators or protecting shells. In many species such hard tissues are made of biominerals with a large inorganic component and minor organic parts.

Several studies on the topic aim to better understand details of the nanostructure, the crystallographic texture and complex twin patten of such biominerals. The studies often have the goal to design and synthsize novel technological material which mimics relevant functions of such biological structures.

Some related examples will be presented and may underline the challenges to be faced in order to disentangle the construction [1] and other characteristic features of biocompatible material which developed its qualities over geological times [2, 3].

[1] Patent: https://patentscope.wipo.int/search/en/detail.jsf?docId=WO2006048198.
[2] A. Becker, U. Bismayer, M. Epple, H. Fabritius, B. Hasse, J. Shi, A. Ziegler, *Dalton Trans.* 551 (2003).
[3] He Jianhan, Shanrong Zhao, Zhuliang Wei and Ulrich Bismayer, *Z. Kristallogr*. **231** (2016) 673.

Evaluation of Differences between Fe_3O_4 Micro- and Nanoparticles Properties

Z. Duriagina, T. Tepla, V. Kulyk

Lviv Polytechnic National University, Lviv, Ukraine

Recently nano- and microsized powder materials based on Fe_3O_4, especially in combination with bioselective elements have been widely used. High chemical activity of Fe_3O_4 particles is caused by their higher ability to ion or atomic exchange, adsorption and formation of surface ligaments with other adsorbed particles. This guarantees the creation of bioparticles with their further use in biosensorics and in enzymatic reactions. Detailed characterization of Fe_3O_4 particles is therefore necessary in order to obtain accurate relationship between their size, electronic, magnetic and structural properties.

Nanoparticles by the sizes and mass occupy the intermediate place between single molecule and living cells. Still the main advantage of these materials is their ability to perform the preset functions under the effect of external magnetic field. However, nanoparticles synthesis has remained until now a complicated task. This is related with the difficulty of formation of homodispersive population of checked-size magnetic particles. Physical and chemical properties of magnetic Fe_3O_4 particles are determined by their size, structure and method of preparation. In particular, the process of synthesis of ferromagnetic iron oxide powders should be directed to obtaining the powder of specific fraction both as to the size and as to the shape. Size factor of powder particles affect their adsorption characteristics, which are determined by the surface energy level. Materials science approaches to the formation of the desired shape and character of the distribution as to the powder fractions will improve their functional properties.

To estimate the sizes of Fe_3O_4 atomic-force microscopy was used, which software products allowed the establishment of the scanned particles structure. Investigation data prove the results of microscopic investigations on the spherical nanoparticles accumulation. Two types of structural inhomogeneity can be distinguished on the investigated sample surface: conglomerates of conical-like nanoparticles and granular texture of substrate. Surface topography is characterized by a rough relief with morphological regions of blocked structure. Blocks are characterized by non-isometric round form with no surface faceting. Use of Fe_3O_4 nanoparticles with the aim of their functionalization application of shells, medical aids and markers on them) or introduction in a living organism for hyperthermia, foresees the application of surface coating. In this case the analysis of the dimensions and properties of nanoparticles using a simple method becomes more complex [1]. In such cases magnetic methods become one of the methods of particles categorization.

It is known that powder particles of Fe_3O_4 retain magnetization even if no external magnetic field is present, possessing own magnetic moment. However, remaining magnetization has a negative effect –a tendency of nanoparticles to agglomeration. Besides the technology of obtaining crystalline nanoparticles with high saturation magnetization needs further improvement. Moreover, nanoparticles lose their stability with time. This occurs due to the decrease of their free surface energy as a result of agglomeration. Therefore, for the effective use of such magnetic particles their chemical stability should be ensured by applying the corresponding coating on their surface.

[1] G. De Crozals, R. Bonnet, C. Farre, C. Chaix, Nanoparticles with multiple properties for biomedical applications: A strategic guide, *Nano Today* **11**(4) (2016) 435-463.

Photocatalytic Activity of Compositions of Type H_2O_2-TiO_2:S,C-HAp/FAp in Visible Light

A. Barylyak[1], Ya. Bobitski[2], B.Cieniek[2], I. Stefaniuk[2], I. Yaremchuk[3], V. Zinchenko[4]

[1]*Danylo Halytsky Lviv National Medical University, Pekarska Str. 69, 79000 Lviv, Ukraine*
[2]*Faculty of Mathematics and Natural Sciences, University of-Rzeszow, Pigonia 1, 35-959 Rzeszow, Poland*
[3]*Department of Photonics, Lviv Polytechnic National University, S. Bandera Str. 12, 79013 Lviv, Ukraine*
[4]*A.V. Bogatsky Physical-Chemical Institute NAS of Ukraine, Lustdorfskaya Road 86, 65080 Odessa, Ukraine*

Recently, considerable attention is devoted to photocatalytic processes, mechanisms and the search new materials for photocatalysis processes. Oxide materials are effective to initiate catalytic reactions. Titanium oxide (TiO_2) has been a subject of considerable attention due to its semiconductor properties, photosensitivity in the ultraviolet light; high photocatalytic properties and applications to clean air, water, and decomposition of organic compounds, bleaching, disinfection and others.

However, using high-energy ultraviolet excitation is limited or unacceptable in some biomedical applications. Thus, there is important to create of photocatalytic materials sensibilized in the visible range of the spectrum. Hydrogen peroxide is widely used as a generator of free radicals in the process of bleaching and whitening. However, the concentration of hydrogen peroxide in biomedical applications strongly regulated or limited to 6%. The catalytic properties of calcium apatite, for example hydroxyapatite, which is a component of bone, are well known. Their nanoscale compositions are used in the processes of remineralization of dental hard tissues.

The main idea of this work is to create a catalyst composition consisting of nanostructured apatite calcium (hydroxyapatite (Hap), fluorideapatite (Fap)), titanium dioxide and reduced concentrations of the hydrogen peroxide sensitive in the visible light to achieve whitening synergetic bleaching effect with simultaneous remineralization of teeth.

TiO_2 was sensibilized in the visible light using doping with S and C. The reactivity of the compositions under blue (460nm) and green radiation (525nm) LEDs was measured by method of electron magnetic resonance. The ESR spectra under blue light and green light irradiations for $Ti0_2$, $Ti0_2$:S,C and FAP-$Ti0_2$:S,C / HAP-$Ti0_2$:S,C samples with limited presence of H_2O_2 were obtained. EPR spectra of all samples nanopowders were investigated at room temperature using the EPR spectrometer. All samples were researched in the dark and under blue light radiation and green light radiation LEDs with illumination 0.01 W/cm^2. The characteristic DMPO-OH spin adduct after irradiation of $Ti0_2$ and FAp-$Ti0_2$, was obtained. The spin adduct indicated that HO• was generated through excitation of Ti02:S,C under blue light irradiation. The spin adduct of superoxide generated from samples HAp during green light irradiation was observed. Our study using EPR spectroscopy and spin trapping has shown that HO• generation through excitation of FAp-$Ti0_2$ is greater than that of HAp-Ti02. It means, that the composition based on $Ti0_2$ doped with S, nanoFAp at limitation of 6% hydrogen peroxide can be used for photocatalytic processes initiated bleaching- remineralization using LED visible radiation spectrum, including the light source for polymerization, which is available in every dentists office.

Quantum-Chemical Studies of Optical Properties of Pirydynsteryl

P.Y. Kobzar[1], O. L. Pavlenko[1], V.V. Kurdyukov[2], O.D. Kachkovsky[3]

[1] *Taras Shevchenko National University of Kyiv, Faculty of Physics, 64/13 Volodymyrska Str., 1601 Kyiv, Ukraine*
[2] *Institute of Organic Chemistry, Color and Structure of Organic Compounds Department , National Academy of Sciences of Ukraine, 5 Murmanska Str., 02660 Kyiv, Ukraine*
[3] *Institute of Bioorganic Chemistry and Petrochemistry, National Academy of Sciences of Ukraine, 1 Murmanska Str., 02660 Kyiv, Ukraine*

Quantum mechanical simulation was performed using the software package Gaussian 09. Molecular optimization was performed using Hartree-Fock HF / 6-31G (d, p), DFT / B3LYP / 6-31G (d, p) methods. Characteristics of electronic transitions calculated by ZINDO / S and TD SCF methods.

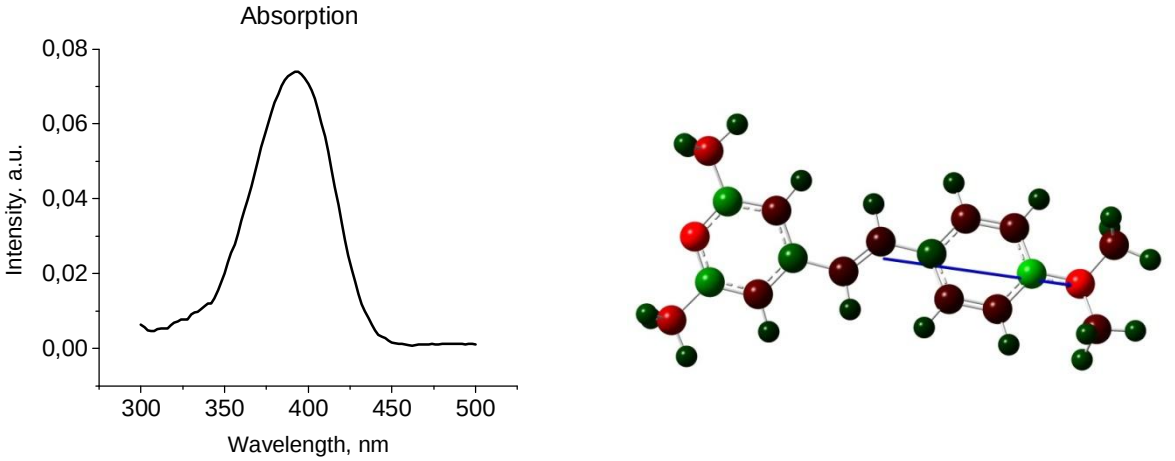

Fig.1. Optimized geometry of pirydynsteryl and calculated absorption spectrum. Perin charge distribution (red - negatively charged, green - positively charged particles). The arrow shows the magnitude and direction of the dipole moment. Also on figure depicted in acetonitrile absorption spectra of the molecule pirydynsterylu.

Calculations show There is a peak in the vicinity of 328 nm and experimental 392 nm.

The magnitude of dipole moment equal to 5.22 Debye charge distribution is due, in particular, as a result of having two nitrogen atoms that have large negative charges -0.5 electronic units, compared with the carbon atoms.

The most negatively charged nitrogen atoms of the molecule can react with pirydynsteryl electron acceptor group other molecules and atoms with a deficit of electron density.

Explain the nature peaks can using quantum-chemical calculations of electronic transitions in the molecule pyridine. The most pronounced is the transition between HOMO and LUMO levels, this level has much more power oscillator. Ionization potential of the molecule that is responsible for transferring electrons to other compounds, calculated by AM1, HF and DFT is 8.26, 7.44 and 6.2 eV, respectively.

Quantum-Chemical Studies of Electron Transitions of Merocyanine Derivatives of Cyclohexadienon

R.S. Iakovyshen[1,*], E.L. Pavlenko[1], N.P. Kulish[1], O.D. Kachkovsky[2], V.V. Kurdyukov[3]

[1]*Taras Shevchenko National University of Kyiv, Faculty of Physics, 64/13 Volodymyrska Street, 01601 Kyiv, Ukraine*
[2]*Institute of Bioorganic Chemistry and Petrochemistry, National Academy of Sciences of Ukraine, 1 Murmanska Street, 03660 Kyiv, Ukraine*
[3]*Color and Structure of Organic Compounds, Department of Institute of Organic Chemistry, National Academy of Sciences of Ukraine, 5 Murmanska Street, 03660 Kyiv, Ukraine*
*iakovyshen@ukr.net

Neutral merocyanines are donor-acceptor substituted polymethine molecules, and as such, they represent an important class of organic chromophores with other linear conjugated system, e.g. polymethinic dyes, squaraines, cyanine bases and polyenes.

In this report presented the results of quantum chemical investigation of the electron structure and nature of electron transitions ofmerocyanine derivatives of the cyclohexadienon with variable donor residues Het.

The chemical constitution of variable donor terminal groups to have an important influence on the electronic structure of merocyanine molecules and their electron transitions. In the Gaussian 03 software package performed molecule modeling, quantum chemical calculations of molecular geometry and distribution of the electron density in the main and excited states. Quantum-chemical calculations of optimized molecular geometry were performed using the DFT/CAM-B3LYP//6-31G(d, p) method; electron transition characteristics were calculated using the TD-DFT/CAM-B3LYP//6-31G(d, p) method and the semi-empirical ZINDO method. Of course, calculated and experimental data do not match perfectly, which is typical for quantum-chemical estimations, however, the correlation is sufficient to correctly analyze the nature of electron transitions.

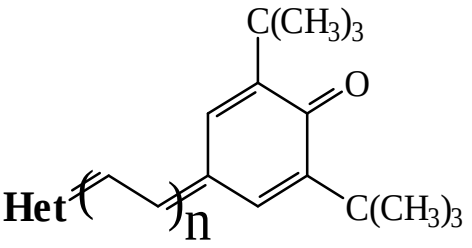

The dependence of atomic charge alternation on the chemical constitution of the donor terminal group is estimated by

$$\Delta q_\mu = |q_{\mu+1} - q_\mu|,$$

where q_μ is the charge at the μ-th atom. A simple quantum-chemical approximation showed that BLA bonds (bond length alternation) can have a positive or a negative value, depending on the donor and/or acceptor strengths of the terminal groups.

The degree of bond alternation is calculated by the following formulas:

$$\Delta l_\nu = (-1)^{-\nu}(l_{\nu+1} - l_\nu),$$

where l_ν is the length of the ν-th bond.

The mutual dispositions of delocalized MOs and local π-orbitals as well as n-MO depend on the donor properties of the variable terminal residues, Het; calculated energies of the frontier and several nearest levels of the merocyanines.

[1] N. Tyutulkov, J. Fabian, A. Mehlhorn, F. Dietz, A. Tatjer, *Polymethine Dyes. Structure and properties*, St. Kliment Ohridski University Press, Sofia, 1991.

Sorption of Neodymium and Gadolinium on Transcarpathian Clinoptilolite

V.O. Vasylechko[1,2], E.T. Stechynska[1], O.D. Stashkiv[1], G.V. Gryshchouk[1], I.O. Patsay[1]

[1] *Department of Analytical Chemistry, Ivan Franko National University of Lviv*
[2] *Department of Natural Sciences and Environment Protection, Lviv University of Trade and Economics*

Most of the lanthanides (Ln) are closely similar in their chemical properties that causes difficulties in separation and quantitative determination of these elements. In most cases, the quantitative determination methods include the pretreatment procedure of samples such as separation, concentration and removal of rare earth elements (REE). Solid-phase extraction with using different sorbents is one of the way to solve the pretreatment problem of the technological solutions and wastewaters. More often for this purpose are used natural zeolites, which have several advantages in comparison with other sorbents. For example, these natural aluminosilicates have mechanical strength, good stability in aggressive medium and under thermal treatment, ability to sorb the trace amounts of analytes, high sorption capasite and selectivity, possibility of easy modification and regeneration of the sorbent, low cost and accessibility. The sorption properties of the clinoptilolite towards Nd(III) and Gd(III) under dynamic conditions have been studied. Nd and Gd – are of the most popular elements of cerium and yttrium subgroups, respectively. These Ln have been widely used in the electronics, nuclear power, as components of magnetic alloys and phosphors. The zeolite compositions with these REE have the biological activity. The clinoptilolite used in this investigation was obtained from the deposit near the village of Sokirnytsia in Ukrainian Transcarpathian region. The previous analysis has shown that the main component was present at 85-90%, the specific surface area, determined by water sorption was 59 $m^2 \cdot g^{-1}$. The chemical composition of Transcarpathian clinoptilolite is (in %): SiO_2, 67.29; TiO_2, 0.26; Al_2O_3, 12.32; Fe_2O_3, 1.26; FeO, 0.25; MgO, 0.99; CaO, 3.01; Na_2O, 0.66; K_2O, 2.76; H_2O, 10.90. It has been established, that the efficiency of the sorption of Nd(III) and Gd(III) mainly depends on the acidity solutions of Ln and previously thermal treatment of the clinoptilolite samples.

The trace amounts of Nd(III) most effectively sorb on the zeolite from the neutral medium at pH 6.5. However, the best concentration of Gd(III) occurs from the low basic solutions at pH 9,5. Sorption capacity of Transcarpation clinoptilolite towords Nd(III) and Gd(III) ions are 1810 and 6500 μg per 1 g of sorbent, respectively. The trace amounts of Nd(III) mainly exist in the cationic forms of the aqueous complexes $[Nd(H_2O)_9]^{3+}$ in the solutions at pH 6.5. The low basic solutions of Gd(III) have hydroxycomplexes – $[Gd(OH)(H_2O)_7]^{2+}$, $[Gd(OH)_2(H_2O)_6]^{+}$ and $[Gd(OH)_3(H_2O)_5]^{0}$. It has showed, that Nd(III) sorb in general on the clinoptilolite using ion-exchange mechanism. The sorption of Gd(III) on the clinoptilolite takes place by the adsorption of the dissolved hydrolysed forms of Gd(III) on the aluminosilicate surface except the ion-exchange mechanism. The differences on the sorption mechanisms of these Ln give the possibility to separate Nd(III) and Gd(III) in the solutions at pH 9.5. In this optimum condition the clinoptilolite maximum sorbs Gd(III) and practically do not sorbs Nd(III). Despite the sorption capacity of the clinoptilolite depends on the temperature of its previously thermal treatment, Nd(III) most effectively sorbs at the non-roasted clinoptilolite samples. The buffer solutions have been used for maintain of pH, ionic power of the solutions and for the improvements of the metrological characteristics of the preconcentration methods of Ln. In the case of the concentration of Nd(III) the best results have been obtained with thrys-buffer solution. The trace amounts of Gd(III) most effectively sorb with borate buffer solution. The solutions of the mineral acids are the best desorbents of Ln from the clinoptilolite. Because, they provide 100 % removal REE from the zeolite matrix. The influence of the macrocomponents of the water on the sorption of Nd(III) and Gd(III) on the clinoptilolite has been studied. The obtained results showed that Transcarpathian clinoptilolite may be used for removal Nd(III) and Gd(III) from the technological solutions.

Authors Index

D

E

F

G

H

I

J

K

L

M

N

O

P

R

S

T

U

V

W

Y

Z

НАУКОВЕ ВИДАННЯ

Збірник тез

Міжнародної наукової конференції “Оксидні матеріали електронної техніки – отримання, властивості, застосування”

OMEE-2017

29 травня – 2 червня, 2017
Львів, Україна

Відповідальний за випуск *В. Швед*
Комп’ютерний набір *Н. В. Мартинюк*

Один електронний оптичний диск CD-ROM.
Об’єм даних у мегабайтах 5,86 Мб.
Наклад 30 прим. Зам. 170795.

Видавець і виготівник: Видавництво Львівської політехніки
Свідоцтво суб’єкта видавничої справи ДК № 4459 від 27.12.2012 р.

вул. Ф. Колесси, 4, Львів, 79013
тел. +380 32 2582146, факс +380 32 2582136
vlp.com.ua, ел. пошта: vmr@vlp.com.ua